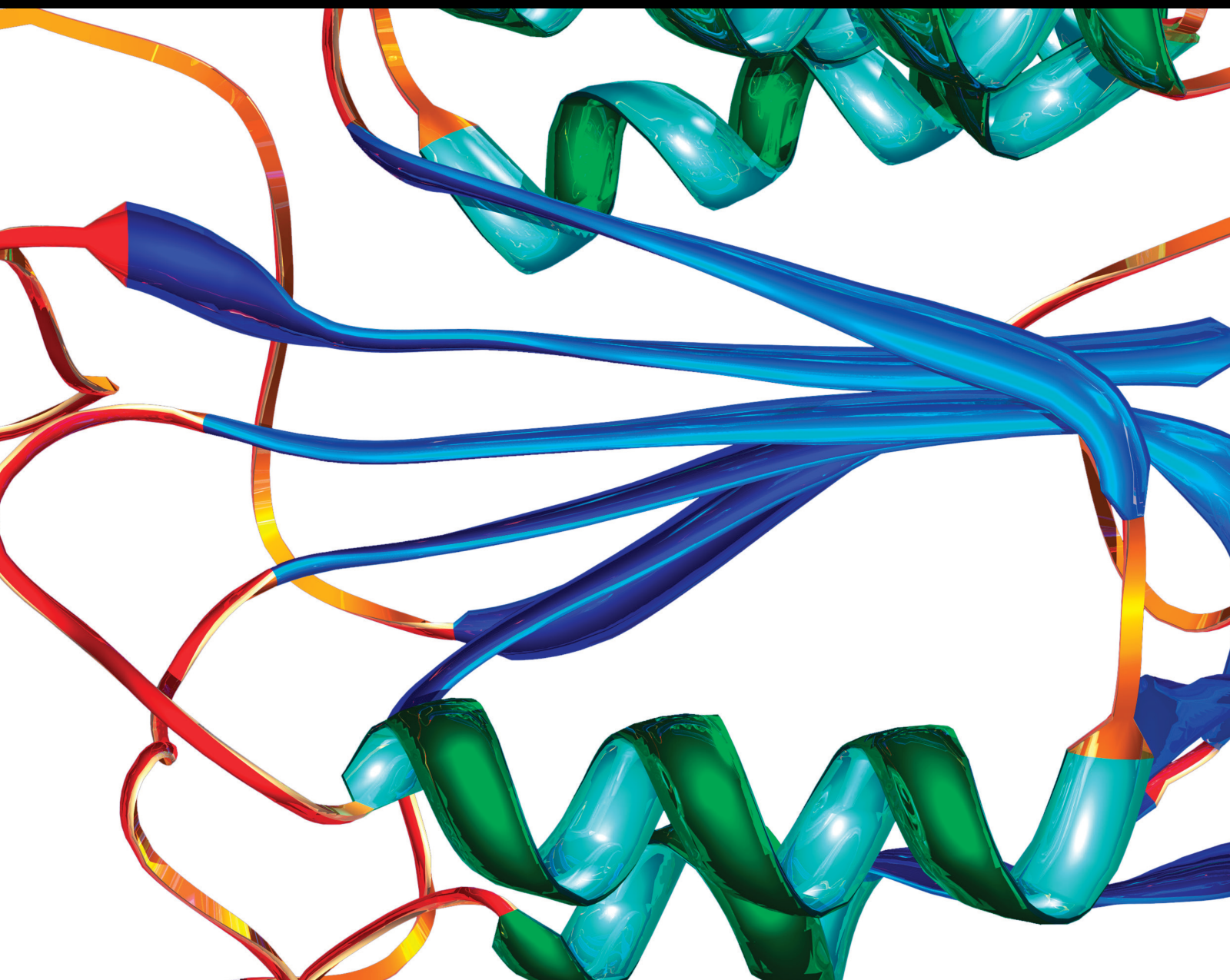


Possible Biomarkers in Malignant and Benign Neurological Disease 2021

Lead Guest Editor: Wen-Jun Tu

Guest Editors: Xianwei Zeng, Baoqiang Guo, and Han-Cheng Qiu





**Possible Biomarkers in Malignant and Benign
Neurological Disease 2021**

Disease Markers

Possible Biomarkers in Malignant and Benign Neurological Disease 2021

Lead Guest Editor: Wen-Jun Tu

Guest Editors: Xianwei Zeng, Baoqiang Guo, and Han-Cheng Qiu



Copyright © 2022 Hindawi Limited. All rights reserved.

This is a special issue published in "Disease Markers." All articles are open access articles distributed under the Creative Commons Attribution License, which permits unrestricted use, distribution, and reproduction in any medium, provided the original work is properly cited.

Chief Editor

Paola Gazzaniga, Italy

Associate Editors


Donald H. Chace , USA
Mariann Harangi, Hungary
Hubertus Himmerich , United Kingdom
Yi-Chia Huang , Taiwan
Giuseppe Murdaca , Italy
Irene Rebelo , Portugal

Academic Editors

Muhammad Abdel Ghafar, Egypt
George Agrogiannis, Greece
Mojgan Alaeddini, Iran
Atif Ali Hashmi , Pakistan
Cornelia Amalinei , Romania
Pasquale Ambrosino , Italy
Paul Ashwood, USA
Faryal Mehwish Awan , Pakistan
Atif Baig , Malaysia
Valeria Barresi , Italy
Lalit Batra , USA
Francesca Belardinilli, Italy
Elisa Belluzzi , Italy
Laura Bergantini , Italy
Sourav Bhattacharya, USA
Anna Birková , Slovakia
Giulia Bivona , Italy
Luisella Bocchio-Chiavetto , Italy
Francesco Paolo Busardó , Italy
Andrea Cabrera-Pastor , Spain
Paolo Cameli , Italy
Chiara Caselli , Italy
Jin Chai, China
Qixing Chen, China
Shaoqiu Chen, USA
Xiangmei Chen, China
Carlo Chiarla , Italy
Marcello Ciaccio , Italy
Luciano Colangelo , Italy
Alexandru Corlateanu, Moldova
Miriana D'Alessandro , Saint Vincent and the Grenadines
Waaqo B. Daddacha, USA
Xi-jian Dai , China
Maria Dalamaga , Greece


Serena Del Turco , Italy
Jiang Du, USA
Xing Du , China
Benoit Dugue , France
Paulina Dumnicka , Poland
Nashwa El-Khazragy , Egypt
Zhe Fan , China
Rudy Foddis, Italy
Serena Fragiotta , Italy
Helge Frieling , Germany
Alain J. Gelibter, Italy
Matteo Giulietti , Italy
Damjan Glavač , Slovenia
Alvaro González , Spain
Rohit Gundamaraju, USA
Emilia Hadziyannis , Greece
Michael Hawkes, Canada
Shih-Ping Hsu , Taiwan
Menghao Huang , USA
Shu-Hong Huang , China
Xuan Huang , China
Ding-Sheng Jiang , China
Esteban Jorge Galarza , Mexico
Mohamed Gomaa Kamel, Japan
Michalis V. Karamouzis, Greece
Muhammad Babar Khawar, Pakistan
Young-Kug Kim , Republic of Korea
Mallikarjuna Korivi , China
Arun Kumar , India
Jinan Li , USA
Peng-fei Li , China
Yiping Li , China
Michael Lichtenauer , Austria
Daniela Ligi, Italy
Hui Liu, China
Jin-Hui Liu, China
Ying Liu , USA
Zhengwen Liu , China
César López-Camarillo, Mexico
Xin Luo , USA
Zhiwen Luo, China
Valentina Magri, Italy
Michele Malaguarnera , Italy
Erminia Manfrin , Italy
Utpender Manne, USA


Alexander G. Mathioudakis, United Kingdom


Andrea Maugeri , Italy

Prasenjit Mitra , India

Ekansh Mittal , USA

Hiroshi Miyamoto , USA

Naoshad Muhammad , USA

Chiara Nicolazzo , Italy

Xing Niu , China

Dong Pan , USA

Dr.Krupakar Parthasarathy, India

Robert Pichler , Austria

Dimitri Poddighe , Kazakhstan

Roberta Rizzo , Italy


Maddalena Ruggieri, Italy

Tamal Sadhukhan, USA


Pier P. Sainaghi , Italy


Cristian Scheau, Romania


Jens-Christian Schewe, Germany

Alexandra Scholze , Denmark

Shabana , Pakistan

Anja Hviid Simonsen , Denmark

Eric A. Singer , USA


Daniele Sola , Italy

Timo Sorsa , Finland


Yaying Sun , China

Mohammad Tarique , USA

Jayaraman Tharmalingam, USA


Sowjanya Thatikonda , USA

Stamatios E. Theocharis , Greece

Tilman Todenhöfer , Germany

Anil Tomar, India

Alok Tripathi, India

Drenka Trivanović , Germany

Natacha Turck , Switzerland

Azizah Ugusman , Malaysia

Shailendra K. Verma, USA

Aristidis S. Veskoukis, Greece

Arianna Vignini, Italy

Jincheng Wang, Japan


Zhongqiu Xie, USA


Yuzhen Xu, China

Zhijie Xu , China


Guan-Jun Yang , China

Yan Yang , USA

Chengwu Zeng , China

Jun Zhang Zhang , USA

Qun Zhang, China


Changli Zhou , USA

Heng Zhou , China

Jian-Guo Zhou, China

Contents

lncRNA DARS-AS1 Promoted Osteosarcoma Progression through Regulating miR-532-3p/CCR7

Yan Xue, Hongmiao Liu, Guangchen Nie, and Xiaoping Ren 

Research Article (9 pages), Article ID 4660217, Volume 2022 (2022)

Tumor Necrosis Factor- α : The Next Marker of Stroke

Yimeng Xue , Xianwei Zeng , Wen-Jun Tu , and Jizong Zhao 





Review Article (8 pages), Article ID 2395269, Volume 2022 (2022)

Intraoperative Use of Topical Retropharyngeal Steroids for Dysphagia after Anterior Cervical Fusion: A Systematic Review and Meta-Analysis

Hang Yu , Hui Dong , Binjia Ruan , Xiaohang Xu , and Yongxiang Wang 


Research Article (9 pages), Article ID 7115254, Volume 2021 (2021)

CircLDLR Promotes Papillary Thyroid Carcinoma Tumorigenicity by Regulating miR-637/LMO4 Axis

Yuan-ming Jiang , Wei Liu , Ling Jiang , and Hongbin Chang 

Research Article (12 pages), Article ID 3977189, Volume 2021 (2021)

IL-38 and IL-36 Target Autophagy for Regulating Synoviocyte Proliferation, Migration, and Invasion in Rheumatoid Arthritis

Zhe Hao and Yi Liu 


Research Article (11 pages), Article ID 7933453, Volume 2021 (2021)

mtDNA in the Pathogenesis of Cardiovascular Diseases

Lili Wang , Qianhui Zhang , Kexin Yuan , and Jing Yuan 


Research Article (8 pages), Article ID 7157109, Volume 2021 (2021)

Recanalization Treatment of Acute Ischemic Stroke Caused by Large-Artery Occlusion in the Elderly: A Comparative Analysis of “the Elderly” and “the Very Elderly”

Qi Wang, Yi-Qun Zhang, Han-Cheng Qiu, Yin-Dan Yao, Ao-Fei Liu, Chen Li, and Wei-Jian Jiang 




Research Article (9 pages), Article ID 3579074, Volume 2021 (2021)

H19 Overexpression Improved Efficacy of Mesenchymal Stem Cells in Ulcerative Colitis by Modulating the miR-141/ICAM-1 and miR-139/CXCR4 Axes

Ming-li Zhao , Tao Chen, Teng-hui Zhang, Feng Tian, and Xiao Wan



Research Article (14 pages), Article ID 7107705, Volume 2021 (2021)

Effect of ORF7 of SARS-CoV-2 on the Chemotaxis of Monocytes and Neutrophils In Vitro

Gang Wang , Jun Guan, Guojun Li, Fengtian Wu, Qin Yang, Chunhong Huang, Junwei Shao, Lichen Xu, Zixuan Guo, Qihui Zhou, Haihong Zhu , and Zhi Chen 


Research Article (9 pages), Article ID 6803510, Volume 2021 (2021)

Association between Plasma Homocysteine Concentrations and the First Ischemic Stroke in Hypertensive Patients with Obstructive Sleep Apnea: A 7-Year Retrospective Cohort Study from China

Nanfang Li , Xintian Cai , Qing Zhu, Xiaoguang Yao, Mengyue Lin, Lin Gan, Le Sun, Na Yue, Yingli Ren, Jing Hong, Yue Ma, Run Wang, Jina Yili, and Qin Luo



Research Article (11 pages), Article ID 9953858, Volume 2021 (2021)

Immune Checkpoints: Therapeutic Targets for Pituitary Tumors

Ding Nie, Yimeng Xue, Qiuyue Fang, Jianhua Cheng, Bin Li, Dawei Wang, Chuzhong Li, Songbai Gui, Yazhuo Zhang, and Peng Zhao 



Review Article (7 pages), Article ID 5300381, Volume 2021 (2021)

Plaque Length Predicts the Incidence of Microembolic Signals in Acute Anterior Circulation Stroke

Liming Zhao, Hongqin Zhao, Yicheng Xu, Aijuan Zhang, Jiatang Zhang , and Chenglin Tian 

Research Article (7 pages), Article ID 2005369, Volume 2021 (2021)

The Prognostic Determinant of Interleukin-10 in Patients with Acute Ischemic Stroke: An Analysis from the Perspective of Disease Management

Wen Sun , Shuhui Wang , and Shanji Nan 

Research Article (9 pages), Article ID 6423244, Volume 2021 (2021)

Research Article

lncRNA DARS-AS1 Promoted Osteosarcoma Progression through Regulating miR-532-3p/CCR7

Yan Xue,^{1,2} Hongmiao Liu,³ Guangchen Nie,² and Xiaoping Ren ^{1,4,5}

¹Hand and Microsurgery Center, The Second Affiliated Hospital of Harbin Medical University, Harbin 150081, China

²Department of Orthopaedics, The fifth hospital of Harbin, Harbin Heilongjiang 150040, China

³Department of Pathology, The general hospital of Heilongjiang Farms & Land reclamation administration, Harbin, Heilongjiang 150086, China

⁴State Province Key Laboratories of Biomedicine Pharmaceuticals, Harbin Medical University, Harbin, Heilongjiang 150086, China

⁵Heilongjiang Medical Science Institute, Harbin Medical University, Harbin, Heilongjiang 150086, China

Correspondence should be addressed to Xiaoping Ren; enrxiaoping@126.com

Received 4 November 2021; Revised 29 December 2021; Accepted 7 January 2022; Published 5 April 2022

Academic Editor: Wen-Jun Tu

Copyright © 2022 Yan Xue et al. This is an open access article distributed under the Creative Commons Attribution License, which permits unrestricted use, distribution, and reproduction in any medium, provided the original work is properly cited.

Background. lncRNAs have been indicated to involve in cell invasion, proliferation, and metastasis. However, function of DARS-AS1 in osteosarcoma remains poorly explored. **Methods.** DARS-AS1 and miR-532-3p level were measured using qRT-PCR. CCK-8 assay and cell invasion assay were done to study cell functions. Luciferase reporter assay was performed to study the mechanism about DARS-AS1 and miR-532-3p. **Results.** We firstly showed that DARS-AS1 expression is upregulated in 73.5% (25/34) of cases with osteosarcoma. Moreover, DARS-AS1 expression is overexpressed in osteosarcoma specimens than in nontumor samples. The DARS-AS1 is overexpressed in the osteosarcoma cell lines (Saos-2, SOSP-9607, U2OS, and MG-63) compared to hFOB. Overexpression of DARS-AS1 promotes cell growth and invasion in MG-63 osteosarcoma cell. DARS-AS1 plays as one sponge for miR-532-3p in osteosarcoma cell, and miR-532-3p overexpression inhibits luciferase activity of DARS-AS1-WT, not DARS-AS1-MUT in MG-63 cell. Ectopic expression of DARS-AS1 inhibits miR-532-3p expression in MG-63 cell. Furthermore, miR-532-3p expression is downregulated in osteosarcoma specimens compared to in paired nontumor samples. MiR-532-3p expression is downregulated in osteosarcoma cell lines compared to hFOB. MiR-532-3p expression is negatively associated with DARS-AS1 expression in osteosarcoma specimens. miR-532-3p directly regulates CCR7 expression in osteosarcoma cell. Elevated DARS-AS1 expression enhances cell growth and invasion via regulating CCR7. **Conclusions.** These data firstly suggested that DARS-AS1 exerted as one oncogene in osteosarcoma partly via regulating miR-532-3p/CCR7.

1. Background

Osteosarcoma is a primary bone malignancy that influences growing bones of adolescents and children and is interrelated with high morbidity [1–3]. The development of several therapeutic methods for osteosarcoma such as radiotherapy, multiagent chemotherapy, and precise tumor excision has ameliorated the prognosis of osteosarcoma [4–6]. However, the five-year surgical rate of these patients diagnosed with advanced stage is still discontent [7–9]. Thus, it is urgent to find novel biomarkers and treatment targets for osteosarcoma cases.

Long noncoding RNAs (lncRNAs) are one type of the noncoding RNAs (ncRNAs) with length exceed that of 200 nucleotides and can modulate gene expression in posttranscriptional or transcriptional level [10–13]. Recent data have suggested that lncRNAs play crucial roles in a lot of cellular functions including differentiation, invasion, proliferation, migration, development, apoptosis, and metastasis [14–18]. Increasing evidences have revealed that lncRNAs are dysregulated in various cancers such as lung carcinoma, bladder cancer, gastric carcinoma, hepatocellular carcinoma, and also osteosarcoma [19–24]. Studies revealed that DARS-AS1 exerted oncogenic roles in human tumors such as

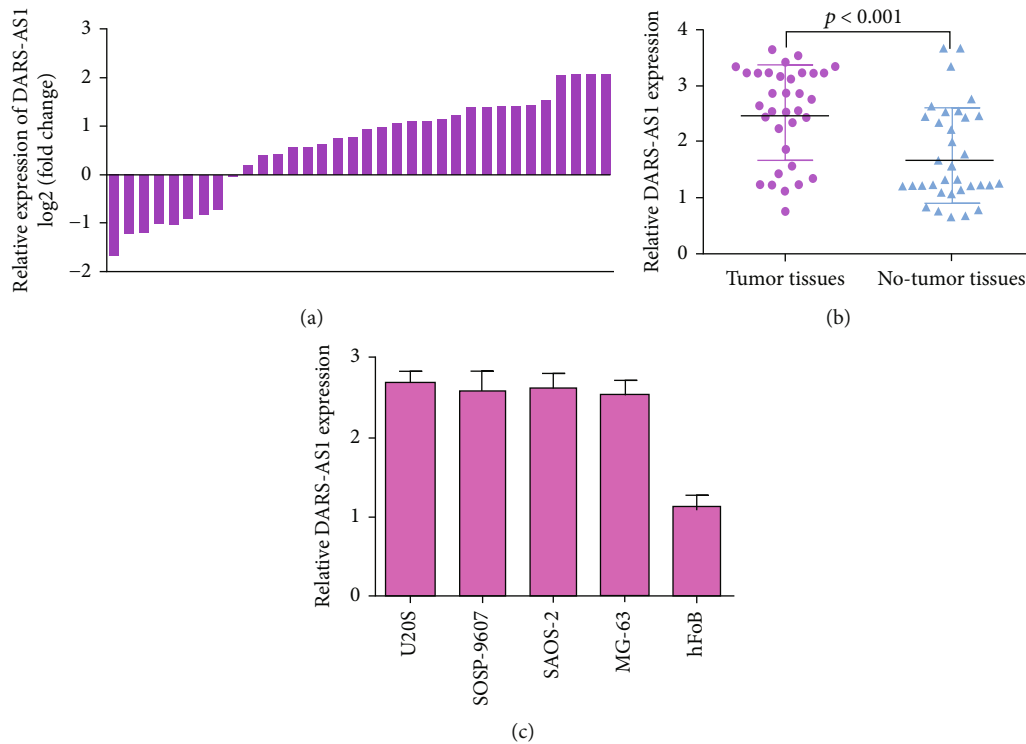


FIGURE 1: DARS-AS1 was highly expressed in osteosarcoma cells and specimens. (a) The DARS-AS1 expression in osteosarcoma specimens and pair no-tumor samples was analyzed with qRT-PCR analysis. (b) DARS-AS1 expression was upregulated in the osteosarcoma specimens compared to in the pair no-tumor samples. (c) The DARS-AS1 expression was overexpressed in osteosarcoma cell lines (U2OS, SOSP-9607, Saos-2, and MG-63) than in one normal osteoblast line (hFOB).

thyroid cancer, myeloma, lung cancer, and ovarian cancer [25–28]. For example, Zheng et al. [27] revealed that DARS-AS1 level was increased in thyroid tumor specimens and was associated with poor prognosis, distant metastasis, and pathological stage, and DARS-AS1 facilitated thyroid tumor cell migration and proliferation via regulating miR-129. Liu et al. [28] demonstrated that DARS-AS1 induced nonsmall cell lung tumor progression through modulating miR-532-3p. Yan [26] showed that DARS-AS1 was upregulated via HIF-1 in myeloma. DARS-AS1 induced myeloma cell tumorigenesis and survival via binding RBM39. Huang et al. [25] showed that expression of DARS-AS1 was upregulated in ovarian tumor specimens and silenced DARS-AS1 expression suppressed cell invasion, migration, and proliferation. However, its function in osteosarcoma remains poorly explored.

We firstly revealed that the DARS-AS1 expression was upregulated in osteosarcoma specimens and cell lines. DARS-AS1 promoted cell growth and invasion in MG-63 osteosarcoma cell.

2. Experimental Materials and Methods

2.1. Clinical Specimens. Thirty pairs of osteosarcoma tissues and pair no-tumor samples were collected from the Second Affiliated Hospital of Harbin Medical University and immediately stored in the liquid nitrogen.

2.2. Cell Culture and Transfect. Four osteosarcoma cell lines (Saos-2, MG-63, SOSP-9607, and U2OS) and a normal osteoblast line (hFOB) were obtained from the American Type Culture Collection (ATCC, USA). These cell lines were plated in the DMEM medium supplemented with FBS, penicillin, and streptomycin. siRNA-control and siRNA-CCR7, miR-532-3p mimic and scramble, pcDNA-DARS-AS1, siRNA-DARS-AS1, and pcDNA-control and siRNA-control plasmids were collected from the Ribobio (Guangzhou, China). Cell transfection was conducted by using Lipofectamine2000 (Invitrogen, CA, USA) according to the manufacturer's protocol. The sequences of siCCR7: 5'-GCGUC AACCC UUUCU UGUATT-3' and 3'-UACAA GAAAG GGUUG ACGCAG-5'; miR-532-3p mimic: 5'-CCUCCCACACCCAAGGCUUGCA-3'.

2.3. RNA Extraction and qRT-PCR. Total cellular and tissue RNA was extracted by using TRIzol kit (Invitrogen, USA) following manufacturer's instruction. Complementary DNAs (cDNAs) were composed, and qRT-PCR analysis was done using SYBR Green (Bio-Rad, Berkeley, CA) on the real-time PCR ABI7500 instrument. The expression of lncRNA and mRNA was compared to GAPDH using the 2^{-DDCT} way. qRT-PCR primers were amplified as follows: GAPDH: forward 5'-AGGTCCACCACTGACACGTT-3', reverse, 5'-GCCTCAAGATCATCAGCAAT-3'; miR-532-3p: forward 5'-CCUCCCACACCCAAGGCUUGCA-3', reverse, 5'-

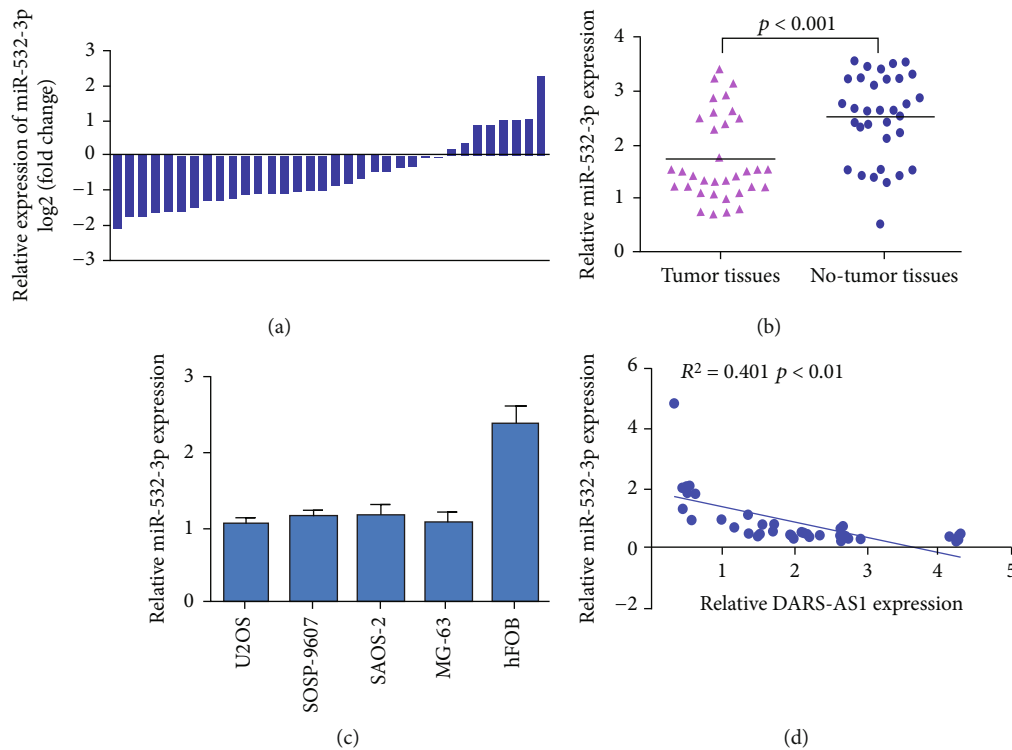


FIGURE 2: miR-532-3p was decreased in osteosarcoma cells and specimens. (a) The miR-532-3p expression in osteosarcoma specimens and pair no-tumor samples was analyzed with qRT-PCR method. (b) miR-532-3p expression was lower in the osteosarcoma specimens than in the pair no-tumor samples. (c) The miR-532-3p expression was downregulated in osteosarcoma cell lines (U2OS, SOSP-9607, Saos-2, and MG-63) compared to in one normal osteoblast line (hFOB). (d) Pearson's correlation assay indicated that miR-532-3p expression was negatively associated with DARS-AS1 expression in osteosarcoma specimens.

CAAGCCUUGGGUGUGGGAGGUU-3'; DARS-AS1: forward 5'-AGCCAAGGACTGGTCTCTTTT-3', reverse, 5'-CTGTACTGGTGGGAAGAGCC-3'; and miR-532-3p: forward 5'-CGTTT CCAAC TGTATG-3', reverse, 5'-CAAC GGCGGATGGCC-3'. The following conditions of qRT-PCR were noted: 40 seconds at the 95°C, 45 cycles for 12 seconds at 95°C, and 60°C for 40 seconds.

2.4. Cell Proliferation and Invasion Assay. For cell proliferation, cell was kept into the 96-well dish at 5×10^3 cells/well. The cell growth rate was analyzed using CCK-8 (DOJINDO, Japan) following manufacturer's protocol at the different time points. The absorbance at 450 nm was determined on the microtiter reader. For cell invasion, Bio-Coat Matrigel chambers (BD Biosciences, Germany) was used. For cell invasion assay, cells were seeded on the top chamber (Matrigel coated filter) in the serum-free medium, and FBS (10%) was conducted as a chemoattractant. After incubation for 48 hours, the cell that invaded to lower side was fixed and counted.

2.5. Luciferase Reporter Assay. Cell was cotransfected pMIR vector containing the diverse mutant or wild type DARS-AS1 and mutant or wild type CCR7, along with pRL-TK control plasmid and miR-532-3p mimic or scramble control by using Lipofectamine2000 (Invitrogen, USA). After 2 days, cell was harvested and then analyzed with the Dual Luciferase

Assay kit (Promega, USA) following manufacturer's protocol.

2.6. Statistical Analysis. Data are indicated as means + SD (Standard Deviation) based on 3 independent experiments and determined by using SPSS version 12.0 software (SPSS, Chicago, USA). Statistical significance was regarded as P value < 0.05 . The significant difference was analyzed by one-way analysis of variance or Student's t tests.

3. Results

3.1. DARS-AS1 Was Highly Expressed in Osteosarcoma Cells and Specimens. DARS-AS1 expression in osteosarcoma specimens and paired nontumor samples was analyzed with qRT-PCR analysis. As presented in Figure 1(a), DARS-AS1 expression was upregulated in 73.5% (25/34) of cases with osteosarcoma. Moreover, DARS-AS1 expression was higher in osteosarcoma specimens than in paired nontumor samples (Figure 1(b)). DARS-AS1 expression was overexpressed in osteosarcoma cell lines (U2OS, SOSP-9607, Saos-2, MG-63, and HOS) than in one normal osteoblast line (hFOB) (Figure 1(c)).

3.2. miR-532-3p Expression Was Decreased in Osteosarcoma Cells and Specimens. miR-532-3p expression in osteosarcoma specimens and paired nontumor samples was analyzed with qRT-PCR method. As presented in Figure 2(a), miR-

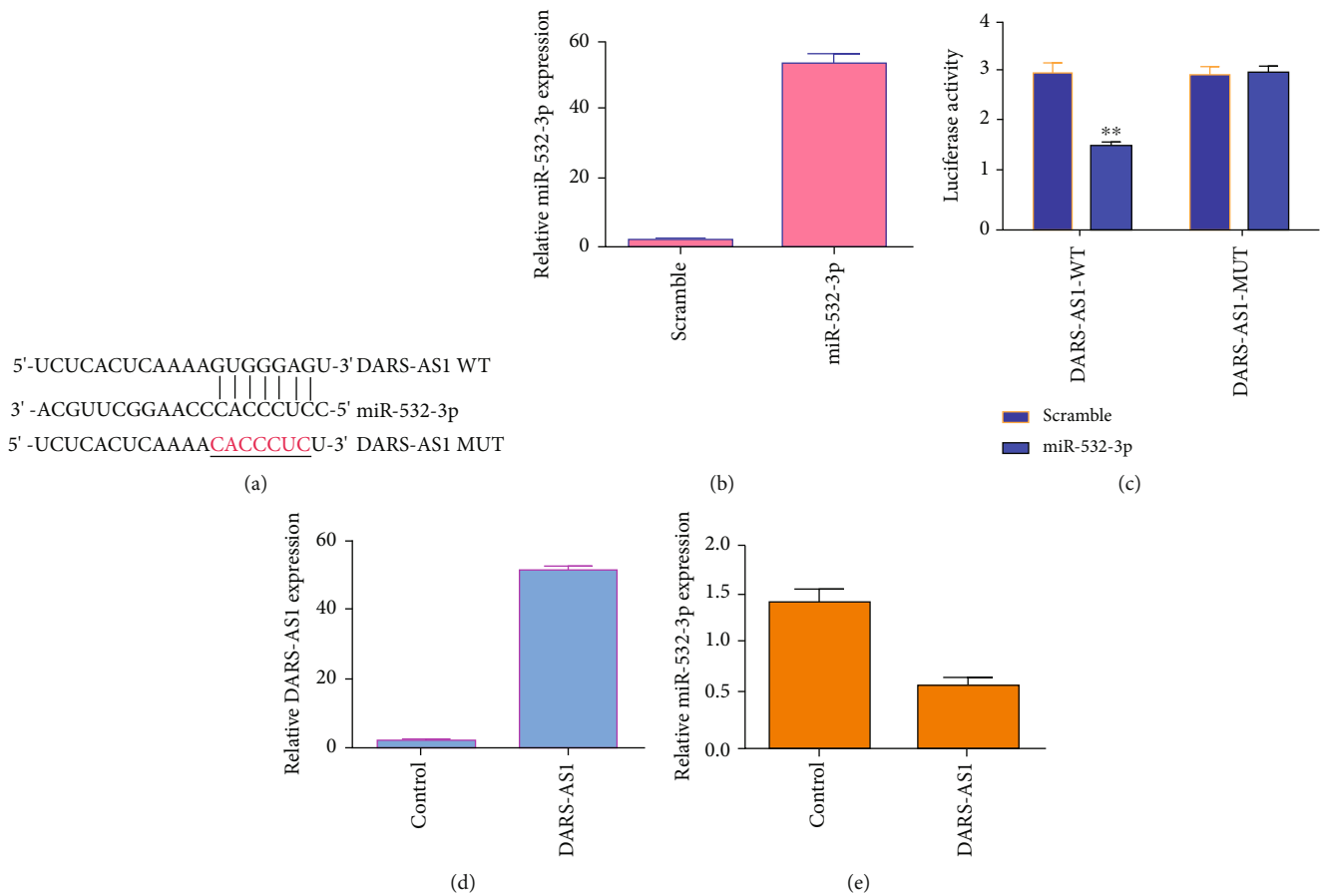


FIGURE 3: DARS-AS1 played as a sponge for miR-532-3p in osteosarcoma cell. (a) DARS-AS1 has potential binding sites of miR-532-3p. (b) The expression of miR-532-3p was significantly upregulated in the MG-63 osteosarcoma cell after treated with miR-532-3p mimics. (c) Overexpression of miR-532-3p decreased luciferase activity of DARS-AS1-WT, not DARS-AS1-MUT in the MG-63 cell. (d) The expression of DARS-AS1 was significantly upregulated in the MG-63 osteosarcoma cell after treated with pcDNA-DARS-AS1 plasmid. (e) Ectopic expression of DARS-AS1 inhibited the miR-532-3p level in the MG-63 cell. $**p < 0.01$.

532-3p expression was downregulated in 76.5% (26/34) of cases with osteosarcoma. Moreover, miR-532-3p expression was lower in the osteosarcoma specimens than in the paired nontumor samples (Figure 2(b)). miR-532-3p expression was decreased in osteosarcoma cell lines (U2OS, SOSP-9607, Saos-2, MG-63, and HOS) than in hFOB (Figure 2(c)). Furthermore, Pearson's correlation assay indicated that miR-532-3p expression was negatively associated with DARS-AS1 expression in osteosarcoma specimens (Figure 2(d)).

3.3. DARS-AS1 Played as a Sponge for miR-532-3p in Osteosarcoma Cell. To study the relationship between DARS-AS1 and miR-532-3p, we observed that DARS-AS1 has potential binding sites of miR-532-3p (Figure 3(a)). The expression of miR-532-3p was significantly upregulated in MG-63 osteosarcoma cell after treated with miR-532-3p mimics (Figure 3(b)). Then, we carried out luciferase analysis to indicate that overexpression of miR-532-3p decreased luciferase activity of DARS-AS1-WT, not DARS-AS1-MUT in the MG-63 cell (Figure 3(c)). The expression of DARS-AS1 was significantly upregulated in the MG-63 osteosarcoma cell after treated with pcDNA-DARS-AS1 plasmid

(Figure 3(d)). Ectopic expression of DARS-AS1 inhibited miR-532-3p level in MG-63 cell (Figure 3(e)).

3.4. miR-532-3p Directly Regulated CCR7 Expression in Osteosarcoma Cell. To study the relationship between CCR7 and miR-532-3p, we observed that CCR7 has potential binding sites of miR-532-3p (Figure 4(a)). Then, we carried out luciferase analysis to show that overexpression of miR-532-3p suppressed luciferase activity of CCR7-WT, not CCR7-MUT in the MG-63 cell (Figure 4(b)). Elevated expression of miR-532-3p inhibited the CCR7 expression in the MG-63 cell (Figure 4(c)). Moreover, ectopic expression of DARS-AS1 promoted CCR7 expression in the MG-63 cell (Figure 4(d)).

3.5. DARS-AS1 Promoted Cell Growth and Invasion in MG-63 Osteosarcoma Cell. CCK-8 assay results indicated that overexpression of DARS-AS1 enhanced cell proliferation in the MG-63 cells (Figure 5(a)). Ectopic expression of DARS-AS1 increased ki-67 expression in the MG-63 cells (Figure 5(b)). Elevated expression of DARS-AS1 promoted cyclin D1 expression in the MG-63 cells (Figure 5(c)).

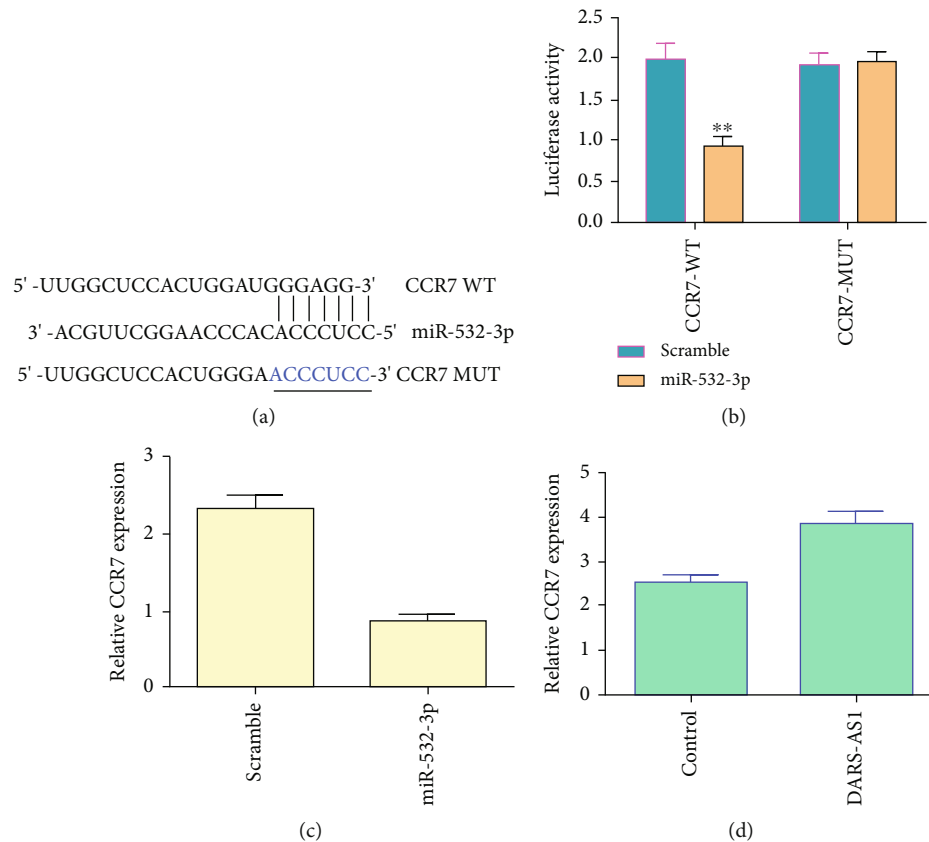


FIGURE 4: miR-532-3p directly regulated CCR7 expression in osteosarcoma cell. (a) CCR7 has potential binding sites of miR-532-3p. (b) Overexpression of miR-532-3p suppressed luciferase activity of CCR7-WT, not CCR7-MUT in the MG-63 cell. (c) Elevated expression of miR-532-3p inhibited the CCR7 expression in the MG-63 cell. (d) Ectopic expression of DARS-AS1 promoted CCR7 expression in the MG-63 cell. ** $p < 0.01$.

Moreover, ectopic expression of DARS-AS1 promoted cell invasion in the MG-63 cell (Figures 5(d) and 5(e)).

3.6. Downregulated Expression of DARS-AS1 Inhibited Cell Growth in MG-63 Osteosarcoma Cell. The expression of DARS-AS1 was significantly downregulated in MG-63 osteosarcoma cell after treated with si-DARS-AS1 (Figure 6(a)). Knockdown of DARS-AS1 suppressed cell proliferation in MG-63 cells (Figure 6(b)). Inhibited expression of DARS-AS1 suppressed the expression of cyclin D1 (Figure 6(c)) and ki-67 (Figure 6(d)).

3.7. Elevated Expression of DARS-AS1 Enhanced Cell Growth and Invasion via Regulating CCR7. To study whether DARS-AS1/CCR7 derived osteosarcoma progression, rescue experiments were performed. We confirmed that the expression of CCR7 was downregulated in the MG-63 cell after treated with si-CCR7 (Figure 7(a)). CCK-8 assay indicated that downregulation of CCR7 suppressed cell proliferation in the DARS-AS1-overexpressing MG-63 cell (Figure 7(b)). Knockdown of CCR7 inhibited ki-67 (Figure 7(c)) and cyclin D1 (Figure 7(d)) expression in the DARS-AS1-overexpressing MG-63 cell. CCR7 knockdown suppressed cell invasion in the DARS-AS1-overexpressing MG-63 cell (Figures 7(e) and 7(f)).

3.8. Discussion. Our study identified that DARS-AS1 acted as one oncogenic lncRNA in the development of osteosarcoma. We firstly revealed that DARS-AS1 expression was higher in osteosarcoma specimens than in paired nontumor samples. DARS-AS1 promoted cell growth and invasion in MG-63 osteosarcoma cell. We found that DARS-AS1 played as a sponge for miR-532-3p in osteosarcoma cell, and ectopic expression of DARS-AS1 inhibited miR-532-3p level in MG-63 cell. Furthermore, miR-532-3p expression was lower in osteosarcoma specimens than in nontumor samples and miR-532-3p expression was negatively associated with DARS-AS1 expression in osteosarcoma specimens. miR-532-3p directly regulated CCR7 expression in osteosarcoma cell. Elevated expression of DARS-AS1 enhanced cell growth and invasion via regulated CCR7. These data suggested that DARS-AS1 exerted as one oncogene in osteosarcoma partly via regulating miR-532-3p/CCR7.

Studies revealed that DARS-AS1 exerted an oncogenic role in several human tumors such as thyroid cancer, lung cancer, myeloma, and ovarian cancer [25–28]. For example, Zheng et al. [27] revealed that DARS-AS1 expression was increased in thyroid tumor specimens and was associated with poor prognosis, distant metastasis, and pathological stage, and DARS-AS1 facilitated thyroid tumor cell migration and proliferation via regulating miR-129. Liu et al.

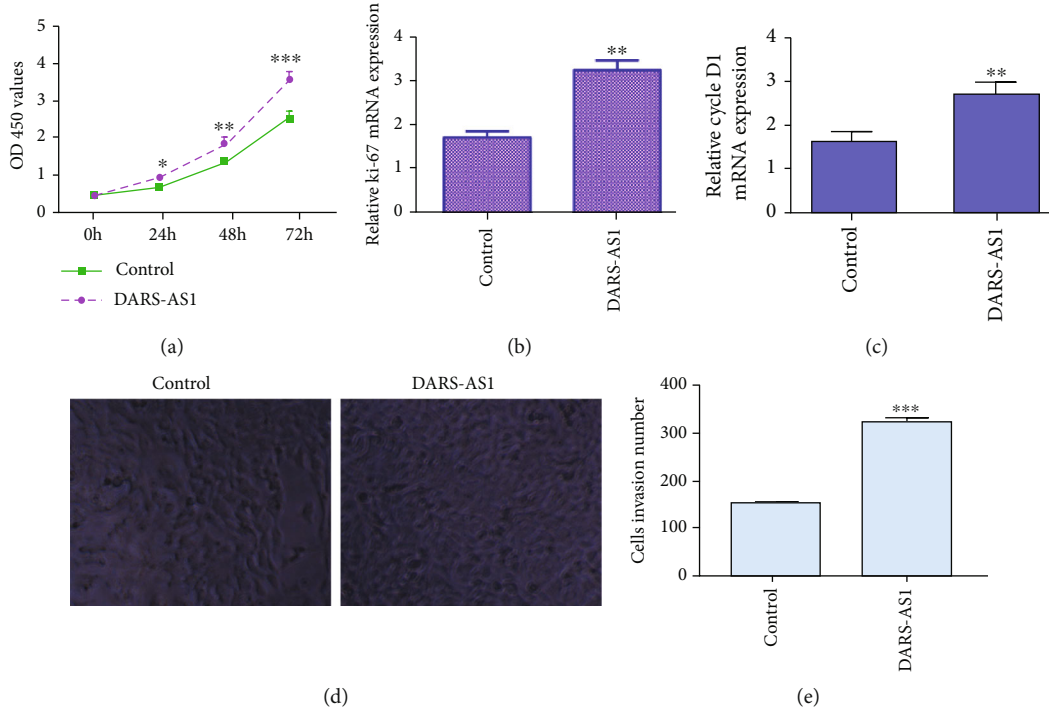


FIGURE 5: DARS-AS1 promoted cell growth and invasion in MG-63 osteosarcoma cell. (a) CCK-8 assay results indicated that overexpression of DARS-AS1 enhanced cell proliferation both in the MG-63 cells. (b) Ectopic expression of DARS-AS1 increased ki-67 expression both in the MG-63 cells. (c) Elevated expression of DARS-AS1 promoted cyclin D1 expression both in the MG-63 cells. (d) Ectopic expression of DARS-AS1 promoted cell invasion in the MG-63 cell. (e) The relative invasive cells were shown. * $p < 0.05$, ** $p < 0.01$, and *** $p < 0.001$.

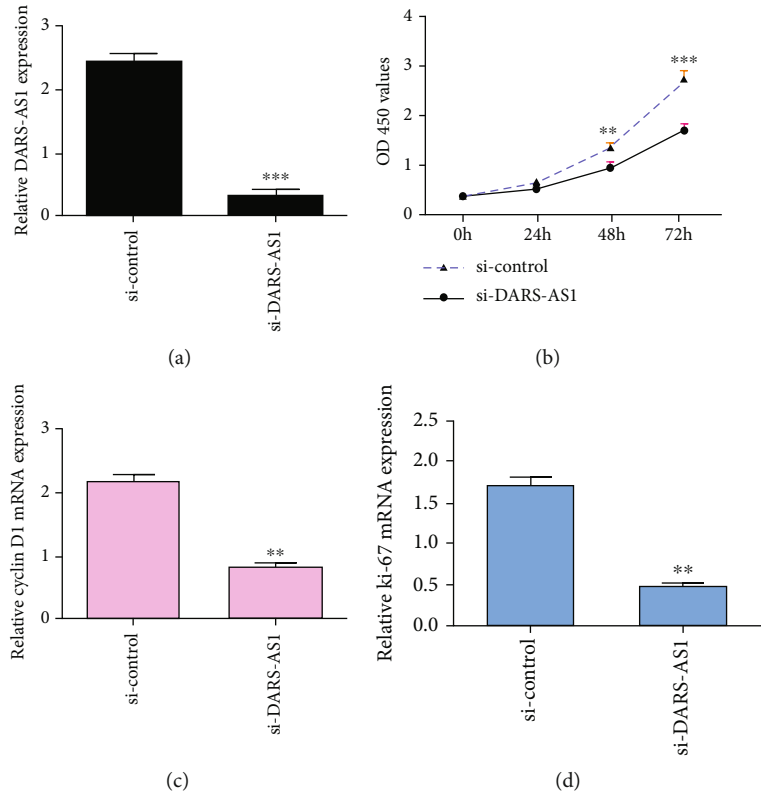


FIGURE 6: DARS-AS1 promoted cell growth in MG-63 osteosarcoma cell. (a) The expression of DARS-AS1 was detected by RT-qPCR assay. (b) Knockdown of DARS-AS1 suppressed cell proliferation in the MG-63 cells. (c) The expression of cyclin D1 was detected by RT-qPCR assay. (d) Inhibition expression of DARS-AS1 suppressed ki-67 expression. * $p < 0.05$, ** $p < 0.01$, and *** $p < 0.001$.

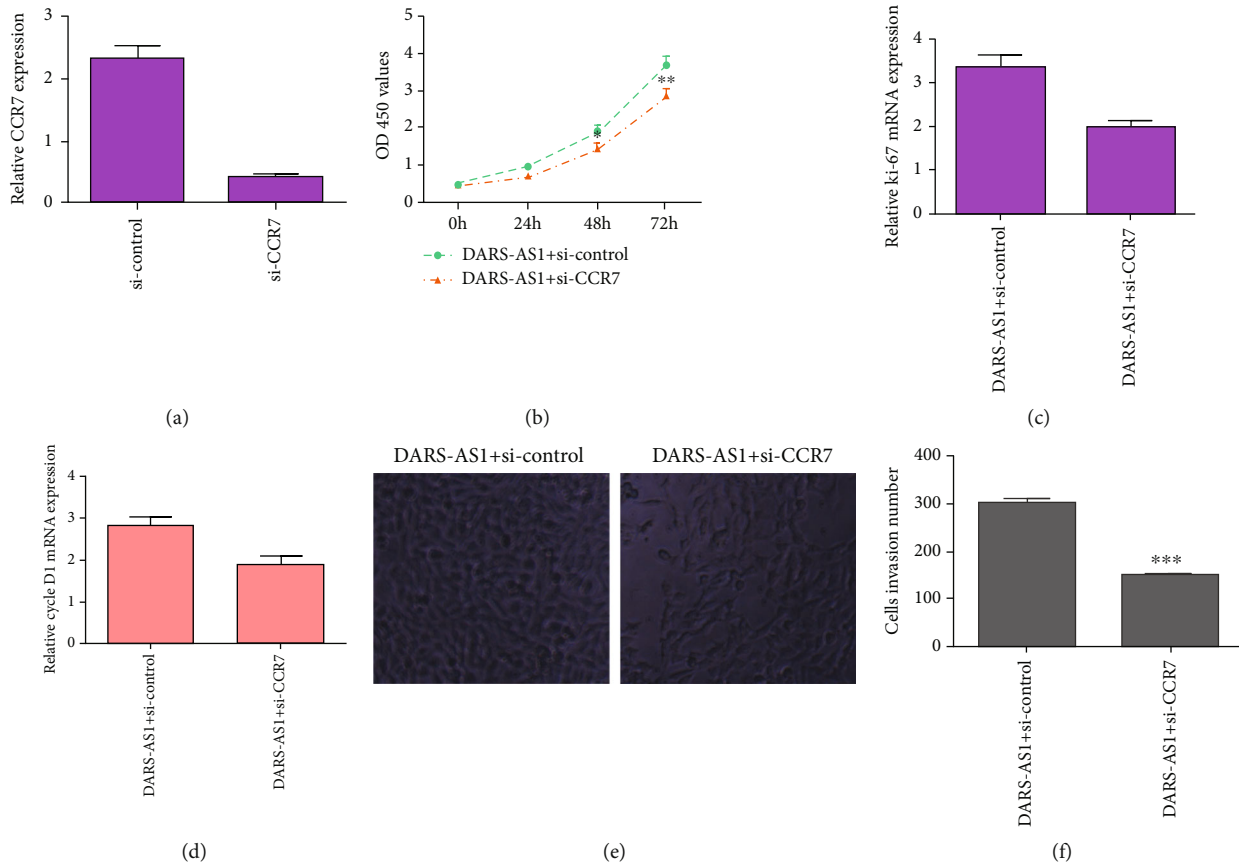


FIGURE 7: Elevated expression of DARS-AS1 enhanced cell growth and invasion via regulated CCR7. (a) The expression of CCR7 was downregulated in the MG-63 cell after treated with si-CCR7 by using qRT-PCR. (b) CCK-8 assay indicated that downregulation expression of CCR7 suppressed cell proliferation in the DARS-AS1-overexpressing MG-63 cell. (c) The expression of ki-67 was analyzed by qRT-PCR assay. (d) The expression of cyclin D1 was analyzed by qRT-PCR assay. (e) Downregulation expression of CCR7 inhibited cell invasion in the DARS-AS1-overexpressing MG-63 cell. (f) The relative invasive cells were shown. * $p < 0.05$, ** $p < 0.01$, and *** $p < 0.001$.

[28] found that DARS-AS1 induced nonsmall cell lung tumor progression through modulating miR-532-3p. Yan [26] showed that DARS-AS1 was upregulated via HIF-1 in myeloma. DARS-AS1 induced myeloma cell tumorigenesis and survival via binding RBM39. Huang et al. [25] indicated that expression of DARS-AS1 was upregulated in ovarian tumor specimens, and silenced DARS-AS1 expression suppressed cell invasion, migration, and proliferation via modulating miR-532-3p. Its role in osteosarcoma remains poorly explored. We firstly studied the expression level of DARS-AS1 in osteosarcoma specimens and paired nontumor samples. Our data indicated that DARS-AS1 expression was upregulated in 73.5% (25/34) of cases with osteosarcoma. Moreover, DARS-AS1 expression was higher in osteosarcoma specimens than in paired nontumor samples. DARS-AS1 promoted cell growth and invasion in MG-63 osteosarcoma cell. These results suggested that DARS-AS1 acted as one oncogenic role in the development of osteosarcoma.

Recent references have suggested that lncRNAs played roles in a lot of tumors via modulating miRNAs expression [16, 29–31]. For instance, lncRNA HOXA-AS2 suppressed osteosarcoma cell invasion, viability, and migration via sponging miR-124-3p [32]. Li et al. [33] indicated that

lncRNA NR2F1-AS1 promoted osteosarcoma progression through sponging miR-483-3p. lncRNA SND1-IT1 promoted osteosarcoma migration and proliferation through regulating miRNA-665 expression [34]. lncRNA SPRY4-IT1 induced osteosarcoma progression through sponging miR-101 [35]. Moreover, lncRNA DARS-AS1 promoted ovarian cancer cell metastasis and growth via sponging miR-532-3p [25]. We also observed that DARS-AS1 has potential binding sites of miR-532-3p in osteosarcoma. Previous study demonstrated that miR-532-3p expression was downregulated in the osteosarcoma tissues [36]. We also found that miR-532-3p expression was lower in osteosarcoma specimens than in paired nontumor samples. Moreover, the data of Pearson's correlation assay indicated that miR-532-3p expression was negatively associated with DARS-AS1 expression in osteosarcoma specimens. miR-532-3p directly regulated CCR7 expression in osteosarcoma cell. Previous study demonstrated that miR-532-3p inhibited TSCC progression through regulating CCR7 and it suggested that CCR7 might play important roles in the development of osteosarcoma [37]. CCR7 are involved in tumor migration and metastasis [38]. We firstly showed that elevated expression of DARS-AS1 enhanced cell growth and

invasion via regulating CCR7. It suggested that DARS-AS1/CCR7 axis might be one novel therapeutic target for osteosarcoma.

4. Conclusions

Our findings showed that DARS-AS1 expression was upregulated in osteosarcoma cells and tissues, and elevated expression of DARS-AS1 enhanced cell growth and invasion via regulating miR-532-3p/CCR7. These data suggested that DARS-AS1 exerted as one oncogene in osteosarcoma partly via regulating miR-532-3p/CCR7.

Abbreviations

miR-532-3p:	microRNA-532-3p
lncRNAs:	Long noncoding RNAs
ncRNAs:	Noncoding RNAs
ATCC:	American type culture collection
FBS:	Fetal bovine serum
cDNAs:	Complementary DNAs
CCR7:	C-C chemokine receptor 7.

Data Availability

The authors can make data available on request through an email to the corresponding author, enrxaoping@126.com, Prof. Dr. Ren.

Ethical Approval

This study was performed with the approval of Clinical Ethics Committee of the Second Affiliated Hospital of Harbin Medical University.

Consent

Each patient has written an informed consent.

Conflicts of Interest

The authors declare that they have no conflicts of interest.

Authors' Contributions

YX, HL, GN, and XR have all contributed to design and wrote the manuscript. Yan Xue and Hongmiao Liu are co-first authors.

References

- [1] D. Zhao, P. Jia, W. Wang, and G. Zhang, "VEGF-mediated suppression of cell proliferation and invasion by miR-410 in osteosarcoma," *Molecular and Cellular Biochemistry*, vol. 400, no. 1-2, pp. 87–95, 2015.
- [2] Y. Zhang, G. Duan, and S. Feng, "MicroRNA-301a modulates doxorubicin resistance in osteosarcoma cells by targeting AMP-activated protein kinase alpha 1," *Biochemical and Biophysical Research Communications*, vol. 459, no. 3, pp. 367–373, 2015.
- [3] Z. W. Ba, L. Gu, S. Hao, X. Wang, Z. Cheng, and G. Nie, "Downregulation of lncRNACASC2 facilitates osteosarcoma growth and invasion through miR-181a," *Cell Proliferation*, vol. 51, no. 1, 2018.
- [4] X. H. Sun, X. L. Geng, J. Zhang, and C. Zhang, "miRNA-646 suppresses osteosarcoma cell metastasis by downregulating fibroblast growth factor 2 (FGF2)," *Tumour Biology*, vol. 36, no. 3, pp. 2127–2134, 2015.
- [5] Z. Li, J. Shen, M. T. V. Chan, and W. K. K. Wu, "The long non-coding RNA SPRY4-IT1: An emerging player in tumorigenesis and osteosarcoma," *Cell Proliferation*, vol. 51, no. 4, 2018.
- [6] R. D. Xu, F. Feng, X. Yu, Z. Liu, and L. Lao, "LncRNA SNHG4 promotes tumour growth by sponging miR-224-3p and predicts poor survival and recurrence in human osteosarcoma," *Cell Proliferation*, vol. 51, no. 6, 2018.
- [7] N. Bilbao-Aldaiturriaga, A. Gutierrez-Camino, I. Martin-Guerrero et al., "Polymorphisms in miRNA processing genes and their role in osteosarcoma risk," *Pediatric Blood & Cancer*, vol. 62, no. 5, pp. 766–769, 2015.
- [8] C. Yang, K. Wu, S. Wang, and G. Wei, "Long non-coding RNA XIST promotes osteosarcoma progression by targeting YAP via miR-195-5p," *Journal of Cellular Biochemistry*, vol. 119, no. 7, pp. 5646–5656, 2018.
- [9] J. Zhao, C. Zhang, Z. Gao, H. Wu, R. Gu, and R. Jiang, "Retracted: Long non-coding RNA ASBEL promotes osteosarcoma cell proliferation, migration, and invasion by regulating microRNA-21," *Journal of Cellular Biochemistry*, vol. 119, no. 8, pp. 6461–6469, 2018.
- [10] S. B. Zhu, W. Fu, L. Zhang et al., "LINC00473 antagonizes the tumour suppressor miR-195 to mediate the pathogenesis of Wilms tumour viaIKK α ," *Cell Proliferation*, vol. 51, no. 1, 2018.
- [11] Z. Li, X. Li, X. Chen et al., "Emerging roles of long non-coding RNAs in neuropathic pain," *Cell Proliferation*, vol. 52, no. 1, 2019.
- [12] Y. F. Zou, Y. Zhong, J. Wu et al., "Long non-codingPANDARas a novel biomarker in human cancer: A systematic review," *Cell Proliferation*, vol. 51, no. 1, p. 51(1), 2018.
- [13] J. M. Zhang, M. Yin, G. Peng, and Y. Zhao, "CRNDE: An important oncogenic long non-coding RNA in human cancers," *Cell Proliferation*, vol. 51, no. 3, 2018.
- [14] K. L. She, H. Yan, J. Huang, H. Zhou, and J. He, "miR-193b availability is antagonized by LncRNA-SNHG7 forFAIM2-induced tumour progression in non-small cell lung cancer," *Cell Proliferation*, vol. 51, no. 1, 2018.
- [15] Q. Chen, X. Huang, and R. Li, "LncRNA MALAT1/miR-205-5p axis regulates MPP-induced cell apoptosis in MN9D cells by directly targeting LRRK2," *American Journal of Translational Research*, vol. 10, no. 2, pp. 563–572, 2018.
- [16] Y. Pan, Y. Wu, J. Hu et al., "Long noncoding RNA HOTAIR promotes renal cell carcinoma malignancy through alpha-2, 8-sialyltransferase 4 by sponging microRNA-124," *Cell Proliferation*, vol. 51, no. 6, 2018.
- [17] Z. Li, X. Li, C. Chen et al., "Long non-coding RNAs in nucleus pulposus cell function and intervertebral disc degeneration," *Cell Proliferation*, vol. 51, no. 5, 2018.
- [18] C. Zhang, C. Su, Q. Song, F. Dong, S. Yu, and J. Huo, "LncRNA PICART1 suppressed non-small cell lung cancer cells proliferation and invasion by targeting AKT1 signaling pathway," *American Journal of Translational Research*, vol. 10, no. 12, pp. 4193–4201, 2018.

- [19] K. S. Ye, S. Wang, H. Zhang, H. Han, B. Ma, and W. Nan, "Long noncoding RNA GAS5 suppresses cell growth and epithelial-mesenchymal transition in osteosarcoma by regulating the miR-221/ARHI pathway," *Journal of Cellular Biochemistry*, vol. 118, no. 12, pp. 4772–4781, 2017.
- [20] Y. Zhuang, H. Jiang, H. Li et al., "Down-regulation of long non-coding RNA AFAP1-AS1 inhibits tumor cell growth and invasion in lung adenocarcinoma," *American Journal of Translational Research*, vol. 9, no. 6, pp. 2997–3005, 2017.
- [21] J. H. He, Z. P. Han, J. M. Liu et al., "Overexpression of long non-coding RNA MEG3 inhibits proliferation of hepatocellular carcinoma huh 7 cells via negative modulation of miRNA-664," *Journal of Cellular Biochemistry*, vol. 118, no. 11, pp. 3713–3721, 2017.
- [22] Y. Zhang, Y. W. Dang, X. Wang et al., "Comprehensive analysis of long non-coding RNA PVT1 gene interaction regulatory network in hepatocellular carcinoma using gene microarray and bioinformatics," *American Journal of Translational Research*, vol. 9, no. 9, pp. 3904–3917, 2017.
- [23] H. X. Zhu, X. Li, Y. Song, P. Zhang, Y. Xiao, and Y. Xing, "Long non-coding RNA ANRIL is up-regulated in bladder cancer and regulates bladder cancer cell proliferation and apoptosis through the intrinsic pathway," *Biochemical and Biophysical Research Communications*, vol. 467, no. 2, pp. 223–228, 2015.
- [24] W. Peng, S. Si, Q. Zhang et al., "Long non-coding RNA MEG3 functions as a competing endogenous RNA to regulate gastric cancer progression," *Journal of Experimental & Clinical Cancer Research*, vol. 34, no. 1, p. 79, 2015.
- [25] K. Huang, W. S. Fan, X. Y. Fu, Y. L. Li, and Y. G. Meng, "Long noncoding RNA DARS-AS1 acts as an oncogene by targeting miR-532-3p in ovarian cancer," *European Review for Medical and Pharmacological Sciences*, vol. 23, no. 6, pp. 2353–2359, 2019.
- [26] H. Yan, "Hypoxia-induced long non-coding RNA DARS-AS1 regulates RBM39 stability to promote myeloma malignancy," *Clinical Lymphoma Myeloma & Leukemia*, vol. 19, no. 10, pp. E101–E101, 2019.
- [27] W. Zheng, X. Tian, L. Cai et al., "LncRNA DARS-AS1 regulates microRNA-129 to promote malignant progression of thyroid cancer," *European Review for Medical and Pharmacological Sciences*, vol. 23, no. 23, pp. 10443–10452, 2019.
- [28] D. Liu, H. Liu, Z. Jiang, M. Chen, and S. Gao, "Long non-coding RNA DARS-AS1 promotes tumorigenesis of non-small cell lung cancer via targeting miR-532-3p," *Minerva Medica*, vol. 112, no. 3, pp. 408–409, 2019.
- [29] Y. Li, L. Zhou, C. Lu et al., "Long non-coding RNA FAL1 functions as a ceRNA to antagonize the effect of miR-637 on the down-regulation of AKT1 in Hirschsprung's disease," *Cell Proliferation*, vol. 51, no. 5, 2018.
- [30] C. Tian, Y. Deng, Y. Jin, S. Shi, and H. Bi, "Long non-coding RNA RNCR3 promotes prostate cancer progression through targeting miR-185-5p," *American Journal of Translational Research*, vol. 10, no. 5, pp. 1562–1570, 2018.
- [31] Z. H. Wu, Y. He, D. Li et al., "Long noncoding RNA MEG3 suppressed endothelial cell proliferation and migration through regulating miR-21," *American Journal of Translational Research*, vol. 9, no. 7, pp. 3326–3335, 2017.
- [32] L. Y. Wang, L. J. Wang, and X. H. Zhang, "Knockdown of lncRNA HOXA-AS2 inhibits viability, migration and invasion of osteosarcoma cells by miR-124-3p/E2F3," *Oncotargets and Therapy*, vol. Volume 12, pp. 10851–10861, 2019.
- [33] S. Li, K. Zheng, Y. Pei, W. Wang, and X. Zhang, "Long non-coding RNA NR2F1-AS1 enhances the malignant properties of osteosarcoma by increasing forkhead box A1 expression via sponging of microRNA-483-3p," *Aging (Albany NY)*, vol. 11, no. 23, pp. 11609–11623, 2019.
- [34] X. M. Jin, B. Xu, Y. Zhang et al., "LncRNA SND1-IT1 accelerates the proliferation and migration of osteosarcoma via sponging miRNA-665 to upregulate POU2F1," *European Review for Medical and Pharmacological Sciences*, vol. 23, no. 22, pp. 9772–9780, 2019.
- [35] H. Yao, G. Hou, Q. Y. Wang, W. B. Xu, H. Q. Zhao, and Y. C. Xu, "LncRNA SPRY4-IT1 promotes progression of osteosarcoma by regulating ZEB1 and ZEB2 expression through sponging of miR-101 activity," *International Journal of Oncology*, vol. 56, no. 1, pp. 85–100, 2019.
- [36] Z. Shi, K. Wang, Y. Xing, and X. Yang, "CircNRP1 encapsulated by bone marrow mesenchymal stem cell-derived extracellular vesicles aggravates osteosarcoma by modulating the miR-532-3p/AKT3/PI3K/AKT Axis," *Frontiers in Oncology*, vol. 11, p. 658139, 2021.
- [37] C. J. Feng, H. I. So, S. Yin et al., "MicroRNA-532-3p suppresses malignant behaviors of tongue squamous cell carcinoma via regulating CCR7," *Frontiers in Pharmacology*, vol. 10, 2019.
- [38] R. Du, G. Tang, Z. Tang, and Y. Kuang, "Ectopic expression of CC chemokine receptor 7 promotes prostate cancer cells metastasis via Notch1 signaling," *Journal of Cellular Biochemistry*, vol. 120, no. 6, pp. 9639–9647, 2019.

Review Article

Tumor Necrosis Factor- α : The Next Marker of Stroke

Yimeng Xue ^{1,2}, Xianwei Zeng ³, Wen-Jun Tu ^{1,4} and Jizong Zhao ^{1,2,5,6,7}

¹Department of Neurosurgery, Beijing Tiantan Hospital, Capital Medical University, Beijing, China

²Savaid Medical School, University of Chinese Academy of Sciences, Beijing, China

³Rehabilitation Hospital of the National Research Center for Rehabilitation Technical Aids, Beijing, China

⁴Institute of Radiation Medicine, Chinese Academy of Medical Science & Peking Union Medical College, Tianjin, China

⁵Center of Stroke, Beijing Institute for Brain Disorders, Beijing, China

⁶Beijing Key Laboratory of Translational Medicine for Cerebrovascular Disease, Beijing, China

⁷China National Clinical Research Center for Neurological Diseases, Beijing, China

Correspondence should be addressed to Wen-Jun Tu; tuwenjun@irm-cams.ac.cn and Jizong Zhao; zhaojz205@163.com

Received 14 October 2021; Revised 5 January 2022; Accepted 19 February 2022; Published 27 February 2022

Academic Editor: Shih-Ping Hsu

Copyright © 2022 Yimeng Xue et al. This is an open access article distributed under the Creative Commons Attribution License, which permits unrestricted use, distribution, and reproduction in any medium, provided the original work is properly cited.

Although there is no shortage of research on the markers for stroke, to our knowledge, there are no clear markers that can meet the needs of clinical prediction and treatment. The inflammatory cascade is a critical process that persists and functions throughout the stroke process, ultimately worsening stroke outcomes and increasing mortality. Numerous inflammatory factors, including tumor necrosis factor (TNF), are involved in this process. These inflammatory factors play a dual role during stroke, and their mechanisms are complex. As one of the representatives, TNF is the primary regulator of the immune system and plays an essential role in the spread of inflammation. In researches done over the last few years, tumor necrosis factor- α (TNF- α) has emerged as a potential marker for stroke because of its essential role in stroke. This review summarizes the latest research on TNF- α in stroke and explores its potential as a therapeutic target.

1. Introduction

Stroke is the leading cause of death and long-term disability worldwide, and its incidence is increasing at younger ages [1, 2]. The high mortality and disability rates place a severe burden on society [3, 4]. Thus, the search for biomarkers that can predict disease prognosis or targeted therapy is significant to improve the treatment and reduce the disability rate [5]. However, there are no specific markers that can provide predictive and therapeutic information as far as we know. Previous studies by Simats et al. have summarized the role of inflammatory biomarkers in helping predict outcomes in stroke patients which may even become therapeutic targets [6]. The inflammatory response process runs through the entire stroke course [7]. In this cascade of inflammatory changes, cytokines like interleukin (IL), TNF, and interferon (IFN) act as central mediators in the inflammatory cascade and are considered as a therapeutic target and prognostic biomarker [8]. The researchers observed changes in the con-

centrations of several types of these cytokines in the cerebrospinal fluid and blood of stroke patients, and these changes were associated with prognosis [9–12]. TNF- α is an emerging molecule that is a kind of pleiotropic cytokine as the primary regulatory factor of the immune system that can be produced by a variety of cell types and is involved in a wide range of pathological processes [13, 14]. It plays a homeostasis and pathophysiological role in the central nervous system. Under pathological conditions, microglia release large amounts of TNF- α , which is a crucial component of the neuroinflammatory response associated with various neurological diseases [15]. Based on several robust pieces of evidence, changes in TNF- α were associated with stroke injury and stroke recovery [16–18]. For example, Tuttolomondo et al. reported that TNF- α expression was elevated after stroke, which stimulated the expression of tissue factors and leukocyte adhesion molecules and inhibited the fibrinolytic system [19]. Although several studies have reported contrary results, the use of TNF- α as a marker of stroke remains

promising. In addition to the role of TNF- α in stroke, anti-TNF- α -based antistroke therapies have received increasing attention from the researchers. In a preclinical study, TNF- α receptor inhibitors reduce brain damage by reducing inflammatory responses in a rat model of ischemic stroke [20]. Therefore, this article reviews the research progress of TNF- α and its antagonists and discusses its application prospect in the treatment of stroke.

2. TNF- α Molecule and Its Receptor

TNF- α is produced by various cells, but its primary source is the cells of the immune system, such as macrophages, lymphoid cells, and mast cells [14, 21]. In these cells, TNF- α is first synthesized into transmembrane protein (tmTNF- α), which is then cleaved by matrix metalloproteinase TNF- α -converting enzyme (TACE) to release soluble TNF- α (sTNF- α) homotrimer and can bind to two types of receptors, namely, TNF receptor (TNFR) type 1 (TNFR1) and type 2 (TNFR2) [15, 21–23]. These two receptors are expressed differently in various cells and differ functionally [24]. Unlike TNFR1, which is ubiquitously expressed in all cell types, TNFR2 is expressed by some immune cells and preferentially by some Treg cells, some endothelial cells, and nerve tissue cells [13, 25]. The TNF-signaling complex structure enables TNF- α to induce inflammation and cell death or to induce tolerance to ischemia after stroke [26]. The main role of TNFR1 is to initiate apoptosis through its death domain and also to induce cell survival mechanisms [27]. Activation of the TNFR2 pathway by TNF- α contributes to immune response and inflammation [28]. It can affect the activation of many intracellular signaling pathways and ultimately lead to cell survival, cell migration, apoptosis, and necrosis (Figure 1) [29–31].

Although TNF- α has a higher affinity for TNFR2 than for TNFR1, most of the biological activities of TNF- α are initiated by TNFR1 [32]. The structure of TNFR1 includes a death domain (DD), which is constitutively expressed in most cell types and is activated by TNF- α in the form of membrane binding (mTNF- α) or soluble (sTNF- α) [33]. Activation of TNFR1 leads to trimer formation, which promotes DD recruitment of TNFR1-associated death domains (TRADD), and TRADD further recruits serine/threonine-protein kinase (RIPK) and TNFR-associated factor (TRAF) 2 [34–36]. The specific process can be described as TNFR1 binds to trimer TNF- α to release death domain silencer (SODD) protein. The TNFR-associated death domain (TRADD) binds to the TNFR1 death domain (DD) and recruits adapter protein receptor-interacting protein (RIP), TNFR-associated factor 2 (TRAF2), and Fas-associated death domain (FADD). When TNFR1 signals apoptosis, FADD binds to procaspase-8 and activates it, eventually initiating the protease cascade reaction. Activation of endonuclease (such as EndoG) mediates DNA breakage and leads to apoptosis. When TNFR1 signals survival, TRAF2 is recruited to the complex, inhibiting apoptosis by cytoplasmic apoptotic protein inhibitor (cIAP). Activation of TRAF2 results in activation of cFos/cJun transcription factors through mitogen-activated protein kinase (MAPK) and cJun

N-terminal kinase (JNK) [37, 38]. The TNFR1 core signaling complex is thus formed and stabilized by RIPK1 ubiquitination, which ultimately mediates a cellular response. For example, cytokine signaling and cell survival are induced by activation of the NF- κ B, JNK, and p38 pathways [39, 40]. The apoptotic pathway would be activated in the absence of complete ubiquitination of RIPK1, leading to cell apoptosis or necrosis [41].

TNFR2 has no dead domain and is only fully activated by mTNF- α [42]. TNFR2 forms trimer and directly recruits TRAF2, TRAF1, or TRAF3 [43]. The nuclear factor kappa-light chain enhancer (NF- κ B), Akt (protein kinase B), and mitogen-activated protein kinase (MAPK) of B cells are then activated to initiate their biological function [44, 45]. For example, it promotes cell activation, migration, and proliferation; plays a protective role in cells; affects the amplification and function of Treg; and also mediates apoptosis through its cooperation with TNFR1 [45–47].

3. Physiological Role of TNF- α Molecule in the Central Nervous System

In the adult brain, TNF is mainly derived from glia, astrocytes, and microglia, and its levels are low, but its role in the central nervous system (CNS) is complex and multipotent [48–50]. First, TNF- α regulates normal neurotransmitter processes in different ways. For example, it not only can induce a rapid increase in AMPA receptors but also can decrease AMPAR levels in cortical surface and hippocampal neurons (a process achieved in the striatum through the elimination of Ca²⁺ permeability inhibition) and enhance tetrodotoxin insensitive Na⁺ channel currents in the plasma membrane of dorsal root ganglion (DRG) neurons. Furthermore, it also regulates the release of glutamate by astrocytes [51–57]. Second, TNF- α plays a dual role in neurogenesis through different inductive environments and receptor subtypes [58]. For example, TNF- α can cause progenitor cell death by abruptly stopping cell division [59]. It exerts neuroprotective effects when it binds to TNFR2 receptors expressed by human neural stem cells [60]. Third, TNF- α can affect endothelial cells in CNS. These pathways include influencing the morphology of endothelial cells, thereby affecting BBB permeability, enhancing the adhesion between leukocytes and endothelial cells, thereby facilitating leukocyte migration to the central nervous system and inducing angiogenic mediators that affect vascular endothelial cells proliferation [61–63].

4. TNF- α in Stroke

The etiology of vascular lesions is obviously redox reaction and stress-dependent [64]. In stroke, neurovascular units can become dysfunctional due to the lack of oxygen and nutrients [65]. During ischemia, changes in the brain include the release of glutamate, the production of reactive oxygen species (ROS) that cause oxidative stress, and activation of microglia, which can affect the secretion of proinflammatory mediators [66, 67]. Oxidative stress and inflammatory response have bidirectional effects on the

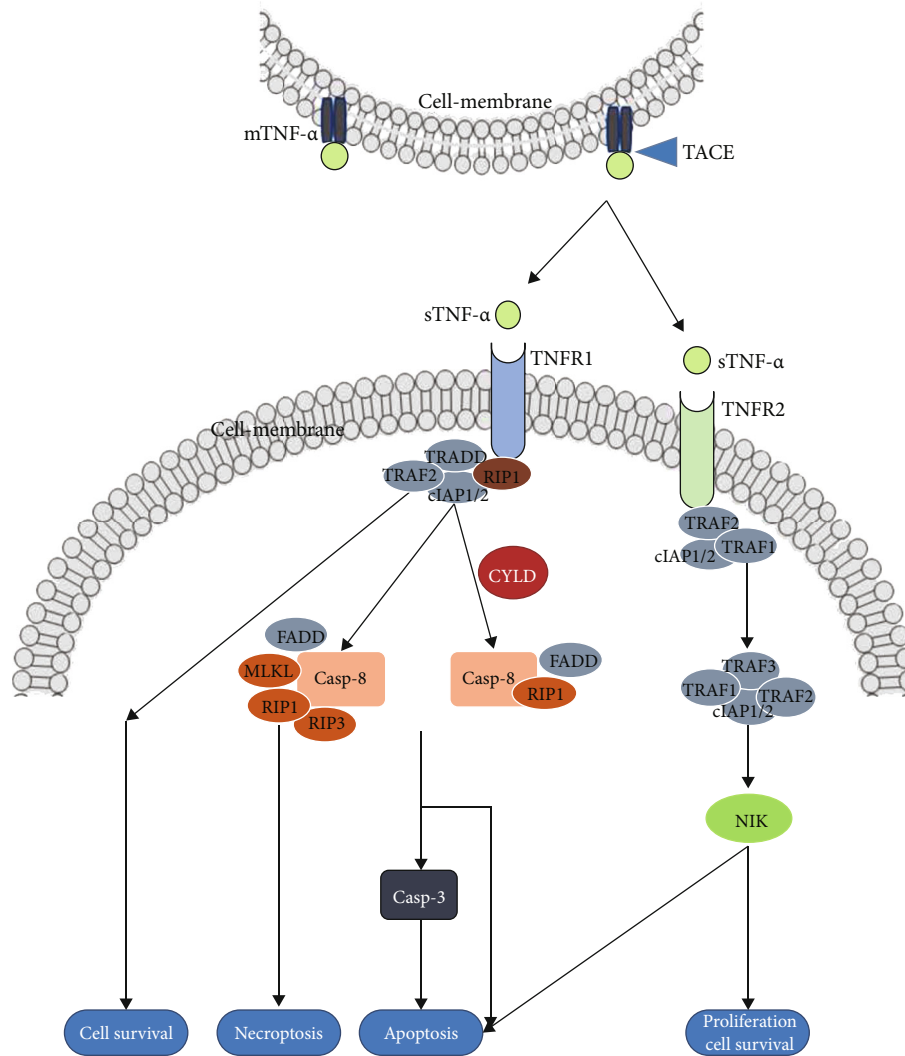


FIGURE 1: TNF- α binds to receptors and affects intracellular signal transduction. MTNF- α is hydrolyzed and cleaved by TACE to produce STNF- α . STNF- α binds to TNFR1 and TNFR2 through different signaling pathways, ultimately leading to a series of outcomes, including necrosis, apoptosis, survival, and proliferation.

whole stroke process. When blood vessels are occluded or underperfused, the immune response begins near the ischemic parenchyma and then extends to the ischemic zone, eventually spreading throughout the body, and microglia are activated and promote the release of TNF- α [68, 69]. Studies have shown that levels of TNF- α in brain tissue may continue to rise 1 day after ischemic injury and correlate with their severity [70, 71]. TNF- α is a core mediator in the immune processes of infection control, autoimmunity, allergic diseases, and antitumor activity [15]. The mechanism of TNF- α 's influence on vascular endothelium includes stimulating the expression of tissue factors and leukocyte adhesion molecules, activating matrix metalloproteinases, and producing oxidative stress through xanthine oxidase [61, 72]. These actions trigger local segments of blood vessels and lead to local inflammation, thrombosis, and bleeding [73]. Other studies have shown that TNF- α can disrupt the protective barrier between brain circulation. These effects include, first, stimulating the activation and proliferation of

astrocytes and microglia and, second, regulating apoptosis factors, such as cysteine. Third, matrix metalloproteinase (MMP) transcription is induced in ischemia and penumbra inflammation. The last induced transcription of cytokines, such as IL-1 and IL-6 [74–77]. In addition, TNF can also induce ischemia tolerance and regulate the signal transduction of cerebral hypoxia and ischemia tolerance [78, 79]. In stroke outcomes, TNF- α is associated with epileptic seizures, movement disorders, spasms, aphasia, pain, depression, and cognitive impairment [80–83]. Zaremba et al. found that the level of TNF- α in cerebrospinal fluid (CSF) was significantly increased in stroke patients, and the increase of CSF and SERUM TNF- α in the first 24 hours of stroke was also significantly associated with the severity of a neurological stroke and the degree of dysfunction according to SSS and BI scores [84]. However, in a clinical study, the researchers found that the level of TNF- α was not associated with functional outcomes after acute stroke [85]. We speculate that this is because of how TNF- α plays

TABLE 1: Current research reports on use of TNF inhibitors in stroke.

Drug name	Drug type	Research type	Describe	Ref.	Year
R-7050	TNF- α receptor inhibitors	Preclinical	Using a rat model of permanent cerebral ischemia, pretreatment with R-7050 offered protection against poststroke neurological deficits, brain infarction, edema, oxidative stress, and caspase 3 activations.	[20]	2021
Adalimumab	TNF- α -neutralizing antibody	Preclinical	Older animals treated with adalimumab show a tendency to reduce poststroke defects and improve survival in older animals after stroke.	[92]	2021
Infliximab	TNF- α inhibitor	Preclinical	Improving stroke outcomes in a mouse model of rheumatoid arthritis.	[18]	2019
Alpha-lipoic acid and etanercept	Free radical scavenger/TNF- α inhibitor	Preclinical	By inhibiting peripheral TNF- α and downregulating microglia activation, it has protective effect on ischemic stroke rats.	[99]	2015
Infliximab and etanercept	TNF- α inhibitor	Preclinical	Compared with untreated rats, the volume of cerebral infarction was significantly reduced in the etanercept or infliximab group.	[86]	2015
Etanercept	TNF- α inhibitor	Preclinical	Decreased middle cerebral artery remodeling but increased cerebral ischemia injury in hypertensive rats.	[100]	2014
CNTO5048	TNF- α antibody	Preclinical	In a mouse model of intracerebral hemorrhage, posttraumatic treatment with CNTO5048 reduced neuroinflammation and improved functional outcomes.	[101]	2013
Etanercept	TNF- α inhibitor	Clinical	Perispinal administration of etanercept improves clinical symptoms in patients with chronic neurological dysfunction following stroke and traumatic brain injury.	[102]	2012
CTfRMAB-TNFR	Fusion protein	Preclinical	CTfRMAB-TNFR fusion protein treatment can reduce hemispheric, cortical, and subcortical stroke volume and neurological deficits and prevent stroke.	[103]	2012

a role in stroke prognosis, which is complex and diverse, and these specific mechanisms need to be further investigated. Doll et al. reviewed several preclinical and clinical studies suggesting that TNF- α has neurotoxic or neuroprotective effects in stroke. There were also conflicting findings when TNF- α was used to predict prognosis. These seem to indicate that the action of TNF- α is complex and bidirectional [26]. Because TNF- α ligand-receptor interactions are involved in almost every aspect of stroke-induced brain injury, it is a promising direction to use TNF- α as an inflammatory marker to predict the outcome of stroke. On the other hand, when TNF- α is used as a potential therapeutic target for stroke, blocking TNF- α can reduce focal ischemic injury and improve clinical outcomes [83, 86].

5. TNF- α Inhibitors

Ischemic stroke is a catastrophic disease. Unfortunately, because of the limited time window for treatment, only a small number of patients receive tissue plasminogen activator (tPA), which is the primary treatment; as a result, most patients receive only supportive care [6, 26]. It is urgent to renew the therapeutic drugs in the clinic. The positive effects of treatment targeting TNF- α in stroke have been demonstrated in preclinical studies over the past few years (Table 1). There are three effective ways to interfere with TNF- α action by blocking receptors, interfering with TNF- α signal transduction, and removing TNF- α protein in effectors [87]. Currently, TNF- α inhibitors, including enanercept, infliximab, adalimumab, pertuzumab, and golimumab, are mainly used to treat autoimmune diseases or inflammatory

diseases [87–89]. Intraventricular injection of TNFR1 decoy receptors or anti-TNF- α antibodies, as well as systemic injection of TACE inhibitors, can reduce ischemic brain damage in stroke [90, 91]. After injecting TNF- α receptor inhibitor R-7050 into stroke rats, Lin et al. found that R-7050 reversed neuronal changes, TNF- α receptor/NF- κ B inflammatory signaling, and BBB destruction and ultimately reduced the area of cerebral infarction [20]. In another study, in older animals, mice treated with adalimumab (TNF- α -inhibiting antibody) reduced poststroke defects and improved poststroke survival [92]. When the preclinical experiment is transformed into clinical application, the researchers must overcome the adverse reactions. These include the most worrisome severe infections, malignancies, heart failure, and nerve demyelination, as well as other general side effects, such as headache, rash, anemia, pharyngitis, diarrhea, nausea, and abdominal pain [88, 93, 94]. Finally, the safety of anti-TNF- α agents during pregnancy or lactation needs to be further explored [88]. In the meantime, the researchers are still working to develop other types of inhibitors to improve stroke outcomes. For example, the IL-2/IL-2R antibody complex enhances Treg-induced neuroprotective effects by inhibiting TNF- α induced inflammation [95]. Contreras et al. proposed that the trimer TNF-R2 extracellular domain might be an innovative TNF- α antagonist [96]. Targeting P2X4 receptors improves postcentral stroke pain through the TNF- α /TNFR1/GABAAR pathway [97]. Given the fact that TNF- α inhibitors are less effective at penetrating BBB, the researchers are also looking for new types of inhibitors that can more easily move through BBB and act more effectively in the damaged areas [98].

These emerging studies provide new research ideas for anti-TNF- α treatment of stroke.

6. Conclusion

In conclusion, although some current studies do not support TNF- α as a clear marker of stroke, we still believe that it is desirable to focus on TNF- α in the following studies, considering that TNF- α is involved in the occurrence, development, and prognosis of stroke and has an indicative effect on the disease. Therefore, it is a promising research direction to use TNF- α as a biomarker of stroke development process or prognosis. At the same time, anti-TNF- α therapy can reduce brain damage in stroke, and it is also worth exploring as a therapeutic target. To make TNF- α be a reliable marker of stroke, the specific role and mechanism it plays in stroke, the protective effect and mechanism of anti-TNF- α treatment against brain injury, and how to reduce the side effects of antibodies are the primary issues that need to be further studied and solved by the researchers. There is a reason to believe that the next marker of stroke is on the horizon with the ongoing research.

Data Availability

Please contact the corresponding author (Pro. Tu) for the data request.

Ethical Approval

Ethical approval is not applicable.

Consent

Consent is not applicable.

Conflicts of Interest

The authors have no conflict of interest relevant to this study.

Acknowledgments

This study was supported by grants from the China Postdoctoral Science Foundation (Nos. 2019M660921 and 2020T130436); Science Foundation for Post Doctorate Research of the Beijing (Nos. 2017-ZZ-123 and 2020-ZZ-005); and Natural Science Foundation of Tianjin (No. 19JCYBJC26600).

References

- [1] E. J. Benjamin, P. Muntner, A. Alonso et al., "Heart disease, and stroke statistics-2019 update: a report from the American Heart Association," *Circulation*, vol. 139, no. 10, pp. e56–e528, 2019.
- [2] C. O. Johnson, M. Nguyen, G. A. Roth et al., "Global, regional, and national burden of stroke, 1990-2016: a systematic analysis for the Global Burden of Disease Study 2016," *The Lancet Neurology*, vol. 18, no. 5, pp. 439–458, 2019.
- [3] M. Tsalta-Mladenov and S. Andonova, "Health-related quality of life after ischemic stroke: impact of sociodemographic and clinical factors," *Neurological Research*, vol. 43, no. 7, pp. 553–561, 2021.
- [4] W. J. Tu, B. H. Chao, L. Ma et al., "Case-fatality, disability and recurrence rates after first-ever stroke: a study from bigdata observatory platform for stroke of China," *Brain Research Bulletin*, vol. 175, pp. 130–135, 2021.
- [5] S. Dolati, J. Soleymani, S. Kazem Shakouri, and A. Mobed, "The trends in nanomaterial-based biosensors for detecting critical biomarkers in stroke," *Clinica Chimica Acta*, vol. 514, pp. 107–121, 2021.
- [6] A. Simats, T. García-Berrocso, and J. Montaner, "Neuroinflammatory biomarkers: from stroke diagnosis and prognosis to therapy," *Biochimica et Biophysica Acta*, vol. 1862, no. 3, pp. 411–424, 2016.
- [7] J. Faura, A. Bustamante, F. Miró-Mur, and J. Montaner, "Stroke-induced immunosuppression: implications for the prevention and prediction of post-stroke infections," *Journal of Neuroinflammation*, vol. 18, no. 1, pp. 127–127, 2021.
- [8] M. Teymuri Kheravi, S. Nayebifar, S. M. Aletaha, and S. Sarhadi, "The effect of two types of exercise preconditioning on the expression of TrkB, TNF- α , and MMP2 genes in rats with stroke," *BioMed Research International*, vol. 2021, Article ID 5595368, 7 pages, 2021.
- [9] E. Tarkowski, L. Rosengren, C. Blomstrand et al., "Early intrathecal production of interleukin-6 predicts the size of brain lesion in stroke," *Stroke*, vol. 26, 8 pages, 1995.
- [10] K. Fassbender, S. Rossol, T. Kammer et al., "Proinflammatory cytokines in serum of patients with acute cerebral ischemia: kinetics of secretion and relation to the extent of brain damage and outcome of disease," *Journal of the Neurological Sciences*, vol. 122, no. 2, pp. 135–139, 1994.
- [11] N. Vila, J. Castillo, A. Dávalos, and A. Chamorro, "Proinflammatory cytokines and early neurological worsening in ischemic stroke," *Stroke*, vol. 31, no. 10, pp. 2325–2329, 2000.
- [12] N. Vila, J. Castillo, A. Dávalos, A. Esteve, A. M. Planas, and A. Chamorro, "Levels of anti-inflammatory cytokines and neurological worsening in acute ischemic stroke," *Stroke*, vol. 34, no. 3, pp. 671–675, 2003.
- [13] X. Cheng, Y. Shen, and R. Li, "Targeting TNF: a therapeutic strategy for Alzheimer's disease," *Drug Discovery Today*, vol. 19, no. 11, pp. 1822–1827, 2014.
- [14] B. B. Aggarwal, "Tumour necrosis factors receptor associated signalling molecules and their role in activation of apoptosis, JNK and NF-kappaB," *Annals of the Rheumatic Diseases*, vol. 59, no. 90001, 2000.
- [15] G. Olmos and J. Lladó, "Tumor necrosis factor alpha: a link between neuroinflammation and excitotoxicity," *Mediators of Inflammation*, vol. 2014, Article ID 861231, 12 pages, 2014.
- [16] R. Fischer and O. Maier, "Interrelation of oxidative stress and inflammation in neurodegenerative disease: role of TNF," *Oxidative Medicine and Cellular Longevity*, vol. 2015, Article ID 610813, 18 pages, 2015.
- [17] F. C. Barone, B. Arvin, R. F. White et al., "Tumor necrosis factor- α ," *Stroke*, vol. 28, no. 6, pp. 1233–1244, 1997.
- [18] N. R. Bonetti, C. Diaz-Cañestro, L. Liberale et al., "Tumour necrosis factor- α inhibition improves stroke outcome in a mouse model of rheumatoid arthritis," *Scientific Reports*, vol. 9, no. 1, p. 2173, 2019.

- [19] A. Tuttolomondo, D. di Raimondo, R. di Sciacca, A. Pinto, and G. Licata, "Inflammatory cytokines in acute ischemic stroke," *Current Pharmaceutical Design*, vol. 14, no. 33, pp. 3574–3589, 2008.
- [20] S.-Y. Lin, Y. Y. Wang, C. Y. Chang et al., "TNF- α receptor inhibitor alleviates metabolic and inflammatory changes in a rat model of ischemic stroke," *Antioxidants*, vol. 10, no. 6, p. 851, 2021.
- [21] G. Epstein Shochet, E. Brook, L. Israeli-Shani, E. Edelstein, and D. Shitrit, "Fibroblast paracrine TNF- α signaling elevates integrin A5 expression in idiopathic pulmonary fibrosis (IPF)," *Respiratory Research*, vol. 18, no. 1, p. 122, 2017.
- [22] R. C. Bates and A. M. Mercurio, "Tumor necrosis factor- α stimulates the epithelial-to-mesenchymal transition of human colonic organoids," *Molecular Biology of the Cell*, vol. 14, no. 5, pp. 1790–1800, 2003.
- [23] C. R. Engwerda, M. Ato, S. Stäger, C. E. Alexander, A. C. Stanley, and P. M. Kaye, "Distinct roles for lymphotoxin- α and tumor necrosis factor in the control of Leishmania donovani infection," *The American Journal of Pathology*, vol. 165, no. 6, pp. 2123–2133, 2004.
- [24] B. B. Aggarwal, "Signalling pathways of the TNF superfamily: a double-edged sword," *Nature Reviews Immunology*, vol. 3, no. 9, pp. 745–756, 2003.
- [25] X. Chen, M. Bäumel, D. N. Männel, O. M. Z. Howard, and J. J. Oppenheim, "Interaction of TNF with TNF receptor type 2 promotes expansion and function of mouse CD4+CD25+ T regulatory cells," *Journal of Immunology*, vol. 179, no. 1, pp. 154–161, 2007.
- [26] D. N. Doll, T. L. Barr, and J. W. Simpkins, "Cytokines: their role in stroke and potential use as biomarkers and therapeutic targets," *Aging and Disease*, vol. 5, no. 5, pp. 294–306, 2014.
- [27] R. van Horssen, T. L. Ten Hagen, and A. M. Eggermont, "TNF- α in cancer treatment: molecular insights, antitumor effects, and clinical utility," *The Oncologist*, vol. 11, no. 4, pp. 397–408, 2006.
- [28] D. Laha, R. Grant, P. Mishra, and N. Nilubol, "The role of tumor necrosis factor in manipulating the immunological response of tumor microenvironment," *Frontiers in Immunology*, vol. 12, article 656908, 2021.
- [29] C. F. Ware, "Network communications: lymphotoxins, LIGHT, and TNF," *Annual Review of Immunology*, vol. 23, no. 1, pp. 787–819, 2005.
- [30] M. K. McCoy and M. G. Tansey, "TNF signaling inhibition in the CNS: implications for normal brain function and neurodegenerative disease," *Journal of Neuroinflammation*, vol. 5, no. 1, pp. 45–45, 2008.
- [31] S. Harashima, T. Horiuchi, N. Hatta et al., "Outside-to-inside signal through the membrane TNF- α induces E-selectin (CD62E) expression on activated human CD4+ T cells," *Journal of Immunology*, vol. 166, no. 1, pp. 130–136, 2001.
- [32] L. A. Tartaglia and D. V. Goeddel, "Two TNF receptors," *Immunology Today*, vol. 13, no. 5, pp. 151–153, 1992.
- [33] O. A. Diaz Arguello and H. J. Haisma, "Apoptosis-inducing TNF superfamily ligands for cancer therapy," *Cancers*, vol. 13, no. 7, 2021.
- [34] D. W. Banner, A. D'Arcy, W. Janes et al., "Crystal structure of the soluble human 55 kd TNF receptor-human TNF beta complex: implications for TNF receptor activation," *Cell*, vol. 73, no. 3, pp. 431–445, 1993.
- [35] H. Hsu, H. B. Shu, M. G. Pan, and D. V. Goeddel, "TRADD-TRAF2 and TRADD-FADD interactions define two distinct TNF receptor 1 signal transduction pathways," *Cell*, vol. 84, no. 2, pp. 299–308, 1996.
- [36] H. Hsu, J. Huang, H. B. Shu, V. Baichwal, and D. V. Goeddel, "TNF-dependent recruitment of the protein kinase RIP to the TNF receptor-1 signaling complex," *Immunity*, vol. 4, no. 4, pp. 387–396, 1996.
- [37] H. B. Shu, M. Takeuchi, and D. V. Goeddel, "The tumor necrosis factor receptor 2 signal transducers TRAF2 and c-IAP1 are components of the tumor necrosis factor receptor 1 signaling complex," *Proceedings of the National Academy of Sciences of the United States of America*, vol. 93, no. 24, pp. 13973–13978, 1996.
- [38] J. E. Vince, D. Pantaki, R. Feltham et al., "TRAF2 must bind to cellular inhibitors of apoptosis for tumor necrosis factor (tnf) to efficiently activate nf- κ b and to prevent tnf-induced apoptosis," *The Journal of Biological Chemistry*, vol. 284, no. 51, pp. 35906–35915, 2009.
- [39] C. Dostert, M. Grusdat, E. Letellier, and D. Brenner, "The TNF family of ligands and receptors: communication modules in the immune system and beyond," *Physiological Reviews*, vol. 99, no. 1, pp. 115–160, 2019.
- [40] T. L. Haas, C. H. Emmerich, B. Gerlach et al., "Recruitment of the linear ubiquitin chain assembly complex stabilizes the TNF-R1 signaling complex and is required for TNF-mediated gene induction," *Molecular Cell*, vol. 36, no. 5, pp. 831–844, 2009.
- [41] P. Gough and I. A. Myles, "Tumor necrosis factor receptors: pleiotropic signaling complexes and their differential effects," *Frontiers in Immunology*, vol. 11, article 585880, 2020.
- [42] D. Faustman and M. Davis, "TNF receptor 2 pathway: drug target for autoimmune diseases," *Nature Reviews Drug Discovery*, vol. 9, no. 6, pp. 482–493, 2010.
- [43] Y. Mukai, T. Nakamura, M. Yoshikawa et al., "Solution of the structure of the TNF-TNFR2 complex," *Science Signaling*, vol. 3, no. 148, 2010.
- [44] S. Yang, J. Wang, D. D. Brand, and S. G. Zheng, "Role of TNF-TNF receptor 2 signal in regulatory T cells and its therapeutic implications," *Frontiers in Immunology*, vol. 9, pp. 784–784, 2018.
- [45] Y. Sheng, F. Li, and Z. Qin, "TNF receptor 2 makes tumor necrosis factor a friend of tumors," *Frontiers in Immunology*, vol. 9, pp. 1170–1170, 2018.
- [46] S. Ahmad, N. A. Azid, J. C. Boer et al., "The key role of TNF-TNFR2 interactions in the modulation of allergic inflammation: a review," *Frontiers in Immunology*, vol. 9, pp. 2572–2572, 2018.
- [47] J. Medler and H. Wajant, "Tumor necrosis factor receptor-2 (TNFR2): an overview of an emerging drug target," *Expert Opinion on Therapeutic Targets*, vol. 23, no. 4, pp. 295–307, 2019.
- [48] L. M. Boulanger, "Immune proteins in brain development and synaptic plasticity," *Neuron*, vol. 64, no. 1, pp. 93–109, 2009.
- [49] J. L. Flynn, M. M. Goldstein, J. Chan et al., "Tumor necrosis factor- α is required in the protective immune response against mycobacterium tuberculosis in mice," *Immunity*, vol. 2, no. 6, pp. 561–572, 1995.
- [50] D. Fresegna, S. Bullitta, A. Musella et al., "Re-examining the role of TNF in MS pathogenesis and therapy," *Cell*, vol. 9, no. 10, p. 2290, 2020.

- [51] M. Lewis, L. A. Tartaglia, A. Lee et al., "Cloning and expression of cDNAs for two distinct murine tumor necrosis factor receptors demonstrate one receptor is species specific," *Proceedings of the National Academy of Sciences of the United States of America*, vol. 88, no. 7, pp. 2830–2834, 1991.
- [52] D. Stellwagen and R. C. Malenka, "Synaptic scaling mediated by glial TNF- α ," *Nature*, vol. 440, no. 7087, pp. 1054–1059, 2006.
- [53] E. C. Beattie, D. Stellwagen, W. Morishita et al., "Control of synaptic strength by glial TNF α ," *Science*, vol. 295, no. 5563, pp. 2282–2285, 2002.
- [54] F. Ogoshi, H. Z. Yin, Y. Kuppumbatti, B. Song, S. Amindari, and J. H. Weiss, "Tumor necrosis-factor-alpha (TNF- α) induces rapid insertion of Ca²⁺-permeable α -amino-3-hydroxyl-5-methyl-4-isoxazole-propionate (AMPA)/kainate (Ca-A/K) channels in a subset of hippocampal pyramidal neurons," *Experimental Neurology*, vol. 193, no. 2, pp. 384–393, 2005.
- [55] P. He, Q. Liu, J. Wu, and Y. Shen, "Genetic deletion of TNF receptor suppresses excitatory synaptic transmission via reducing AMPA receptor synaptic localization in cortical neurons," *The FASEB Journal*, vol. 26, no. 1, pp. 334–345, 2012.
- [56] G. Perea, M. Navarrete, and A. Araque, "Tripartite synapses: astrocytes process and control synaptic information," *Trends in Neurosciences*, vol. 32, no. 8, pp. 421–431, 2009.
- [57] X. Jin and Gereau RW 4th, "Acute p38-mediated modulation of tetrodotoxin-resistant sodium channels in mouse sensory neurons by tumor necrosis factor-alpha," *The Journal of Neuroscience*, vol. 26, no. 1, pp. 246–255, 2006.
- [58] S. L. Montgomery and W. J. Bowers, "Tumor necrosis factor-alpha and the roles it plays in homeostatic and degenerative processes within the central nervous system," *Journal of Neuroimmune Pharmacology*, vol. 7, no. 1, pp. 42–59, 2012.
- [59] E. Cacci, J. H. Claassen, and Z. Kokaia, "Microglia-derived tumor necrosis factor-alpha exaggerates death of newborn hippocampal progenitor cells In Vitro," *Journal of Neuroscience Research*, vol. 80, no. 6, pp. 789–797, 2005.
- [60] U. Heldmann, P. Thored, J. H. Claassen, A. Arvidsson, Z. Kokaia, and O. Lindvall, "TNF- α antibody infusion impairs survival of stroke-generated neuroblasts in adult rat brain," *Experimental Neurology*, vol. 196, no. 1, pp. 204–208, 2005.
- [61] J. S. Pober and R. S. Cotran, "Cytokines and endothelial cell biology," *Physiological Reviews*, vol. 70, no. 2, pp. 427–451, 1990.
- [62] N. Sato, T. Goto, K. Haranaka et al., "Actions of tumor necrosis factor on cultured vascular endothelial cells: morphologic modulation, growth inhibition, and cytotoxicity," *Journal of the National Cancer Institute*, vol. 76, no. 6, pp. 1113–1121, 1986.
- [63] W. Pan, J. E. Zadina, R. E. Harlan, W. TJO, W. A. Banks, and A. J. Kastin, "Tumor necrosis factor- α : a neuromodulator in the CNS," *Neuroscience and Biobehavioral Reviews*, vol. 21, no. 5, pp. 603–613, 1997.
- [64] M. Maciejczyk, M. Bielas, A. Zalewska, and K. Gerreth, "Salivary biomarkers of oxidative stress and inflammation in stroke patients: from basic research to clinical practice," *Oxidative Medicine and Cellular Longevity*, vol. 2021, Article ID 5545330, 22 pages, 2021.
- [65] G. J. del Zoppo, "Stroke and neurovascular protection," *The New England Journal of Medicine*, vol. 354, no. 6, pp. 553–555, 2006.
- [66] U. Dirnagl, C. Iadecola, and M. A. Moskowitz, "Pathobiology of ischaemic stroke: an integrated view," *Trends in Neurosciences*, vol. 22, no. 9, pp. 391–397, 1999.
- [67] J. T. Coyle and P. Puttfarcken, "Oxidative stress, glutamate, and neurodegenerative disorders," *Science*, vol. 262, no. 5134, pp. 689–695, 1993.
- [68] X. Zhou, F. Yu, X. Feng et al., "Immunity and inflammation predictors for short-term outcome of stroke in young adults," *The International Journal of Neuroscience*, vol. 128, no. 7, pp. 634–639, 2018.
- [69] B. H. Clausen, M. Degn, N. A. Martin et al., "Systemically administered anti-TNF therapy ameliorates functional outcomes after focal cerebral ischemia," *Journal of Neuroinflammation*, vol. 11, no. 1, p. 203, 2014.
- [70] T. Liu, R. K. Clark, P. C. McDonnell et al., "Tumor necrosis factor-alpha expression in ischemic neurons," *Stroke*, vol. 25, no. 7, pp. 1481–1488, 1994.
- [71] J. Zaremba and J. Losy, "Early TNF-alpha levels correlate with ischaemic stroke severity," *Acta Neurologica Scandinavica*, vol. 104, no. 5, pp. 288–295, 2001.
- [72] K. S. Mark, W. J. Trickler, and D. W. Miller, "Tumor necrosis factor-alpha induces cyclooxygenase-2 expression and prostaglandin release in brain microvessel endothelial cells," *The Journal of Pharmacology and Experimental Therapeutics*, vol. 297, no. 3, pp. 1051–1058, 2001.
- [73] J. M. Hallenbeck, "The many faces of tumor necrosis factor in stroke," *Nature Medicine*, vol. 8, no. 12, pp. 1363–1368, 2002.
- [74] N. Badiola, C. Malagelada, N. Llecha et al., "Activation of caspase-8 by tumour necrosis factor receptor 1 is necessary for caspase-3 activation and apoptosis in oxygen-glucose deprived cultured cortical cells," *Neurobiology of Disease*, vol. 35, no. 3, pp. 438–447, 2009.
- [75] C. C. Hughes, D. K. Male, and P. L. Lantos, "Adhesion of lymphocytes to cerebral microvascular cells: effects of interferon-gamma, tumour necrosis factor and interleukin-1," *Immunology*, vol. 64, no. 4, pp. 677–681, 1988.
- [76] H. Loppnow and P. Libby, "Proliferating or interleukin 1-activated human vascular smooth muscle cells secrete copious interleukin 6," *The Journal of Clinical Investigation*, vol. 85, no. 3, pp. 731–738, 1990.
- [77] V. W. Yong, C. Power, P. Forsyth, and D. R. Edwards, "Metalloproteinases in biology and pathology of the nervous system," *Nature Reviews. Neuroscience*, vol. 2, no. 7, pp. 502–511, 2001.
- [78] H. Nawashiro, K. Tasaki, C. A. Ruetzler, and J. M. Hallenbeck, "TNF-alpha pretreatment induces protective effects against focal cerebral ischemia in mice," *Journal of Cerebral Blood Flow and Metabolism*, vol. 17, no. 5, pp. 483–490, 1997.
- [79] B. Cheng, S. Christakos, and M. P. Mattson, "Tumor necrosis factors protect neurons against metabolic-excitotoxic insults and promote maintenance of calcium homeostasis," *Neuron*, vol. 12, no. 1, pp. 139–153, 1994.
- [80] M. Liang, L. Zhang, and Z. Geng, "Advances in the development of biomarkers for poststroke epilepsy," *BioMed Research International*, vol. 2021, Article ID 5567046, 8 pages, 2021.
- [81] Y. Chen, J. Pu, Y. Liu et al., "Pro-inflammatory cytokines are associated with the development of post-stroke depression in

- the acute stage of stroke: a meta-analysis," *Topics in Stroke Rehabilitation*, vol. 27, no. 8, pp. 620–629, 2020.
- [82] M. A. Grigolashvili and R. M. Mustafina, "The role of the inflammatory process in the development of post-stroke cognitive impairment," *Zh Nevrol Psikhiatr Im S S Korsakova*, vol. 121, no. 3, pp. 16–21, 2021.
- [83] E. Tobinick, N. M. Kim, G. Reyzin, H. Rodriguez-Romanace, and V. DePuy, "Selective TNF inhibition for chronic stroke and traumatic brain injury," *CNS Drugs*, vol. 26, no. 12, pp. 1051–1070, 2012.
- [84] J. Zaremba and J. Losy, "Early TNF- α levels correlate with ischaemic stroke severity," *Acta Neurologica Scandinavica*, vol. 104, no. 5, pp. 288–295, 2001.
- [85] H. Flores-Cantú, F. Góngora-Rivera, F. Lavalle-González et al., "Tumor necrosis factor alpha, prognosis and stroke subtype etiology," *Medicina Universitaria*, vol. 18, no. 73, pp. 194–200, 2016.
- [86] C. A. Arango-Dávila, A. Vera, A. C. Londoño et al., "Soluble or soluble/membrane TNF- \pm inhibitors protect the brain from focal ischemic injury in rats," *The International Journal of Neuroscience*, vol. 125, no. 12, pp. 936–940, 2015.
- [87] A. K. Frankola, H. N. Greig, W. Luo, and D. Tweedie, "Targeting TNF-Alpha to elucidate and ameliorate neuroinflammation in neurodegenerative diseases," *CNS & Neurological Disorders Drug Targets*, vol. 10, no. 3, pp. 391–403, 2011.
- [88] V. Gerriets, P. Bansal, A. Goyal, and K. Khaddour, *Tumor necrosis factor inhibitors*, StatPearls Publishing LLC., Treasure Island (FL), 2021.
- [89] D. H. Present, P. Rutgeerts, S. Targan et al., "Infliximab for the treatment of fistulas in patients with Crohn's disease," *The New England Journal of Medicine*, vol. 340, no. 18, pp. 1398–1405, 1999.
- [90] X. Wang, G. Z. Feuerstein, L. Xu et al., "Inhibition of tumor necrosis factor- α -converting enzyme by a selective antagonist protects brain from focal ischemic injury in rats," *Molecular Pharmacology*, vol. 65, no. 4, pp. 890–896, 2004.
- [91] H. Nawashiro, D. Martin, and J. M. Hallenbeck, "Neuroprotective effects of TNF binding protein in focal cerebral ischemia," *Brain Research*, vol. 778, no. 2, pp. 265–271, 1997.
- [92] L. Liberale, N. R. Bonetti, Y. M. Puspitasari et al., "TNF- α antagonism rescues the effect of ageing on stroke: perspectives for targeting inflamm-ageing," *European Journal of Clinical Investigation*, vol. 51, no. 11, article e13600, 2021.
- [93] X. Mariette, M. Matucci-Cerinic, K. Pavelka et al., "Malignancies associated with tumour necrosis factor inhibitors in registries and prospective observational studies: a systematic review and meta-analysis," *Annals of the Rheumatic Diseases*, vol. 70, no. 11, pp. 1895–1904, 2011.
- [94] F. Wolfe and K. Michaud, "Biologic treatment of rheumatoid arthritis and the risk of malignancy: analyses from a large US observational study," *Arthritis and Rheumatism*, vol. 56, no. 9, pp. 2886–2895, 2007.
- [95] M. C. Borlongan, C. Kingsbury, F. E. Salazar et al., "IL-2/IL-2R antibody complex enhances Treg-induced neuroprotection by dampening TNF- α inflammation in an In Vitro stroke model," *Neuromolecular Medicine*, vol. 23, no. 4, pp. 540–548, 2021.
- [96] M. A. Contreras, L. Macaya, V. Manrique et al., "A trivalent TNF-R2as a new tumor necrosis factor alpha-blocking molecule," *Proteins*, vol. 89, no. 11, pp. 1557–1564, 2021.
- [97] J. Lu, X. Guo, M. Yan et al., "P2X4R contributes to central disinhibition via TNF- α /TNFR1/GABA_AR pathway in post-stroke pain rats," *The Journal of Pain*, vol. 22, no. 8, pp. 968–980, 2021.
- [98] V. Manrique-Suárez, L. Macaya, M. A. Contreras et al., "Design and characterization of a novel dimeric blood-brain barrier penetrating TNF α inhibitor," *Proteins*, vol. 89, no. 11, pp. 1508–1521, 2021.
- [99] M.-H. Wu, C. C. Huang, C. C. Chio et al., "Inhibition of peripheral TNF- α and downregulation of microglial activation by alpha-lipoic acid and etanercept protect rat brain against ischemic stroke," *Molecular Neurobiology*, vol. 53, no. 7, pp. 4961–4971, 2016.
- [100] P. W. Pires, S. S. Girgla, G. Moreno, J. L. McClain, and A. M. Dorrance, "Tumor necrosis factor- α inhibition attenuates middle cerebral artery remodeling but increases cerebral ischemic damage in hypertensive rats," *American Journal of Physiology. Heart and Circulatory Physiology*, vol. 307, no. 5, pp. H658–H669, 2014.
- [101] B. Lei, H. N. Dawson, B. Roulhac-Wilson, H. Wang, D. T. Laskowitz, and M. L. James, "Tumor necrosis factor alpha antagonism improves neurological recovery in murine intracerebral hemorrhage," *Journal of Neuroinflammation*, vol. 10, no. 1, 2013.
- [102] E. Tobinick, N. M. Kim, G. Reyzin, H. Rodriguez-Romanace, and V. DePuy, "Selective TNF inhibition for chronic stroke and traumatic brain injury: an observational study involving 629 consecutive patients treated with perispinal etanercept," *CNS Drugs*, vol. 26, no. 12, pp. 1051–1070, 2012.
- [103] R. K. Sumbria, R. J. Boado, and W. M. Pardridge, "Brain protection from stroke with intravenous TNF α decoy receptor-Trojan horse fusion protein," *Journal of Cerebral Blood Flow and Metabolism*, vol. 32, no. 10, pp. 1933–1938, 2012.

Research Article

Intraoperative Use of Topical Retropharyngeal Steroids for Dysphagia after Anterior Cervical Fusion: A Systematic Review and Meta-Analysis

Hang Yu ^{1,2}, Hui Dong ^{2,3}, Binjia Ruan ^{2,3}, Xiaohang Xu ^{1,2} and Yongxiang Wang ²

¹Clinical Medical College of Yangzhou University, Yangzhou, China

²Northern Jiangsu People's Hospital Affiliated to Yangzhou University, Yangzhou, China

³The Yangzhou School of Clinical Medicine of Dalian Medical University, Yangzhou, China

Correspondence should be addressed to Yongxiang Wang; wyx918spine@126.com

Received 4 November 2021; Accepted 14 December 2021; Published 31 December 2021

Academic Editor: Wen-Jun Tu

Copyright © 2021 Hang Yu et al. This is an open access article distributed under the Creative Commons Attribution License, which permits unrestricted use, distribution, and reproduction in any medium, provided the original work is properly cited.

Purpose. The anterior cervical approach is commonly used clinically for cervical spondylosis, but it also results in frequent postoperative dysphagia, which can increase the risk of complications and poor treatment satisfaction in severe cases. Intraoperative local application of retropharyngeal steroids has an impact on reducing the occurrence and severity of dysphagia; however, the results of current studies vary. The meta-analysis of this randomized trial was to evaluate the effectiveness and safety of intraoperative topical retropharyngeal steroids for the control of dysphagia after anterior cervical spine surgery. **Methods.** Two authors searched electronic databases such as PubMed, MEDLINE, EMBASE, Cochrane Library, and Google Scholar, respectively. The search terms were “Dysphagia,” “Steroids,” “Anterior Cervical Discectomy and Fusion,” etc. A random effects model was used to conduct a meta-analysis based on deviance information criteria. **Results.** A total of 8 studies were included in this meta-analysis after screening of 792 studies. Bazaz scores were not significantly different in the steroid group at one day postoperatively ($P = 0.38$), and dysphagia was significantly improved at 14 days postoperatively (95% CI: 0.15 to 0.64; $P = 0.002$). PSTSI was significantly improved one day ($P = 0.03$) and 14 days after surgery ($P < 0.0001$). VAS scores were all lower versus controls ($P < 0.001$). **Conclusion.** Perioperative local retropharyngeal steroid administration as an adjunct to anterior cervical spine surgery reduces the incidence and severity of dysphagia compared with placebo control. However, future high-quality randomized controlled studies could incorporate nonsubjective dysphagia measures and long-term follow-up on the occurrence of associated complications or other side effects.

1. Introduction

The current standard approach for the treatment of cervical disc disease is anterior cervical spinal fusion (ACDF) using the Smith-Robinson technique. This approach is considered relatively safe and effective; however, it has been reported to be associated with complications such as dysphagia, airway damage, and vocal disturbances in up to 79% of patients [1–3]. Although the exact pathophysiological mechanism of dysphagia after anterior cervical spine surgery is not fully understood, some studies have been proposed that it may be the effect of local soft-tissue edema, paralysis of the recurrent laryngeal nerve, or prevertebral soft-tissue swelling (PSTS)

[4–6]. Severe dysphagia after ACDF has been demonstrated to lead to malnutrition, aspiration, increased risk of pulmonary complications, and increased medical costs [7].

To reduce the incidence and severity of dysphagia, steroids are often used in clinical practice. Corticosteroids are known anti-inflammatory agents that inhibit the production of inflammatory prostaglandins and cytokines. This inflammatory process is responsible for the swelling of the soft tissues, which eventually leads to compression of the esophagus and trachea. Several studies have shown that the use of systemic corticosteroids after anterior cervical spine surgery is beneficial in reducing the incidence and severity of dysphagia [8–10]. While these results are encouraging,

systemic administration of corticosteroids is also associated with systemic side effects; this may be a limitation of this route of administration. For this reason, the efficacy of topical application of corticosteroids to the retropharyngeal space for anterior cervical fusion has been investigated. However, the reported results are not the same [11, 12], and the association between local application of corticosteroids on postoperative tissue swelling and dysphagia has not been well described. Therefore, to provide clear and uniform conclusions using the best available evidence, a systematic review and meta-analysis of randomized controlled trials was conducted. The primary and secondary objectives of this study were to determine whether the intraoperative application of topical corticosteroids in anterior cervical surgery has substantial clinical benefit in reducing the severity of dysphagia and identify any clinically relevant complications associated with corticosteroid therapy.

2. Materials and Methods

The study was conducted following the guidelines outlined in the PRISMA (preferred reporting items for systematic reviews and meta-analysis) statement [13]. The data included in this study are from published studies and are not directly relevant to the patients. Therefore, ethics committee approval and informed consent were not required.

2.1. Identification of Studies. A comprehensive literature search was conducted, to identify all published studies evaluating the efficacy of topically applied corticosteroids for anterior cervical fusion. Two independent reviewers conducted a systematic electronic search of PubMed, MEDLINE, EMBASE, the Cochrane Library, and Google Scholar. The search date is from the beginning to June 31, 2021. The keywords used for the search are “Dysphagia,” “Deglutition Disorders,” “Swallowing Disorders,” “Steroids,” “Cervical Vertebrae,” “Anterior Cervical Discectomy and Fusion,” “ACDF” and their near synonyms, etc. There are no restrictions based on publication date, language, or follow-up.

2.2. Assessment of Eligibility. The following criteria were used for study inclusion: (1) adult patients with cervical spondylosis undergoing single- or multilevel anterior decompression-only fusion; (2) perioperative topical corticosteroids, placebo in the control group, and no other interventions for dysphagia; and (3) RCT design.

The exclusion criteria are as follows: (1) trials that explicitly include cases of trauma, tumor, or infection; (2) abstracts, letters, or conference proceedings; and (3) studies for which no extractable data are available.

2.3. Selection of Literature. It was filtered by scanning the titles of each study to filter out inappropriate articles. An independent reviewer then reviewed the abstracts of the remaining studies and selected those that were potentially relevant to our study. Two authors independently reviewed the full text of these articles as well as the references for additional research. We then critically evaluated the studies according to the inclusion and exclusion criteria and

assessed the quality of the randomized controlled trials according to the suggested checklist. All differences were resolved by consensus through discussion and further confirmed by a third author.

2.4. Assessment of Risk of Bias and Data Extraction. Study quality was assessed using version 2 of the Cochrane Risk of Bias Tool for Randomized Trials (RoB 2). Two reviewers applied all criteria to each study independently, using a uniform methodology. Clinical outcome data from individual studies were independently extracted into spreadsheets by 2 reviewers and reviewed against the original information to avoid errors. Data extracted from the study included identifiers, study characteristics, patient demographics, interventions, surgical data, perioperative PSTS, clinical dysphagia outcomes, visual analog scale (VAS), and complications, and disagreements were resolved through discussion and negotiation. PSTS is measured as the ratio of the measured anterior soft-tissue thickness of the vertebral body to the anterior-posterior (AP) diameter of each vertebral body. To compare the overall PSTS of the two groups, the mean PSTS at C3, 4, and 5 where edema was observed to be most pronounced was defined as the prevertebral soft-tissue swelling index (PSTSI). PSTSI eliminates interindividual differences, such as vertebral width or any other abnormalities in the cervical or retropharyngeal space, facilitating comparisons with other postoperative patients as well as with the patients themselves [14, 15].

2.5. Statistical Analysis. The meta-analysis was analyzed using Review Manager 5.3 (RevMan 5.3. Ink, Cochrane Collaboration, Oxford, United Kingdom). The I^2 statistic (ranging from 0 to 100%) was used to quantify the heterogeneity between studies. I^2 values $>50\%$ indicate significant heterogeneity, and random effects analysis was used to compare heterogeneous results. There is likely to be a high degree of heterogeneity between different randomized controlled trials due to clinical and methodological factors. Thus, even if I^2 is small, the random effects model is applicable to the entire meta-analysis. Continuous variables are reported as mean differences and 95% confidence intervals, such as time to surgery, and dichotomous variables (e.g., complications) are reported as risk ratios and 95% confidence intervals; P value < 0.05 was considered to indicate a significant difference. Funnel plots were performed to assess publication bias.

3. Results

3.1. Search Results. The flowchart of the search is shown in Figure 1. The search yielded 792 studies, of which 39 were duplicates. 742 studies were excluded based on title, abstract, and full-text screening, leaving 12 possible articles. Three other studies were excluded after full-text review because they did not use topical steroids or were not RCTs. Of the nine articles included, all were eligible for the meta-analysis. These studies included a total of 632 patients, of which 327 constituted the topical steroid group and the placebo group consisted of the remaining 305 patients. Table 1 summarizes the characteristics of the eight included articles.

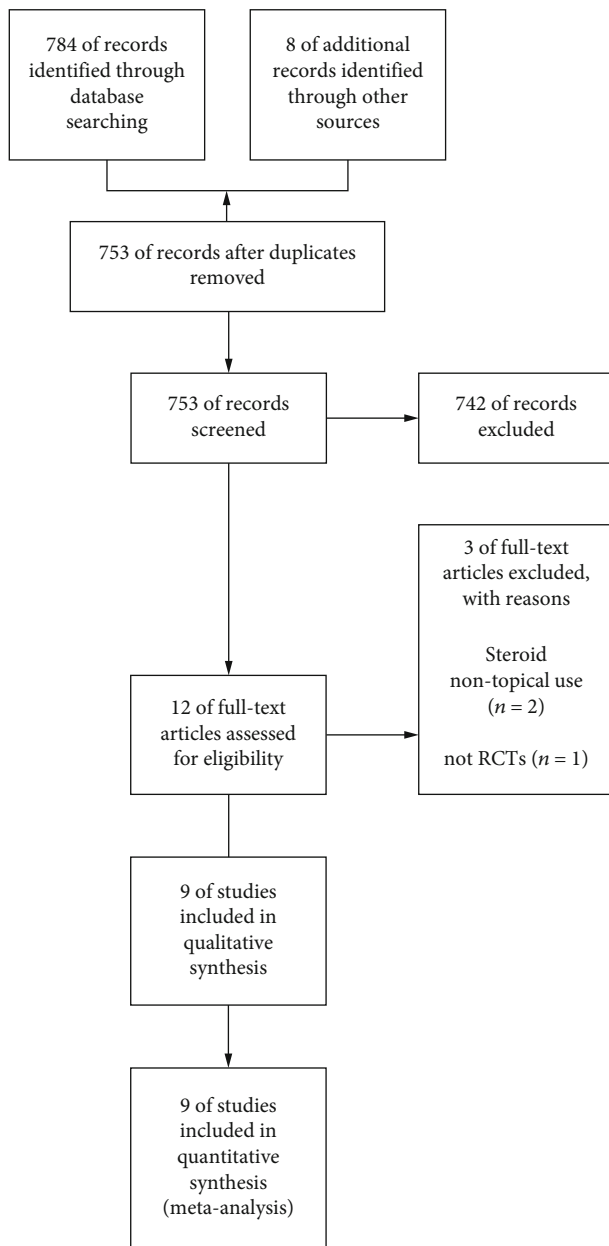


FIGURE 1: PRISMA flowchart for the literature search.

3.2. Risk of Bias. The Cochrane risk of bias assessment for RCTs is shown in Figure 2. Two studies were found to have a “high” risk of bias, primarily attributable to the randomization process and outcome measures. For all studies, we used the modified Jadad scale to evaluate the qualities of them, where 3-5 scores mean high quality and 0-2 scores mean low quality. For quality assessment, all studies included in our research were of high quality [22] (Table 2).

3.3. Primary Outcome. In this series, the most commonly used tool for assessing dysphagia is the Bazaz scale [20, 21, 23] or its modified version, the Modified Dysphagia Scoring System (MDSS) [18, 19]. The Bazaz scale and MDSS have 4 levels: none, mild, moderate, and severe. Meta-analysis of the Bazaz scale of dysphagia showed no significant difference

on the postoperative day ($P = 0.38$); however, at 2 weeks postoperatively, the overall incidence and severity of dysphagia were significantly lower in the patients in the topical steroid group than in the control group ($P = 0.002$) (Figure 3). Meta-analysis showed statistically significantly lower PSTSI in the topical steroid group than in the control group both one day after surgery and 2 weeks after surgery (1 day, $P = 0.03$ and 2 weeks, $P < 0.0001$) (Figure 4).

3.4. Secondary Outcome. A total of five studies reported VAS scores at the follow-up time points. VAS scores were significantly lower in the topical steroid group than in the control group one day postoperatively ($I^2 = 38\%$, $P < 0.0001$) versus 2 weeks postoperatively ($I^2 = 72\%$, $P = 0.002$) (Figure 5).

3.5. Publication Bias and Sensitivity Analysis. We performed funnel plotting of the postoperative Bazaz score as well as the PSTSI, and the funnel plot shows a symmetric distribution (Figures 6 and 7). Although the statistical power was limited by the total number of studies, no significant bias was found.

To determine the effect of each study on postoperative Bazaz scores, postoperative PSTSI, and VAS scores, we perform a sensitivity analysis to verify the robustness of our results. No significant effect on the results was observed after excluding any single study, suggesting that the results of this meta-analysis are relatively robust.

4. Discussion

ACDF is an effective treatment for degenerative cervical spine disease when nonsurgical treatment has failed. Despite the clinical success of ACDF, postoperative problems may arise that the most common is dysphagia, the prevalence of which can be as high as 79%. Our meta-analysis of 632 patients in eight randomized trials found that topical steroids significantly reduced the occurrence and severity of dysphagia and improved neck pain after ACDF surgery. This is similar to the results of two previous systematic reviews and a meta-analysis [24–26]; they support the use of steroids to prevent dysphagia in patients undergoing anterior cervical fusion surgery. However, they included studies that also included systemic intravenous application of steroid hormones. Considering that topically applied steroids have a lower risk of systemic reactions or complications, our study compared the efficacy of topical steroid application with placebo control only. However, on the first postoperative day, there was no significant difference in the incidence of dysphagia between the two groups of patients. It is likely that the initial dysphagia on the first postoperative day is more of a mechanistic effect caused by the inherent manipulation of the esophagus by surgery [19], rather than due to swelling or inflammation, as the swelling of the anterior neck tissue gradually increases in the days following the procedure. And the topical application of steroids is a combination of steroids with gelatin sponges, which may delay the distribution and action of the drug, thus preventing any apparent effect on the first postoperative day [17]. There are no

TABLE 1: Baseline characteristics of studies included in the systematic review.

Study (year)	Experimental data			Control data			Outcomes recorded	Follow-up (month)
	Patients	Mean age (yr)	Male (%)	Patients	Mean age (yr)	Male (%)		
Dahapute 2020 [15]	25	50.4	76	25	50.4	76	PSTS, VAS, NDI	12
Ryan 2021 [16]	37	59	41	36	57	50	Bazaz, EAT-10	3
Kim 2021 [17]	56	58.1	48.2	53	58.4	54.7	EAT-10, SWAL-QOL, VAS, NDI	1
Haws 2018 [12]	55	49.4	56.4	49	50.6	61.2	PSTS, SWAL-QOL, VAS	3
Jekins 2018 [18]	29	55.6	51.7	21	54	52.3	Bazaz, EAT-10, VAS neck pain, NDI	12
Edwards 2016 [19]	27	54	41	23	54.5	39	Modified Dysphagia Scoring System	1
Lee 2011 [11]	25	54.3	72	25	50.9	56	PSTS, VAS, NDI	22
Seddighi 2017 [20]	38	49.3	47.3	38	50.2	42.1	Bazaz, PSTS, VAS	6
Grasso 2019 [21]	35	46.1	51.4	35	45.5	48.5	Bazaz, VAS	12

	Random sequence generation (selection bias)	Allocation concealment (selection bias)	Blinding of participants and personnel (performance bias)	Blinding of outcome assessment (detection bias)	Incomplete outcome data (attrition bias)	Selective reporting (reporting bias)	Other bias
Dahapute 2020	+	+	+	+	+	?	?
Edwards 2016	+	+	+	+	?	+	-
grasso 2019	?	?	?	+	+	?	?
Haws 2018	+	+	+	+	+	+	+
Jekins 2018	+	+	+	+	?	+	?
Kim 2021	+	+	+	+	+	?	?
Lee 2011	+	?	-	?	+	?	?
Ryan 2021	+	+	+	+	+	+	?
Seddighi 2017	+	?	?	+	?	+	?

FIGURE 2: Risk-of-bias assessment.

studies examining the exact pharmacokinetics of this route and method of administration [16].

The prevertebral soft tissues observed on a lateral radiograph consist of the muscles, ligaments, and cervical fascia of the pharynx or esophagus. Dissecting and stretching them during ACDF, edematous and inflammatory changes occur which leads to muscle and subperiosteal hemorrhage and soft-tissue swelling, resulting in the development of PSTS [27]. Dysphagia is common after ACDF surgery, and several studies have shown that the occurrence and severity of post-operative dysphagia are related to the degree of PSTS. Related reports indicate that the most severe PSTS occurs around the C4 vertebral body [14], and this is consistent with the findings of Suk et al. Therefore, the mean value of PSTS at C3, 4, and 5 (PSTSI) was used as the standardized comparison parameter. This meta-analysis found that topical steroid hormone application reduced the degree of PSTSI in patients on the first postoperative day, and at the second postoperative week, the PSTSI values were significantly lower in the steroid group compared to the control group. The incidence of painful dysphagia immediately after surgery was significantly lower in the steroid group than in the control group, and recovery was also faster; this is attributed to the control of the local inflammatory response by steroids and the subsequent reduction of the PSTS effect.

Esophageal perforation, one of the most dreaded complications of ACDF, has an incidence of 0.02% to 1.52% [28]. Topical steroids, on the other hand, increase the chance of perforation because they may reduce the ability of soft tissues to heal on their own. Only one study in this analysis reported 2 cases of delayed esophageal perforation [11]; they cautioned against the use of topical retropharyngeal steroids in patients with a long history of chronic steroid application. Corticosteroids reduce inflammation by decreasing neutrophil adhesion to the vascular endothelium and inhibit macrophages by limiting chemotaxis, phagocytosis, and cytokine release. However, while steroids suppress inflammation, they also increase the risk of infection. Dahapute et al.'s study

TABLE 2: Results of equality evaluation of included trials.

Study (year)	Random sequence generation	Allocation concealment	Blindness	Withdrawal and lost visits	Modified Jadad scale
Dahapute 2020	Random grouping	Appropriate	Appropriate	Describe	7
Ryan 2021	Random grouping	Appropriate	Appropriate	Describe	7
Kim 2021	Random grouping	Appropriate	Appropriate	Describe	7
Haws 2018	Random grouping	Appropriate	Appropriate	Describe	7
Jekins 2018	Random grouping	Appropriate	Appropriate	Unclear	6
Edwards 2016	Random grouping	Appropriate	Appropriate	Unclear	6
Lee 2011	Random grouping	Unclear	Unclear	Describe	5
Seddighi 2017	Random grouping	Unclear	Unclear	Unclear	4
Grasso 2019	Random grouping	Unclear	Unclear	Unclear	4

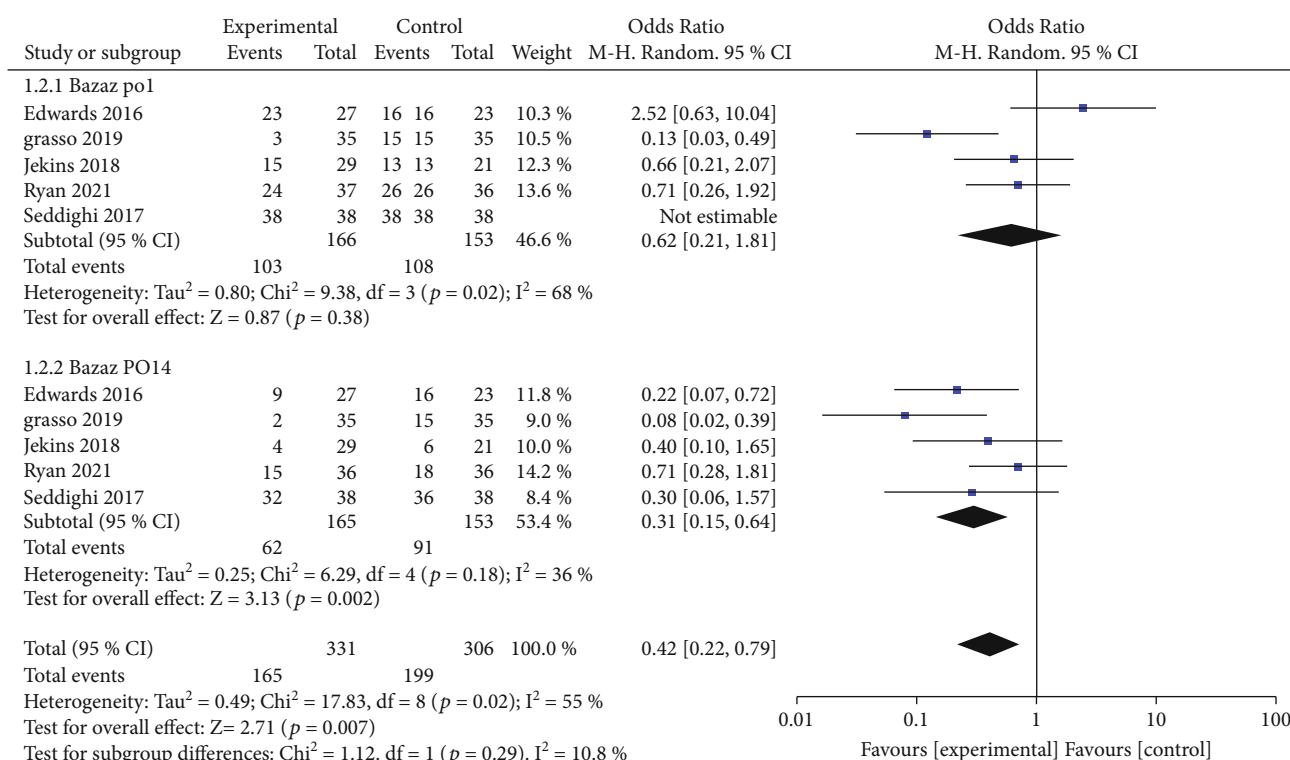


FIGURE 3: Primary outcome on the first postoperative day. Bazaz assessed no significant difference in the incidence and severity of dysphagia between the two groups. However, the steroid group was significantly lower than the control group at 14 days postoperatively. PO: postoperative.

showed that there were no significant differences in postoperative inflammatory indicators of white blood cell count and CPR between the two groups, and one case of infection was reported in the placebo group. Corticosteroids can promote apoptosis of osteoblasts and bone cells, which may affect bone healing as well as increase the risk of prosthetic joints. In this meta-analysis, although some studies reported cases of postoperative pseudarthrosis, but at subsequent follow-up, there were signs of bone nonunion in both groups, while excluding the possibility of a significant effect of steroids on bone healing [15]. However, this result should be interpreted with caution, because two of the eight studies did not report infection rates and four did not report pseu-

darthrosis rates. It is possible that the distant adverse effects and complications of steroids were not captured due to the short follow-up period.

The current study observed some limitations. Given the variation in the types and doses of steroids used in each study, we are unable to provide information on the best treatment regimen for reducing the rate and severity of postoperative dysphagia after ACDF, and better treatment doses may exist. We suggest that a relevant randomized controlled trial could be conducted to find the best clinical treatment option to reduce postoperative dysphagia using different types and different doses of topical steroids. Currently, one of the challenges in evaluating dysphagia is that there is no

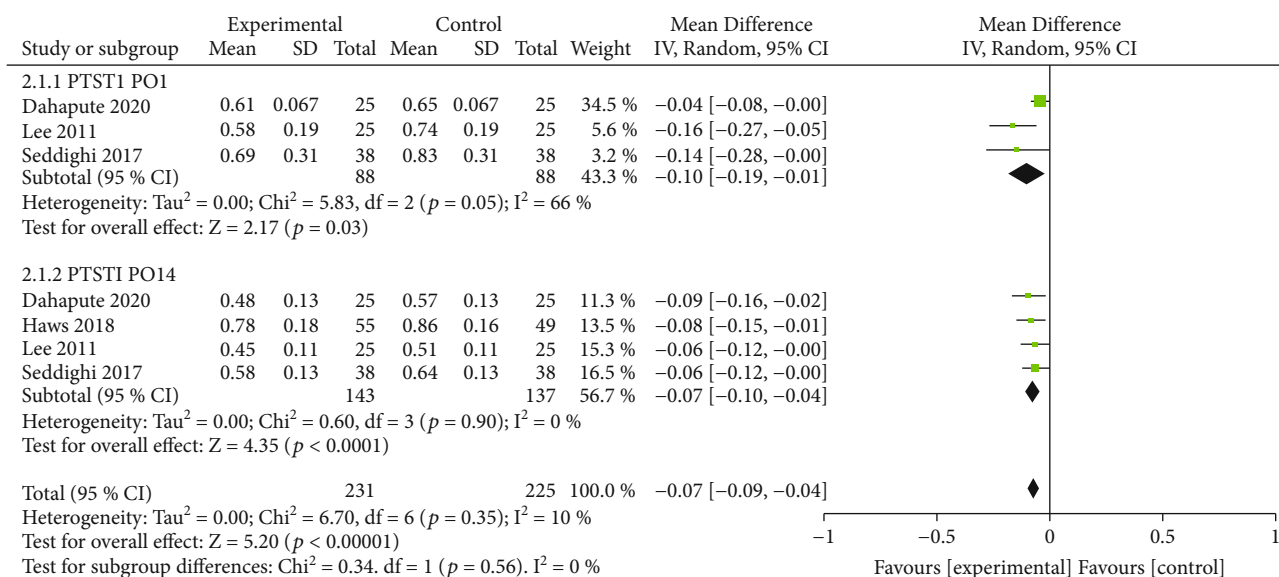


FIGURE 4: PSTSI was significantly different in the steroid group on the first postoperative day and on postoperative day 14.

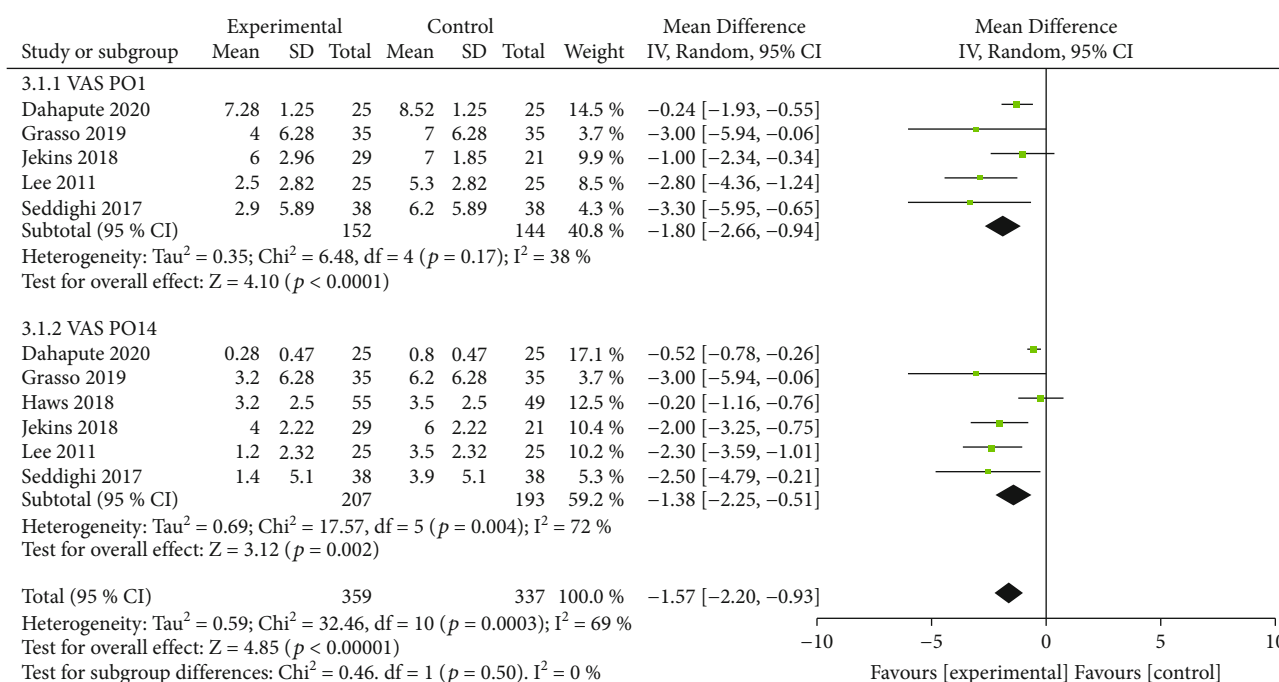


FIGURE 5: Secondary outcome VAS scores was significantly lower in the steroid group than in the control group on both postoperative day 1 and day 14.

“gold standard” outcome indicator. Therefore, the included studies took different outcome scores for the postoperative dysphagia measure, so comparable data were not available for some of the studies, which may have biased the results. Also, differences in the design, definition, and outcome measures of studies of postoperative dysphagia in ACDF may be one reason for the wide variation in reported prevalence. Although relevant patient-centered dysphagia questionnaires and indicators have been validated, there is a subjective component to patient response, and more invasive

modalities such as barium swallow tests and video laryngeal endoscopy can eliminate this subjective factor. In addition, the greatest change in dysphagia severity in the included study population appeared to occur in the first 2 weeks postoperatively. However, incidence and severity were measured only a small number of times during this period, thus obscuring the exact onset and duration of postoperative dysphagia that may be reduced by topical steroids in patients undergoing ACDF surgery. In the included studies, the short- to medium-term follow-up may have missed the time

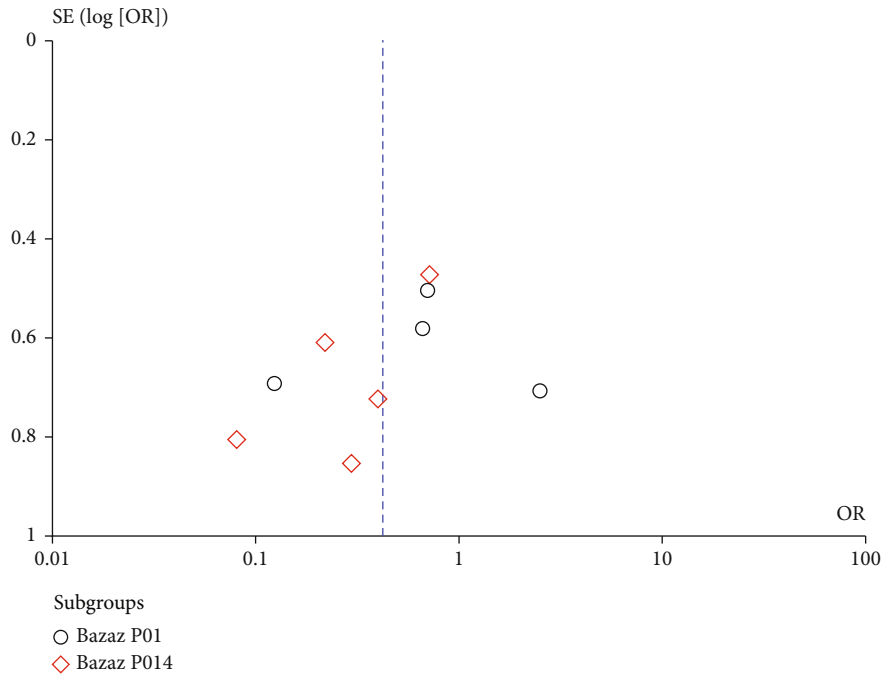


FIGURE 6: Funnel plot of the Bazaz scores.

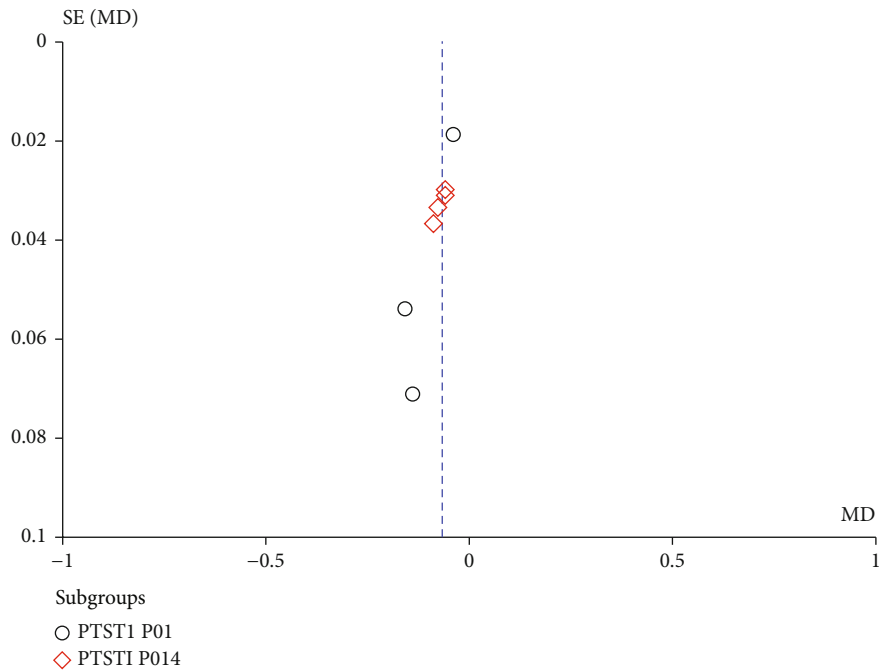


FIGURE 7: Funnel plot of the PSTSI.

to maximum benefit for patients, as well as long-term outcome indicators, including fusion rates. However, we can say with confidence that the use of topically applied steroids is effective and does not significantly increase the risk of complications. But the differences between the included studies make it difficult to provide clear and specific recommendations. Therefore, future studies could include nonsubjective measures of dysphagia, more frequent documentation

of patient-reported dysphagia, larger study populations, subgroup analyses, and cost-effectiveness analyses of intraoperative steroid use to reduce dysphagia after ACDF surgery.

5. Conclusion

This meta-analysis found moderate-quality evidence supporting perioperative topical steroid administration as an

adjunct to anterior cervical spine surgery to reduce the incidence and severity of dysphagia compared with placebo. Future high-quality randomized comparative effectiveness trials are assured.

Abbreviations

ACDF: Anterior cervical spinal fusion
 PSTS: Prevertebral soft-tissue swelling
 PSTSI: Prevertebral soft-tissue swelling index
 MDSS: Modified Dysphagia Scoring System.

Data Availability

The data supporting this meta-analysis are from previously reported studies and datasets, which have been cited. The processed data are available from the corresponding author upon request.

Conflicts of Interest

The authors have no relevant financial or nonfinancial interests to disclose.

Authors' Contributions

Hang Yu and Hui Dong contributed equally to this work and should be considered as co-first authors. Hang Yu contributed to research design, acquisition of data, analysis and interpretation of data, and writing—original draft. Hui Dong contributed to acquisition of data, analysis and interpretation of data, and writing—original draft. Binjia Ruan and Xiaohang Xu contributed to acquisition of data, analysis and interpretation of data, and methodology. Yongxiang Wang contributed to conceptualization, research design, revision, and supervision.

Acknowledgments

This study was supported by the National Natural Science Foundation of China (82072423).

References

- [1] C. A. Smith-Hammond, K. C. New, R. Pietrobon, D. J. Curtis, C. H. Scharver, and D. A. Turner, "Prospective analysis of incidence and risk factors of dysphagia in spine surgery patients: comparison of anterior cervical, posterior cervical, and lumbar procedures [J]," *Spine (Phila Pa 1976)*, vol. 29, no. 13, pp. 1441–1446, 2004.
- [2] K. K. Anderson and P. M. Arnold, "Oropharyngeal dysphagia after anterior cervical spine surgery: a review [J]," *Global Spine J*, vol. 3, no. 4, pp. 273–285, 2013.
- [3] P. G. Campbell, S. Yadla, J. Malone et al., "Early complications related to approach in cervical spine surgery: single-center prospective study [J]," *World Neurosurgery*, vol. 74, no. 2-3, pp. 363–368, 2010.
- [4] N. Nagoshi, L. Tetreault, H. Nakashima et al., "Risk factors for and clinical outcomes of dysphagia after anterior cervical surgery for degenerative cervical myelopathy: results from the AOSpine International and North America Studies [J]," *The Journal of Bone and Joint Surgery. American Volume*, vol. 99, no. 13, pp. 1069–1077, 2017.
- [5] M. J. Lee, R. Bazaz, C. G. Furey, and J. Yoo, "Risk factors for dysphagia after anterior cervical spine surgery: a two-year prospective cohort study [J]," *The Spine Journal*, vol. 7, no. 2, pp. 141–147, 2007.
- [6] L. H. Riley 3rd, R. L. Skolasky, T. J. Albert, A. R. Vaccaro, and J. G. Heller, "Dysphagia after anterior cervical decompression and Fusion," *Spine (Phila Pa 1976)*, vol. 30, no. 22, pp. 2564–2569, 2005.
- [7] H. M. Starmer, L. H. Riley 3rd, A. T. Hillel, L. M. Akst, S. R. A. Best, and C. G. Gourin, "Dysphagia, short-term outcomes, and cost of care after anterior cervical disc surgery," *Dysphagia*, vol. 29, no. 1, pp. 68–77, 2014.
- [8] K. J. Song, S. K. Lee, J. H. Ko, M. J. Yoo, D. Y. Kim, and K. B. Lee, "The clinical efficacy of short-term steroid treatment in multilevel anterior cervical arthrodesis [J]," *The Spine Journal*, vol. 14, no. 12, pp. 2954–2958, 2014.
- [9] S. B. Jeyamohan, T. J. Kenning, K. A. Petronis, P. J. Feustel, D. Drazin, and D. J. DiRisio, "Effect of steroid use in anterior cervical discectomy and fusion: a randomized controlled trial [J]," *Journal of Neurosurgery. Spine*, vol. 23, no. 2, pp. 137–143, 2015.
- [10] M. Pedram, L. Castagnera, X. Carat, G. Macouillard, and J. M. Vital, "Pharyngolaryngeal lesions in patients undergoing cervical spine surgery through the anterior approach: contribution of methylprednisolone [J]," *European Spine Journal*, vol. 12, no. 1, pp. 84–90, 2003.
- [11] S. H. Lee, K. T. Kim, K. S. Suk, K. J. Park, and K. I. Oh, "Effect of retropharyngeal steroid on prevertebral soft tissue swelling following anterior cervical discectomy and fusion: a prospective, randomized study [J]," *Spine (Phila Pa 1976)*, vol. 36, no. 26, pp. 2286–2292, 2011.
- [12] B. E. Haws, B. Khechen, A. S. Narain et al., "Impact of local steroid application on dysphagia following an anterior cervical discectomy and fusion: results of a prospective, randomized single-blind trial [J]," *Journal of Neurosurgery. Spine*, vol. 29, no. 1, pp. 10–17, 2018.
- [13] D. Moher, A. Liberati, J. Tetzlaff, and D. G. Altman, "Preferred reporting items for systematic reviews and meta-analyses: the PRISMA statement [J]," *International Journal of Surgery*, vol. 8, no. 5, pp. 336–341, 2010.
- [14] K. S. Suk, K. T. Kim, S. H. Lee, and S. W. Park, "Prevertebral soft tissue swelling after anterior cervical discectomy and fusion with plate fixation [J]," *International Orthopaedics*, vol. 30, no. 4, pp. 290–294, 2006.
- [15] A. Dahapute, S. Sonone, S. Bhaladhare et al., "Prospective randomized controlled trial to study the effect of local steroids in the retropharyngeal space after anterior cervical discectomy and fusion [J]," *Global Spine J*, vol. 11, no. 6, pp. 826–832, 2021.
- [16] R. A. Curto and C. C. Edwards, "Does local steroid reduce dysphagia after cervical disc replacement? A prospective, randomized, placebo-controlled, double-blinded study [J]," *Clin Spine Surg*, vol. 34, no. 6, pp. E329–E336, 2021.
- [17] H. J. Kim, R. Alluri, D. Stein et al., "Effect of topical steroid on swallowing following ACDF: results of a prospective double-blind randomized control trial [J]," *Spine (Phila Pa 1976)*, vol. 46, no. 7, pp. 413–420, 2021.
- [18] T. J. Jenkins, R. Nair, S. Bhatt et al., "The effect of local versus intravenous corticosteroids on the likelihood of dysphagia and

- dysphonia following anterior cervical discectomy and fusion: a single-blinded, prospective, randomized controlled trial [J],” *The Journal of Bone and Joint Surgery. American Volume*, vol. 100, no. 17, pp. 1461–1472, 2018.
- [19] C. C. Edwards, C. Dean, C. C. Edwards, D. Phillips, and A. Blight, “Can dysphagia following anterior cervical fusions with rhBMP-2 be reduced with local dexamethasone Application?,” *Spine*, vol. 41, no. 7, pp. 555–562, 2016.
- [20] M. Hasani Barzi, M. Nikoobakht, N. Hasani Barzi, F. Khanali, and Z. Yazdi, “Effect of local steroid injection on prevertebral soft tissue swelling following anterior cervical discectomy and fusion [J],” *International Clinical Neuroscience Journal*, vol. 4, no. 3, pp. 84–90, 2017.
- [21] G. Grasso, L. Leone, and F. Torregrossa, “Dysphagia prevention in anterior cervical discectomy surgery: results from a prospective clinical study [J],” *World Neurosurgery*, vol. 125, p. e1176, 2019.
- [22] A. R. Jadad, R. A. Moore, D. Carroll et al., “Assessing the quality of reports of randomized clinical trials: is blinding necessary? [J],” *Controlled Clinical Trials*, vol. 17, no. 1, pp. 1–12, 1996.
- [23] R. Bazaz, M. J. Lee, and J. U. Yoo, “Incidence of dysphagia after anterior cervical spine surgery - a prospective study [J],” *Spine*, vol. 27, no. 22, pp. 2453–2458, 2002.
- [24] J. W. Liu, Y. Q. Zhang, Y. Hai, N. Kang, and B. Han, “Intravenous and local steroid use in the management of dysphagia after anterior cervical spine surgery: a systematic review of prospective randomized controlled trials (RCTs) [J],” *European Spine Journal*, vol. 28, no. 2, pp. 308–316, 2019.
- [25] S. A. Zadegan, S. B. Jazayeri, A. Abedi, H. N. Bonaki, A. R. Vaccaro, and V. Rahimi-Movaghgar, “Corticosteroid administration to prevent complications of anterior cervical spine fusion: a systematic review [J],” *Global Spine J*, vol. 8, no. 3, pp. 286–302, 2018.
- [26] S. Garcia, N. E. Schaffer, N. Wallace, B. B. Butt, J. Gagnier, and I. S. Aleem, “Perioperative corticosteroids reduce dysphagia severity following anterior cervical spinal fusion: a meta-analysis of randomized controlled trials [J],” *The Journal of Bone and Joint Surgery. American Volume*, vol. 103, no. 9, pp. 821–828, 2021.
- [27] A. Frempong-Boadu, J. K. Houten, B. Osborn et al., “Swallowing and speech dysfunction in patients undergoing anterior cervical discectomy and fusion: a prospective, objective preoperative and postoperative assessment [J],” *Journal of Spinal Disorders & Techniques*, vol. 15, no. 5, pp. 362–368, 2002.
- [28] S. H. Halani, G. R. Baum, J. P. Riley et al., “Esophageal perforation after anterior cervical spine surgery: a systematic review of the literature [J],” *Journal of Neurosurgery. Spine*, vol. 25, no. 3, pp. 285–291, 2016.

Research Article

CircLDLR Promotes Papillary Thyroid Carcinoma Tumorigenicity by Regulating miR-637/LMO4 Axis

Yuan-ming Jiang ¹, Wei Liu ¹, Ling Jiang ², and Hongbin Chang ²

¹Department of Otolaryngology, Wuhan No.1.Hospital, Wuhan 430030, China

²General Surgery, Wuhan Hanyang Hospital, Wuhan 430000, China

Correspondence should be addressed to Hongbin Chang; hongbin-chang@cug.edu.cn

Received 24 September 2021; Revised 3 November 2021; Accepted 15 November 2021; Published 9 December 2021

Academic Editor: Wen-Jun Tu

Copyright © 2021 Yuan-ming Jiang et al. This is an open access article distributed under the Creative Commons Attribution License, which permits unrestricted use, distribution, and reproduction in any medium, provided the original work is properly cited.

Background. Circular RNAs (circRNAs) have been reported to play important roles in the development and progression of papillary thyroid carcinoma (PTC). However, the function and molecular mechanism of circRNA low-density lipoprotein receptor (circLDLR) in the tumorigenesis of PTC remain unknown. **Results.** In this study, circLDLR was found to be markedly upregulated in PTC tissues and cell lines, and knockdown of circLDLR inhibited PTC cell proliferation, migration, and invasion but induced apoptosis *in vitro*. Moreover, circLDLR acted as a sponge for miR-637, and miR-637 interference reversed the anticancer effects of circLDLR knockdown on PTC cells. LMO4 was verified to be a target of miR-637; LMO4 upregulation abolished miR-637 mediated inhibition of cell growth and metastasis in PTC. Additionally, circLDLR could indirectly modulate LMO4 via acting as a sponge of miR-637 in PTC cells. Besides that, xenograft analysis showed that circLDLR knockdown suppressed tumor growth *in vivo* via regulating LMO4 and miR-637. **Conclusion.** Taken together, these results demonstrated that circLDLR promoted PTC tumorigenesis through miR-637/LMO4 axis, which may provide a novel insight into the understanding of PTC tumorigenesis and be useful in developing potential targets for PTC treatment.

1. Introduction

Thyroid cancer is the most common type of human malignancies in endocrine system and is histologically categorized into papillary, follicular, medullary, anaplastic, and poorly differentiated thyroid cancer [1, 2], among which, papillary thyroid carcinoma (PTC) is the most common type of thyroid carcinomas with a rising prevalence at an average annual rate of nearly 4% in recent years [1, 2]. Early PTC has relatively good survival, while the 5-year survival rate of PTC with advanced stage is only 59% [3]. Importantly, although great advance in the clinical treatment of PTC, including surgery and/or physiotherapy or chemotherapy, recurrence and metastasis still occurred with high rates [4]. Thus, it is of great significance to further identify the pathogenesis of PTC to develop novel effective treatments for PTC.

Circular RNAs (circRNAs) are one of stable and highly conservative noncoding RNA molecules with a covalently closed loop lacking the 5'-end cap and the 3'-end poly A tail

[5, 6]. Increasing studies have shown the involvement of circRNAs in the tumorigenesis of many types of malignancy, such as gastric cancer [7], bladder cancer [8], hepatocellular carcinoma [9], and so on. Besides, previous studies also revealed that abnormal expression of circRNAs is drawn into the initiation and progression of PTC through by affecting the malignant behaviors of cancer cells [10, 11]. Circular RNA low-density lipoprotein receptor (circLDLR, hsa_circ_0003892) is a derived from LDLR gene with the length of 544 bp; it locates at chr19: 11230767-11238761. According to the analysis of GSE93522 dataset, the expression of circLDLR was found to be aberrantly upregulated in PTC. However, the biological functions of circLDLR in the progression of PTC remain unknown.

MicroRNAs (miRNAs) are one of small noncoding RNAs and can modulate specific gene expression programs by regulating posttranslational processes [9]. miRNAs have been documented to be involved in a variety of biological functions in cancers, thus affecting tumor progression [12].

Recently, Yuan et al. demonstrated that lncRNA HOTTIP promoted PTC progression by inducing cell malignant biological behavior via targeting miR-637 [13]. However, the action and molecular mechanism of miR-637 in PTC progression remain vague. Additionally, it is well known that miRNAs commonly exert their functions through targeting 3'-UTR of their target genes [14]. LIM-only protein 4 (LMO4) is a member of LIM domain only proteins (LMOs), which belongs to a subfamily of LIM-containing proteins [15]. Previous study showed LMO4 was increased in PTC and promoted cell growth, migration, and invasion via circBACH2/miR-139-5p/LMO4 axis [16]. Thus, it is not clear whether LMO4 is involved in PTC tumorigenesis as a target of miR-637.

In this study, we investigated the function of circLDLR in PTC carcinogenesis *in vitro* and *in vivo* and evaluated whether circLDLR exerted its biological functions via circLDLR/miR-637/LMO4 in regulating cell biological behaviors of PTC.

2. Materials and Methods

2.1. Clinical Specimens. Tumor tissues and para-tumor samples were collected from 45 PTC patients in Wuhan No.1.Hospital and then immediately stored at -80°C until RNA isolation. The screening of included PTC patients was shown in Fig. S1. Follow-up was conducted regularly every 3 months in the first 2 years after surgery and reduced to every 6 months from the third year. The last follow-up was performed in April 2019. We had obtained the agreement of the Ethics Committee of Wuhan No.1.Hospital, and written informed consent was collected from all patients before this study.

2.2. Cell Culture and Transfection. Human thyroid follicular epithelial cell line Nthy-ori 3-1 and human thyroid cancer cell lines (TPC-1, IHH-4) were purchased from Shanghai Academy of Life Science (Shanghai, China) and then were grown in RPMI-1640 medium (Gibco, Carlsbad, CA, USA) in accompany with 10% fetal bovine serum (FBS, Gibco) at 37°C with 5% CO_2 .

Small interfering RNA (siRNA) sequences targeting circLDLR (si-circLDLR, 5'-GTCCTCCCCATCGGACAAA GTdtdt-3'), pcDNA3.1-circLDLR overexpression vector (circLDLR), pcDNA3.1-LIM domain only 4 (LMO4) overexpression vector (LMO4), their negative control (si-NC: 5'-TTCTCCGAACGTGTCACGT-3', circ-NC, vector), lentiviral particles stably expressing either short hairpin RNA-(shRNA-) targeting circLDLR (sh-circLDLR, 5'-CCGGT CCTCCCCATCGGACAAAGTCTC GAGACTTTGTCCGA TGGGGAGGACTTTTTG-3') or a scrambled control sequence (sh-NC, 5'-TTCTCCGAACGTGTCACGTTCAA GAGACGTGACACGTTCCGA G AATTTTTT-3') were designed and synthesized by Invitrogen (Carlsbad, CA, USA). The miR-637 mimic (sense, 5'-ACUGGGGCUU UCUGGCUCUGCGU-3, antisense, 5'-GCAGAGCCC GAA GCCCCCAGUUU-3'), miR-637 inhibitor (anti-miR-637)

(5'-ACGCAGAGC CCGAAAGCCCCAGU-3'), and their negative control (mimic control (NC): sense, 5'-UUCUCC GAACGUGUCAGUTT-3', antisense, 5-ACGUGA CAGC UUCGGAG AATT-3'; and inhibitor control (anti-NC): sense, 5'-CAGUACUU UUGUGUAGUCA A-3') were achieved by RiboBio (Guangzhou, China). The transfection was conducted using Lipofectamine 3000 (Invitrogen) for 48 h.

2.3. Quantitative Real-Time Polymerase Chain Reaction (qRT-PCR). The isolation of total RNA was performed with the help of Trizol reagent (Invitrogen). A PARIS Kit (Invitrogen) was used to define the subcellular localization of circLDLR according to the manufacturer's instructions. Complementary DNA (cDNA) generation was conducted using a High-Capacity cDNA Reverse Transcription Kit (Qiagen, Valencia, CA, USA), and then, qPCR was implemented by a miScript SYBR Green PCR Kit (Qiagen). The relative expression was detected using the $2^{-\Delta\Delta\text{Ct}}$ method with glyceraldehyde-3-phosphate dehydrogenase (GAPDH) or U6 small nuclear B noncoding RNA (U6) as an internal control. The PCR reaction program started at 95°C for 2 min, 40 cycles for 95°C for 10 s followed by 60°C for 30 s. The same experiment was repeated three times, and the average was taken. The primer sequences are as follows: circLDLR: F, 5'-CGTTGATGATATCTGTCCAAAATACTTTGTC-3', R, 5'-CGATGGGGAGGACAATGGACAGAGCCCTC-3'; miR-637: F, 5'-ACUGGGGCUUUCUGGCUCUGCGU-3', R, 5'-ACGCAGAGCCCCGAAAGCCCCAGU-3'; LMO4: F, 5'-GGGATCGGTTCCACTACATCA-3', R, 5'-GGTGAC AATGAGGAAGGGCTA-3'; GAPDH: F 5'-GAGAAACCT GCCAAGTATGATGAC-3', R 5'-GGAGTTGCTGTTGA AGTCAC-3', U6: F, 5'-CTCGCTTCGGCAGCACA-3', R, 5'-AACGCTTCACGAATTTGCGT-3'.

2.4. RNase R Treatment. The RNA ($2\ \mu\text{g}$) was interacted with or without RNase R ($3\ \text{U}/\text{mg}$, Qiagen) at 37°C for 20 min. Then, the resulting RNA was purified using an RNeasy MinElute Cleanup Kit (Qiagen) and subjected to qRT-PCR analysis. The results represent as the average of three independent replicates.

2.5. Cell Proliferation Analysis. For cell counting kit-8 (CCK-8) assay, TPC-1 and IHH-4 cells transfected with the assigned vector were placed in 96-well plates overnight (1×10^4 cells/well) and then incubated with $10\ \mu\text{L}$ CCK-8 solution (Beyotime, Shanghai, China) for another 2 h at 24, 48, 72, or 96 h. Subsequently, the absorbance at 450 nm was measured. The experiment was repeated at least three times.

For colony formation assay, transfected cells (5000/well) with RPMI-1640 medium were seeded in 6-well plates, and the medium was replaced with new medium every 3 days. Finally, the typical images were photographed, and the number of visible colonies (≥ 50 cells) was counted after 14 days of incubation. The experiment was repeated three times.

2.6. Flow Cytometer. Transfected TPC-1 and IHH-4 cells (1×10^4 cells/ μL) were collected and resuspended in binding buffer; then, 10 μL Annexin V-FITC and propidium iodide (PI) were added into the cell suspension and interacted for 15 min under darkness. The apoptotic cells were evaluated by FACScan flow cytometer within 1 h. Three replicate wells were set in each group, and the experiment was repeated three times.

2.7. Transwell Assay. The invasion ability of cells was detected by a 24-well transwell chamber (8 μm ; Corning Costar, Cambridge, MA) precoated with Matrigel. Following transfection, cells suspended in serum-free medium (3×10^5 cells/mL) were seeded in the upper chamber of transwell; then, 500 μL complete medium mixed with 10% FBS was added into the lower chambers. 24 h later, invaded cells were counted by a microscope. The results represent as the average of three independent replicates.

2.8. Wound Healing Assays. Cell migration was analyzed by wound healing assays. Transfected cells were seeded into a 6-well plate (1×10^4 cells/mL) overnight. Then, a sterile micropipette tip was utilized to create wounds in cell monolayers, followed by washing with PBS to remove free-floating cells and cell debris. After 24 h, representative images were captured, and the distance was measured to calculate cell migration. Experiments were performed three times, and the average was taken.

2.9. Western Blot. Proteins were extracted using RIPA lysis buffer (Beyotime, Beijing, China). Extractive proteins were separated by sodium dodecyl sulfate polyacrylamide gel electrophoresis and then shifted onto polyvinylidene fluoride membranes. The antibodies used in this study included cleaved-caspase3 (C-caspase3) (1:1000, ab2302, Abcam, Cambridge, MA, USA), matrix metalloproteinase 2 (MMP2) (1:5000; ab92536, Abcam), MMP9 (1:2000, ab38898, Abcam), LMO4 (1:5000, ab131030, Abcam), proliferating cell nuclear antigen (PCNA) (1:5000, ab29, Abcam), GAPDH (1:10000, ab181602, Abcam) primary antibodies (overnight, 4°C), and HRP-conjugated secondary antibody (1:3000, Sangon, Shanghai, China) (1 h, 37°C). The same experiment was repeated three times.

2.10. Dual-Luciferase Reporter Assay. The bioinformatics analysis was executed by the online database CircInteractome (<https://circinteractome.nia.nih.gov/>) or Targetscan (http://www.targetscan.org/vert_71/). Dual-luciferase reporter assay was used for validating the interaction between miR-637 and circLDLR or LMO4. Wild (wt) type and mutant (mut) circLDLR and LMO4 3' UTR containing the predicted binding sites of miR-637 were cloned into the pmirGLO Vector (Promega, Shanghai, China) to generate pmirGLO-circLDLR-wt, pmirGLO-circLDLR-mut, pmirGLO-LMO4-wt, or pmirGLO-LMO4-mut. Then, these constructed vectors combined with miR-637 mimic or mimic control (miR-NC) were cotransfected into TPC-1 and IHH-4 cells using Lipofectamine 3000 (Invitrogen). 48 h later, the luciferase activity normalized to Renilla luciferase activity was examined by a dual

luciferase assay kit (Promega). The same experiment was repeated three times.

2.11. RNA Immunoprecipitation (RIP) Assay. TPC-1 and IHH-4 cells were lysed RIP buffer (Millipore, Billerica, MA, USA), and cellular lysates were incubated with magnetic beads conjugated with human anti-Argonaute2 (Ago2) antibody (Millipore) or normal mouse IgG (Millipore) at 4°C for 4 h, followed by interaction with Proteinase K to digest the protein. Finally, immunoprecipitated RNA was extracted, and purified RNA was subjected to qRT-PCR analysis. Analyses were performed in triplicates.

2.12. Xenograft Experiments In Vivo. BALB/c nude mice ($N = 6$, 4-6 weeks old) were obtained from National Laboratory Animal Center (Beijing, China). 1×10^6 TPC-1 cells stably transfected with sh-circLDLR or sh-NC were subcutaneously injected into the flanks of the nude mice. Tumor size was determined each week to calculate tumor volume. At day 35, mice were euthanized, and tumors of each group were weighed and harvested for molecular analysis. Mice were killed by cervical dislocation after deep anesthesia with 2% isoflurane. All experiments were done in Wuhan No.1.Hospital and approved by the Animal Research Committee of Wuhan No.1.Hospital.

2.13. Statistical Analysis. Data of at least three experiments were shown as mean values with standard deviation (SD). All statistical analyses were performed using the GraphPad Prism 7 software. Statistical differences between groups were analyzed using Student's *t*-test, one-way or two-way analysis of variance (ANOVA) followed by Tukey's test as appropriate. The correlation analysis was carried out with Pearson correlation analysis. *P* value < 0.05 (*), *P* value < 0.01 (**), or *P* value < 0.001 (***) was considered as statistically significant.

3. Results

3.1. CircLDLR Expression in PTC and Its Correlation with Overall Survival. The expression of circLDLR in 45 PTC tissues and matched normal tissues was detected, and qRT-PCR analysis displayed that circLDLR was remarkably elevated in tumor tissues relative to those in normal tissues (Figure 1(a)). Then, the correlations of circLDLR expression and special clinicopathological parameters of PTC were analyzed; it was proved that higher circLDLR expression was correlated with advanced TNM stages, tumor size, and lymph node metastasis (Table 1, $P < 0.05$). Besides that, patients with PTC were divided into two groups depending on the median level of circLDLR expression, and we found that patients in the high circLDLR group had a significantly shorter overall survival than those in the low circLDLR group (Figure 1(b)). Then, the expression of circLDLR in cells was measured; as expected, circLDLR also was higher in PTC cell lines (TPC-1 and IHH-4) than those in normal Nthy-ori 3-1 cell lines (Figure 1(c)). Afterwards, the stability of circLDLR was investigated. Total RNA from proliferating TPC-1 and IHH-4 cells was treated with RNase R; by contrast with linear LDLR mRNA, circLDLR could resistant to

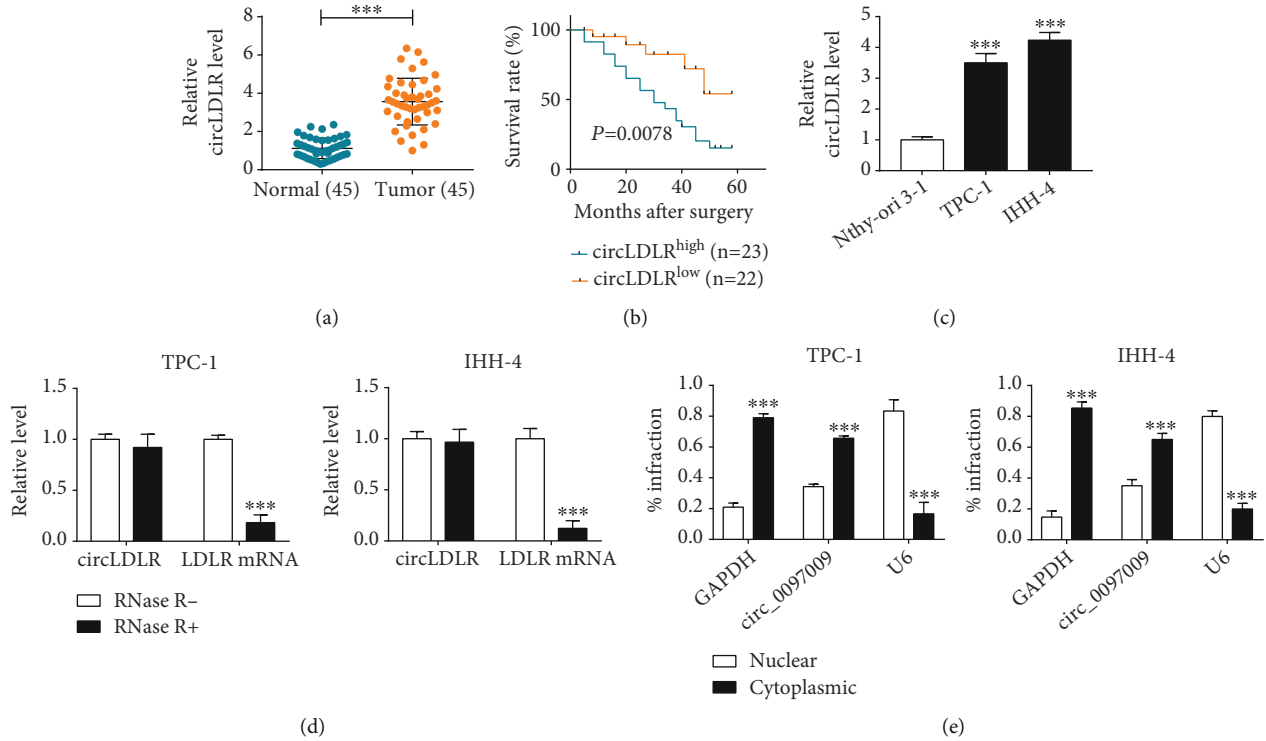


FIGURE 1: CircLDLR expression in PTC and its correlation with overall survival. (a) qRT-PCR analysis of circLDLR expression in 45 PTC tissues and matched normal tissues. (b) Kaplan-Meier survival curve analysis for the correlation between circLDLR expression and overall survival rate in PTC. (c) qRT-PCR analysis of circLDLR expression in PTC cell lines (TPC-1 and IHH-4) and normal Nthy-ori 3-1 cell lines. (d) qRT-PCR analysis of circLDLR and LDLR mRNA expression in TPC-1 and IHH-4 cells in the presence or absence of RNase R (e) Nuclear and cytoplasmic fraction experiment displaying the location of circLDLR in TPC-1 and IHH-4 cells. *** $P < 0.001$.

the degradation by RNase R, indicating circLDLR stably functioned as a typical circRNA (Figure 1(d)). Besides that, qRT-PCR indicated that circLDLR was distributed mainly in the cytoplasm (Figure 1(e)). These data confirmed that circLDLR expression was elevated in PTC, and high circLDLR predicted poor overall survival in patients with PTC.

3.2. CircLDLR Knockdown Suppresses Cell Malignant Phenotypes in PTC. To explore the function of circLDLR in PTC, TPC-1 and IHH-4 cells were transfected with si-circLDLR or si-NC; then, qRT-PCR analysis showed that circLDLR expression was significantly reduced by si-circLDLR as expected (Figure 2(a)). Subsequently, CCK-8 assay indicated that circLDLR knockdown inhibited the proliferation of TPC-1 and IHH-4 cells (Figure 2(b)); similarly, colony formation analysis also revealed that circLDLR silencing decreased the number of colonies formed in TPC-1 and IHH-4 cells (Figure 2(c)). Conversely, the apoptosis of TPC-1 and IHH-4 cells was induced by circLDLR knockdown (Figure 2(d)). Meanwhile, transwell assay suggested that the invasion ability of TPC-1 and IHH-4 cells was suppressed by circLDLR downregulation (Figure 2(e)); besides, wound-healing assay showed that circLDLR knockdown also inhibited the migration of TPC-1 and IHH-4 cells (Figures 2(f) and 2(g)). Moreover, the expression of C-caspase3 was upregulated, while MMP2 and MMP9 expression was downregu-

TABLE 1: Correlation between circLDLR expression and clinicopathological parameters of papillary thyroid carcinoma patients ($n = 45$).

Clinical feature	n	circLDLR		P value
		High	Low	
Age				0.449
≥ 45	24	11	13	
< 45	21	12	9	
Gender				0.884
Man	23	12	11	
Woman	22	11	11	
TNM stage				0.011
I/II	18	5	13	
III/IV	27	18	9	
Tumor size (cm^3)				< 0.001
≥ 3	24	18	6	
< 3	21	5	16	
Lymph node metastasis				0.005
N0	23	7	16	
N1	22	16	6	

lated by circLDLR knockdown in TPC-1 and IHH-4 cells (Figures 2(h) and 2(i)). Taken together, circLDLR knockdown suppressed PTC progression.

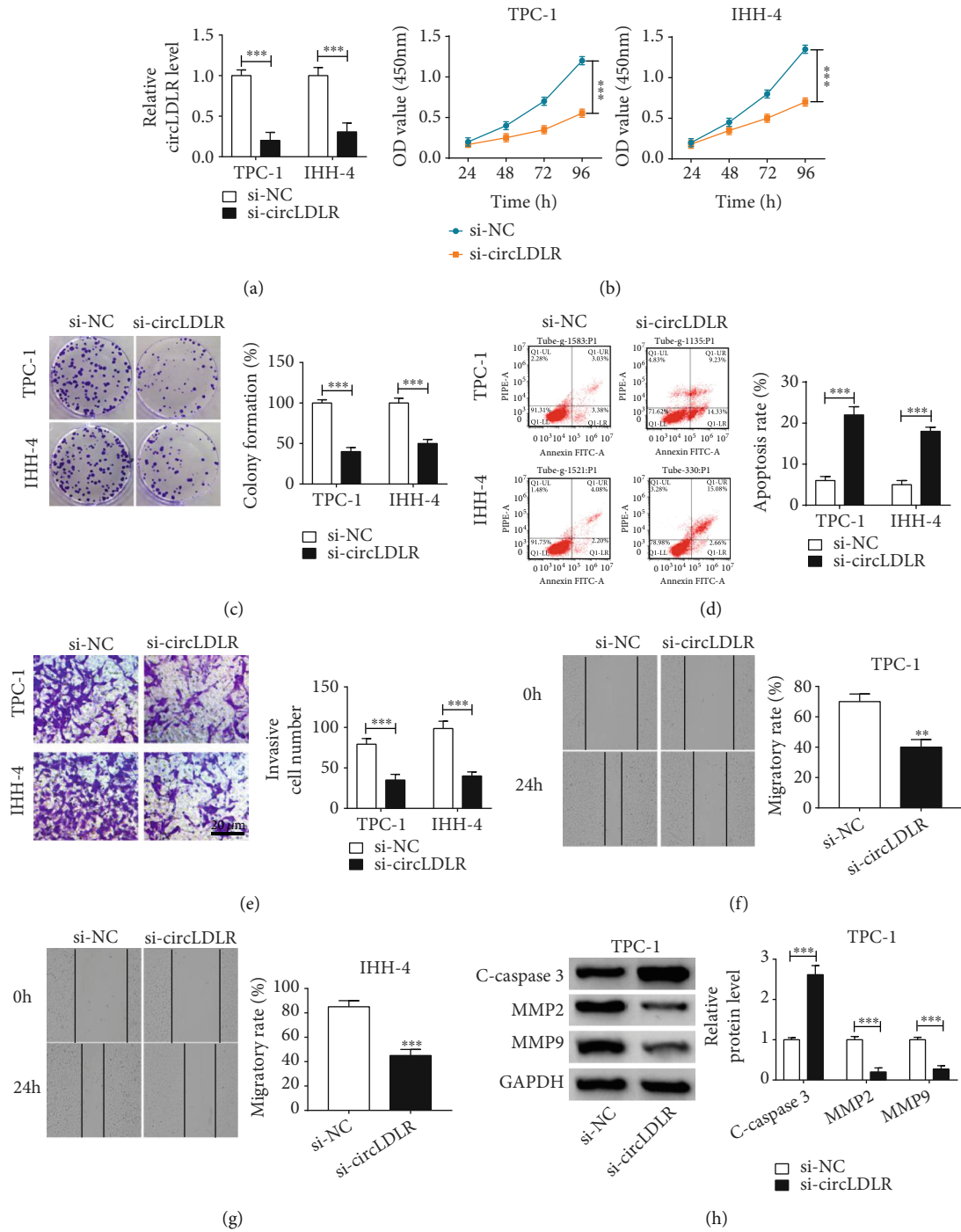
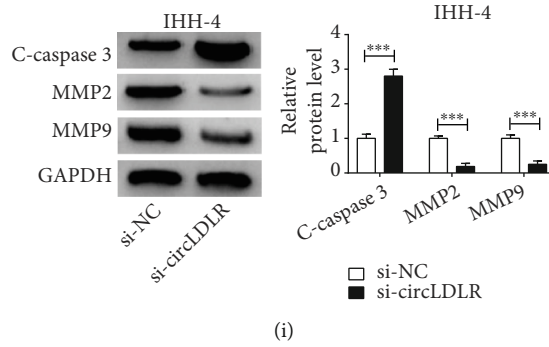


FIGURE 2: Continued.



(i)

FIGURE 2: CircLDLR knockdown suppresses cell malignant phenotypes in PTC. TPC-1 and IHH-4 cells were transfected with si-circLDLR or si-NC. (a) qRT-PCR analysis of circLDLR expression in TPC-1 and IHH-4 cells after transfection. (b, c) The proliferation analysis of TPC-1 and IHH-4 cells using CCK-8 assay and colony formation assay. (d) Flow cytometry analysis of apoptosis of TPC-1 and IHH-4 cells. (e-g) The analysis of invasion and migration abilities of TPC-1 and IHH-4 cells using transwell assay and wound healing assay. (h, i) Western blot analysis of C-caspase3, MMP2, and MMP9 protein levels. ** $P < 0.01$, *** $P < 0.001$.

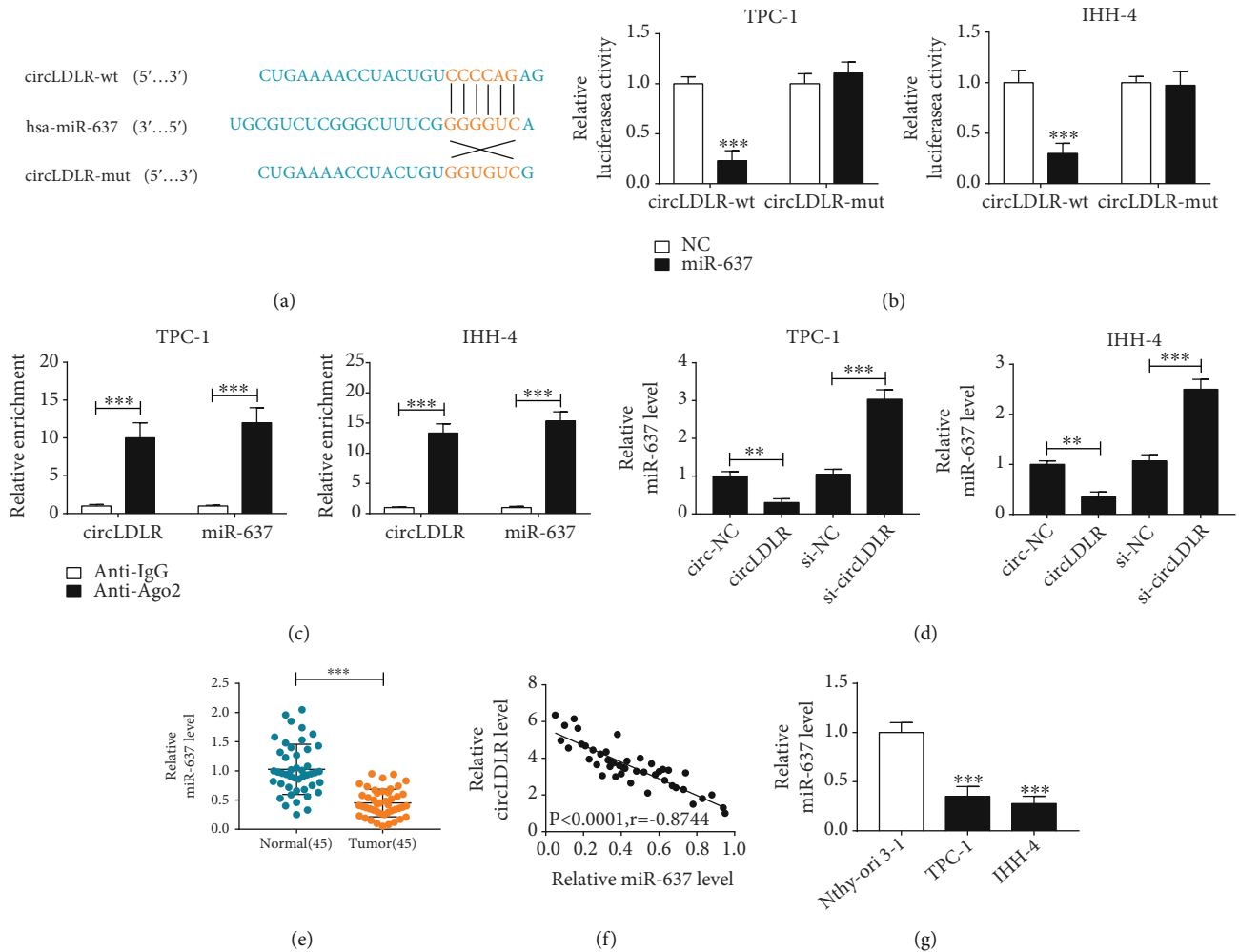


FIGURE 3: CircLDLR functions as an efficient miR-637 sponge in PTC cells. (a) Potential binding sites of circLDLR in miR-637 sequences. (b, c) Interaction analysis between circLDLR in miR-637 in TPC-1 and IHH-4 cells using the dual-luciferase reporter assay and RIP assay. (d) qRT-PCR analysis of miR-637 expression in TPC-1 and IHH-4 cells transfected with circ-NC, circLDLR, si-circLDLR, or si-NC. (e) Levels detection of miR-637 in 45 PTC tissues and matched normal tissues with qRT-PCR. (f) The correlation analysis between circLDLR and miR-637 using Pearson correlation analysis. (g) qRT-PCR analysis of miR-637 expression in PTC cell lines (TPC-1 and IHH-4) and normal Nthy-ori 3-1 cell lines. ** $P < 0.01$, *** $P < 0.001$.

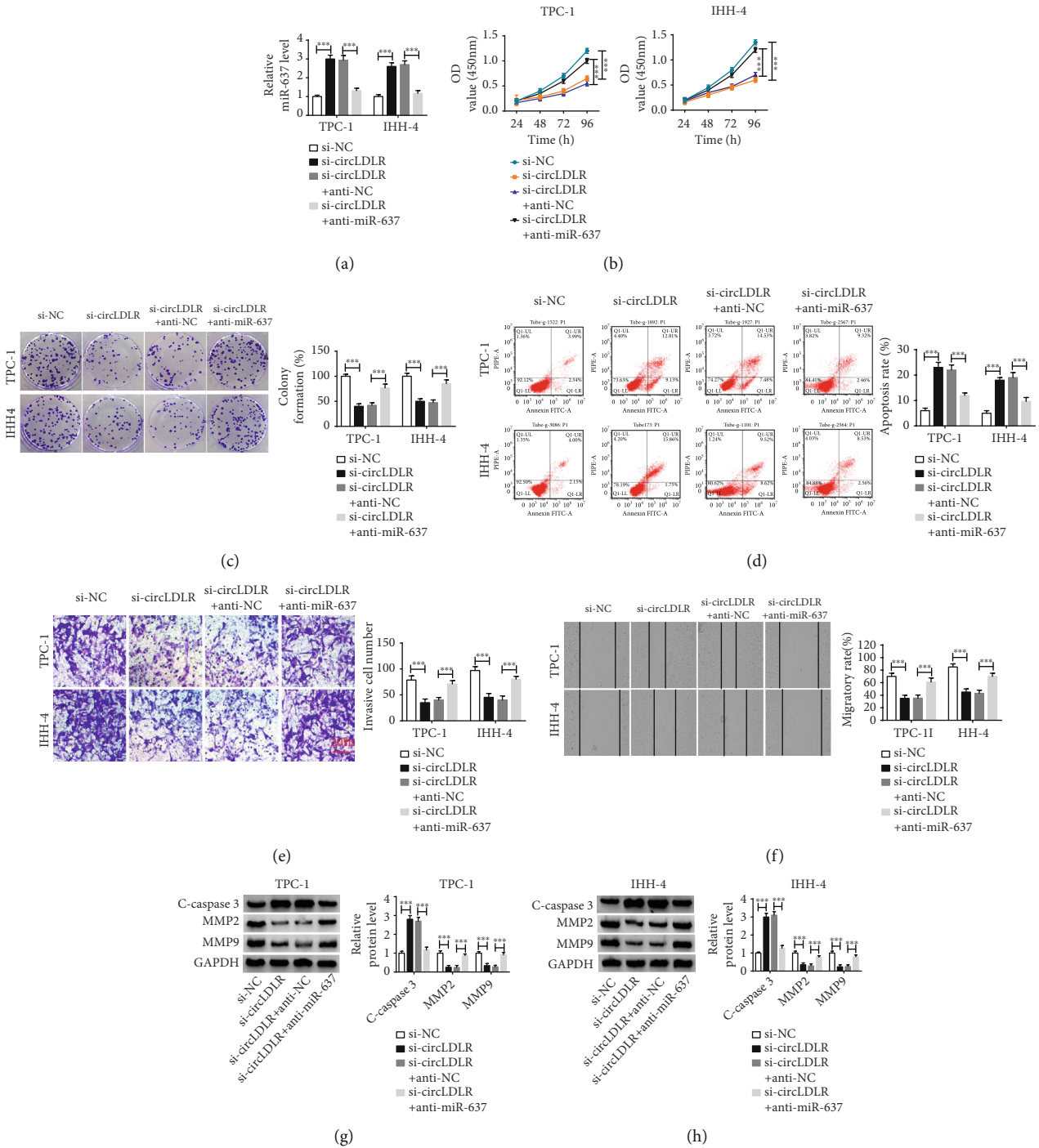


FIGURE 4: miR-637 interference reverses the antitumor effects induced by si-circLDLR in PTC cells. TPC-1 and IHH-4 cells were transfected with si-NC, si-circLDLR, si-circLDLR + anti-NC, or si-circLDLR + anti-miR-637. (a) qRT-PCR analysis of miR-637 expression after transfection. (b, c) The proliferation analysis of TPC-1 and IHH-4 cells using CCK-8 assay and colony formation assay. (d) Apoptosis analysis of TPC-1 and IHH-4 cells using flow cytometry. (e, f) Analysis of TPC-1 and IHH-4 cell migration and invasion with transwell assay and wound healing assay. (g, h) Levels detection of C-caspase3, MMP2, and MMP9 protein levels using western blot. *** $P < 0.001$.

3.3. CircLDLR Functions as an Efficient miR-637 Sponge in PTC Cells. It has been reported that circRNAs can act as miRNA sponges to modulate the expression of downstream mRNAs [17]. Thus, whether circLDLR enhanced the malignant biological behaviors of PTC cell by sponging miRNAs was explored. According to prediction of CircInteractome,

seven miRNAs with high score were selected, and we found that circLDLR knockdown significantly led to an increase of miR-637 expression in TPC-1 cells (Fig. S2). Thus, we hypothesized that miR-637 might be a target of circLDLR. The binding sites of miR-637 on circLDLR are shown in Figure 3(a). Then, the dual luciferase reporter assay

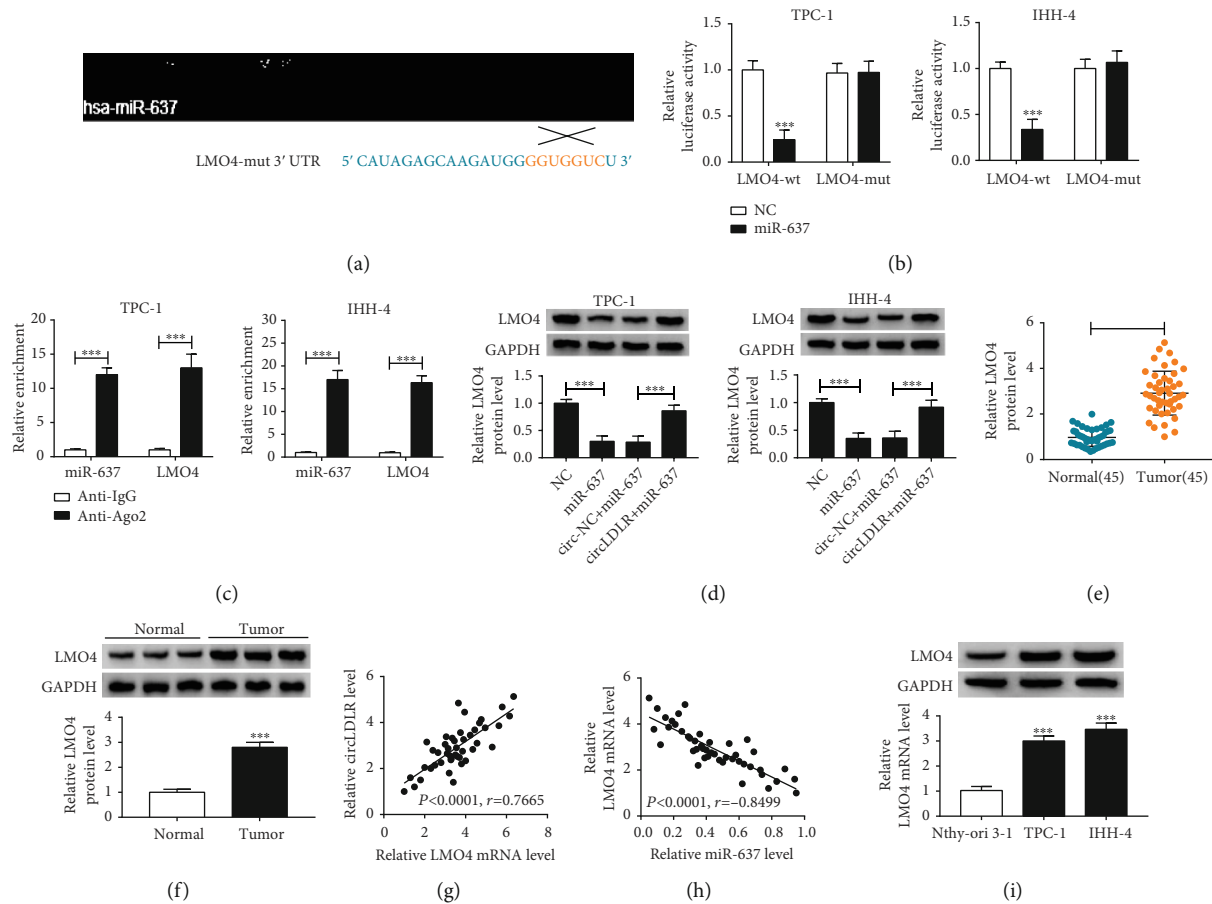


FIGURE 5: LMO4 is a target of miR-637, and circLDLR regulates LMO4 via miR-637 in PTC cells. (a) The predicted binding sites of miR-637 on LMO4 sequences. (b) Luciferase activity detection in TPC-1 and IHH-4 cells cotransfected with the reporter plasmid and the indicated miRNAs using the dual-luciferase reporter assay. (c) qRT-PCR analysis of miR-637 and LMO4 expression in TPC-1 and IHH-4 cells pulled down by Anti-Ago2 or Anti-IgG. (d) Western blot analysis of LMO4 level in TPC-1 and IHH-4 cells transfected with NC, miR-637, circ-NC + miR-637, and circLDLR + miR-637. (e, f) Level detection of LMO4 in 45 PTC tissues and matched normal tissues with qRT-PCR and western blot. (g, h) Correlation analysis between LMO4 and circLDLR or miR-637 in PTC tissues with Pearson correlation analysis. (i) Level detection of LMO4 in PTC cell lines (TPC-1 and IHH-4) and normal Nthy-ori 3-1 cell lines with western blot. *** $P < 0.001$.

exhibited that miR-637 overexpression dramatically reduced the luciferase activity of the circLDLR-wt group in TPC-1 and IHH-4 cells but not the circLDLR-mut group (Figure 3(b)). In the meanwhile, we discovered that circLDLR and miR-637 pulled down by Anti-Ago2 was predominantly enriched in the Ago2 overexpression group compared with the control Anti-IgG group in TPC-1 and IHH-4 cells (Figure 3(c)). These results confirmed that circLDLR targeted miR-637 in PTC. Additionally, qRT-PCR analysis indicated that miR-637 expression was inhibited by circLDLR overexpression but was elevated by circLDLR downregulation in TPC-1 and IHH-4 cells (Figure 3(d)). Subsequently, the expression of miR-637 in PTC was detected, and miR-637 was decreased in PTC tissues (Figure 3(e)) and was negatively correlated with circLDLR (Figure 3(f)). Also, miR-637 had a low expression in TPC-1 and IHH-4 cells compared with the normal Nthy-ori 3-1 cell lines (Figure 3(g)). Therefore, these results indicated that miR-637 was a target of circLDLR and might be associated with the development of PTC.

3.4. MiR-637 Interference Reverses the Antitumor Effects Induced by si-circLDLR in PTC Cells. We then investigated whether circLDLR promoted the progression of PTC by interacting with miR-637. TPC-1 and IHH-4 cells were transfected with si-NC, si-circLDLR, si-circLDLR + anti-NC, or si-circLDLR + anti-miR-637, and qRT-PCR analysis showed that miR-637 inhibition attenuated si-circLDLR-induced elevation of miR-637 in TPC-1 and IHH-4 cells (Figure 4(a)), suggesting the success of transfection. After that, rescue assay was conducted, and results showed miR-637 interference reversed circLDLR knockdown-mediated impairments of the proliferation (Figures 4(b) and 4(c)), invasion (Figure 4(e)) and migration (Figure 4(f)), and promotion of apoptosis (Figure 4(d)) in TPC-1 and IHH-4 cells. Accordingly, western blot analysis also confirmed miR-637 inhibition could partly abate si-circLDLR-mediated migration and invasion inhibition and apoptosis enhancement, evidenced by the change in C-caspase3, MMP2, and MMP9 protein levels in TPC-1 and IHH-4 cells (Figures 4(g) and 4(h)). In all, we verified that

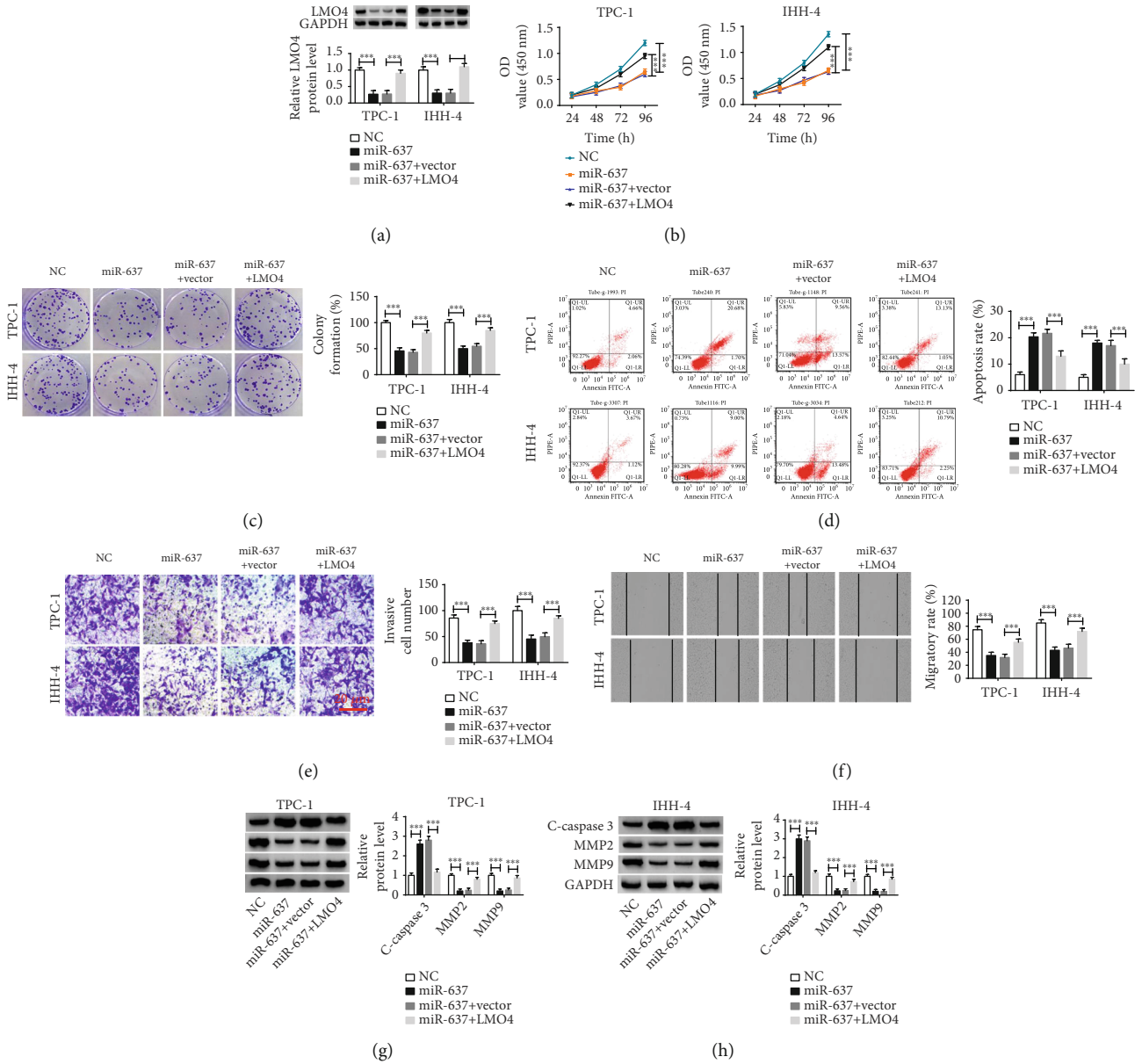


FIGURE 6: MiR-637 suppresses cell malignant phenotypes in PTC cells by targeting LMO4. TPC-1 and IHH-4 cells were transfected with NC, miR-637, miR-637 + vector, or miR-637 + LMO4. (a) Western blot analysis of LMO4 expression in TPC-1 and IHH-4 cells after transfection. (b, c) The proliferation analysis of TPC-1 and IHH-4 cells using CCK-8 assay and colony formation assay. (d) Flow cytometry analysis of apoptosis of TPC-1 and IHH-4 cells. (e, f) The analysis of invasion and migration abilities of TPC-1 and IHH-4 cells using transwell assay and wound healing assay. (g, h) Western blot analysis of C-caspase3, MMP2, and MMP9 protein levels. ***P < 0.001.

circLDLR promoted PTC progression partly by downregulating miR-637.

3.5. LMO4 Is a Target of miR-637 and circLDLR Regulates LMO4 via miR-637 in PTC Cells. The related target genes of miR-637 were further predicted. According to the prediction of TargetsScan program, LMO4 was found that might be a target of miR-637 with putative binding sites (Figure 5(a)). Then, a reduction of luciferase activity in TPC-1 and IHH-4 cells cotransfected with LMO4-wt and miR-637 mimic was detected (Figure 5(b)). Moreover, RIP assay displayed that LMO4 and miR-637 expression was notably enriched in

Ago2 immunoprecipitates relative to the control IgG immunoprecipitates (Figure 5(c)). These data revealed that LMO4 was a target of miR-637. Afterwards, we discovered that LMO4 expression was decreased by miR-637 overexpression, and miR-637 overexpression reversed circLDLR-induced increase of LMO4 level in TPC-1 and IHH-4 cells (Figure 5(d)). Thus, a circLDLR/miR-637/LMO4 axis in PTC was identified. After that, the expression of LMO4 was analyzed; we found that LMO4 expression was upregulated in PTC tumor tissues at mRNA and protein levels (Figures 5(e) and 5(f)). Besides that, LMO4 was positively correlated with circLDLR (Figure 5(g)), while negatively

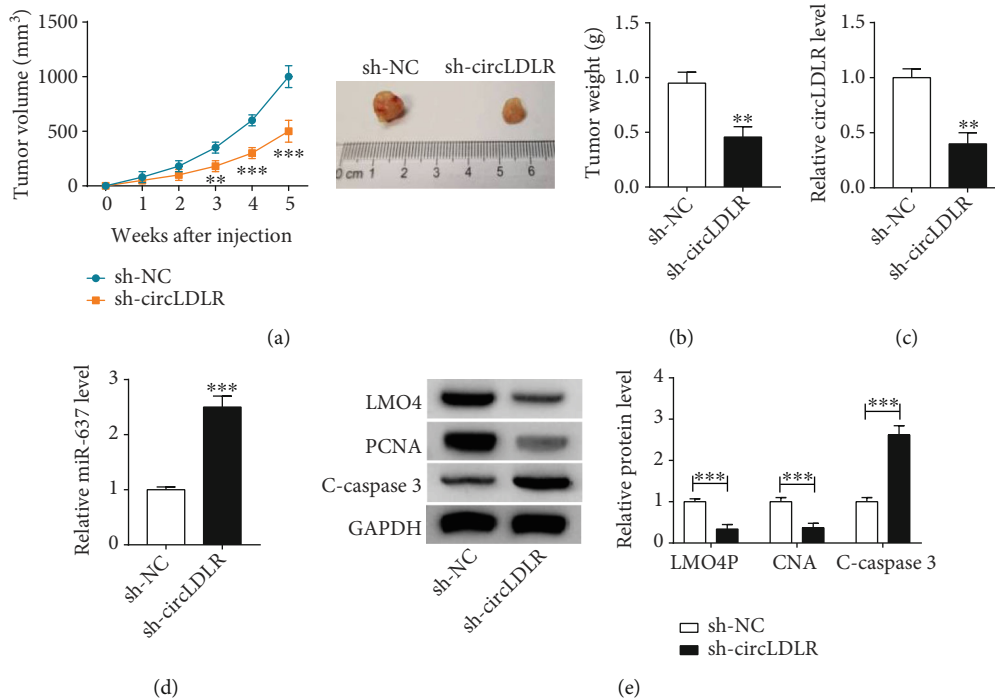


FIGURE 7: CircLDLR knockdown impedes the growth of xenograft tumors *in vivo*. TPC-1 cells stably transfected with sh-circLDLR or sh-NC were subcutaneously injected into the flanks of the nude mice to establish xenograft models. (a, b) The detection of the size and weight of xenograft tumors. (c, d) qRT-PCR analysis of circLDLR and miR-637 levels in tumor masses. (e) Western blot analysis of LMO4, PCNA, and C-caspase3 levels in in tumor masses. ** $P < 0.01$, *** $P < 0.001$.

correlated with miR-637 (Figure 5(h)) in PTC tissues, further suggesting the relationship among circLDLR, miR-637, and LMO4 in PTC. Similarly, LMO4 was also elevated in PTC cell lines (Figure 5(i)). These results suggested that miR-637 targeted LMO4 and circLDLR regulated LMO4 via miR-637 in PTC cells.

3.6. MiR-637 Suppresses Cell Malignant Phenotypes in PTC Cells by Targeting LMO4. Given the axis of circLDLR/miR-637/LMO4 in PTC cells, we further studied whether LMO4 was involved in the action of circLDLR/miR-637 axis in PTC progression. TPC-1 and IHH-4 cells were transfected with NC, miR-637, miR-637 + vector, or miR-637 + LMO4, and then qRT-PCR analysis showed that LMO4 overexpression rescued miR-637 mimic-induced decrease of LMO4 in TPC-1 and IHH-4 cells (Figure 6(a)). Then, functional experiments were conducted. Results exhibited that miR-637 re-expression impaired the proliferation (Figures 6(b) and 6(c)), invasion (Figure 6(e)), and migration (Figure 6(f)) but induced apoptosis (Figure 6(d)) in TPC-1 and IHH-4 cells. Besides that, miR-637 overexpression led to the increase of C-caspase3 and decrease of MMP2 and MMP9 in TPC-1 and IHH-4 cells (Figures 6(g) and 6(h)). Thus, miR-637 inhibited PTC progression. However, rescue assay showed that the antitumor functions of miR-637 were significantly reversed by LMO4 overexpression in TPC-1 and IHH-4 cells (Figures 6(b) and 6(h)). Altogether, miR-637 suppressed PTC progression partly by targeting LMO4.

3.7. CircLDLR Knockdown Impedes PTC Growth In Vivo. To investigate the functions of circLDLR *in vivo*, a xenograft tumor model was established. As shown in Figures 7(a) and 7(b), circLDLR knockdown suppressed the growth of xenograft tumors, evidenced by the smaller size and lighter weight of tumors in the sh-circLDLR group. In addition, knockdown of circLDLR decreased the levels of circLDLR and LMO4 (Figures 7(c) and 7(e)) but increased the level of miR-637 (Figure 7(d)) in xenograft tumors. Furthermore, western bolt analysis showed that PCNA was decreased, but C-caspase3 was increased in the xenograft tumors of the sh-circLDLR group compared with the sh-NC group, furthering revealing circLDLR silencing suppressed tumor growth *in vivo*. Collectively, circLDLR silencing hindered tumor growth *in vivo* via regulating miR-637 and LMO4.

4. Discussion

PTC is the most frequent endocrine malignancy and generally has a good prognosis. Nevertheless, accumulating evidence has exhibited that early stage extradural invasion, lymph node metastasis, distant metastases, and recurrence occasionally occur in some cases, which lead to a poor prognosis, even death in PTC patients [14, 18]. Up to date, increasing researches have reported the implication of circRNAs in the development and progression of cancers through modulating diverse cellular processes [16, 19, 20]. In PTC, some circRNAs have also been indicated to be

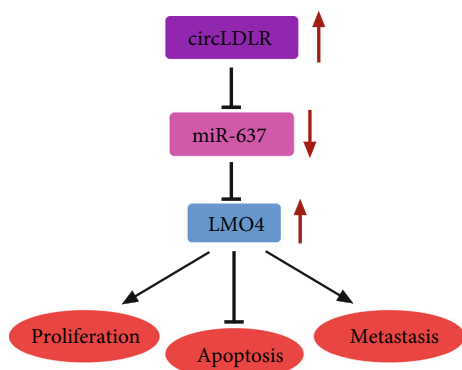


FIGURE 8: The schematic diagram illustrates circLDLR/miR-637/LMO4 axis in PTC tumorigenesis. CircLDLR promotes proliferation and metastasis and suppresses apoptosis of PTC through miR-637/LMO4 axis.

implicated in cancer progression. For example, Wei et al. found that circZFR promoted cell proliferation and invasion in PTC via upregulating C8orf4 expression through miR-1261 [21]. Bi et al. revealed that circRNA_102171 contributed to the progression PTC by activating CTNNBIP1/Wnt/ β -catenin [22]. Thus, circRNAs may be promising candidates for controlling the progression of PTC.

According to the analysis of GSE93522 dataset, the expression of circLDLR was found to be aberrantly upregulated in PTC. Importantly, we also observed that circLDLR was elevated in clinical PTC tissues and cell lines, and high circLDLR expression predicted poor prognosis. However, the biological function of circLDLR in PTC tumorigenesis was not reported yet. Sustained proliferation and metastatic progression are the major drivers of lethality in cancers, and metastasis accounts for the vast majority of patient mortality [28-30]. Thus, the role of circLDLR in PTC cell growth and metastasis was investigated. We found that knockdown of circLDLR inhibited PTC cell proliferation, invasion, and migration but facilitated apoptosis *in vitro*. Moreover, clinical relevance of circLDLR was validated by the observed suppression in ccRCC tumorigenic in nude mice after circLDLR silencing. Altogether, we demonstrated that circLDLR siRNA might be a promising molecule for the treatment of PTC.

It has been identified that circRNAs can function as miRNA sponges to modulate gene expression through abolishing the activity of miRNAs [17]. Subsequently, whether circLDLR served its biological function by acting as miRNA sponge was investigated. Through bioinformatics analysis and interaction analysis, we confirmed that miR-637 was a target of circLDLR in PTC cells. MiR-637 is a well-recognized tumor suppressor. For instance, miR-637 suppressed hepatoma cell viability and invasion via targetedly degrading the expression of AKT1 [23]. MiR-637 decrease was related to poor overall survival and accelerated malignant properties of glioma cells by targeting AKT1 [24]. However, the function of miR-637 in PTC remains unclear. In our work, miR-637 was downregulated in PTC tissues and cell lines; then, we discovered that restoration of miR-637 suppressed cell malignant phenotypes in PTC, thereby hindering cancer progression. After that, rescue assay sug-

gested miR-637 inhibition reversed the inhibitory effects of circLDLR knockdown on PTC tumorigenesis. Therefore, the role of circLDLR/miR-637 axis in the development of PTC was firstly identified.

Recently, growing evidence has identified the involvement of LMO4 in the tumorigenesis. LMO4 has been identified to mediate interactions between multiprotein complexes and DNA, which modulates the expression of genes participated in modulating various biological processes, like cell survival and mammalian development [25]. Additionally, Wang et al. revealed that LMO4 facilitated tumor cell malignant phenotypes in gastric cancer via activating PI3K-Akt-mTOR signaling [26]. Zhou et al. demonstrated that LMO4 suppressed p53-mediated repression of cell proliferation in breast cancer by blocking p53 [27]. Thus, dysregulation of LMO4 plays an important role in the carcinogenesis of cancer. In this study, the expression of LMO4 was found to be elevated in PTC; besides, LMO4 was confirmed to be a target of miR-637, and LMO4 upregulation attenuated the antitumor effects of miR-637 in PTC cells. Thus, the anticancer function of the miR-637/LMO4 pathway in PTC was demonstrated. More importantly, this study also detected that circLDLR could indirectly regulate LMO4 expression via miR-637 in PTC.

In summary, our findings firstly proved that circLDLR acted as an oncogene to promote PTC progression by promoting cancer cell malignant biological behaviors via miR-637/LMO4 pathway (Figure 8). This study offers an improved understanding of the pathogenesis of PTC and reveals a novel regulatory pathway, which may be targeted for therapeutic benefits. Nevertheless, further investigations are needed to probe whether circLDLR/miR-637/LMO4 can affect the phenotypes of normal cells, thus uncovering the clinical applicability of these molecules as the anticancer drug.

Data Availability

No data were used to support this study.

Conflicts of Interest

The authors declare that there are no competing interests associated with the manuscript.

Authors' Contributions

Yuan-ming Jiang, Wei Liu, and Ling Jiang contributed equally to this work.

Supplementary Materials

Figure S1: the diagram of the screening of included PTC patients. Figure S2: the selection of the potential targeted miRNAs of circLDLR. (*Supplementary Materials*)

References

- [1] W. Chen, R. Zheng, P. D. Baade et al., "Cancer statistics in China, 2015," *CA: a Cancer Journal for Clinicians*, vol. 66, no. 2, pp. 115-132, 2016.

- [2] Y. Yang, Q. Chen, W.-Y. Yu et al., "Herbal active ingredients: an emerging potential for the prevention and treatment of papillary thyroid carcinoma," *BioMed Research International*, vol. 2020, 10 pages, 2020.
- [3] B. R. Haugen, E. K. Alexander, K. C. Bible et al., "2015 American Thyroid Association management guidelines for adult patients with thyroid nodules and differentiated thyroid cancer: the American Thyroid Association guidelines task force on thyroid nodules and differentiated thyroid cancer," *Thyroid*, vol. 26, no. 1, pp. 1–133, 2016.
- [4] T. Takano, "Natural history of thyroid cancer," *Endocrine Journal*, vol. no. p. E117, 2017.
- [5] A. Rybak-Wolf, C. Stottmeister, P. Glazar et al., "Circular RNAs in the mammalian brain are highly abundant, conserved, and dynamically expressed," *Molecular Cell*, vol. 58, no. 5, pp. 870–885, 2015.
- [6] Y. Li, Q. Zheng, C. Bao et al., "Circular RNA is enriched and stable in exosomes: a promising biomarker for cancer diagnosis," *Cell Research*, vol. 25, no. 8, pp. 981–984, 2015.
- [7] W. L. Mo, J. T. Jiang, L. Zhang et al., "Circular RNA hsa_circ_0000467 promotes the development of gastric cancer by competitively binding to microRNA miR-326-3p," *BioMed Research International*, vol. 2020, 10 pages, 2020.
- [8] Z. Ding, G. Li, Z. Deng, and P. Li, "Circ-PRMT5 enhances the proliferation, migration and glycolysis of hepatoma cells by targeting miR-188-5p/HK2 axis," *Annals of Hepatology*, vol. 19, no. 3, pp. 269–279, 2020.
- [9] L. He and G. J. Hannon, "MicroRNAs: small RNAs with a big role in gene regulation," *Nature Reviews Genetics*, vol. 5, no. 7, pp. 522–531, 2004.
- [10] G. Wu, W. Zhou, X. Lin et al., "RETRACTED: circRASSF2 acts as ceRNA and promotes papillary thyroid carcinoma progression through miR-1178/TLR4 signaling pathway," *Molecular Therapy Nucleic Acids*, vol. 19, pp. 1153–1163, 2020.
- [11] M. Ye, H. Hou, M. Shen, S. Dong, and T. Zhang, "Circular RNA circFOXM1 plays a role in papillary thyroid carcinoma by sponging miR-1179 and regulating HMGB1 expression," *Molecular Therapy-Nucleic Acids*, vol. 19, pp. 741–750, 2020.
- [12] T. A. Farazi, J. I. Spitzer, P. Morozov, and T. Tuschl, "miRNAs in human cancer," *The Journal of Pathology*, vol. 223, no. 2, pp. 102–115, 2011.
- [13] Q. Yuan, Y. Liu, Y. Fan et al., "LncRNA HOTTIP promotes papillary thyroid carcinoma cell proliferation, invasion and migration by regulating miR-637," *The International Journal of Biochemistry & Cell Biology*, vol. 98, pp. 1–9, 2018.
- [14] X. Cai, Z. Zhao, J. Dong et al., "Circular RNA circBACH2 plays a role in papillary thyroid carcinoma by sponging miR-139-5p and regulating LMO4 expression," *Cell Death & Disease*, vol. 10, no. 3, pp. 1–12, 2019.
- [15] N. Wang, K. Lin, Z. Lu et al., "The LIM-only factor LMO4 regulates expression of the BMP7 gene through an HDAC2-dependent mechanism, and controls cell proliferation and apoptosis of mammary epithelial cells," *Oncogene*, vol. 26, no. 44, pp. 6431–6441, 2007.
- [16] J.-H. He, Y.-G. Li, Z.-P. Han et al., "The CircRNA-ACAP2/Hsa-miR-21-5p/Tiam1 regulatory feedback circuit affects the proliferation, migration, and invasion of colon cancer SW480 cells," *Cellular Physiology and Biochemistry*, vol. 49, no. 4, pp. 1539–1550, 2018.
- [17] J. Wang, D. Wang, D. Wan et al., "Circular RNA in invasive and recurrent clinical nonfunctioning pituitary adenomas: expression profiles and bioinformatic analysis," *World Neurosurgery*, vol. 117, pp. e371–e386, 2018.
- [18] J. J. Sancho, T. W. J. Lennard, I. Paunovic, F. Triponez, and A. Sitges-Serra, "Prophylactic central neck dissection in papillary thyroid cancer: a consensus report of the European Society of Endocrine Surgeons (ESES)," *Langenbeck's Archives of Surgery*, vol. 399, no. 2, pp. 155–163, 2014.
- [19] H.-F. Liang, X.-Z. Zhang, B.-G. Liu, G.-T. Jia, and W.-L. Li, "Circular RNA circ-ABC10 promotes breast cancer proliferation and progression through sponging miR-1271," *American Journal of Cancer Research*, vol. 7, no. 7, pp. 1566–1576, 2017.
- [20] Z.-J. Zhao and J. Shen, "Circular RNA participates in the carcinogenesis and the malignant behavior of cancer," *RNA Biology*, vol. 14, no. 5, pp. 514–521, 2017.
- [21] H. Wei, L. Pan, D. Tao, and R. Li, "Circular RNA circZFR contributes to papillary thyroid cancer cell proliferation and invasion by sponging miR-1261 and facilitating C8orf4 expression," *Biochemical and Biophysical Research Communications*, vol. 503, no. 1, pp. 56–61, 2018.
- [22] W. Bi, J. Huang, C. Nie et al., "CircRNA circRNA_102171 promotes papillary thyroid cancer progression through modulating CTNBP1-dependent activation of β -catenin pathway," *Journal of Experimental & Clinical Cancer Research*, vol. 37, no. 1, p. 275, 2018.
- [23] Y. Du and Y. Wang, "MiR-637 inhibits proliferation and invasion of hepatoma cells by targeted degradation of AKT1," *European Review for Medical and Pharmacological Sciences*, vol. 23, no. 2, pp. 567–575, 2019.
- [24] T. Que, Y. Song, Z. Liu et al., "Decreased miRNA-637 is an unfavorable prognosis marker and promotes glioma cell growth, migration and invasion via direct targeting Akt1," *Oncogene*, vol. 34, no. 38, pp. 4952–4963, 2015.
- [25] W. Wang, S. Wu, M. Guo, and J. He, "LMO4 is a prognostic marker involved in cell migration and invasion in non-small-cell lung cancer," *Journal of Thoracic Disease*, vol. 8, no. 12, pp. 3682–3690, 2016.
- [26] N. Wang, Q. Dong, and X.-N. Zhou, "LMO4 promotes the invasion and proliferation of gastric cancer by activating PI3K-Akt-mTOR signaling," *American Journal of Translational Research*, vol. 11, no. 10, pp. 6534–6543, 2019.
- [27] X. Zhou, M. Sang, W. Liu et al., "LMO4 inhibits p53-mediated proliferative inhibition of breast cancer cells through interacting p53," *Life Sciences*, vol. 91, no. 9-10, pp. 358–363, 2012.

Research Article

IL-38 and IL-36 Target Autophagy for Regulating Synoviocyte Proliferation, Migration, and Invasion in Rheumatoid Arthritis

Zhe Hao and Yi Liu 

Department of Rheumatology and Immunology, West China Hospital, Sichuan University, Chengdu, 610041 Sichuan, China

Correspondence should be addressed to Yi Liu; yi2006liu@163.com

Received 9 September 2021; Revised 9 October 2021; Accepted 3 November 2021; Published 20 November 2021

Academic Editor: Wen-Jun Tu

Copyright © 2021 Zhe Hao and Yi Liu. This is an open access article distributed under the Creative Commons Attribution License, which permits unrestricted use, distribution, and reproduction in any medium, provided the original work is properly cited.

Rheumatoid arthritis (RA) is an autoimmune disease leading to severe joint damage and disability. Fibroblast-like synoviocytes (FLSs) mostly contribute to the joint inflammation and destruction in RA through distinct mechanisms. However, little is known about newly discovered interleukin- (IL-) 36 and IL-38 involving in the pathology of RA. Here, we assessed the effect of IL-36 and IL-38 on RA-FLS function using IL-36 and IL-38 overexpression plasmids. We found that IL-36 inhibited synoviocytes proliferation while IL-38 showed an opposite influence. Furthermore, IL-36 and IL-38 significantly sequestered or accelerated RA-FLS migration and invasion capacity, respectively. Mechanically, IL-36 and IL-38 targeted autophagy for RA-FLS modulation. Using autophagy inhibitor 3-MA and inducer compound rapamycin, we found that autophagy negatively regulated the survival, migration, and invasion of synovial cells. Based on these results, IL-38 in combination with autophagy inhibitor 3-MA treatment demonstrated the strongest blockage of the above three activities of RA-FLS, and IL-38 overexpression reversed rapamycin-inhibited cell proliferation, migration, and invasion. Moreover, injection of IL-36 can improve the symptoms of RA in a rat model of RA. Taken together, we conclude that IL-38 and IL-36 target autophagy for regulating synoviocyte proliferation, migration, and invasion in RA.

1. Introduction

Rheumatoid arthritis (RA) is a chronic, inflammatory, systemic, autoimmune arthritides characterized by immunoglobulin G and citrullinated protein-specific autoantibodies induced synovial inflammation and hyperplasia, ultimately leading to cartilage damage and bone destruction [1]. It is related to systemic disorders such as cardiovascular, pulmonary, and skeletal dysfunction, among which accompanied cardiovascular disease ascribes to the most common cause of mortality of RA patients [2]. Epidemiological researches have reported that RA has a fairly constant global prevalence with the range of 0.5-1.0% in white population [3]. The cause of the disease is complex and is associated with interplays of risk factors like genetics, female sex, and environmental factors. Some biomarkers have been found to be related with RA [4, 5]. During the progress of RA, the resident fibroblast-like synoviocytes (FLSs) assume a semiautonomous and aggressive phenotype, constituting the fundamental mecha-

nism for RA pathogenesis [6]. RA-FLS can proliferate in an anchorage-independent manner without contact inhibition. The increasing number of FLS thus contributes to the transformation of synovial lining into invasive pannus, which can migrate between joints and is directly responsible for cartilage and bone damage [7]. In addition, activated RA-FLS can produce a range of inflammatory cytokines, chemokines, and proangiogenic factors, facilitating the recruitment and proliferation of immune cells such as T cells and B cells, to maintain adaptive immune organization and joint inflammation as well as joint angiogenesis [8]. Therefore, instead of focusing on altering proinflammation cytokines and the immune signaling, targeting RA-FLS to deactivate its autonomous and aggressive phenotypes can be promising strategies for RA therapy.

Interleukin- (IL-) 38 and IL-36 belong to IL-1 cytokine family, which can be divided into three subfamilies as IL-1, IL-18, and IL-36 subfamily by precursor protein length, and play crucial roles in innate and adaptive immunity [9].

Recent studies have suggested both proinflammation and anti-inflammation properties of IL-38, depending on the protein concentration, existing form, posttranslational modification, or cellular environmental context. However, in most cases, IL-38 acts as an antagonist of receptors IL-1R1, IL-36R, or IL-1RAPL1 or recruits inhibitory coreceptor like single Ig IL-1-related receptor (SIGIRR) to suppress proinflammation responses. By inhibiting their binding with specific ligands like IL-1 β , IL-33, or IL-36, IL-38 sequesters downstream NF- κ B, AP1, and JNK signaling pathways [10], therefore, mechanically regulating the progression of numerous disease comprising cancer, myocardial infarction, and autoimmune diseases such as RA [11]. Indeed, emerging studies have indicated that IL-38 is involved in RA pathology. First of all, IL-38 expression was found significantly improved in the serum, synovial tissue, and synovial fluid in RA patients and was associated with production of inflammation cytokines like IL-1 β , IL-6, or IL-1Ra [12]. Gene polymorphism of IL-38 was also related to the occurrence of RA [13]. Moreover, IL-38 administration was found to alleviate RA severity in both collagen-induced and K/BxN-induced RA mouse model through inhibiting proinflammation responses [14]. However, the function of IL-38 in RA besides immune regulation has not been well described yet.

Unlike IL-38, IL-36 exhibit proinflammation characteristic through heterodimeric receptor complex IL-36R and IL-1RAcP. Upon binding to the receptors, Myd88 is recruited and phosphorylates IRAKs, followed by TRAF6 conjunction and ubiquitination, and ultimately activates MAPK and NF- κ B signaling pathway, leading to the production of IFNs, inflammation cytokines, and chemokines like IFN- γ , IL-8, or CXCL1 [15]. It has been reported that IL-36 expression is related to many diseases such as psoriasis, arthritis, obesity, and other chronic diseases [16]. IL-36 and IL-36R were both found elevated in the synovium in RA patients and RA-inducing animal models, with the ability to activate IL-6 and IL-8 secretion in RA-FLS [17, 18], while the molecular mechanism of IL-36 in RA pathology remains to be studied.

Autophagy is a highly conserved endogenous self-degradation process for organelle, proteins, or intracellular pathogens [19], thus maintaining cellular homeostasis and deciding cell fate. Autophagy is a dynamic and multiple-step cellular process, involving initiation, phagophore nucleation and elongation, autophagosome maturation, and autolysosome fusion and degradation [20]. Emerging evidence has identified the importance of autophagy in rheumatic disease, such as systemic lupus erythematosus, rheumatoid arthritis, or osteoarthritis [21, 22]. In RA, many different types of cells present disorder of autophagy, including FLSs, activated T cells, and osteoblast, all of which largely contribute to the pathogenesis of RA [23–25]. Dysfunction of autophagy in RA-FLS leads to hyperplasia of synovial tissue, and downregulated autophagy in cartilage cells is responsible for cell death and cartilage destruction. Mechanically, autophagy results in apoptosis resistance in synovium, T cells, and osteoclasts, promoting their proliferation and survival, therefore, exacerbating RA progression. The function of autophagy in other molecular mechanisms of RA is complex and not well established.

Therefore, we hypothesized that IL-38 and IL-36 α may regulate the disease progression of RA, and autophagy may be involved in the process. In this study, we sought to validate the crosstalk of inflammation cytokines IL-36/IL38 and autophagy in determining the process of RA pathology, trying to provide some new insights in RA regulation. The therapeutic effect of IL-36 for RA was also primarily investigated.

2. Materials and Methods

2.1. Cell Culture and Stimulation. SW982 cell line was purchased from the Cell Bank of Type Culture Collection of Chinese Academy of Sciences and was cultured in Leibovitz's L-15 Medium (Solarbio, Beijing, China) containing 10% fetal bovine serum (Thermo Fisher, Waltham, MA, USA), 100 U/mL penicillin and 100 mg/mL streptomycin at 37°C in 5% CO₂, respectively. For autophagy inhibition or initiation, cells were treated with 10 mmol/L of 3-MA or rapamycin (10 nmol/L; Sigma Aldrich, St. Louis, MO, USA) for 24 hours, after transfection with recombinant plasmid.

2.2. Plasmid Construction and Transient Transfection. IL-38 and IL-36 gene sequence information were obtained from NCBI gene database and the target IL-38 or IL-36 DNA fragment was directly synthesized with NheI and KpnI restriction enzyme cutting site added to N-terminal or C-terminal, respectively. Target gene was inserted ahead of EGFP gene sequence into pcDNA3.1-EGFP vector for fusion protein expression. After double-enzyme digesting, DNA ligase, transduction, and bacterial colony amplification, plasmids were extracted for NheI and KpnI digestion and sequencing validation. Plasmid DNA was transfected into cells using lipofectamine 2000 transfection reagent (Thermo Fisher) according to manufacturer's instruction.

2.3. RNA Extraction and Quantitative Real-Time PCR. Cells were harvested 24 hours after transfection with indicated plasmids and lysed with Trizol reagent (Thermo Fisher). Total RNA was isolated according to manufacturer's procedure. Briefly, after lysing in 1 volume of Trizol for 5 min, 1/5 volume of chloroform was added for homogenization vigorously and incubated for 3 min. After centrifuging at 12000 g, 4°C for 15 min, the upper aqueous phase was gathered, and 1/2 volume of isopropanol was added for incubation at room temperature for 10 min, followed by centrifuging at 12000 g, 4°C for 15 min. The RNA pellet was washed with 1 mL 75% ethanol, centrifuged at 12000 g, 4°C for 5 min. After air dried, RNA was dissolved in RNase-free water and stored at -70°C until use.

For quantitative real-time PCR analysis, PrimeScript II Reverse Transcriptase (Takara, Japan) was used for first-strand cDNA synthesis according to manufacturer's protocol. The cDNA was amplified, and gene expression was determined with Bio-Rad CFX connect detection system using iTaq Universal SYBR Green Supermix (Bio-Rad, Hercules, CA, USA). PCR amplification was performed as follows: 95°C for 5 min followed by 40 cycles consisting of

95°C for 15 s, 55°C for 15 s, and 72°C for 30 s. mRNA transcript levels were normalized to GAPDH. The following gene-specific primer sequences were used: 5'-GGGAAA CTGTGGCGTGAT-3' (sense) and 5'-GAGTGGGTGTC GCTGTTGA-3' (antisense) for GAPDH; 5'-ACCAAC CCGAGCCTGTGA-3' (sense) and 5'-CCCAGTTCTTG GGTAAGGATG-3' (antisense) for IL-36; 5'-GACAAC TGCTGTGCAGAGAAG-3' (sense) and 5'-GGCCTCTTC ACCACCTTTGT-3' (antisense) for IL-38.

2.4. Western Blot. Cells were lysed in RIPA buffer with PMSF (Solarbio, Wuhan, China), and extracted-protein concentration was determined using Bio-Rad Protein Assay (Bio-Rad). Western blot analysis was performed with indicated antibodies in accordance with the Western blotting protocol provided by Cell Signaling Technology with modification. Specific antibody against IL-38 was purchased from Abcam (Cambridge, MA, USA). Primary antibodies against GAPDH, IL-36 α and LC3, and HRP-conjugated goat-anti-rabbit IgG secondary antibody were obtained from Bioswamp (Wuhan, China). Briefly, protein samples were loaded onto SDS-PAGE gel and electrotransferred to PVDF membrane, then incubated the membrane in blocking buffer for 1 h at room temperature followed by primary antibody (1:1000 dilution) incubation with gentle agitation overnight at 4°C. The next day, the membrane was incubated with species appropriate for HRP-conjugated secondary antibody in blocking buffer (1:20000 dilution) with gentle agitation for one hour at room temperature. The proteins were detected with Clarity Western ECL Substrate (Bio-Rad) for digital imaging using Tannon-5200 (Tannon, Shanghai, China).

2.5. Immunofluorescence Assay. SW982 cells were plated in 35 mm confocal dishes (Ibidi, Lochhamer, Germany). After treatment, cells were fixed with 4% paraformaldehyde in PBS pH 7.4 for 10 min at room temperature. Then, permeabilization was performed by incubating the samples for 10 min at 4°C with PBS containing 0.1–0.25% Triton X-100. Samples were then blocked in PBS containing 5% normal serum and 0.3% Triton X-100 for 1 hour at room temperature, followed by incubation with diluted primary antibody in PBS containing 1% BSA and 0.3% Triton™ X-100 overnight at 4°C. Next day, samples were incubated with Alexa Fluor 594-conjugated goat anti-rabbit secondary antibody (Bioswamp, Wuhan, China) for one or two hours in the dark before nuclear staining with DAPI for 5 min at room temperature. Dishes were stored at 4°C protected from light for long-term storage. Cells were finally imaged using inverted immunofluorescent microscope (DMIL LED, Leica, Wetzlar, Germany).

2.6. EdU Proliferation Assay. Cell Light Edu Apollo 567 In Vitro Imaging Kit was supplied by Guangzhou RiboBio (China, Guangzhou) and used for determining the proliferation of SW982 cells according to manufacturer's instructions. After experimentation, 100 μ L, 50 μ M EdU was added into the cell culture medium for incubation for 2 hours. Fixation was performed at room temperature for 15 min using 4% paraformaldehyde diluted in PBS, followed

by permeabilization with 0.5% Triton X-100 and incubated 20 min at room temperature. Fluorescent EdU detection was performed after EdU staining with Apollo567 and nuclear staining with Hoechst 33258. Images were collected using immunofluorescent microscope (DMIL LED, Leica).

2.7. Wound Healing Assay. Wound healing assays were performed to determine the migration ability of SW982 synovial cells after different treatments. Reference lines were marked to guarantee the same area of image acquisition. Cells were seeded into 24-well plates and grew to 80% confluence for transfection or stimulation. 24 hours later, a linear wound was created in the cellular monolayer with a same 200 μ L pipette tip in each well. After scratch, gently wash cell monolayer to remove detached cells. Cells were continually cultured at 37°C with 5% CO₂, and images of the wound were captured at 0, 24, or 48 hours upon the wound creation using a phase contrast inverted microscope with appropriate magnification.

2.8. Transwell Cell Invasion Assay. The cell invasion assays were performed using Corning BioCoat Matrigel invasion chamber (Corning, NY, USA), with a pore size of 8 μ m polyethylene terephthalate membrane precoated with Matrigel. SW982 cells transfected with indicated plasmids or treated with correspondent chemical reagents were resuspended in serum free medium and were seeded in the upper well at the concentration of 104/mL.

L-15 media containing 20% FBS was added to the lower chamber as the chemoattractant. Cells were incubated for 48 hours, and noninvaded cells were gently removed; the remaining cells downside of the membrane surface were stained with 0.1% crystal violet at room temperature for 5 min. Cells were imaged with Inverted Laboratory Microscope Leica DM IL LED and analyzed from randomly selected different fields.

2.9. Animal Model of RA. Fifteen specific-pathogen-free (SPF) male SD rats (weighing 180–220 g) were purchased from Hubei Animal Experiment Center. Rats were maintained under SPF conditions with a room temperature of 22–26°C and humidity of 50–60% under a 12-hr light/dark cycle with access to food and water ad libitum. All animal procedures were approved by the Institutional Animal Care and Use Committee of the local institution.

Rats were randomly divided into three groups: control, model, and treatment groups ($n = 5$ per group). Rats in the model and treatment groups were injected with 50 μ L of type II collagen (2 mg/mL) combined with incomplete Freund's adjuvant in the articular cavity of hind ankle joint at the first and 7th day. Rats in the control group were injected with the same volume of incomplete Freund's adjuvant. Rats in the treatment group were injected with recombinant IL-36 from the first day to the 10th day. All rats were sacrificed until the 28th day. Before sacrifice, the body weight and the swelling and color of the feet and joints were recorded, and the length and thickness of the ankles and feet were measured and compared. After the rats were sacrificed, the ankle joint

synovium was collected for hematoxylin-eosin (HE) staining to observe the inflammation and infiltration.

2.10. HE Staining. Collected ankle joint synovium were fixed in 10% formaldehyde for more than 24 hr. The samples were dehydrated in alcohol, embedded in paraffin, and cut into 3 μ m sections. Subsequently, the sections were deparaffinized and rehydrated, then subjected to HE staining following a standard protocol. Images were captured under a microscope (DMIL LED, Leica, Wetzlar, Germany).

2.11. Statistical Analysis. The data are expressed as the means \pm SD and are representative of three independent experiments. Statistical differences between the experimental groups were calculated using GraphPad Prism software. The means obtained for the different groups were compared by one-way ANOVA followed by the Tukey post hoc test. A value of $P < 0.05$ was considered statistically significant.

3. Results

3.1. IL-38 and IL-36 Regulate Synoviocyte Proliferation, Migration, and Invasion. First, we want to determine the effect of IL-36 and IL-38 on the proliferation of FLS in RA pathology. The expression of IL-38 and IL-36 overexpression construct was first assessed. As shown in Figure 1(a), both IL-36 and IL-38 encoding plasmid successfully expressed plenty of EGFP fusion protein validated by microscope examination. mRNA and protein expression of IL-36 and IL-38 were confirmed with RT-PCR and Western blot (Figures 1(b)–1(d)).

EdU cell proliferation assay was performed to evaluate the proliferation of SW982 cells transfected with IL-36 or IL-38 expression plasmids. The results showed that compared with the control, IL-36 overexpression reduced the cell proliferation, whereas IL-38 overexpression increased the cell proliferation (Figure 2(a)). Then, the effect of IL-36 and IL-38 on the migration and invasion of SW982 cells was investigated. As shown in Figure 2(b), the wound widths in IL-38 overexpressed cells were dramatically narrowed at both 24 hr and 48 hr. However, cells that migrated toward the scratch were attenuated by IL-36. Simultaneously, the number of cells penetrated through Matrigel-coated transwell membranes increased significantly in the presence of IL-38 while the cells infiltrated into the other side of the monolayer filter were suppressed by IL-36 overexpression. These data demonstrated that IL-38 facilitated while IL-36 impaired the migration and invasion capacity of SW982 cells. Taken together, our results suggested that IL-36 and IL-38 regulated proliferation, migration, and invasion of the synoviocytes in an opposite manner.

3.2. IL-38 and IL-36 Modulate Autophagy. Next, the effect of IL-36 and IL-38 on autophagy in SW982 cells was investigated. LC3-I is diffuse cytosolic distributed and LC3-II puncta is focus distributed, which can be indicated by the bright intensity and location of the fluorescence. As shown in Figure 3(a), fluorescence was focused and bright in the IL-36 expression group while was diffused in the IL-38 overexpression group. Western blot results in Figure 3(b)

showed that IL-36 potentiated conversion of LC3-I into LC3-II while IL-38 suppressed LC3-II accumulation. These data demonstrated that IL-36 accelerated and IL-38 impeded autophagy.

3.3. IL-38 Promotes Autophagy-Inhibited Cell Proliferation. Since IL-38 impeded autophagy, next, we investigated whether IL-38 regulates RA-FLS proliferation via autophagy. SW982 synovial cells were treated with autophagy initiation inhibitor 3-methyladenine (3-MA) or inducer rapamycin (Rapa) with or without IL-38 encoding plasmids transfection. As shown in Figure 4(a), in the untransfected group, LC3-II turnover was alleviated by 3-MA and exacerbated by rapamycin treatment. Immunoblot analysis also indicated that IL-38 inhibited LC3-II formation, and this inhibition was a little aggravated by the addition of 3-MA. Moreover, IL-38 overexpression mitigated rapamycin-induced LC3-II accumulation comparison with only rapamycin-treated group. EdU staining assay showed that inhibition of autophagy by 3-MA promoted SW982 cell proliferation, and by contrast, initiation of autophagy by rapamycin greatly restrained the red fluorescent light intensity (Figure 4(b)). In addition, IL-38 overexpression significantly enhanced cell proliferation in both untreated or 3-MA or rapamycin-treated groups. Combination treatment of IL-38 and 3-MA exhibited the strongest ability to accelerate cell proliferation, and IL-38 overexpression reversed the rapamycin-mediated blockage of cell proliferation. In conclusion, these data demonstrated that IL-38 promoted autophagy-inhibited synovial cell proliferation.

3.4. IL-38 Facilitates Synoviocyte Migration and Invasion via Autophagy. Then, we investigated how autophagy regulated synovial cell migration and invasion, as well as the role of IL-38 in these processes. Wound healing analysis showed that 3-MA treatment enhanced the migration ability of SW982 cells at both 24 hr and 48 hr, and autophagy initiated by rapamycin slowed down cell migration (Figure 5(a)). In addition, we found that IL-38 overexpression group displayed similar narrow wound width in comparison with 3-MA group. In line with this, IL-38 and 3-MA treatment together maximally improved cell wound healing speed, while IL-38 restored the cell healing capacity diminished by rapamycin. These data collectively suggested that IL-38 promoted synoviocyte migration, which was inhibited by autophagy.

Next, we evaluated the influence of IL-38 and autophagy on cell invasion using transwell assay. As shown in Figure 5(b), 3-MA treatment led to increasing SW982 cells translocated from the coated filter to the downside serum containing culture medium. Rapamycin addition alleviated the number of cells stained with crystal violet, suggesting impaired invasion ability. After IL-38 transfection, more cells managed to move across the transwell membrane compared to the control group. In line with the aforementioned results, IL-38 overexpression accelerated 3-MA-induced cell invasion and reversed the rapamycin downregulated number of transmembrane cells. Taken together, these findings demonstrated that IL-38 facilitates synoviocyte migration and invasion via autophagy.

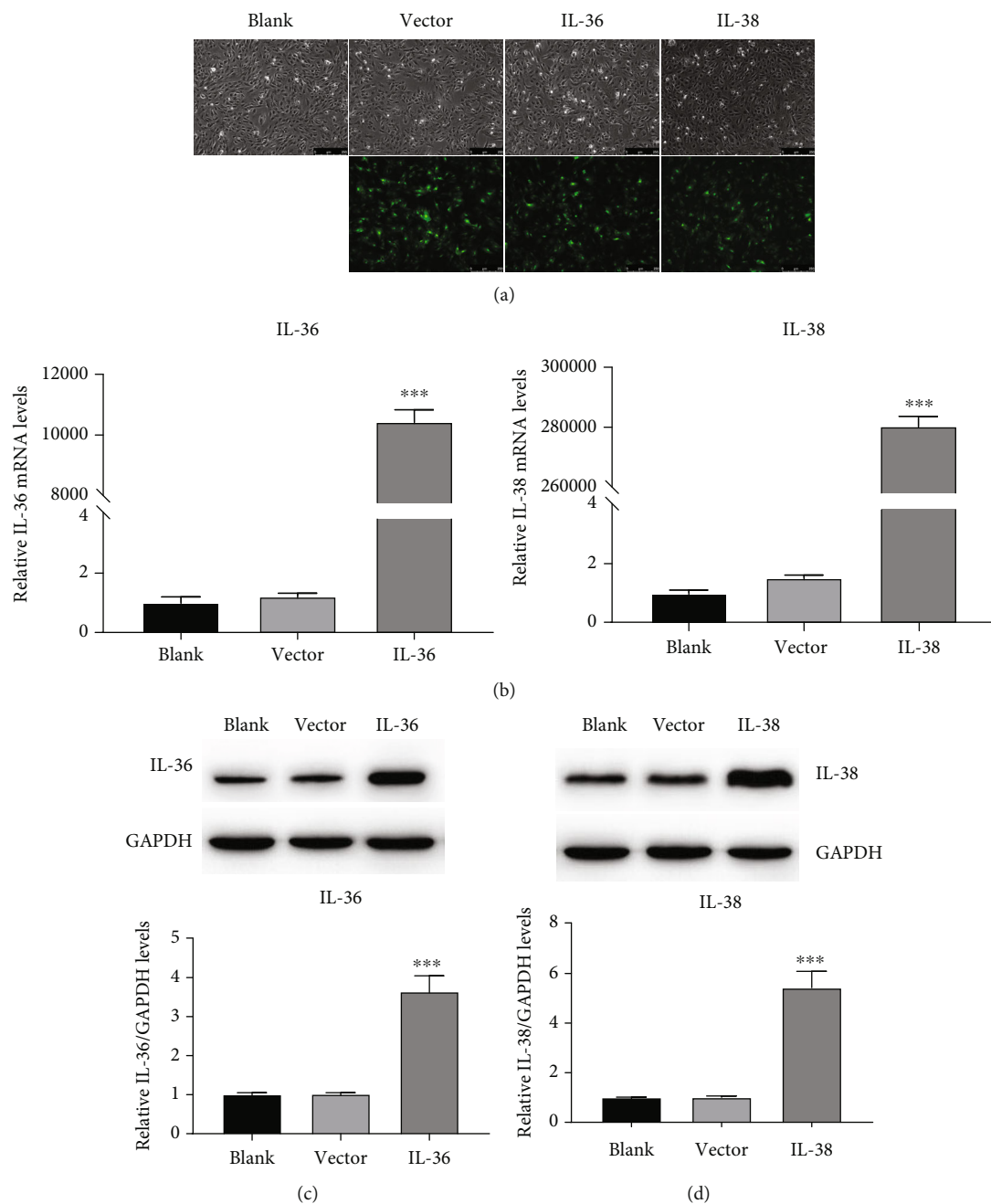


FIGURE 1: Identification of IL-38 and IL-36 overexpression construct. (a) SW982 cells were transfected with EGFP fusion IL-36 or IL-38 encoding plasmids or empty vector. Cells were examined under microscopy (100x) for EGFP expression. Representative images are presented from three biological replicates. (b) SW982 cells were transfected with empty vector or IL-36 (left panel) or IL-38 (right panel) or left untransfected, followed by total RNA isolation 24 hours posttransfection and subjected to qRT-PCR analysis. (c) SW982 cells were transfected with the indicated plasmids for 24 hours followed by Western blot detection for IL-36 or IL-38 expression; GAPDH was used as control. Data represent the mean from three independent experiments with SD. *** $P < 0.001$ compared to the control group.

3.5. IL-36 Treatment Improve the Symptoms of RA in a Rat Model. Since IL-36 showed protective effect against synovocytes, we next explored the therapeutic effect of IL-36 α in the rat model. The morphological observation results showed that compared with the control group, the weight of the rats in the model and treatment groups was significantly reduced, and the weight of the rats in the treatment group was higher than that of the model group without significant

difference (Figure 6(a)). The foot length, width, plantar thickness, and ankle width of rats in the model and treatment groups were significantly larger than those of rats in the control group, but these indicators of rats in the treatment group were significantly lower than those of the model group (Figure 6(a)). The HE staining results showed that the cells in the control rats were neatly arranged without inflammatory cell infiltration, but cells in the model rats had severe

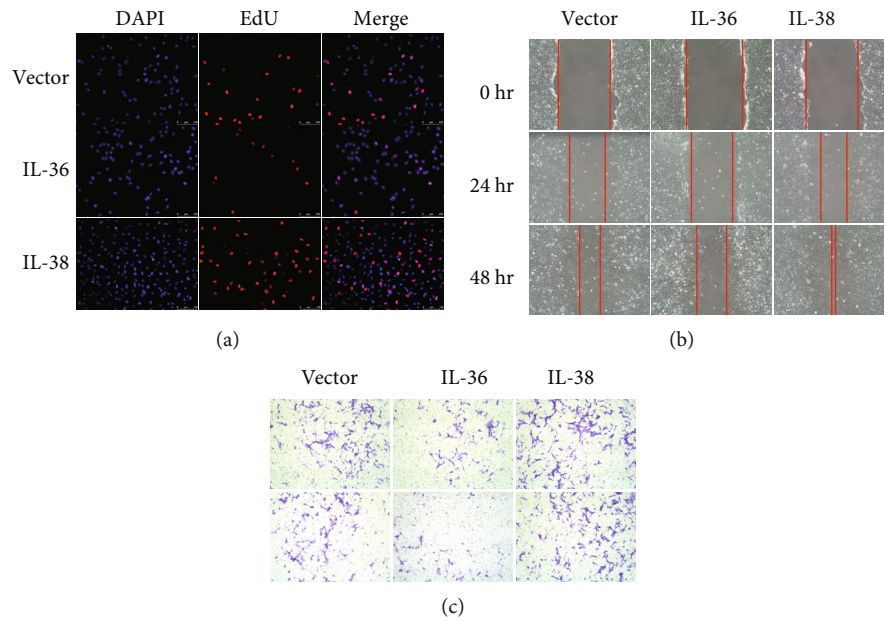


FIGURE 2: IL-38 and IL-36 regulate synovioocyte proliferation, migration, and invasion. (a) SW982 cells transfected with indicated plasmids for 24 hours were incubated with EdU followed by fixation and permeabilization and then subjected to EdU staining with Apollo567 and nuclear staining with Hoechst 33258. Representative micrographs (200x) from three independent experiments are shown. (b) SW982 cells were transfected with the indicated constructs for 24 hours followed by scratching to form a linear wound with pipette tip. Cells were then cultured for indicated hours, and images of the wound were captured using a phase contrast inverted microscope with 100x magnification. (c) SW982 cells with IL-36 or IL-38 or empty vector transfection for 24 hours were digested by trypsin and resuspended and placed into upside of the transwell. Cells were cultured for 48 hours and were determined by crystal violet staining and microscopy (100x). Representative images are presented from at least three biological replicates.

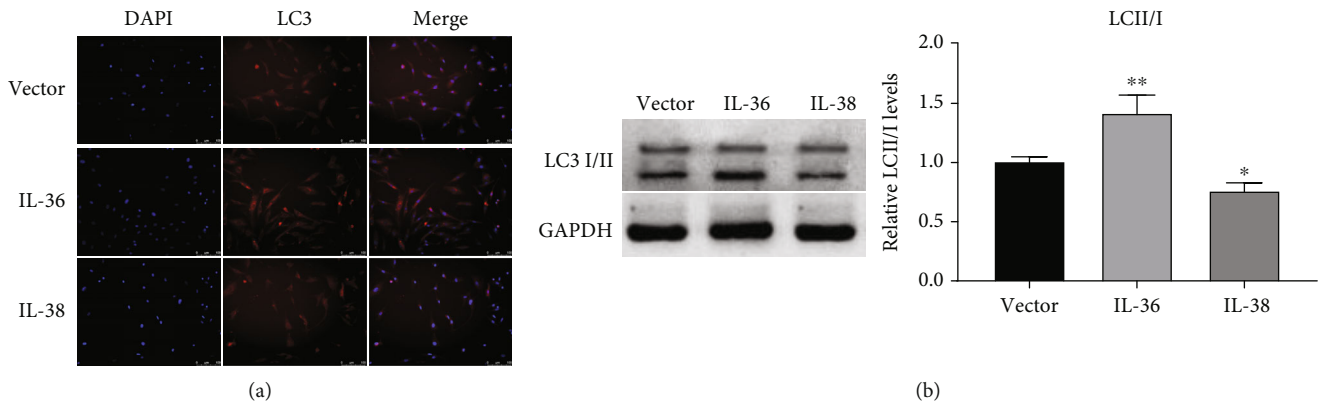
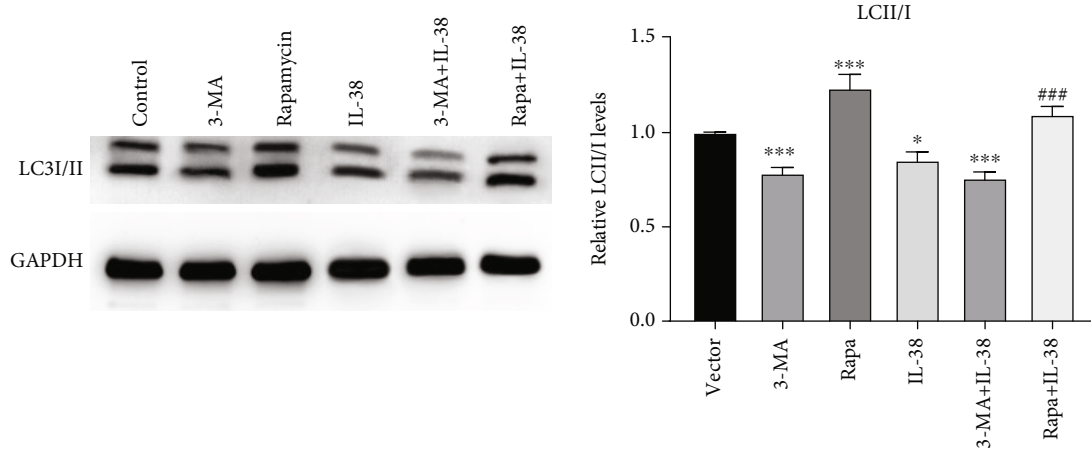


FIGURE 3: IL-38 and IL-36 modulate autophagy. (a) SW982 cells were transfected with IL-36 or IL-38 overexpression construct or empty vector for 24 hours. Cells were then subjected to immunofluorescent staining using LC3 antibody, and nucleus were labeled with DAPI. Representative micrographs (100x) from three dependent experiments were shown. (b) SW982 cells with the indicated plasmids transfection for 24 hours were harvested and lysed in RIPA buffer and subjected to SDS-PAGE and Western blot analysis. The endogenous LC3I/II turnover was assessed using LC3 specific antibody. GAPDH was detected as control. The data are representative of three independent experiments. * $P < 0.05$, ** $P < 0.01$ compared to the vector group.

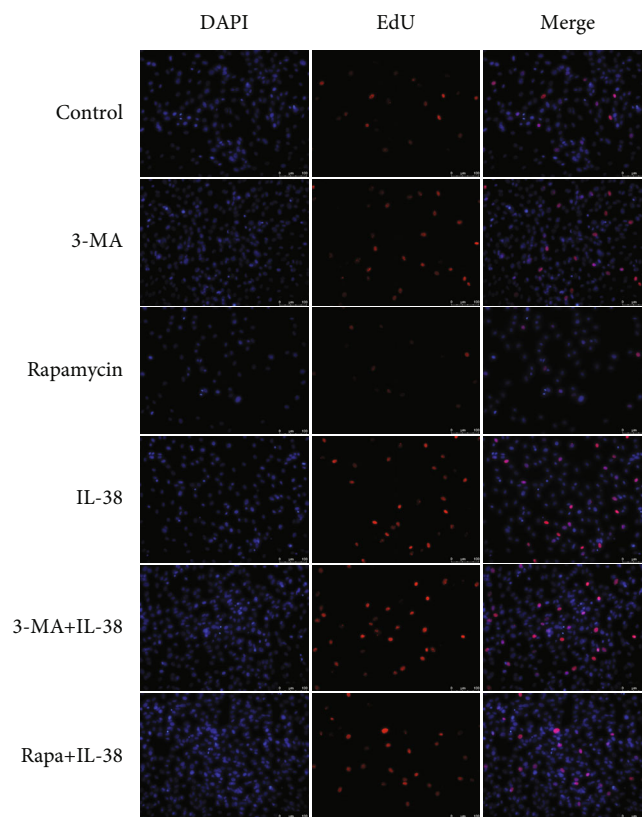
inflammatory cell infiltration, while cells in the treatment rat had almost no inflammatory cell infiltration, which was comparable to that in the control group (Figure 6(b)). These data suggest that IL-36 treatment can improve the redness and swelling of the paws, relieve the symptoms of paw arthritis, and inhibit the inflammation in the joint synovium.

4. Discussion

In this study, we found that IL-38 enhanced synovial cell proliferation, migration, and invasion while IL-36 exhibited contrary function. IL-36 accelerated and IL-38 impeded synovial cell autophagy, which may contribute to RA pathology. Further experiments showed that IL-38 promoted



(a)



(b)

FIGURE 4: IL-38 promotes autophagy-inhibited cell proliferation. (a) SW982 cells were transfected with IL-38 overexpression plasmids or empty vector and treated with 3-MA or rapamycin or left untreated. Cells were cultured for 24 hours and then collected and lysed for immunoblotting analysis. The endogenous LC3II/I turnover was assessed using LC3 specific antibody. GAPDH was detected as control. * $P < 0.05$, *** $P < 0.001$ compared to the vector group; ### $P < 0.001$ compared to the Rapa group. (b) SW982 cells were transfected with empty vector or IL-38 overexpression plasmids and treated with 3-MA or rapamycin or left untreated. Cells were cultured for 24 hours before EdU proliferation assay. Representative micrographs (200x) from three independent experiments are shown.

autophagy-restrained synovial cell proliferation, migration, and invasion. Moreover, injection of IL-36 can improve the symptoms of RA in a rat model of RA. Our data together suggested crucial roles of IL-38 and IL-36 for determining RA-FLS fate and ultimately regulating joint damages.

RA is a chronic inflammatory disease with the main pathological feature of proliferative synovial lining tissue

caused by hyperplasia of FLS [6]. RA is also characterized as cartilage and bone destruction caused by synovium transformation into the invasive tissue and aggressive phenotypes of FLSs such as migration and invasion [26]. Both IL-38 and IL-36 were found to be elevated in RA patients [12, 13, 17, 18]. The present study found that IL-38 enhanced while IL-36 inhibited synovial cell proliferation, migration, and

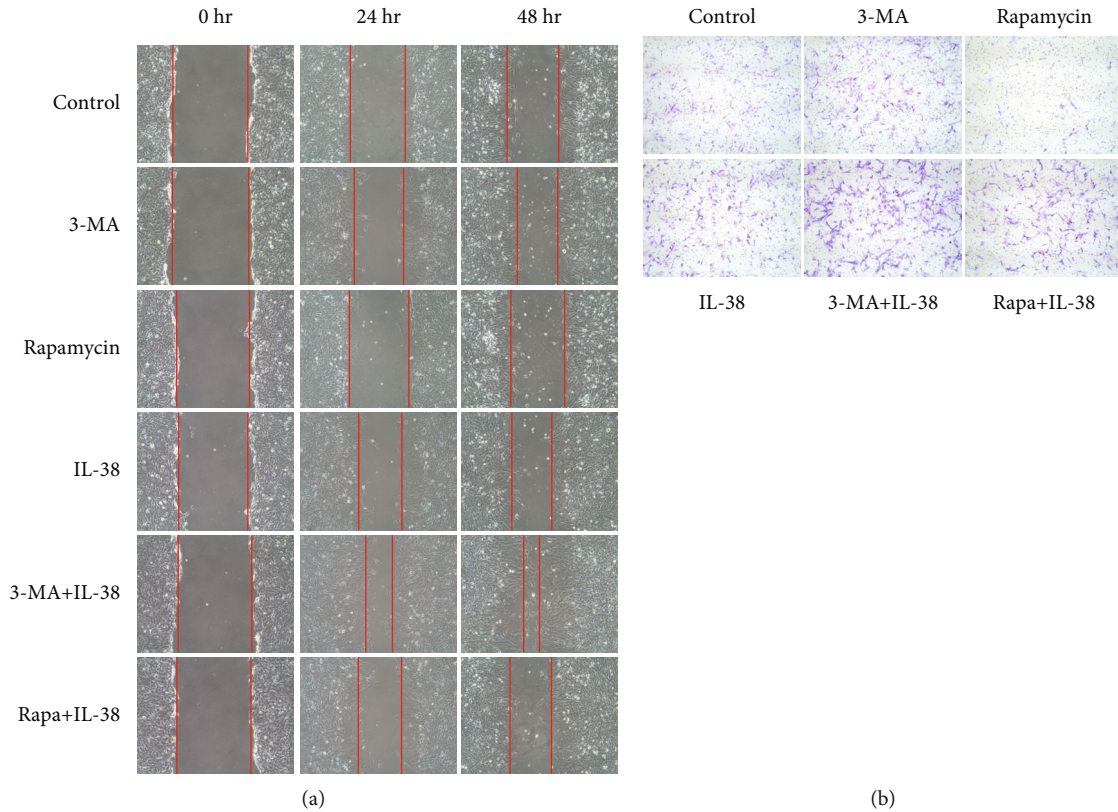


FIGURE 5: IL-38 facilitates synoviocyte migration and invasion via autophagy. (a) SW982 cells were transfected with IL-38 overexpression plasmids or empty vector and treated with 3-MA or rapamycin or left untreated. Cells were cultured for 12 hours followed by wound healing assay. Images of the wound were captured at 0, 24, and 48 hours after the wound was created. Representative micrographs (100x) from three independent experiments are shown. (b) S SW982 cells were transfected with IL-38 overexpression plasmids or empty vector and treated with 3-MA or rapamycin or left untreated. Cells were cultured for 24 hours and then digested by trypsin, resuspended, and seeded into upside well of the transwell system. After cultured for 24 hours, cells were subjected to crystal violet staining and microscopy examination. Three separate experiments were performed with consistent results, and represented images are shown.

invasion. IL-38 can bind with IL-36R and function as an antagonist to IL-36, thus interrupting IL-36 binding to heterodimeric receptor complex IL-36R/IL-1RAcP [27]. IL-36 binds to the IL-36R leading to nuclear factor kappa B/mitogen-activated protein kinase-mediated cytokine release [15]. Recently, a study reported that IL-36R may mediate the crosstalk between plasma cells and FLS [28]. Therefore, by competing IL-36R, elevated IL-38 and IL-36 together promoted FLS proliferation and migration, thus contributing to the pathogenesis of RA. Moreover, our preliminary study in rats showed that IL-36 treatment can relieve the symptoms of paw arthritis and inhibit the inflammation in the joint synovium of RA rats, indicating its possible clinical application.

Autophagy is a fundamental intracellular degradation process with multiple roles in immunity, thus maintaining cellular homeostasis and deciding cell fate [19]. Recent studies have revealed the involvement of autophagy in RA pathogenesis including elevated autophagy in RA-FLS for apoptosis resistance [29, 30]. Dysfunction of autophagy in RA-FLS leads to hyperplasia of synovial tissue, and down-regulated autophagy in cartilage cells is responsible for cell

death and cartilage destruction. The present study found that IL-36 accelerated and IL-38 impeded synovial cell autophagy. For now, there are barely a few references studying the relationship of IL-38 and IL-36 with autophagy. A recent report in 2020 reported that IL-36 activated autophagy to ablate the immune inhibitory of CD4+CD25+ Treg [31], thus aggravating host immune response and the development of sepsis. This is consistent with our conclusion that IL-36 promoted autophagy in RA for synoviocyte hyperplastic activity. No previous work characterized the role of IL-38 in autophagy. In consideration of the resemblance in anti-inflammation, IL-10 was described to suppress autophagy through activating PI3K/Akt/mTOR and JAK/STAT signal pathway. Indeed, de Graaf et al. currently found that IL-38 prevented the induction of trained immunity by inhibition of mTOR signaling [32]. This finding could be one theoretical foundation of our study. Also, IL-38 signaling results in the production of many inflammatory cytokines such as IL-2, IL-6, IL-13, and IL-17, all of which have the ability to participate in the autophagy process. IL-6 signals through STAT3/Bcl-2 to decline the expression of autophagy protein Beclin 1 for autophagy inhibition [33]; IL-17 activates

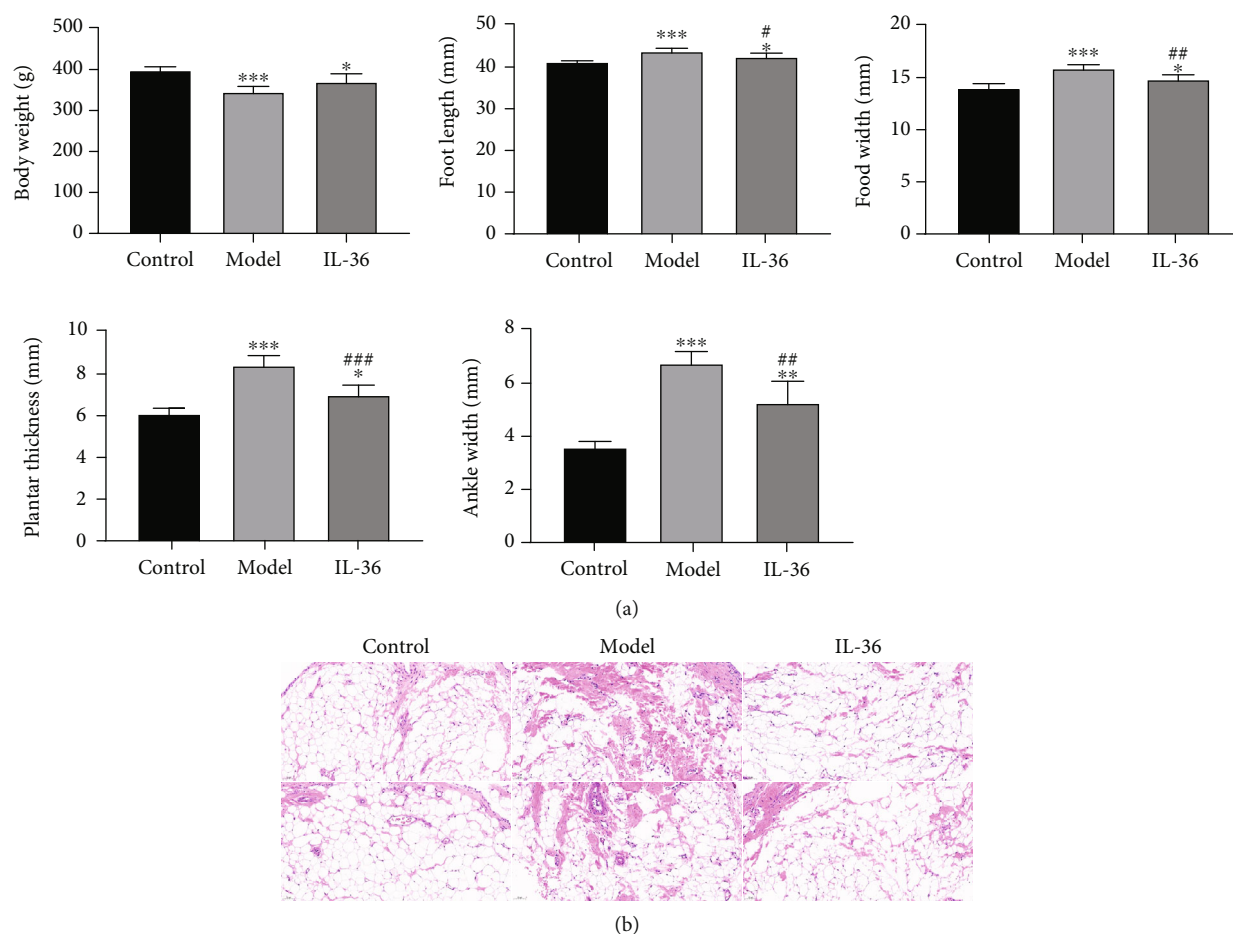


FIGURE 6: IL-36 treatment improve the symptoms of RA in a rat model. A rat model of RA was developed by injecting type II collagen combined with incomplete Freund's adjuvant to the articular cavity of hind ankle joint of the rat at the first and 7th day. Rats in the treatment group were injected with recombinant IL-36 from the first day to 10th day. All rats were sacrificed until the 28th day. (a) The body weight and the length and thickness of the ankles and feet were measured and compared. * $P < 0.05$, ** $P < 0.01$, *** $P < 0.001$ compared to the vector group; # $P < 0.05$, ## $P < 0.01$, ### $P < 0.001$ compared to the model group. (b) HE staining of the ankle joint synovium to show the inflammation and infiltration.

TAB2/3-mediated MAPK pathway to block autophagy progression [34]. Therefore, IL-38 might indirectly target autophagy for RA regulation.

IL-38 and IL-36 affect synovial cell proliferation, migration, and invasion, and they also modulate synovial cell autophagy. Autophagy is reported to modulate cell migration and invasion through different mechanisms [35–37]. Therefore, the effect of IL-38 and autophagy interaction on synovial cell proliferation, migration, and invasion was further studied. IL-36 was not further studied due to its inhibited effects on RA-FLS biological process. Our data showed that IL-38 promoted synovial cell proliferation, migration, and invasion via autophagy. Distinct mechanisms of pathogenesis and progression of RA are positively and negatively related to autophagy. Autophagy contributes to the microorganism elimination or immunological tolerance to prevent RA, whereas autophagy accelerates citrullinated antigen presentation and T cell and B cell activation [38]. Therefore, the modulation of cell events of IL-38 via autophagy may contribute to the immune regulation during RA.

In conclusion, here, we propose a working model of IL-36 and IL-38 regulating FLS function via autophagy, which connects newly discovered IL-36/IL-38 immune regulation with autophagy, providing the possibility of clinical application targeting both pathways. Preliminary in vivo study suggested that IL-36 has the potential for clinical application.

5. Conclusions

In conclusion, here, we propose a working model of IL-36 and IL-38 regulating FLS function via autophagy, which connects newly discovered IL-36/IL-38 immune regulation with autophagy, providing the possibility of clinical application targeting both pathways.

Data Availability

The data used to support the findings of this study are available from the corresponding author upon request.

Conflicts of Interest

The authors declare that they have no conflicts of interest.

References

- [1] J. S. Smolen, D. Aletaha, A. Barton et al., "Rheumatoid arthritis," *Nature Reviews. Disease Primers*, vol. 4, p. 18001, 2018.
- [2] D. L. Scott, F. Wolfe, and T. W. Huizinga, "Rheumatoid arthritis," *Lancet*, vol. 376, pp. 1094–1108, 2010.
- [3] K. D. Deane and V. M. Holers, "The natural history of rheumatoid arthritis," *Clinical Therapeutics*, vol. 41, pp. 1256–1269, 2019.
- [4] F. S. Azzeh and O. A. Kensara, "Vitamin D is a good marker for disease activity of rheumatoid arthritis disease," *Disease Markers*, vol. 2015, 2015.
- [5] F. Ingegnoli, R. Castelli, and R. Gualtierotti, "Rheumatoid factors: clinical applications," *Disease Markers*, vol. 35, 734 pages, 2013.
- [6] B. Bartok and G. S. Firestein, "Fibroblast-like synoviocytes: key effector cells in rheumatoid arthritis," *Immunological Reviews*, vol. 233, pp. 233–255, 2010.
- [7] S. Lefevre, A. Knedla, C. Tennie et al., "Synovial fibroblasts spread rheumatoid arthritis to unaffected joints," *Nature Medicine*, vol. 15, pp. 1414–1420, 2009.
- [8] I. B. McInnes and G. Schett, "The pathogenesis of rheumatoid arthritis," *The New England Journal of Medicine*, vol. 365, pp. 2205–2219, 2011.
- [9] L. Xie, Z. Huang, H. Li, X. Liu, S. Zheng, and W. Su, "IL-38: a new player in inflammatory autoimmune disorders," *Biomolecules*, vol. 9, 2019.
- [10] F. L. van de Veerdonk, D. M. de Graaf, L. A. Joosten, and C. A. Dinarello, "Biology of IL-38 and its role in disease," *Immunological Reviews*, vol. 281, pp. 191–196, 2018.
- [11] M. A. Boutet, G. Bart, M. Penhoat et al., "Distinct expression of interleukin (IL)-36alpha, beta and gamma, their antagonist IL-36Ra and IL-38 in psoriasis, rheumatoid arthritis and Crohn's disease," *Clinical and Experimental Immunology*, vol. 184, pp. 159–173, 2016.
- [12] S. I. Takenaka, S. Kaieda, T. Kawayama et al., "IL-38: a new factor in rheumatoid arthritis," *Biochem Biophys Rep*, vol. 4, pp. 386–391, 2015.
- [13] M. A. Boutet, A. Nerviani, and C. Pitzalis, "IL-36, IL-37, and IL-38 cytokines in skin and joint inflammation: a comprehensive review of their therapeutic potential," *International Journal of Molecular Sciences*, vol. 20, 2019.
- [14] M. A. Boutet, A. Najm, G. Bart et al., "IL-38 overexpression induces anti-inflammatory effects in mice arthritis models and in human macrophages in vitro," *Annals of the Rheumatic Diseases*, vol. 76, pp. 1304–1312, 2017.
- [15] F. Diomedea, M. Zingariello, M. Cavalcanti et al., "MyD88/ERK/NFkB pathways and pro-inflammatory cytokines release in periodontal ligament stem cells stimulated by *Porphyromonas gingivalis*," *European Journal of Histochemistry*, vol. 61, p. 2791, 2017.
- [16] D. Boraschi, P. Italiani, S. Weil, and M. U. Martin, "The family of the interleukin-1 receptors," *Immunological Reviews*, vol. 281, pp. 197–232, 2018.
- [17] S. Frey, A. Derer, M. E. Messbacher et al., "The novel cytokine interleukin-36alpha is expressed in psoriatic and rheumatoid arthritis synovium," *Annals of the Rheumatic Diseases*, vol. 72, pp. 1569–1574, 2013.
- [18] C. Lamacchia, G. Palmer, E. Rodriguez et al., "The severity of experimental arthritis is independent of IL-36 receptor signaling," *Arthritis Research & Therapy*, vol. 15, p. R38, 2013.
- [19] D. Glick, S. Barth, and K. F. Macleod, "Autophagy: cellular and molecular mechanisms," *The Journal of Pathology*, vol. 221, pp. 3–12, 2010.
- [20] B. Levine, N. Mizushima, and H. W. Virgin, "Autophagy in immunity and inflammation," *Nature*, vol. 469, pp. 323–335, 2011.
- [21] Y. Feng, B. Li, X. Y. Li, and Z. B. Wu, "The role of autophagy in rheumatic disease," *Current Drug Targets*, vol. 19, pp. 1009–1017, 2018.
- [22] J. S. Rockel and M. Kapoor, "Autophagy: controlling cell fate in rheumatic diseases," *Nature Reviews Rheumatology*, vol. 12, pp. 517–531, 2016.
- [23] K. Xu, Y. S. Cai, S. M. Lu et al., "Autophagy induction contributes to the resistance to methotrexate treatment in rheumatoid arthritis fibroblast-like synovial cells through high mobility group box chromosomal protein 1," *Arthritis Research & Therapy*, vol. 17, p. 374, 2015.
- [24] J. M. Ireland and E. R. Unanue, "Autophagy in antigen-presenting cells results in presentation of citrullinated peptides to CD4 T cells," *The Journal of Experimental Medicine*, vol. 208, pp. 2625–2632, 2011.
- [25] K. Xu, P. Xu, J. F. Yao, Y. G. Zhang, W. K. Hou, and S. M. Lu, "Reduced apoptosis correlates with enhanced autophagy in synovial tissues of rheumatoid arthritis," *Inflammation Research*, vol. 62, pp. 229–237, 2013.
- [26] G. Nygaard and G. S. Firestein, "Restoring synovial homeostasis in rheumatoid arthritis by targeting fibroblast-like synoviocytes," *Nature Reviews Rheumatology*, vol. 16, pp. 316–333, 2020.
- [27] F. L. van de Veerdonk, A. K. Stoeckman, G. Wu et al., "IL-38 binds to the IL-36 receptor and has biological effects on immune cells similar to IL-36 receptor antagonist," *Proceedings of the National Academy of Sciences of the United States of America*, vol. 109, pp. 3001–3005, 2012.
- [28] V. Schmitt, M. Hahn, V. Kästle et al., "Interleukin-36 receptor mediates the crosstalk between plasma cells and synovial fibroblasts," *European Journal of Immunology*, vol. 47, pp. 2101–2112, 2017.
- [29] Y. M. Chen, C. Y. Chang, H. H. Chen et al., "Association between autophagy and inflammation in patients with rheumatoid arthritis receiving biologic therapy," *Arthritis Research & Therapy*, vol. 20, p. 268, 2018.
- [30] Y. Dai and S. Hu, "Recent insights into the role of autophagy in the pathogenesis of rheumatoid arthritis," *Rheumatology*, vol. 55, pp. 403–410, 2016.
- [31] Y. Ge, M. Huang, N. Dong, and Y. M. Yao, "Effect of interleukin-36beta on activating autophagy of CD4+CD25+ regulatory T cells and its immune regulation in sepsis," *The Journal of Infectious Diseases*, vol. 222, pp. 1517–1530, 2020.
- [32] D. M. de Graaf, L. U. Teufel, F. L. van de Veerdonk et al., "IL-38 prevents induction of trained immunity by inhibition of mTOR signaling," *Journal of Leukocyte Biology*, vol. 110, no. 5, pp. 821–998, 2021.
- [33] B. Qin, Z. Zhou, J. He, C. Yan, and S. Ding, "IL-6 inhibits starvation-induced autophagy via the STAT3/Bcl-2 signaling pathway," *Scientific Reports*, vol. 5, p. 15701, 2015.

- [34] Y. Zhou, P. W. Wu, X. W. Yuan, J. Li, and X. L. Shi, "Interleukin-17A inhibits cell autophagy under starvation and promotes cell migration via TAB2/TAB3-p38 mitogen-activated protein kinase pathways in hepatocellular carcinoma," *European Review for Medical and Pharmacological Sciences*, vol. 20, pp. 250–263, 2016.
- [35] Y. Wang, H. Xiong, D. Liu et al., "Autophagy inhibition specifically promotes epithelial-mesenchymal transition and invasion in RAS-mutated cancer cells," *Autophagy*, vol. 15, pp. 886–899, 2019.
- [36] L. Zhang, X. Liu, L. Song, H. Zhai, and C. Chang, "MAP7 promotes migration and invasion and progression of human cervical cancer through modulating the autophagy," *Cancer Cell International*, vol. 20, p. 17, 2020.
- [37] W. Zhou, Q. Shen, H. Wang et al., "Knockdown of YAP/TAZ inhibits the migration and invasion of fibroblast synovial cells in rheumatoid arthritis by regulating autophagy," *Journal of Immunology Research*, vol. 2020, 2020.
- [38] M. Vomero, C. Barbati, T. Colasanti et al., "Autophagy and rheumatoid arthritis: current knowledges and future perspectives," *Frontiers in Immunology*, vol. 9, article 1577, 2018.

Research Article

mtDNA in the Pathogenesis of Cardiovascular Diseases

Lili Wang , Qianhui Zhang , Kexin Yuan , and Jing Yuan 

Department of Cardiology, Hebei General Hospital, Shijiazhuang, Hebei Province, China

Correspondence should be addressed to Lili Wang; drwanglili@126.com

Received 21 August 2021; Revised 6 October 2021; Accepted 24 October 2021; Published 9 November 2021

Academic Editor: Wen-Jun Tu

Copyright © 2021 Lili Wang et al. This is an open access article distributed under the Creative Commons Attribution License, which permits unrestricted use, distribution, and reproduction in any medium, provided the original work is properly cited.

The incidence rate of cardiovascular disease (CVD) has been increasing year by year and has become the main cause for the increase of mortality. Mitochondrial DNA (mtDNA) plays a crucial role in the pathogenesis of CVD, especially in heart failure and ischemic heart diseases. With the deepening of research, more and more evidence showed that mtDNA is related to the occurrence and development of CVD. Current studies mainly focus on how mtDNA copy number, an indirect biomarker of mitochondrial function, contributes to CVD and its underlying mechanisms including mtDNA autophagy, the effect of mtDNA on cardiac inflammation, and related metabolic functions. However, no relevant studies have been conducted yet. In this paper, we combed the current research status of the mechanism related to the influence of mtDNA on the occurrence, development, and prognosis of CVD, so as to find whether these mechanisms have something in common, or is there a correlation between each mechanism for the development of CVD?

1. Introduction of mtDNA Structure and Function

[1] mtDNA itself is a small, double-stranded circular molecule, and human mtDNA is 16,569 bp in length. mtDNA encodes 13 polypeptide subunits of the oxidative phosphorylation (OXPHOS) enzyme complexes, 22 transfer RNAs, and 2 ribosome RNAs, which are needed for mitochondrial respiration [2]. Unlike nuclear DNA (nDNA), mtDNA lacks histone protection and efficient DNA repair function, making it vulnerable to damage. We know that DNA is the major genetic material and contains genetic information. About 30% of the genetic profile in mtDNA is used to encode, and about 70% is used to encode the proteins within the mitochondria, so the disease caused by changes in mtDNA will have the corresponding genetic nature. A growing number of studies have shown that mtDNA plays an important role in the regulation of innate immunity and can induce inflammatory disease via affecting cell stress. Mitochondrial dysfunction, resulting in release of mtDNA called damage-associated molecular pattern (DAMP), can trigger natural immunity, leading to DAMP activation of inflammation. Furthermore, the characteristics of mtDNA

and bacterial DNA are similar; 30 released mtDNA molecules can cause CVDs such as atherosclerosis by inducing inflammatory reaction. The decrease of mtDNA increased autophagy regulating function, and CVD after myocardial cell damage can also lead to line body dysfunction, release more mtDNA to cells, and cause CVD through various mechanisms, which form a circle. Therefore, it is significant to study the multiple mechanisms of mtDNA on the occurrence, development, and prognosis of CVD, which can provide new ideas for clinical treatment.

2. mtDNA Copy Number and CVD

mtDNA is the only relatively independent genome that exists in organelles. It can control and encode part of proteins, and it can indirectly reflect mitochondrial function. The copy number of mtDNA in the genome can predict CVD's occurrence, development, and prognosis. Foram et al. showed that the copy number of mtDNA is inversely proportional to CVD events, and the influence on CVD risk assessment of young individuals is significantly increased [3]. However, the sample size of the above studies is small. Therefore, multi-factor analysis of age, region, sex, blood

lipid, blood pressure, smoking status and related drugs should be studied and to determine the application potential of mtDNA in clinic. Christina et al. evaluated 2,507 African-Americans and European-Americans for community arteriosclerosis risk and studied the relationship between mtDNA-CN and nDNA methylation. They have shown that the regulation of mtDNA copy number leads to differences in the methylation and expression of genes associated with signal transduction processes, thus affecting the expression status of crucial genes in human pathophysiological process [4]. In addition, mtDNA copy number plays a certain role in the development of CVD. mtDNA copy number may reflect the degree of mtDNA damage and may be a biomarker of mitochondrial function and a predictor of cardiovascular disease risk. It has been reported in the literature that mtDNA copy number in the cardiomyocytes of patients with heart failure is significantly decreased. Oxidative stress can aggravate heart failure and cardiac remodeling, and the electron transport chain in mitochondria is an important source of oxidative free radicals. In myocardial infarction mice, the expression of the antioxidant gene peroxiredoxin-3 (PRX-3) and mtTFA can, to some extent, increase mtDNA copy number in patients with heart failure, delay pathological myocardial remodeling, and improve the survival rate of mice. Ikeda et al. found that in mice overexpressing mtTFA and Twinkle helical protein, mtDNA copy number was increased by 2 times and myocardial damage in isolated cardiac hypertrophy was alleviated [5]. Therefore, increasing mtDNA copy number becomes a new way to treat myocardial injury mediated by oxidative stress.

mtDNA copy number variation is influenced by environmental and genetic factors, among them, oxidative stress is one of the most important factors. Different effects of these factors on mtDNA copy number need more research to clarify. At the same time, how mtDNA copy number variation works on the prediction of the occurrence and development of diseases and its appropriate application in treatment also will be the important direction of research in the future.

3. mtDNA Inflammatory Response

“Aseptic inflammation of the heart” is usually a secondary response to myocardial damage caused by ischemia injury or heart failure. A growing number of researches have demonstrated that inflammation plays an important role in the physiological and pathological progress of heart failure [6]. The expression level of inflammatory factors in patients with heart failure was significantly higher than that in healthy people [7, 8]. The abnormal expression of inflammatory factors and their receptors are closely associated with the mortality of patients with severe heart failure and the poor prognosis of idiopathic dilated cardiomyopathy [9–11]. Besides, studies have identified that the expression status of TNF- α in serum is closely related to the severity of heart failure [7, 8]. Relative hypomethylation, unique structural characteristics, and vulnerability to oxidative damage make mtDNA a potentially potent DAMP in disease, which activates innate immunity to induce inflammation and type I

interferon responses. Recent studies have found that pattern recognition receptors (PRRs), including TLR-9, NLRP3 inflammasome, and GMP-AMP synthase- (cGAS-) STING pathway, are key promoters of mtDNA-related inflammatory responses [12, 13]. The proinflammatory function of mtDNA was first identified in 2004 by Collins et al. [14]. In this study, the researchers injected mtDNA instead of nDNA into the articular cavity of mice and found that mtDNA could promote the inflammatory response of joints by inducing the secretion of TNF- α in spleen cells. At the same time, it has been reported that loss of mitochondrial DNA attenuates IL-1 β secretion in macrophages by inhibiting activation of inflammasome after treatment with lipopolysaccharide (LPS) and ATP [15]. The way mtDNA participates in inflammatory response is similar to that of bacteria. Significantly, oxidation is necessary in mtDNA-related inflammatory response [16, 17]. When mtDNA binds to TFAM, nucleotide has a high stability; otherwise, mtDNA is in a fragile and easily degraded state. It has been reported that the abnormal expression of TFAM or mtDNA caused by oxidative modification is the decisive factor leading to the combination of TFAM and mtDNA and the instability of nucleoid. However, the role of defective TFAM and mtDNA binding in inflammatory response is still unknown. The study found showed that both cell-free mtDNA and TFAM-bound mtDNA play an important role in inflammatory response [18].

3.1. mtDNA, as an Inflammatory Mediator, Interacts with the following Substances to Produce an Autoimmune Stress Response and Trigger Inflammation

3.1.1. *Toll-Like Receptor 9*. Studies had shown that acute myocardial infarction can cause aseptic inflammation, aggravate tissue damage, and lead to increased levels of mtDNA, which activates the NF- κ B pathway through TLR9 and triggers an innate immune response, leading to myocardial cell damage. In arteriosclerosis, the released mtDNA forms a complex with the human antimicrobial peptide LL-37, which is resistant to degradation of deoxyribonuclease 2 and escapes autophagy recognition, leading to the activation of TLR9-mediated inflammatory response and the sustained activation of TLR9, causes autoimmune activation of chemokines and live cytokines, and exacerbates arteriosclerosis [19]. Increased mtDNA in plasma source exosomes in chronic heart failure triggers an inflammatory response through the TLR9-NF- κ B pathway [20]. mtDNA released in acute myocardial infarction activates TLR9 and aggravates ischemia reperfusion injury through the TLR9-p38 MAPK pathway, thus exacerbating myocardial injury. Myocardial ischemia-reperfusion injury is a challenging clinical problem. During myocardial ischemia-reperfusion injury, a large amount of mtDNA is released, which causes inflammatory reaction and aggravates myocardial injury [21]. Current studies suggest that chloroquine interferes with TLR9-mediated inflammatory signaling and transduction, and PDTIC inhibits NF- κ B and inhibits NF- κ B activation by metal chelation. More suitable drugs and dosages require further study [22].

3.1.2. NLRP3 and Inflammasomes. NLRP3 is the second factor that has been shown to influence the inflammatory response through REDOX and mtDNA. NLRP3 is very sensitive to bacterial infection, viral invasion, and other pathogenic factors [23, 24]. It was found that mtROS activated NLRP3, and the mechanism was closely related to the oxidation of mtDNA [15, 16, 25, 26]. mtROS can influence mtDNA subcellular localization and activate NLRP3 inflammasome by binding NLRP3 [16]. NLRP3 inflammasome is a multiprotein complex composed of NLRP3, which is a spot-like protein with a caspase activation and recruitment domain and is closely related to apoptosis. It has been reported that NLRP3 and ASC colocalize to mitochondrial clusters in the endoplasmic reticulum-perinuclear space when NLRP3 inflammasome is activated, thereby inducing caspase 1 cleavage and activation [27]. When caspase-1 is activated, the expression levels of proinflammatory factors such as IL-1 and IL-18 are significantly increased and thus participate in REDOX inflammatory reactions [28]. Besides, deletion of NLRP3 and caspase-1 genes reduces mtDNA release [15, 26]. It has also been found that nonoxidative mitochondrial DNA can induce IL-1 β secretion by activating inflammatory bodies such as AIM2 [29]. Multiple risk factors of CVD are also considered to activate inflammasomes, so intervention in the activation of inflammasomes can be a prevention and treatment target of cardiovascular disease. Heart function of I/R mice with NLRP3 defect was improved, and hypoxia injury was reduced. Under the action of ATP, ischemic myocardial fibroblasts promote the assembly and upregulation of NLRP3 inflammasomes, thus affecting the infarct size. By constructing a mouse model of ischemic injury, the use of NLRP3 inflammasome inhibitors prevented myocardial cell death and reduced left ventricular systolic function in mice to a certain extent. In heart failure following ischemic heart injury, a strong inflammatory response leads to further injury and dysfunction of cardiac contraction and expansion, and the release of cell debris during tissue injury causes conformational changes in NLRP3 inflammasomes, leading to the activation of caspase-1. Clinical treatment of heart failure patients with IL-1 antagonist injection showed increased oxygen consumption, which is expected to be a new direction of heart failure treatment in the future.

Currently, the NLRP3 inflammasome's influence on heart failure has been largely focused on its mediated role in IL-1 and IL-18 in heart remodeling. The activation of NLRP3 inflammasomes in mice had been shown to induce heart failure by promoting myocardial inflammation and systolic dysfunction by producing proinflammatory IL-1 [30].

3.1.3. Cyclic GMP-AMP Synthetase. When first discovered, the cGAS-STING signaling pathway was thought to be a crucial component of the innate immune system; its function being to detect the existence of cytoplasmic DNA and induce the secretion of inflammatory factors. When the cyclic GMP-AMP synthase (cGAS) senses DNA that should not be present in the cytoplasm, it catalyzes a chemical reaction between GTP and ATP that produces a small molecule called cyclic GMP-AMP (cGAMP); the molecule acts as a

messenger for innate immune system, further activating the immune response. Therefore, cGAS is like a burglar alarm, and cGAMP is the electrical signal generated by the burglar alarm [31, 32]. In recent years, STING has been identified as a cytoplasmic anchored protein capable of directly binding to double-stranded DNA or initiating IFN response via cyclic dinucleotide activation. In addition, the IFN response initiated by STING can also be realized by affecting mtDNA [33, 34]. The mechanism is that when STING binds to mtDNA, cGAS will begin to recruit STING proteins, and STING induces phosphorylation of transcription factor IRF-3 through activation of TANK (NF- κ B activator associated with TRAF family members) binding kinase and NF- κ B signaling pathway [35]. mtDNA also activates cGAS-STING to initiate the production of type 1 interferon (IFN), which triggers an inflammatory response [36]. Recent literature suggests that mtDNA released into the cytoplasm during apoptosis may activate cGAS to produce cGAMP, which enlists STING, and downstream to further activate TBK1-IRF3 signaling pathway to produce IFN-7 and IFN-8. In addition, recent studies have shown that mtDNA produced by herpes virus infection can also activate the cGAS-STING signaling pathway. Activated IRF-3 mediates transcription of nuclear gene products stimulated by type I and type III IFN and IFN leading to mtDNA-induced inflammatory response. In physiological environment, oxidative mtDNA whole-body injection increased IFN-stimulated gene expression in the spleen of wild-type mice, but not in STING-deficient mice. Therefore, the study of cGAS and STING targeted drugs for the treatment of chronic inflammation has a good prospect.

4. mtDNA Autophagy and Cardiovascular Disease

The inflammatory response triggered by mtDNA is closely related to autophagy. Autophagy is a key adaptive mechanism by which excess cytoplasmic components (such as DNA, proteins, mitochondria, and intracellular pathogens) are "confiscated" by double-membrane vacuoles (autophages) that fuse with lysosomes to degrade the cytoplasmic components captured in them for clearance, to protect the cells from stress-induced damage [37]. The pathological process of a variety of CVD is accompanied by changes in the autophagy of cardiac myocytes. Myocardial injury activates autophagy's repair of cells. If the damage is severe, it could cause apoptotic process. In addition, autophagy can limit the inflammatory response by regulating key immune regulators such as NF- κ B10 and STING11. In pathological conditions such as microbial infection and major trauma, when malfunctioning mitochondria and damaged mtDNA accumulate in the cytoplasm beyond the capacity of autophagy, the negative regulatory function of autophagy is lost. As a result, the inflammatory response increased significantly, often accompanied by chronic inflammation, which is caused by abnormal responses to TLR92, TLR12, NLRP35, and/or cGAS-STING13, thus triggering the occurrence and development of CVD [38].

TABLE 1: Cardiovascular diseases associated with pathogenic mtDNA mutations.

Mutation type	Mutant gene mutations in the genes	Disease	Reference
Basepair substitution	mtDNA A4401G		[50]
	mtDNA T14484G		[51]
tRNA genetic mutation	tRNA ^{Met} m.A4435G	Hypertension	[52–58]
	tRNA ^{Leu} m.A3243G		
	tRNA ^{Leu} m.A4263G		
	tRNA ^{Leu} m.T4353C		
	tRNA ^{Phe} m.C593T		
	tRNA ^{Trp} m.C5553T		
	tRNA ^{Glc} m.T4353C		
	tRNA ^{Ile} m.T4291C		
mRNA mutation	tRNA ^{Leu} m.T3253C		
	tRNA ^{Ala} m.A5655G		
tRNA genetic mutation	m.A8701G in ATP6		[59]
	tRNA ^{Thr} m.G15927A		
mtDNA deletion	tRNA ^{Phe} m.T5592C	Coronary atherosclerotic disease	[60]
	tRNA ^{Leu} m.A3243G		
Basepair substitution	mtDNA4977bp Deletion		[61]
mtDNA deletion	mtDNA T16189C		[62]
Basepair substitution	mtDNA4977bp Deletion	Arrhythmia	[63]
tRNA genetic mutation	mtDNA T14709C		[64]
	tRNA ^{Ala} m.4322dupC		[65]
mtDNA rearrangement deletion	tRNA ^{Leu} m.A3243G	Cardiomyopathy	[66]
	7.5 KB deletion between ATPASE6 gene and D loop		
tRNA genetic mutation	mtDNA7436bp Deletion		[67]
tRNA genetic mutation	tRNA ^{Leu} m.A3243G	Heart failure	[68]

Therefore, the research on autophagy inducers will help to improve the loss of autophagy caused by mtDNA, thus reducing the impact of chronic inflammation on CVD. mtDNA that escapes autophagy can trigger an inflammatory response in cardiomyocytes mediated by Toll-like receptor TLR9 and can induce myocarditis and dilated cardiomyopathy [39].

This study provided a new idea for elucidating the mechanism of chronic inflammation in heart failure. By forming a complex with human antimicrobial Peptide LL-37, mtDNA from dead cells or from the structure of NET not only can not be eliminated by DNASE II, the LL-37-mtDNA complex formed at the same time, after entering into the cells, becomes difficult to clear by avoiding the autophagy recognition, resulting in the continuous activation of the TLR9 signaling pathway in the cells [40].

5. mtDNA Mutations and Cardiovascular Disease

In view of the structure of mtDNA and its own genetic characteristics, mtDNA is prone to mutation. Holt and Wallace initially detected mtDNA mutations, respectively, in cells from patients with mitochondrial encephalomyopathy and Leber hereditary neuropathy. Mutations are possible candi-

date risk factors for cardiovascular disease due to the effect of mitochondria on energy metabolism and the generation of reactive oxygen species by evidence-based complementary and alternative drugs. With the improvement of scientific research level, multiple researches have demonstrated that CVD and mtDNA mutations are closely related, such as heart block, myocarditis, and sudden death. These studies provided theoretical and experimental basis for elucidating the pathogenesis of CVD. However, the current research is limited to the detection of some mtDNA mutations in some CVD, but how do the mutated genes change the structure and function of the proteins they encode and how the mtDNA directed proteins affect the occurrence and development of mitochondrial diseases caused by oxidative stress and energy metabolism remain to be further studied.

6. mtDNA and Metabolic Memory in Diabetic Cardiomyopathy

More than 40 years ago, some scholars discovered a disease that can occur independently of cardiovascular disease or hypertension, which was named diabetic cardiomyopathy (DCM). At present, its pathogenesis has not been fully clarified [41]. Multiple pathophysiological mechanisms of DCM

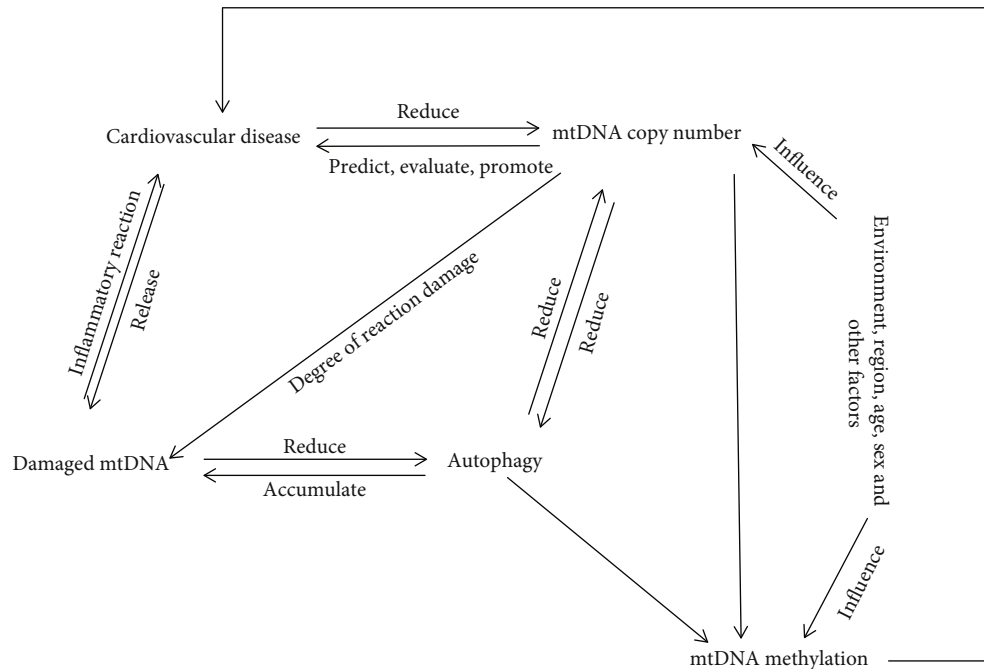


FIGURE 1: Relationship between mtDNA and cardiovascular disease. Multiple mechanisms interact to influence the occurrence, development, and prognosis of cardiovascular disease.

had been identified, such as the existence of hyperglycemia, nonenzymatic glycosylation of macromolecules (such as proteins), disorder of energy metabolism, mitochondrial dysfunction, improper calcium treatment, abnormal reactive oxygen species, inflammation, cardiomyocyte death, and cardiac hypertrophy and fibrosis, resulting in impaired cardiac systolic function. There was also growing evidence that a phenomenon called “metabolic memory” exists in cardiovascular complications of diabetes, suggesting that these pathogenic mechanisms might be controlled by mtDNA epigenetic modifications. While how epigenetic mechanisms work is still not fully understood, a series of studies have demonstrated its importance in modulating the cardiac response to diabetes, and these studies are believed to contribute to an in-depth comprehending of the specific mechanisms of DCM and their possible prevention and/or treatment. Cong et al. found that mitochondrial glucose and lipid metabolism disorders were one of the important mechanisms of DCM. There were two ways to increase ROS in myocardium: mitochondrial and extramitochondrial [42, 43]. Boudina et al. study found enhanced mitochondrial uncoupling and mitochondrial respiratory chain dysfunction in cardiomyocytes of DB/DB mice with type 2 diabetes [44]. In addition, increased UCP3 expression, mitochondrial damage, and reduced heart energy efficiency were reported after cardiac ischemia in DB/DB mice [45]. The dysregulation of mitochondrial Ca^{2+} in DCM is a research hotspot in these years, and the presence of mitochondrial Ca^{2+} regulation disorders in diabetic animal models had been reported in laboratory [46, 47]. Mitochondrial dysfunction has a significant effect on the occurrence and progression of diabetic cardiomyopathy. mtDNA damage of myocardial cells caused by oxidative stress affects the pathogenesis of

diabetic cardiomyopathy significantly. Mitochondrial oxidative stress was considered to be the single cause of mtDNA damage and the underlying cause of mitochondrial dysfunction. The formation of 8-hydroxy-2'-deoxyguanosine (8-OHdG) is a classic manifestation of mtDNA damage, which leads to mutations when the 8-oxoguanosine DNA glycosylase (Ogg1) is not repaired properly; Cividini et al. showed that high glucose induced o-GlcNAcylation of Ogg1 and increased mtDNA damage [48]. Hicks et al. showed that increased oxidative stress induced by diabetes would change the function of mitochondrial topoisomerase, and the activation/inhibition state of mitochondrial topoisomerase would have an important impact on mtDNA integrity and myocardial health in diabetes mellitus. Although mtDNA repair mechanisms have been demonstrated in cardiomyocytes, the mechanisms of this repair have not been fully identified [49]. Therefore, these findings provided a new possible biochemical mechanism for diabetic cardiomyopathy.

7. Summary

From the literature, it is clear that mtDNA plays an important role in keeping mitochondria normal (Table 1). The copy number of mtDNA can reflect the occurrence and development of CVD to some extent. mtDNA damage not only causes a variety of related metabolic diseases in human body but also is an important point of CVD and causes of new coronary CVD. mtDNA is special due to its composition and structure, such as no histone protection and located near the respiratory chain, the main site of endogenous oxygen radicals. It is vulnerable to damage by free radicals and is not easy to repair due to its poor damage repair ability. Because mtDNA is directly related to energy metabolism

in vivo, mtDNA damage can easily lead to reduced ATP synthesis and cause cell senescence and even death. Apoptosis or necrosis is regulated by multiple factors, among which mtDNA damage may be one of the effects of many mechanisms on cardiovascular disease. The physiological mechanism network system constructed by mtDNA copy, injury, senility, apoptosis, autophagy, and so on plays an important role in the occurrence of CVD (Figure 1). The combined effect of mtDNA on CVD needs to be further studied, and the effects of mtDNA polymorphism on cardiovascular diseases should also be studied.

Data Availability

No data were used to support this study.

Conflicts of Interest

The authors declare that there is no conflict of interests regarding the publication of this paper.

References

- [1] J. L. Elson, M. Venter, and F. H. Van der Westhuizen, "The aetiology of cardiovascular disease: a role for mitochondrial DNA?," *Cardiovascular journal of Africa*, vol. 29, no. 2, pp. 122–132, 2018.
- [2] D. A. Brown, J. B. Perry, M. E. Allen et al., "Mitochondrial function as a therapeutic target in heart failure," *Nature Reviews Cardiology*, vol. 14, no. 4, pp. 238–250, 2017.
- [3] F. N. Ashar, Y. Zhang, R. J. Longchamps et al., "Association of mitochondrial DNA copy number with cardiovascular disease," *JAMA Cardiology*, vol. 2, no. 11, pp. 1247–1255, 2017.
- [4] C. A. Castellani, R. J. Longchamps, J. A. Sumpter et al., "Mitochondrial DNA copy number can influence mortality and cardiovascular disease via methylation of nuclear DNA CpGs," *Genome medicine*, vol. 12, no. 1, pp. 1–7, 2020.
- [5] M. Ikeda, T. Ide, T. Fujino et al., "Overexpression of TFAM or twinkle increases mtDNA copy number and facilitates cardioprotection associated with limited mitochondrial oxidative stress," *PloS one*, vol. 10, no. 3, p. e0119687, 2015.
- [6] S. Van Linthout and C. Tschöpe, "Inflammation-cause or consequence of heart failure or both?," *Current Heart Failure Reports*, vol. 14, no. 4, pp. 251–265, 2017.
- [7] G. Torre-Amione, S. Kapadia, C. Benedict, H. Oral, J. B. Young, and D. L. Mann, "Proinflammatory cytokine levels in patients with depressed left ventricular ejection fraction: a report from the Studies of Left Ventricular Dysfunction (SOLVD)," *Journal of the American College of Cardiology*, vol. 27, no. 5, pp. 1201–1206, 1996.
- [8] D. L. Mann, "Inflammatory mediators and the failing heart: past, present, and the foreseeable future," *Circulation Research*, vol. 91, no. 11, pp. 988–998, 2002.
- [9] A. Deswal, N. J. Petersen, A. M. Feldman, J. B. Young, B. G. White, and D. L. Mann, "Cytokines and cytokine receptors in advanced heart failure: an analysis of the cytokine database from the Vesnarinone Trial (VEST)," *Circulation*, vol. 103, no. 16, pp. 2055–2059, 2001.
- [10] A. Yndestad, A. M. Holm, F. Müller et al., "Enhanced expression of inflammatory cytokines and activation markers in T-cells from patients with chronic heart failure," *Cardiovascular Research*, vol. 60, no. 1, pp. 141–146, 2003.
- [11] I. Kindermann, M. Kindermann, R. Kandolf et al., "Predictors of outcome in patients with suspected myocarditis," *Circulation*, vol. 118, no. 6, pp. 639–648, 2008.
- [12] J. Wu, L. Sun, X. Chen et al., "Cyclic GMP-AMP Is an Endogenous Second Messenger in Innate Immune Signaling by cytosolic DNA," *Science*, vol. 339, no. 6121, pp. 826–830, 2013.
- [13] H. Nakayama and K. Otsu, "Mitochondrial DNA as an inflammatory mediator in cardiovascular diseases," *Biochemical Journal*, vol. 475, no. 5, pp. 839–852, 2018.
- [14] L. V. Collins, S. Hajizadeh, E. Holme, I. M. Jonsson, and A. Tarkowski, "Endogenously oxidized mitochondrial DNA induces in vivo and in vitro inflammatory responses," *Journal of Leukocyte Biology*, vol. 75, no. 6, pp. 995–1000, 2004.
- [15] K. Nakahira, J. A. Haspel, V. A. Rathinam et al., "Autophagy proteins regulate innate immune responses by inhibiting the release of mitochondrial DNA mediated by the NALP3 inflammasome," *Nature Immunology*, vol. 12, no. 3, pp. 222–230, 2011.
- [16] K. Shimada, T. R. Crother, J. Karlin et al., "Oxidized mitochondrial DNA activates the NLRP3 inflammasome during apoptosis," *Immunity*, vol. 36, no. 3, pp. 401–414, 2012.
- [17] K. Pazmandi, Z. Agod, B. V. Kumar et al., "Oxidative modification enhances the immunostimulatory effects of extracellular mitochondrial DNA on plasmacytoid dendritic cells," *Free Radical Biology & Medicine*, vol. 77, pp. 281–290, 2014, Epub 2014 Oct 7.
- [18] G. H. Kunkel, P. Chaturvedi, and S. C. Tyagi, "Mitochondrial pathways to cardiac recovery: TFAM," *Heart Failure Reviews*, vol. 21, no. 5, pp. 499–517, 2016.
- [19] M. Bliksøen, L. H. Mariero, M. K. Torp et al., "Extracellular mtDNA activates NF- κ B via toll-like receptor 9 and induces cell death in cardiomyocytes," *Basic Research in Cardiology*, vol. 111, no. 4, p. 42, 2016.
- [20] W. Ye, X. Tang, Z. Yang et al., "Plasma-derived exosomes contribute to inflammation via the TLR9-NF- κ B pathway in chronic heart failure patients," *Molecular Immunology*, vol. 87, pp. 114–121, 2017, Epub 2017 Apr 25.
- [21] J. Yang, J. He, M. Ismail et al., "HDAC inhibition induces autophagy and mitochondrial biogenesis to maintain mitochondrial homeostasis during cardiac ischemia/reperfusion injury," *Journal of molecular and cellular cardiology*, vol. 130, pp. 36–48, 2019.
- [22] C. A. Puyo, A. Earhart, N. Staten et al., "Mitochondrial DNA induces Foley catheter related bladder inflammation via Toll-like receptor 9 activation," *Scientific report*, vol. 8, no. 1, pp. 1–12, 2018.
- [23] N. Kelley, D. Jeltema, Y. Duan, and Y. He, "The NLRP3 inflammasome: an overview of mechanisms of activation and regulation," *International Journal of Molecular Sciences*, vol. 20, no. 13, p. 3328, 2019.
- [24] P. Duewell, H. Kono, K. J. Rayner et al., "NLRP3 inflammasomes are required for atherogenesis and activated by cholesterol crystals," *Nature*, vol. 464, no. 7293, pp. 1357–1361, 2010.
- [25] Z. Zhang, X. Xu, J. Ma et al., "Gene deletion of gabarap enhances Nlrp3 inflammasome-dependent inflammatory responses," *Journal of Immunology*, vol. 190, no. 7, pp. 3517–3524, 2013.
- [26] J. H. Won, S. Park, S. Hong, S. Son, and J. W. Yu, "Rotenone-induced impairment of mitochondrial electron transport chain

- confers a selective priming signal for NLRP3 inflammasome activation," *Journal of Biological Chemistry*, vol. 290, no. 45, pp. 27425–27437, 2015.
- [27] R. Zhou, A. S. Yazdi, P. Menu, and J. Tschopp, "A role for mitochondria in NLRP3 inflammasome activation," *Nature*, vol. 469, no. 7329, pp. 221–225, 2011.
- [28] T. Strowig, J. Henao-Mejia, E. Elinav, and R. Flavell, "Inflammasomes in health and disease," *Nature*, vol. 481, no. 7381, pp. 278–286, 2012.
- [29] Y. Dombrowski, M. Peric, S. Koglin et al., "Honey bee (*Apis mellifera*) venom induces AIM2 inflammasome activation in human keratinocytes," *Allergy*, vol. 67, no. 11, pp. 1400–1407, 2012.
- [30] S. Sano, K. Oshima, Y. Wang et al., "Tet2-mediated clonal hematopoiesis accelerates heart failure through a mechanism involving the IL-1 β /NLRP3 inflammasome," *Journal of the American College of Cardiology*, vol. 71, no. 8, pp. 875–886, 2018.
- [31] H. Ishikawa and G. N. Barber, "The STING pathway and regulation of innate immune signaling in response to DNA pathogens," *Cellular and Molecular Life Sciences*, vol. 68, no. 7, pp. 1157–1165, 2011.
- [32] H. Ishikawa, "STING is an endoplasmic reticulum adaptor that facilitates innate immune signalling," *Nature*, vol. 455, no. 7213, pp. 674–678, 2008.
- [33] A. Rongvaux, R. Jackson, C. C. Harman et al., "Apoptotic caspases prevent the induction of type I interferons by mitochondrial DNA," *Cell*, vol. 159, no. 7, pp. 1563–1577, 2014.
- [34] X. Ning, Y. Wang, M. Jing et al., "Apoptotic caspases suppress type I interferon production via the cleavage of cGAS, MAVS, and IRF3," *Molecular cell*, vol. 74, no. 1, pp. 19–31, 2019.
- [35] G. N. Barber, "STING-dependent cytosolic DNA sensing pathways," *Trends in immunology*, vol. 35, no. 2, pp. 88–93, 2014.
- [36] M. J. White, K. McArthur, D. Metcalf et al., "Apoptotic caspases suppress mtDNA-induced STING-mediated type I IFN production," *Cell*, vol. 159, no. 7, pp. 1549–1562, 2014.
- [37] M. G. De Leo, L. Staiano, M. Vicinanza et al., "Autophagosome-lysosome fusion triggers a lysosomal response mediated by TLR9 and controlled by OCRL," *Nature Cell Biology*, vol. 18, no. 8, pp. 839–850, 2016.
- [38] Y. Y. Lan, D. Londoño, R. Bouley, M. S. Rooney, and N. Hacohen, "Dnase2a deficiency uncovers lysosomal clearance of damaged nuclear DNA via autophagy," *Cell Reports*, vol. 9, no. 1, pp. 180–192, 2014.
- [39] T. Oka, S. Hikoso, O. Yamaguchi et al., "Mitochondrial DNA that escapes from autophagy causes inflammation and heart failure," *Nature*, vol. 485, no. 7397, pp. 251–255, 2012.
- [40] Z. Zhang, P. Meng, Y. Han et al., "Mitochondrial DNA-LL-37 complex promotes atherosclerosis by escaping from autophagic recognition," *Immunity*, vol. 43, no. 6, pp. 1137–1147, 2015, Epub 2015 Dec 8.
- [41] X. Hu, T. Bai, Z. Xu, Q. Liu, Y. Zheng, and L. Cai, "Pathophysiological fundamentals of diabetic cardiomyopathy," *Comprehensive Physiology*, vol. 7, no. 2, pp. 693–711, 2017.
- [42] W. Cong, D. Ruan, Y. Xuan et al., "Cardiac-specific overexpression of catalase prevents diabetes-induced pathological changes by inhibiting NF- κ B signaling activation in the heart," *Journal of molecular and cellular cardiology*, vol. 89, pp. 314–325, 2015.
- [43] S. Ivanović-Matić, D. Bogojević, V. Martinović et al., "Catalase inhibition in diabetic rats potentiates DNA damage and apoptotic cell death setting the stage for cardiomyopathy," *Journal of Physiology and Biochemistry*, vol. 70, no. 4, pp. 947–959, 2014.
- [44] S. Boudina, S. Sena, H. Theobald et al., "Mitochondrial energetics in the heart in obesity-related diabetes: direct evidence for increased uncoupled respiration and activation of uncoupling proteins," *Diabetes*, vol. 56, no. 10, pp. 2457–2466, 2007, Epub 2007 Jul 10.
- [45] N. H. Banke and E. D. Lewandowski, "Impaired cytosolic NADH shuttling and elevated UCP3 contribute to inefficient citric acid cycle flux support of postischemic cardiac work in diabetic hearts," *Journal of Molecular and Cellular Cardiology*, vol. 79, pp. 13–20, 2015.
- [46] J. Fauconnier, J. T. Lanner, S. J. Zhang et al., "Insulin and inositol 1, 4, 5-trisphosphate trigger abnormal cytosolic Ca²⁺ transients and reveal mitochondrial Ca²⁺ handling defects in cardiomyocytes of ob/ob mice," *Diabetes*, vol. 54, no. 8, pp. 2375–2381, 2005.
- [47] D. D. Belke, E. A. Swanson, and W. H. Dillmann, "Decreased sarcoplasmic reticulum activity and contractility in diabetic db/db mouse heart," *Diabetes*, vol. 53, no. 12, pp. 3201–3208, 2004.
- [48] F. Cividini, B. T. Scott, A. Dai et al., "O⁶-GlcNAcylation of 8-oxoguanine DNA glycosylase (Ogg1) impairs oxidative mitochondrial DNA lesion repair in diabetic hearts*," *The Journal of Biological Chemistry*, vol. 291, no. 51, pp. 26515–26528, 2016.
- [49] S. Hicks, N. Labinskyy, B. Piteo et al., "Type II diabetes increases mitochondrial DNA mutations in the left ventricle of the Goto-Kakizaki diabetic rat," *American Journal of Physiology. Heart and Circulatory Physiology*, vol. 304, no. 7, pp. H903–H915, 2013.
- [50] R. Li, Y. Liu, Z. Li, L. Yang, S. Wang, and M. X. Guan, "Failures in mitochondrial tRNAMet and tRNAGln metabolism caused by the novel 4401A>G mutation are involved in essential hypertension in a Han Chinese family," *Hypertension*, vol. 54, no. 2, pp. 329–337, 2009.
- [51] Q. Yang, S. K. Kim, F. Sun et al., "Maternal influence on blood pressure suggests involvement of mitochondrial DNA in the pathogenesis of hypertension: the Framingham Heart Study," *Journal of Hypertension*, vol. 25, no. 10, pp. 2067–2673, 2007.
- [52] Z. Lu, H. Chen, Y. Meng et al., "The tRNA^{Met} 4435A>G mutation in the mitochondrial haplogroup G2a1 is responsible for maternally inherited hypertension in a Chinese pedigree," *European Journal of Human Genetics*, vol. 19, no. 11, pp. 1181–1186, 2011.
- [53] P. C. Hung, H. S. Wang, H. T. Chung, M. S. Hwang, and L. S. Ro, "Pulmonary hypertension in a child with mitochondrial A3243G point mutation," *Brain and Development*, vol. 34, no. 10, pp. 866–868, 2012.
- [54] S. Wang, R. Li, A. Fettermann et al., "Maternally inherited essential hypertension is associated with the novel 4263A>G mutation in the mitochondrial tRNAIle gene in a large Han Chinese family," *Circulation Research*, vol. 108, no. 7, pp. 862–870, 2011.
- [55] Q. Qiu, R. Li, P. Jiang et al., "Mitochondrial tRNA mutations are associated with maternally inherited hypertension in two Han Chinese pedigrees," *Human mutation*, vol. 33, no. 8, pp. 1285–1293, 2012.

- [56] F. H. Wilson, A. Hariri, A. Farhi et al., "A cluster of metabolic defects caused by mutation in a mitochondrial tRNA," *Science*, vol. 306, no. 5699, pp. 1190–1194, 2004.
- [57] M. Zhou, M. Wang, L. Xue et al., "A hypertension-associated mitochondrial DNA mutation alters the tertiary interaction and function of tRNA^{Leu(UUR)}," *The Journal of Biological Chemistry*, vol. 292, no. 34, pp. 13934–13946, 2017.
- [58] Y. Zhu, X. Gu, and C. Xu, "A mitochondrial DNA A8701G mutation partly associated with maternally inherited hypertension and dilated cardiomyopathy in a Chinese pedigree," *Chinese Medical Journal*, vol. 129, no. 15, p. 1890, 2016.
- [59] P. Jiang, M. Wang, L. Xue et al., "A hypertension-associated tRNA^{Ala} mutation alters tRNA metabolism and mitochondrial function," *Molecular and Cellular Biology*, vol. 36, no. 14, pp. 1920–1930, 2016.
- [60] Y. Qin, L. Xue, P. Jiang et al., "Mitochondrial tRNA variants in Chinese subjects with coronary heart disease," *Journal of the American Heart Association*, vol. 3, no. 1, article e000437, 2014.
- [61] L. Sabatino, N. Botto, A. Borghini, S. Turchi, and M. G. Andreassi, "Development of a new multiplex quantitative real-time PCR assay for the detection of the mtDNA4977 deletion in coronary artery disease patients: A link with telomere shortening," *Environmental and molecular mutagenesis*, vol. 54, no. 5, pp. 299–307, 2013.
- [62] N. Botto, S. Berti, S. Manfredi et al., "Detection of mtDNA with 4977 bp deletion in blood cells and atherosclerotic lesions of patients with coronary artery disease," *Mutation Research*, vol. 570, no. 1, pp. 81–88, 2005.
- [63] T. Mazzone, A. Chait, and J. Plutzky, "Cardiovascular disease risk in type 2 diabetes mellitus: insights from mechanistic studies," *Lancet*, vol. 371, no. 9626, pp. 1800–1809, 2008.
- [64] T. N. Kelly, L. A. Bazzano, V. A. Fonseca, T. K. Thethi, K. Reynolds, and J. He, "Systematic review: glucose control and cardiovascular disease in type 2 diabetes," *Annals of Internal Medicine*, vol. 151, no. 6, pp. 394–403, 2009.
- [65] S. Mahjoub, D. Sternberg, R. Boussaada et al., "A novel mitochondrial DNA tRNA^{Ile} (m.4322dupC) mutation associated with idiopathic dilated cardiomyopathy," *Diagnostic Molecular Pathology*, vol. 16, no. 4, pp. 238–242, 2007.
- [66] P. E. Schwarz, U. Gruhl, S. R. Bornstein, R. Landgraf, M. Hall, and J. Tuomilehto, "The European perspective on diabetes prevention: development and implementation of a European guideline and training standards for diabetes prevention (IMAGE)," *Diabetes & Vascular Disease Research*, vol. 4, no. 4, pp. 353–357, 2007.
- [67] L. Vilarinho, F. M. Santorelli, M. J. Rosas, C. Tavares, M. Melo-Pires, and S. DiMauro, "The mitochondrial A3243G mutation presenting as severe cardiomyopathy," *Journal of Medical Genetics*, vol. 34, no. 7, pp. 607–609, 1997.
- [68] S. H. Tay, D. R. Nordli, E. Bonilla et al., "Aortic rupture in mitochondrial encephalopathy, lactic acidosis, and stroke-like episodes," *Archives of Neurology*, vol. 63, no. 2, pp. 281–283, 2006.

Research Article

Recanalization Treatment of Acute Ischemic Stroke Caused by Large-Artery Occlusion in the Elderly: A Comparative Analysis of “the Elderly” and “the Very Elderly”

Qi Wang,^{1,2} Yi-Qun Zhang,³ Han-Cheng Qiu,³ Yin-Dan Yao,³ Ao-Fei Liu,³ Chen Li,³ and Wei-Jian Jiang^{1,3} 

¹The PLA Rocket Force Characteristic Medical Center, The Teaching Hospital of Soochow University, Beijing, China

²Department of Vascular Neurosurgery, New Era Stroke Care and Research Institute, Department of Neurology, Beijing Rehabilitation Hospital, Capital Medical University, Beijing, China

³Department of Vascular Neurosurgery, New Era Stroke Care and Research Institute, The PLA Rocket Force Characteristic Medical Center, Beijing, China

Correspondence should be addressed to Wei-Jian Jiang; jiangweijian2018@163.com

Received 11 June 2021; Revised 27 August 2021; Accepted 31 August 2021; Published 6 October 2021

Academic Editor: Xianwei Zeng

Copyright © 2021 Qi Wang et al. This is an open access article distributed under the Creative Commons Attribution License, which permits unrestricted use, distribution, and reproduction in any medium, provided the original work is properly cited.

Objective. To assess whether the effectiveness and safety of recanalization therapy for acute ischemic stroke (AIS) caused by large-artery occlusion (LAO) differ between patients aged 60–79 years and patients aged ≥ 80 years. **Methods.** We analyzed prospective data of patients with LAO (≥ 60 years) who underwent recanalization therapy at the Department of Vascular Neurosurgery, New Era Stroke Care and Research Institute, PLA Rocket Force Characteristic Medical Center, from November 2013 to July 2017. The data were compared between elderly patients (60–79 years) and very elderly patients (≥ 80 years). The effectiveness of recanalization therapy was evaluated using the 90-day modified Rankin scale (mRS) score, while safety was assessed by the rates of symptomatic intracranial hemorrhage (SICH) and mortality within 30 days. **Results.** A total of 151 patients with AIS induced by LAO were included in this study. Seventy-three patients (48.3% [73/151]) had an overall favorable outcome (mRS score 0–2) after treatment. A higher proportion of patients in the elderly group showed a favorable outcome compared with the very elderly group (58.6% [34/58] vs. 41.6% [39/93], respectively; $P = 0.046$). The incidence of SICH (12.7% vs. 16.13%, respectively; $P = 0.561$) and mortality (10.3% vs. 7.5%, respectively; $P = 0.548$) within 30 days was not significantly different between the two groups. **Conclusion.** Recanalization treatment of LAO is more effective in elderly patients compared with very elderly patients, while the safety of recanalization treatment is comparable between these two groups.

1. Introduction

Acute large-artery occlusion (LAO) has become the most important cause of acute ischemic stroke (AIS) worldwide and is related to the high recurrence rate of ischemic stroke and poor outcomes [1]. Endovascular thrombectomy (ET) and intravenous alteplase thrombolysis (IVT) are currently the preferred vascular recanalization treatments for AIS.

Stroke morbidity and mortality increase with age, and the absolute number of patients with fatal stroke is likely to increase steadily due to population aging, a continued increase in traditional risk factors, and poor management [2].

Age is usually regarded as an important factor affecting the choice of treatment and prognosis, and this consideration is particularly prominent in individuals aged over 80 years [3–6]. However, few randomized controlled trials have investigated large-vessel recanalization treatment in patients aged over 80 years.

With the development of recanalization treatment technology and population aging, the treatment of acute LAO in patients over 80 years of age is receiving increasing attention. In 2013, the Chinese Stroke Association and the American Heart Association/American Stroke Association modified AIS recombinant tissue plasminogen activator (rt-PA) IVT

guidelines. Specifically, an age of greater than 80 years was no longer an absolute exclusion criterion; instead, it became a relative exclusion criterion (level II evidence and grade B recommendation) [7, 8]. Moreover, the inclusion criteria for AIS recanalization therapy in clinical practice have been further expanded. Very elderly patients with low National Institutes of Health Stroke Scale (NIHSS) scores, an Alberta Stroke Program Early Computed Tomography (ASPECT) score of <6, and posterior circulation infarction have been gradually indicated to undergo revascularization therapy.

At the same time, an increasing number of single-center trials began to include very elderly patients over 80 years of age into the scope of intravascular recanalization treatment and compared them with elderly patients aged less than 80 years [9]. It has been emphasized that the safety of ET is comparable between patients aged over 80 years and those aged less than 80 years [10]. However, the relationship between recanalization therapy and clinical outcomes in very elderly patients (those aged over 80 years of age) is not fully understood. Therefore, this study was aimed at assessing whether the benefits and safety of recanalization therapy for acute LAO and AIS are comparable between patients ≥ 80 years of age (very elderly patients) and patients aged 60–79 years (elderly patients) to provide a basis for clinical treatment. Thus, we aimed to assess whether there is a difference in the effectiveness and safety of recanalization therapy for AIS caused by LAO between elderly patients and very elderly patients. We also aimed to provide a basis for the future selection of patients suitable for acute stroke recanalization treatment and to investigate whether recanalization treatment has a better effect in elderly patients compared with very elderly patients. The findings of this study may inform future treatment selection.

2. Materials and Methods

2.1. Patient Information. This study was a retrospective study that included patients aged ≥ 60 years with AIS who were admitted continuously to the Department of Vascular Neurosurgery, New Era Stroke Care and Research Institute, PLA Rocket Force Characteristic Medical Center, from November 2013 to July 2017. Patients were divided into the elderly group (60–79 years) and the very elderly group (≥ 80 years). Patients' baseline characteristics, imaging results, and treatment plans were recorded. This study was approved by the Ethics Committee of PLA Rocket Force Characteristic Medical Center, and written informed consent was obtained from all patients.

The inclusion criteria were as follows: (1) aged ≥ 60 years; (2) met the AIS diagnostic criteria, including clear neurological deficit, presence of an infarct on diffusion-weighted imaging, and no cerebral hemorrhage on head computed tomography (CT) [11]; (3) presence of LAO at the internal carotid artery (ICA), vertebral artery, basilar artery (BA), or main middle cerebral artery (M1), which was related to the stroke event and confirmed by magnetic resonance angiography or digital subtraction angiography; and (4) an onset time window of within 4.5 hours for IVT and within 6 hours for intravascular treatment in patients

with anterior-circulation disease and within 24 hours for patients with posterior-circulation disease.

The exclusion criteria were as follows: (1) coagulation dysfunction, mental disorders, or malignant tumors; (2) liver or kidney dysfunction, organ diseases, or an incomplete medical history; (3) acute cerebral hemorrhage, systemic infection, or blood system disease; (4) bilateral or multiple large-artery disease, perforating artery disease or small-artery disease, a history of surgical or interventional treatment for aortic valve stenosis, or other diseases affecting clinical follow-up and judgment; (5) refusal or failure to comply with the treatment plan or failure to complete follow-up; and (6) participation in other clinical trials.

2.2. Treatment Plan

2.2.1. IVT. For patients who met the requirements for IVT and who had no contraindications to IVT, 0.9 mg/kg rt-PA (Boehringer Ingelheim Pharmaceutical Co., Ltd., Germany) was administered. For patients with a higher bleeding risk, the doctor exercised the decision to administer 0.6 mg/kg rt-PA based on experience.

2.2.2. ET. All surgeries were performed by an experienced neurointerventionist (Professor Jiang Weijian). General or local anesthesia was used depending on the patient's condition and tolerance. Thrombus location was determined using angiography, and the Solitaire AB stent removal device was preferentially used for thrombus removal. The degree of recanalization was measured by modified thrombolysis in cerebral infarction (mTICI), with grade $\geq 2b$ representing successful recanalization and grade 3 representing complete recanalization [12].

2.2.3. Blood Pressure Management. To prevent ischemia-reperfusion injury after recanalization, blood pressure was kept below 180/105 mmHg before surgery and maintained at around 80% of the baseline level but not less than 90/60 mmHg after vascular recanalization.

2.2.4. Antiplatelet Drugs. After ET, patients were routinely treated with dual antiplatelet therapy (oral aspirin 100 mg/day and clopidogrel 75 mg/day). Three months later, single-agent antiplatelet therapy with aspirin 100 mg/day or clopidogrel 75 mg/day was administered long term.

2.2.5. Statins. Patients diagnosed with cerebral infarction were immediately administered statin treatment. For patients with severe atherosclerosis or emergency stent implantation, intensive statin treatment was used.

2.3. Outcome Assessment. The mRS score 90 days after treatment was used as the evaluation standard to determine recovery of neurological function. An mRS score of 0–2 was defined as a good functional prognosis, and an mRS score of 3–6 was defined as a poor prognosis [13]. The mRS score was recorded by a neurologist who followed up patients by telephone or during clinic visits.

The incidence of SICH and mortality within 30 days after treatment was recorded. SICH was defined as subarachnoid

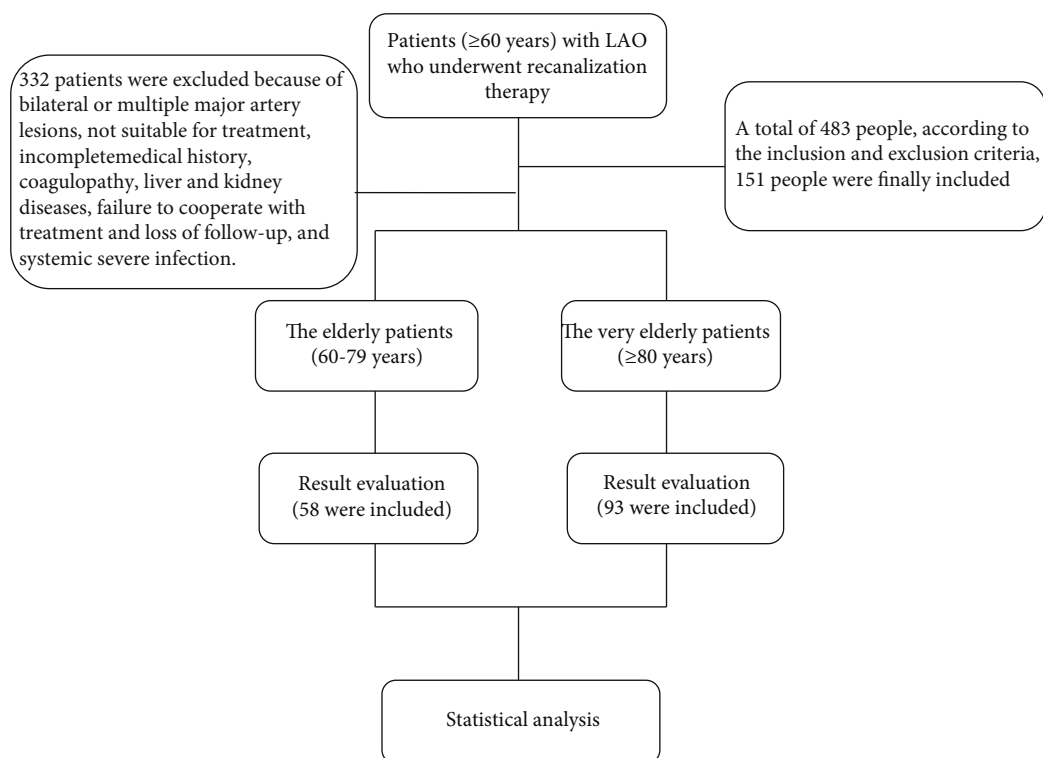


FIGURE 1: Research flow chart.

hemorrhage or cerebral parenchymal hemorrhage with neurological deficit.

2.4. Statistical Analysis. SPSS 22.0 statistical software was used for data analysis. Quantitative data are expressed as mean \pm standard deviation or median (interquartile range (IQR)) depending on whether the data were normally distributed. The *t*-test or the rank-sum test was used to identify differences between two individual groups. Count data are expressed as the number of cases or as a percentage and were compared using the chi-square test. A repeated-measures analysis of variance was used to compare NIHSS and mRS scores at different time points in each group. A *P* value of <0.05 was considered statistically significant. Variables with *P* values of <0.1 in a univariate analysis were included in a multivariate regression analysis. Confounding factors were controlled by stratified analysis and propensity score matching.

3. Results

3.1. Patients' Baseline Characteristics. A total of 483 patients were enrolled from November 2013 to July 2017, according to the inclusion and exclusion criteria; 151 people were finally included, all of whom were diagnosed with AIS caused by LAO (Figure 1). There were 74 men (49% [74/151]) and 77 women (51% [77/151]). Among them, 38.4% of patients (58/151) belonged to the elderly group (60–79 years of age), and 61.6% of patients (93/151) belonged to the very elderly group (80–93 years of age). There were 18 male patients in the elderly group (13.03% [18/58]) and 56 in the very elderly group (60.22% [56/93]). The proportion of male patients in

the very elderly group was significantly higher compared with that in the elderly group ($P < 0.01$).

Before treatment, there were eight patients (13.79% [8/58]) with atrial fibrillation in the elderly group and 27 patients (29.03% [27/93]) with atrial fibrillation in the very elderly group ($P = 0.875$).

The incidence of vascular lesions in the elderly and very elderly groups, respectively, was as follows: ICA (22.4% vs. 26.9%), middle cerebral artery (36.2% vs. 33.3%), BA (29.3% vs. 29%), anterior circulation (40.9% vs. 59.1%), and posterior circulation (34.9% vs. 65.1%). No significant differences were observed between the two groups ($P > 0.05$; Table 1). There was no significant difference in the baseline NIHSS score ($P = 0.163$) or the baseline mRS score ($P = 0.935$) between the elderly group and the very elderly group (Table 1). The specific infarction sites included the basal ganglia, internal capsule, cerebral lobe, watershed region, brainstem, cerebellum, and thalamus (subject to imaging). No significant difference in the number of patients with infarction in these different regions was observed between the two groups ($P = 0.980$) (Table 1).

3.2. Treatment Results

3.2.1. mRS Score. Among all patients in the elderly group, 73 (48.3%) had a favorable 90-day outcome (mRS score 0–2 points). Compared with the elderly group, the very elderly group had a lower proportion of patients with a favorable outcome (41.6% vs. 58.6%, $P = 0.046$) (Figure 2) (Table 2).

3.2.2. Death and Complications. There were 13 deaths (8.6% [13/151]) in the total cohort, and 22 patients (14.6% [22/151]) had SICH. No significant difference in the

TABLE 1: Comparison of baseline characteristics between <80 and ≥80 groups.

Clinical data		All (<i>n</i> = 151)	<80-years-old group (<i>n</i> = 58)	≥80-years-old group (<i>n</i> = 93)	Test used	$\chi^2/t/Z$	<i>P</i>
Gender	Male (<i>n</i> (%))	74 (49.01)	18 (31.03)	56 (60.22)	Chi-square test	12.172 ^a	<0.001
	Female (<i>n</i> (%))	77 (50.99)	40 (68.97)	37 (39.78)			
BMI		24.66 ± 1.73	24.47 ± 1.83	24.77 ± 1.67	<i>t</i> -test	-1.036 ^b	0.302
Time from onset to groin puncture (hours)		6.29 ± 0.72	6.26 ± 0.68	6.30 ± 0.76	<i>t</i> -test	-0.349 ^b	0.727
Time from onset to recanalization (min)		40.43 ± 2.98	40.24 ± 3.16	40.55 ± 2.87	<i>t</i> -test	-0.615 ^b	0.539
Baseline medical history	Hypertension (<i>n</i> (%))	59 (39.07)	23 (39.66)	36 (38.71)	Chi-square test	0.013 ^a	0.908
	Diabetes (<i>n</i> (%))	55 (36.42)	21 (36.21)	34 (36.56)			
	Hyperlipidemia (<i>n</i> (%))	48 (31.79)	18 (31.03)	30 (32.26)			
	Coronary heart disease (<i>n</i> (%))	53 (38.48)	21 (29.97)	32 (34.41)			
	Atrial fibrillation (<i>n</i> (%))	35 (23.18)	8 (13.79)	27 (29.03)			
Vessel involved	Middle cerebral artery (<i>n</i> (%))	43 (28.48)	21 (36.2)	31 (33.3)	Chi-square test	0.418 ^a	0.741
	Internal carotid artery (<i>n</i> (%))	31 (20.53)	13 (22.4)	25 (26.9)			
	Basilar artery (<i>n</i> (%))	35 (23.18)	17 (29.3)	27 (29)			
	Vertebral artery (<i>n</i> (%))	13 (8.61)	7 (12.1)	10 (10.8)			
	Anterior cerebral artery	88 (58.3)	36 (40.9)	52 (59.1)			
	Posterior cerebral artery	63 (41.7)	22 (34.9)	41 (65.1)			
Occlusion site	Basal ganglia	33 (21.9)	13 (24.5)	20 (20.4)	Chi-square test	1.312	0.980
	Inner capsule	7 (4.6)	2 (3.8)	5 (5.1)			
	Brain lobe	26 (17.2)	10 (18.9)	16 (16.3)			
	Watershed	22 (14.6)	7 (13.2)	15 (15.3)			
	Brain stem	41 (27.2)	13 (24.5)	28 (28.6)			
	Cerebellum	10 (6.6)	3 (5.7)	7 (7.1)			
	Thalamus	12 (7.9)	5 (9.4)	7 (7.1)			
Baseline NIHSS, median (IQR)		9 (4, 16)	11 (6, 15.25)	8 (3, 16)	Wilcoxon rank sum test	4.659 ^a	0.163
Baseline mRS, median (IQR)		3 (2, 4)	3 (2, 4)	3 (2, 4)	Wilcoxon rank sum test	0.425 ^a	0.935
Acute treatment (rt-PA)					Chi-square test	4.247 ^a	0.001
0.6 mg/kg		63 (56.8)	13 (20.6)	50 (79.4)			
0.9 mg/kg		48 (43.2)	10 (20.8)	38 (79.2)			

a means chi-square test; b stands for *t*-test.

incidence of mortality or SICH was found between the elderly and the very elderly group (mortality: 10.3% vs. 7.5%, $P = 0.548$; SICH: 12.07% vs. 16.13%, $P = 0.561$) (Table 2). The differences in other complications, including respiratory failure and lung infection, were not statistically significant between the two groups ($P = 0.9$) (Table 2).

3.2.3. Predictor Analysis. Table 3 shows the results of the univariate and multivariate analyses of prognostic factors at 90 days. With the univariate analysis, the factors that predicted a favorable outcome were the male sex (odds ratio (OR) = 3.243, 95% confidence interval (CI): 1.517–6.93, $P = 0.002$) and low-dose rt-PA (OR = 3.170, 95% CI: 1.373–7.320, $P = 0.007$). The factors that significantly predicted a poor outcome were sex, atrial fibrillation (OR = 4.656, 95% CI: 1.772–12.237, $P = 0.002$), and thrombolytic therapy (OR = 2.561, CI: 1.014–6.465, $P = 0.047$). The multivariate regression analysis of predictive factors indi-

cated that the male sex and low-dose rt-PA were predictive factors for a favorable outcome.

3.3. Follow-Up Outcome. The duration of clinical follow-up was 90 days. The proportion of patients with a favorable outcome at 90 days (48.3% [73/151]) was significantly higher compared with that before treatment (36.4% [55/151]) ($P = 0.036$). In the elderly group, the proportion of patients with a favorable outcome at 90 days after treatment was significantly higher compared with that before treatment (58.6% vs. 31%, respectively; $P = 0.015$). The rate of a favorable outcomes at 90 days (25.8%) was not significantly different compared with the rate before treatment (24.5%) in the very elderly group ($P = 0.791$). During the follow-up period, there were five patients (3.3%) with recurrent ischemic stroke, including two patients in the elderly group and three patients in the very elderly group (3.4% vs. 3.2%,

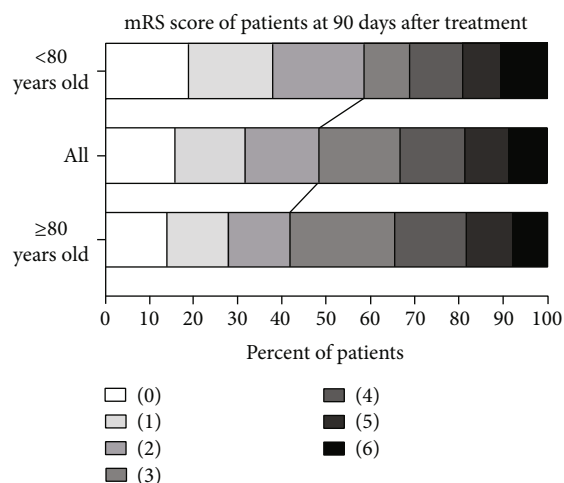


FIGURE 2: Distribution of mRS scores in the elderly group, the very elderly group, and all patients 90 days after treatment. The proportion of patients in each group with different scores was shown (0-6, the higher the score, the more severe the disability). The numbers under the bar represent the proportions of patients in different scoring segments. Due to rounding, the sum of these percentages may not equal 100. The black lines indicate the comparison of the proportion of patients with favorable outcomes (mRS 0-2 points) in different groups. The detailed results were as follows: 90 days after treatment, a total of 73 patients (48.3%) had a favorable outcome (mRS 0-2). In the group of <80 years old and ≥80 years old, 34 patients (58.6%) and 39 patients (41.6%) had a favorable outcomes, respectively. The ratio of favorable outcomes in the former was higher than that in the latter ($P = 0.046$).

respectively; $P = 0.941$). Four patients (2.6%) developed in-stent restenosis 2 months after surgery, including one patient in the elderly group and three patients in the very elderly group (1.7% vs. 3.2%, respectively; $P = 0.576$).

4. Discussion

4.1. Effectiveness Analysis. In this study, the proportion of patients with a favorable outcome 90 days after recanalization treatment differed between the two groups; that is, the proportion of patients with a favorable outcome in the very elderly group was lower compared with that in the elderly group (Figure 2). A meta-analysis involving 1,400 subjects validated this view and proposed that the effectiveness of aortic recanalization therapy in very elderly patients was poorer compared with elderly patients [10, 14]. Most single-center trials and meta-analyses hold the view that 80 years of age is an independent predictor of functional independence and mortality 30 days after ET, and it is also the demarcation point for a rapid decline in functional prognosis [14-16]. In very elderly patients, functional improvement after treatment is limited by neuronal reserve, remodeling ability, and plasticity [14]. Another possible reason is that difficulty in vascular access and increased vascular distortion or atherosclerotic lesions may affect surgical outcomes [15, 16].

Conflicting results have been reported in previous studies. For example, Taichiro et al. showed no significant differ-

ence in the favorable outcome rate between the elderly group and the very elderly group (42% vs. 57%, respectively; $P = 0.261$), and the therapeutic effect of ET treatment between the two groups was also comparable [17]. Yasuhiro et al. proposed that age should not be used as a criterion to exclude elderly patients. They believe that improving recanalization techniques could elevate the success rate of treatment in older patients, but there is still no uniform standard on how to improve the technology [18].

In this study, we suggest that in addition to the above reasons, other baseline factors, such as atrial fibrillation and thrombolysis dose, may also be responsible for the poor prognosis of elderly patients. The lower functional independence of patients in the very elderly group before stroke may also reduce treatment effectiveness [19]. Therefore, age may indeed be a factor to consider when deciding whether recanalization therapy should be selected in the clinic.

4.2. Safety Analysis. In this study, we found no significant difference in safety between the two groups within 30 days after treatment. No significant difference was detected in the rate of SICH or mortality between the elderly and very elderly groups (16.1% vs. 12.1%, respectively; $P = 0.561$; 7.5% vs. 10.3%, respectively; $P = 0.548$). This may be due to the following three reasons. First, a low dose of rt-PA (0.6 mg/kg) was administered to some patients to improve safety in this study. The conditions suitable for low-dose thrombolysis were as follows: advanced age, mild stroke, relative contraindications, bleeding risk, awakening stroke, and overweight [20]. Twelve patients in the elderly group and 34 patients in the very elderly group underwent low-dose rt-PA treatment. The proportion of patients in the very elderly group who underwent low-dose rt-PA treatment was significantly higher compared with the proportion of patients in the elderly group (36.6% vs. 20.7%, respectively; $P = 0.039$). Second, careful treatment selection and active prevention of complications after treatment were adopted to further ensure patient safety. When selecting treatment for patients with a baseline mRS score of ≥2 and an ASPECT score of ≤6, a comprehensive assessment and in-depth communication with family members were carried out to ensure patient safety and successful treatment plan implementation. Finally, the interval from disease onset to treatment was strictly limited to between 4.5 and 6 hours for all patients included in the study [10]. The International Stroke Trial 3 showed no difference in the rate of cerebral hemorrhage and mortality between the very elderly group and the elderly group (4% vs. 3%, respectively; $P = 0.667$), confirming that thrombolytic therapy is safe in the elderly [21]. The results of the EXTEND-IA and REVASCAT studies have confirmed the safety of IVT and bridge endovascular therapy within 6 hours of AIS onset [22]. Therefore, our results are consistent with previous findings that the safety of recanalization treatment is comparable between the elderly and very elderly groups.

4.3. Influencing Factors. In this study, univariate and multivariate analyses indicated that the male sex and low-dose rt-PA thrombolysis were predictive factors for a favorable outcome. Atrial fibrillation and thrombolytic therapy were

TABLE 2: Comparison of treatment outcomes between the elderly group and the very elderly group.

	All	<80 (58)	≥80 (93)	<i>P</i>
mRS at 90 days (<i>M</i> , IQR)	3 (1, 4)	2 (1, 4)	3 (1, 4)	0.246
IVT (<i>M</i> , IQR)	3 (1, 4)	2 (1, 4.5)	3 (1, 4)	0.450
ET (<i>M</i> , IQR)	3 (2, 4)	3 (1.75, 5)	2 (0, 4)	0.486
IVT&ET (<i>M</i> , IQR)	2 (1, 4)	2 (0, 4)	3 (1, 4)	0.173
Before treatment				
Favorable outcomes (mRS 0-2 at 90 days) (<i>n</i> , %)	55 (36.4)	18 (31.0)	37 (39.8)	0.277
90 days after treatment				
Favorable outcomes (mRS 0-2 at 90 days) (<i>n</i> , %)	73 (48.3)	34 (58.6)	39 (41.6)	0.046
Other outcome (mRS 3-6 at 90 days) (<i>n</i> , %)	78 (51.7)	24 (41.4)	54 (58.1)	0.046
SICH (<i>n</i> , %)	22 (14.6)	7 (12.07)	15 (16.13)	0.561
Other complications (<i>n</i> , %)	46 (30.5)	18 (31.0)	28 (30.1)	0.904
Death (mRS 6 at 90 days) (<i>n</i> , %)	13 (8.6)	6 (10.3)	7 (7.5)	0.548
mRS at 90 days in different degrees (<i>n</i> , %)				0.380
0	24 (15.9)	11 (19.0)	13 (14.0)	
1	24 (15.9)	11 (19.0)	13 (14.0)	
2	25 (16.6)	12 (20.7)	13 (14.0)	
3	28 (18.5)	6 (10.3)	22 (23.7)	
4	22 (14.6)	7 (12.1)	15 (16.1)	
5	15 (9.9)	5 (8.6)	10 (10.8)	
6	13 (8.6)	6 (10.3)	7 (7.5)	

Normally distributed data is presented as mean \pm standard deviation and compared using independent sample *t*-test. Data that are not normally distributed is expressed as *M* (P25-P75), and the Wilcoxon rank sum test is used for the comparison between groups. Count data is represented by *n* (%), and the comparison between groups is done by the chi-square (χ^2) test. The multivariate analysis is tested by two-class logistic regression analysis. $P < 0.05$ indicates statistical significance.

predictive of a poor outcome. According to previous meta-analyses and multicenter studies, the main factors affecting the effectiveness of recanalization treatment are baseline functional level (a higher baseline NIHSS score), vascular disease location, thrombolysis dose, time from onset to emergency, operation time, and the proportion of patients with mTICI $> 2b/3$ [10, 14, 23].

We found no significant difference in the baseline functional level or in the distribution of anterior-circulation and posterior-circulation lesions between the two groups in the present study (Table 1). Moreover, we found that the proportion of male patients with a favorable outcome and a poor outcome was 64.4% and 34.6%, respectively (OR = 3.24, $P = 0.002$). Findings from South Korea have shown that the average life expectancy of men is lower than that of women, resulting in a significantly decreased proportion of male patients in the very elderly group, which may have affected the results. Therefore, we speculate that the male sex may be predictive of a favorable outcome. Moreover, an older age and the female sex are also predictors of a poor outcome. Because women have a longer life expectancy than men, women are more likely to be of a higher chronological age when they experience stroke and they may thus have a higher disability rate when classified into the very elderly group [24, 25], which is consistent with previous meta-analysis results [14].

The rate of atrial fibrillation in the very elderly group was higher compared with that in the elderly group (29.03% vs. 13.79%, respectively; $P = 0.031$). The proportion of patients with atrial fibrillation in those with favorable and poor out-

comes was 11% and 34.6%, respectively (OR = 4.656, $P = 0.02$), indicating that atrial fibrillation may be an influencing factor of a poor outcome. Similar findings have been reported in previous studies. The incidence of atrial fibrillation confirmed on admission was significantly higher in patients ≥ 80 years of age compared with patients < 80 years of age (69% vs. 45%, respectively; $P = 0.042$). Moreover, the incidence of cardiogenic thromboembolism in patients aged ≥ 80 years was significantly higher compared with those aged < 80 years (94% vs. 73%, respectively; $P = 0.016$). Therefore, we infer that atrial fibrillation may lead to a higher bleeding risk and a poor prognosis. This may be due to large-artery embolism caused by atrial fibrillation, which causes infarction in the area supplied by the middle cerebral artery. Furthermore, atrial fibrillation is often associated with other high-risk factors, such as hypertension and atherosclerosis, which lead to a significantly higher mortality rate compared with patients without atrial fibrillation or patients with tremor [20, 25].

In this study, 111 patients underwent IVT and 40 patients did not undergo IVT, and there was statistical difference between the two ($P < 0.05$). A significant difference was observed between the number of patients with a poor outcome at 90 days and the number of patients with a favorable outcome (68 vs. 43, respectively; $P < 0.001$). The multivariate analysis showed that IVT is predictive of a poor outcome ($P = 0.047$), which is contrary to previous studies [15, 16, 26, 27]. With a detailed analysis of previous studies, we found that the effect of different rt-PA doses on the results was rarely mentioned. In this study, by

TABLE 3: Multivariate analysis for predictors of good outcome and poor outcomes.

	Univariate logistic regressions for outcome			Multivariate logistic regressions for outcome	
	Favorable outcomes <i>n</i> = 73	Poor outcomes <i>n</i> = 78	<i>P</i>	Odds ratio (95%)	<i>P</i>
Male	47 (64.4)	27 (34.6)	<0.001 ^a	3.243 (1.517, 6.93)	0.002
BMI	24.71 ± 1.68	24.61 ± 1.79	0.726		
Onset to groin time (h)	6 (6, 7)	6 (6, 7)	0.684 ^b		
Onset to IVT time (min)	40 (38, 43)	40.5 (38, 43)	0.419 ^c		
Baseline NIHSS	9 (4, 15)	9 (4, 16)	0.761 ^c		
Hypertension	24 (32.9)	35 (44.9)	0.131 ^a		
Diabetes mellitus	31 (42.5)	24 (30.8)	0.136 ^a		
Hyperlipidemia	19 (26)	29 (37.2)	0.141 ^a		
Coronary heart disease	21 (35.1)	32 (41)	0.143 ^a		
Arterial fibrillation	8 (11)	27 (34.6)	0.001 ^a	4.656 (1.772, 12.237)	0.002
Location			0.565 ^a		
Middle cerebral artery (<i>n</i> (%))	24 (32.9)	28 (35.9)			
Internal carotid artery (<i>n</i> (%))	21 (28.8)	17 (21.8)			
Basilar artery (<i>n</i> (%))	22 (30.1)	22 (28.2)			
Vertebral artery (<i>n</i> (%))	6 (8.2)	11 (14.1)			
Treatment options			0.271 ^a		
Age			0.046 ^a	3.536 (1.344, 9.306)	0.011
<80	34 (46.6)	24 (30.8)			
≥80	39 (53.4)	54 (69.2)			
rt-PA			<0.001 ^a	2.561 (1.014, 6.465)	0.047
No	30 (41.1)	10 (12.8)			
Yes	43 (58.9)	68 (87.2)			
rt-PA 0.6 mg/kg	32 (43.8)	14 (17.9)	0.001 ^a	3.170 (1.373, 7.320)	0.007

“a” indicates chi-square test; “b” indicated *t*-test; “c” indicates *Z* test. The assignment is as follows: favorable outcomes group = 1, poor prognosis group = 0; 0.6 mg/kg = 1, and 0.9 mg/kg = 2. BMI: body mass index.

comparing the effects of different rt-PA doses, we infer that IVT can affect the outcome of recanalization therapy, but the effect is also influenced by the rt-PA dose. In our study, the number of patients in the elderly and very elderly groups who underwent low-dose rt-PA treatment (0.6 mg/kg) was significantly different (13 [20.6%] vs. 50 [79.4%], respectively; *P* = 0.001). Therefore, we speculate that low-dose rt-PA thrombolysis may increase safety but significantly reduce the effectiveness of treatment, thus making IVT a predictive factor for a poor outcome in this study. Similar to our results, Dong et al. recently reported that low-dose rt-PA thrombolysis can reduce the risk of SICH, but it also significantly reduces treatment effectiveness [28].

In previous studies, the influence of age and serum 25 (OH) D concentration on the prognosis of stroke has been noted. According to the DNA methylation algorithm, biological age is probably an independent predictor of 3-month mortality after ischemic stroke, which is unrelated to NIHSS score and vascular risk factors [29]. Tu et al. suggest that 25 (OH) D remains an independent prognostic marker of 90-day mortality and functional outcomes in Chinese patients with AIS; lower serum levels of 25 (OH) D are independently associated with the stroke recurrence and mortality at 24 months in ischemic stroke patients [30, 31]. Cheng et al. suggested that

elevated serum hS-CRP and HCY levels were associated with the risk of PSD 1 year after stroke, and this was likely to be a factor influencing the favorable outcomes at 90 days [32]. Further randomized controlled trials are needed to assess the factors that influence the prognosis of stroke in elderly patients.

This study had several limitations. First, this study was a single-center study; thus, the evaluation may not be sufficiently comprehensive. There is a need to further expand the scope of analysis to include other factors, such as ASPECT score, collateral circulation grading, and the relatively small number of cases after grouping. Second, the overall sample size was small, and this limitation was particularly prominent when the three methods were separately counted. This may have led to a decrease in detection efficiency. In future studies, the inclusion criteria should be optimized, the number of subjects should be increased, and data from multiple research centers should be combined for analysis.

5. Conclusion

In this study, nearly half of the total cohort achieved a good functional prognosis at 3 months after recanalization. Recanalization had comparable safety between patients aged ≥80 years

and patients aged 60–79 years. Although there were no significant differences between the two groups in terms of group size, baseline functional score, and vascular lesions, the benefits of recanalization in very elderly patients were not as good as those in elderly patients. Therefore, we infer that age may be an important factor affecting the outcome of aortic recanalization. Furthermore, we identified other influencing factors. Specifically, sex may affect treatment effectiveness, low-dose rt-PA thrombolysis may improve treatment safety, and atrial fibrillation may predict a poor prognosis. In clinical practice, a comprehensive evaluation of certain factors, such as age, must be considered to achieve better treatment outcomes.

Abbreviations

NIHSS:	The National Institutes of Health Stroke Scale
rtRS:	The modified Rankin scale
DSA:	Digital subtraction angiography
AIS:	Acute ischemic stroke
LAO:	Large artery occlusion
SICH:	Symptomatic intracranial hemorrhage
ET:	Endovascular thrombectomy
IVT:	Intravenous alteplase
rt-PA:	Recombinant tissue plasminogen activator
ASPECT:	Alberta Stroke Program Early CT
DWI:	Diffusion-weighted magnetic resonance imaging
CT:	Computed tomography
ICA:	Internal carotid artery
VA:	Vertebral artery
BA:	Basilar artery
M1:	Main middle cerebral artery
MRA:	Magnetic resonance angiography
mTICI:	Modified thrombolysis in cerebral infarction.

Disclosure

The funders had no role in the design and conduct of the study; in the collection, analysis, and interpretation of the data; and in the preparation, review, or approval of the manuscript.

Conflicts of Interest

All of the authors have no disclosure-conflict of interest.

Authors' Contributions

W-JJ contributed to the conception, design, data analysis, and manuscript revision. QW and Y-QZ collected the data and drafted the manuscript. Y-QZ contributed equally to this work and should be considered co-first authors along with Q-W. H-CQ, A-FL, and CL analyzed data and revised the manuscript. Y-DY reviewed and edited the manuscript.

Acknowledgments

We would like to thank Li Xiang, Department of Record Room, the PLA Rocket Force Characteristic Medical Center, Beijing, 100088, China, for her help in providing data. We thank Emily Woodhouse, PhD, from Liwen Bianji (Edanz) (<http://www.liwenbianji.cn/>), for editing the English text of a draft of this

manuscript. This work was funded by the National Key Basic Research Program of China (973 program) (grant No. 2013CB733800) and National Natural Science Foundation of China (grant Nos. 81471767 and 81871464).

References

- [1] P. B. Gorelick, K. S. Wong, H. J. Bae, and D. K. Pandey, "Large artery intracranial occlusive disease: a large worldwide burden but a relatively neglected frontier," *Stroke*, vol. 39, no. 8, pp. 2396–2399, 2008.
- [2] B.-H. Chao, F. Yan, Y. Hua et al., "Stroke prevention and control system in China: CSPPC-stroke program," *International Journal of Stroke*, vol. 16, no. 3, pp. 265–272, 2021.
- [3] J. S. Balami, B. A. Sutherland, L. D. Edmunds et al., "A systematic review and meta-analysis of randomized controlled trials of endovascular thrombectomy compared with best medical treatment for acute ischemic stroke," *International Journal of Stroke*, vol. 10, no. 8, pp. 1168–1178, 2015.
- [4] O. A. Berkhemer, P. S. Fransen, D. Beumer et al., "A randomized trial of intraarterial treatment for acute ischemic stroke," *The New England Journal of Medicine*, vol. 372, no. 1, pp. 11–20, 2015.
- [5] B. C. Campbell, P. J. Mitchell, T. J. Kleinig et al., "Endovascular therapy for ischemic stroke with perfusion-imaging selection," *The New England Journal of Medicine*, vol. 372, no. 11, pp. 1009–1018, 2015.
- [6] M. Goyal, A. M. Demchuk, B. K. Menon et al., "Randomized assessment of rapid endovascular treatment of ischemic stroke," *The New England Journal of Medicine*, vol. 372, no. 11, pp. 1019–1030, 2015.
- [7] Expert group of scientific statement of Chinese Stroke association, "Scientific statement of Chinese Stroke Association on intravenous thrombolysis in acute ischemic stroke," *Chinese Journal of Stroke*, vol. 12, no. 3, p. 267, 2017.
- [8] E. C. Jauch, J. L. Saver, Adams HP Jr et al., "Guidelines for the early management of patients with acute ischemic stroke: a guideline for healthcare professionals from the American Heart Association/American Stroke Association," *Stroke*, vol. 44, no. 3, pp. 870–947, 2013.
- [9] A. Alawieh, A. Chatterjee, W. Feng et al., "Thrombectomy for acute ischemic stroke in the elderly: a 'real world' experience," *Journal of Neurointerventional Surgery*, vol. 10, no. 12, pp. 1209–1217, 2018.
- [10] M. Goyal, B. K. Menon, W. H. van Zwam et al., "Endovascular thrombectomy after large-vessel ischaemic stroke: a meta-analysis of individual patient data from five randomised trials," *Lancet*, vol. 387, no. 10029, pp. 1723–1731, 2016.
- [11] Chinese stroke association, neurointerventional branch of Chinese stroke society, Chinese association of preventive medicine Interventional group, and committee on prevention and control, "Intravascular therapy for acute ischemic stroke," *Chinese Journal Stroke*, vol. 13, no. 7, pp. 706–711, 2018.
- [12] A. Tamburrini, S. M. Rehman, D. Votano et al., "Penetrating trauma of the thoracic aorta caused by a knitting needle," *Annals of Thoracic Surgery*, vol. 103, no. 2, article e193, 2017.
- [13] X. Li, L. Ling, C. Li, and Q. Ma, "Efficacy and safety of desmoteplase in acute ischemic stroke patients: a systematic review and meta-analysis," *Medicine*, vol. 96, no. 18, article e6667, 2017.

- [14] A. Alawieh, R. M. Starke, A. R. Chatterjee et al., "Outcomes of endovascular thrombectomy in the elderly: a 'real-world' multicenter study," *Journal of Neurointerventional Surgery*, pp. 1–9, 2018.
- [15] P. Guedin, A. Larcher, J. P. Decroix et al., "Prior IV thrombolysis facilitates mechanical thrombectomy in acute ischemic stroke," *Journal of Stroke and Cerebrovascular Diseases*, vol. 24, no. 5, pp. 952–957, 2015.
- [16] R. R. Leker, S. Piskis, J. M. Gomori, and J. E. Cohen, "Is Bridging Necessary? A Pilot Study of Bridging versus Primary Stentriever- Based Endovascular Reperfusion in Large Anterior Circulation Strokes," *Journal of Stroke and Cerebrovascular Diseases*, vol. 24, no. 6, pp. 1163–1167, 2015.
- [17] T. Imahori, K. Tanaka, A. Arai, R. Shiomi, D. Fujiwara, and T. Mori, "Mechanical thrombectomy for acute ischemic stroke patients aged 80 years or older Mechanical thrombectomy for acute ischemic stroke in elderly," *Journal of Stroke and Cerebrovascular Diseases*, vol. 26, no. 12, pp. 2793–2799, 2017.
- [18] Y. Kawabata, N. Nakajima, H. Miyake, S. Fukuda, and T. Tsukahara, "Endovascular treatment of acute ischaemic stroke in octogenarians and nonagenarians compared with younger patients," *The Neuroradiology Journal*, vol. 32, no. 4, pp. 303–308, 2019.
- [19] J. F. Kleine, T. Boeckh-Behrens, S. Prothmann, C. Zimmer, and T. Liebig, "Discrepancy between early neurological course and mid-term outcome in older stroke patients after mechanical thrombectomy," *Journal of Neurointerventional Surgery*, vol. 8, no. 7, pp. 671–676, 2016.
- [20] J. L. Saver, M. Goyal, A. Bonafe et al., "Stent-Retriever thrombectomy after intravenous t-PA vs. t-PA alone in stroke," *The New England Journal of Medicine*, vol. 372, no. 24, pp. 2285–2295, 2015.
- [21] Y. Chen, C.-H. Li, Y.-X. Wang et al., "Safety and effectiveness of intravenous thrombolysis with recombinant tissue plasminogen activator in eighty years and older acute ischemic stroke patients," *European Review for Medical and Pharmacological Sciences*, vol. 19, no. 10, pp. 1852–1858, 2015.
- [22] Z. Di, Z. Shu-ting, and W. Bo, "Interpretation of 'Chinese guidelines for diagnosis and treatment of acute ischemic stroke 2018'," *Chinese Journal of Contemporary Neurology and Neurosurgery*, vol. 19, no. 11, p. 899, 2019.
- [23] J. Z. Willey, G. Ortega, P. M. Pego et al., "Thrombolysis in patients aged over 80 years is equally effective and safe, Thrombolysis in patients over 80 years is effective and safe," *Journal of Stroke and Cerebrovascular Diseases*, vol. 25, no. 6, pp. 1532–1538, 2016.
- [24] M. Kelly-Hayes, A. Beiser, C. S. Kase, A. Scaramucci, R. B. D'Agostino, and P. A. Wolf, "The influence of gender and age on disability following ischemic stroke: the Framingham study," *Journal of Stroke and Cerebrovascular Diseases*, vol. 12, no. 3, pp. 119–126, 2003.
- [25] W. Sun, G. Li, X. Zeng et al., "Clinical and imaging characteristics of cerebral infarction in patients with nonvalvular atrial fibrillation combined with cerebral artery stenosis," *Journal of Atherosclerosis and Thrombosis*, vol. 25, no. 8, pp. 720–732, 2018.
- [26] E. A. Mistry, A. M. Mistry, M. O. Nakawah et al., "Mechanical thrombectomy outcomes with and without intravenous thrombolysis in stroke patients: a meta-analysis," *Stroke*, vol. 48, no. 9, pp. 2450–2456, 2017.
- [27] D. Behme, C. Kabbasch, A. Kowoll et al., "Intravenous Thrombolysis Facilitates Successful Recanalization with Stent-Retriever Mechanical Thrombectomy in Middle Cerebral Artery Occlusions," *Journal of Stroke and Cerebrovascular Diseases*, vol. 25, no. 4, pp. 954–959, 2016.
- [28] Y. Dong, Y. Han, H. Shen et al., "Who may benefit from lower dosages of intravenous tissue plasminogen activator? Results from a cluster data analysis," *Stroke & Vascular Neurology*, vol. 5, no. 4, pp. 348–352, 2020.
- [29] C. Soriano-Tárraga, E. Giralt-Steinhauer, M. Mola-Caminal et al., "Biological age is a predictor of mortality in ischemic stroke," *Scientific Reports*, vol. 8, no. 1, p. 4148, 2018.
- [30] W. J. Tu, S. J. Zhao, D. J. Xu, and H. Chen, "serum 25-hydroxyvitamin D predicts the short-term outcomes of Chinese patients with acute ischaemic stroke," *Clinical Science*, vol. 126, no. 5, pp. 339–346, 2014.
- [31] H. Qiu, M. Wang, D. Mi, J. Zhao, W. Tu, and Q. Liu, "Vitamin D status and the risk of recurrent stroke and mortality in ischemic stroke patients: data from a 24-month follow-up study in China," *The Journal of Nutrition, Health & Aging*, vol. 21, no. 7, pp. 766–771, 2017.
- [32] L. S. Cheng, W. J. Tu, Y. Shen, L. J. Zhang, and K. Ji, "Combination of high-sensitivity C-reactive protein and homocysteine predicts the post-stroke depression in patients with ischemic stroke," *Molecular Neurobiology*, vol. 55, no. 4, pp. 2952–2958, 2018.

Research Article

H19 Overexpression Improved Efficacy of Mesenchymal Stem Cells in Ulcerative Colitis by Modulating the miR-141/ICAM-1 and miR-139/CXCR4 Axes

Ming-li Zhao ¹, Tao Chen,¹ Teng-hui Zhang,² Feng Tian,³ and Xiao Wan⁴

¹Department of General Surgery & Guangdong Provincial Key Laboratory of Precision Medicine for Gastrointestinal Tumor, Nanfang Hospital, The First School of Clinical Medicine, Southern Medical University, Guangzhou, Guangdong 510515, China

²Department of General Surgery, Jinling Hospital, School of Medicine, Nanjing University, Nanjing, Jiangsu 210002, China

³Department of Gastrointestinal Surgery, Provincial Hospital Affiliated to Shandong University, Jinan, Shandong 250012, China

⁴Department of General Surgery, The First Affiliated Hospital of USTC, Division of Life Sciences and Medicine, University of Science and Technology of China, Hefei, Anhui 230001, China

Correspondence should be addressed to Ming-li Zhao; zhao_ming_li@163.com

Received 18 June 2021; Revised 30 July 2021; Accepted 2 September 2021; Published 29 September 2021

Academic Editor: Wen-Jun Tu

Copyright © 2021 Ming-li Zhao et al. This is an open access article distributed under the Creative Commons Attribution License, which permits unrestricted use, distribution, and reproduction in any medium, provided the original work is properly cited.

Overexpression of C-X-C motif chemokine receptor 4 (CXCR4) and intercellular cell adhesion molecule-1 (ICAM-1) may promote homing of mesenchymal stem cells (MSC). In this study, we treated ulcerative colitis animals with MSC preconditioned with or without H19 and compared the therapeutic effect of MSC and MSC-H19. We evaluated the regulatory relationship of H19 vs. miR-141/miR-139 and miR-141/miR-139 vs. ICAM-1/CXCR4. We established an ulcerative colitis mouse model to assess the effect of MSC and MSC-H19. H19 was found to bind to miR-141 and miR-139. The activity of H19 was strongly decreased in cells c-transfected with miR-141/miR-139 and WT H19. ICAM-1 was confirmed to be targeted by miR-141 and CXCR4 was targeted by miR-139. The H19 expression showed a negative regulatory relationship with the miR-141 and miR-139 expression but a positive regulatory relationship with the ICAM-1 and CXCR4 expression. In summary, the overexpression of H19 in MSC downregulated miR-139 and miR-141, thus increasing the activity of their targets ICAM-1 and CXCR4, respectively, to exhibit therapeutic effects in ulcerative colitis.

1. Introduction

As a condition of the gastrointestinal tract system, inflammatory bowel disease (IBD) manifests as ulcerative colitis, Crohn's disease, and persistent inflammation in the stomach. The etiology of IBD remains unclear; although, studies on IBD pathogenesis have shown that the breakdown of the immune system in the digestive tract, including an imbalance in intestinal microbiota, is crucial for the onset of this condition [1, 2].

Mesenchymal stem cells (MSC) are present in many body organs, such as dental pulp, bone marrow, fat, and muscles; furthermore, MSC are linked to the microvasculature in the entire body as pericytes. These cells may differentiate into different types of mesenchymal cells [3]. MSC

produce cytokines and alter the microenvironment required for cell regrowth. MSC possess strong immunomodulatory properties by reducing the proliferation of inflammatory cells as well as the synthesis of cytokines [4]. MSC are presently utilized for the treatment of inflammatory conditions, such as myocarditis, sclerosis, and IBD [5, 6]. While the functions of MSC remain elusive, MSC are used for IBD therapy and have displayed appealing outcomes in animals [7–9].

Noncoding RNA (ncRNA) has been shown to possess significant properties in the regulation of gene functions [10]. ncRNAs have been shown to become significant regulatory factors in the onset, progression, and prognosis of medical conditions [11]. ncRNAs include the extensively studied miRNAs, as well as the lncRNAs, which is one type

of ncRNA recently recognized for their importance. However, although miRNAs have been intensively examined for their functionalities, lncRNAs also comprise a new and possibly crucial class of ncRNAs [12]. LncRNA H19 is located close to the telomeric region of chromosome 11p15.5 [13], and it was reported to be highly expressed in the developing embryo while being significantly downregulated in neonates [14]. Moreover, H19 has been described as an oncogene in several diseases such as bladder cancer, colorectal cancer, or breast cancer [15–17]. Apart from this, H19 silences target genes by upregulating the miR-139 expression. In one study, H19 was significantly upregulated under hypoxic conditions, indicating that H19 participates in cell injury induced by hypoxia [18]. And a previous study showed that miR-139 expression was downregulated in nerve cells and rodent brains under hypoxia [19]. Moreover, H19 was demonstrated to compete with miR-141 and influence the expression of miR-141, as well as the ZEB1 which is the target gene of miR-141, in gastric cancer [20]. By making use of a bioinformatic approach, H19 was shown to bind to miR-139 and miR-141. Therefore, it was supposed that there may be interactions between miR-139/miR-141 and H19 [20, 21].

Bioinformatic results and dual-luciferase assays have suggested that CXCR4 is a direct miR-139 target. Functionally, the suppressive effects of miR-139 on the proliferation of T-ALL cells were reversed by CXCR4 transfection, while the miR-139 overexpression substantially lowered the malignancy of T-ALL cells, and people with very high expression of miR-139 and reduced CXCR4 expression showed greater five-year survival than people with reduced miR-139 expression [22]. Also, the homing and migratory capacity of umbilical cord-derived MSC via regulating CXCR4 could lead to the boosting of protection against liver ischemia/reperfusion injury by rapamycin-preconditioned umbilical cord-derived MSC [23], and by promoting the expression of CXCR4, HIV glycoprotein gp120 has also been found to enhance the migration of MSC [24]. Also, bioinformatic results and dual-luciferase assays have suggested ICAM-1 as a direct target of miR-141. ICAM-1 has been shown to interact with target cells during cytotoxic T cell and natural killer cell-mediated damage [25], and ICAM-1 has also been shown to prevent and reverse dextran sulfate sodium-induced colitis in mice [26].

Moreover, It has been shown that the overexpression of CXCR4 and ICAM-1 may promote the homing of MSC in the treatment of IBD [27, 28]. Furthermore, we suspected that the overexpression of H19 may enhance the expression of CXCR4 and ICAM-1, possibly by the findings that H19 could sponge the expression of miR-139 and miR-141 expression [21]. In this study, we treated ulcerative colitis animals with MSC preconditioned with or without H19 and compared the therapeutic effect of MSC and MSC-H19 in the treatment of ulcerative colitis.

2. Materials and Methods

2.1. Mice. All female C57BL/6 mice (approximately 8 weeks, body weight approximately 20 g) were obtained from the

institutional animal center. Mice were fed a pellet-based diet and drinking water. The study protocol was approved by the institutional ethical committee.

2.2. Preparation of MSC. Bilateral tibias and femurs were isolated from four-week-old female C57BL/6 mice, and bone marrow was rinsed out of the marrow cavity with DMEM (Gibco, New York, NY, USA) and filtered using a cell strainer (70 μ m, BD Biosciences, Franklin Lakes, NJ, USA) prior to spinning for 5 mins at 600 g. The cell pellets were then resuspended in the same medium at 1×10^6 cells/mL. H19- and CXCR4-overexpressing MSC were produced using lentiviral transduction (Thermo Fisher, USA) with pWSLV-07-EF1a-Puro-GFP vectors. The correctness of each plasmid was validated through sequencing. 293 T cells (ATCC, Manassas, VA) were cotransfected with the pWSLV-07-EF1a-H19-Puro-GFP and pWSLV-07-EF1a-Puro-GFP plasmids using Lipofectamine 3000 (Invitrogen, Carlsbad, CA).

2.3. Animal Model. Colitis was triggered by administration of 36–50 kDa DSS (MP Biomedical, Santa Ana, CA). The mice were fed 5% DSS in sterile water for 1 week and then fed regular water for another 14 days (three cycles). The animals were evaluated every day to record food uptake and body weight (body weight change was calculated using the weight on day 0 as a reference). Bodyweight data were collected every 3 days to calculate body weight change (%) (weight at day X /weight at day 0) \times 100, and stool consistency and rectal bleeding occurrence were recorded. Thirty-two C57BL/6 mice were randomly divided into four groups (eight animals/group): a SHAM group (mice treated with PBS), animal model group (mice treated with DSS), and two treatment groups (mice treated with DSS + MSC and mice treated with DSS + MSC-H19). For the two treatment groups, mice were treated with MSC or MSC-H19 (3×10^6 cells/mL) via tail vein injection on days 4, 14, and 24. The animal model establishment was accomplished following previous published protocols [29]. Around 5% of the mice died during our experiment. At the end of the experiments (12 weeks in total), the animals in each group were killed to isolate colons for functional analysis.

2.4. Real-Time PCR. A miRNeasy Mini kit (Qiagen, Valencia, CA) was used with a ReverTra PCR assay kit (Toyobo, Osaka, Japan) and SYBR Green mix (Toyobo, Osaka, Japan) to measure H19, miR-141, CXCR4, ICAM-1, and miR-139 expression with the $2^{-\Delta\Delta C_t}$ method. U6 and β -actin were used for control. The primer sets for H19 were 5'-CTTCTTTAAGTCCGTCTCGTTC-3' (forward) and 5'-GAGGCAGGTAGTGTAGTGGTTC-3' (reverse). The primer sets for miR-141 were 5'-TCTTCCAGTGC AGTGTGG-3' (forward) and 5'-GAACATGTCTGCGT ATCTC-3' (reverse). The primer sets for miR-139 were 5'-CTACAGTGCACGTGTCTC-3' (forward) and 5'-GAAC ATGTCTGCGTATCTC-3' (reverse). The primer sets for CXCR4 mRNA were 5'-GACTGGCATAGTCGGCAAT GGA-3' (forward) and 5'-CAAAGAGGAGGTCAGCCAC TGA-3' (reverse). The primer sets for ICAM-1 mRNA were

5'-AAACCAGACCCTGGAAGTGCAC-3' (forward) and 5'-GCCTGGCATTTCAGAGTCTGCT-3' (reverse).

2.5. Cell Experiments. MSC were divided into 2 groups: (1) a pcDNA group (MSC transfected with pcDNA) and (2) a pcDNA-H19 group (MSC transfected with pcDNA-H19). The cells were cultured in DMEM (Gibco, Waltham, MA) containing 100 U/mL pen-strep and 10% FBS. Cells were passaged using 0.25% trypsin EDTA (Gibco, Thermo Fisher Scientific, Waltham, MA) every week. Similarly, MSC were divided into 2 groups: (1) a scramble control group (MSC transfected with control siRNA) and (2) an H19 siRNA group (MSC transfected with H19 siRNA). The primer sets for H19 siRNA were 5'-AACCCGUAGAUCGGAUCUU GUG-3' (forward) and 5'-CAAGAUCGGAUCUACGGGU UU-3' (reverse). The primer sets for control siRNA were 5'-UUCUCCGAACGUGUCACGUTT-3' (forward) and 5'-ACGUGACACGUUCGGAGAATT-3' (reverse). The transfection of MSC was performed with Lipofectamine 3000, and cells were collected 48 h after transfection for subsequent assays.

2.6. Cell Invasion Assay. Transwell assays (Corning, Corning, NY) were performed using an 8 μ m membrane with a Matrigel coating (BD Biosciences, San Jose, CA).

2.7. Luciferase Assay. According to previous publications, H19 was predicted to bind to miR-141 [20] and miR-139 [21]. To confirm the binding of H19 to miR-141 and miR-139, a luciferase assay was performed by cotransfecting cells with scrambled miRNA control + WT H19, miR-141/miR-139 + WT H19, scrambled miRNA control + MUT H19, and miR-141/miR-139 + MUT H19. In brief, fragments of miR-141 and miR-139 containing miR-141 and miR-139 binding sites were cloned into the pcDNA vector (Promega, Madison, WI) downstream of the luciferase gene to generate wild-type H19 plasmids for miR-141 and miR-139 binding, respectively. At the same time, site-directed mutagenesis was performed at the miR-141 and miR-139 binding sites of H19 to generate mutant H19 plasmids. In the next step, MSC were cotransfected with wild-type/mutant H19 and miR-141 or miR-139 using Lipofectamine 3000. The luciferase activity was tested 48 h later using a dual-Luciferase assay (Promega, Madison, WI).

Moreover, by searching public databases (<http://mirtarbase.mbc.nctu.edu.tw>, <http://www.mirdb.org>), ICAM1 and CXCR4 were shown to, respectively, bind to miR-141 and miR-139. In this study, fragments of ICAM-1 and CXCR4 containing binding sites for miR-141 and miR-139, respectively, were cloned into pcDNA vectors downstream of the luciferase gene to generate wild-type ICAM-1 and CXCR4 plasmids for miR-141 and miR-139 binding, respectively. At the same time, site-directed mutagenesis was performed at the miR-141 and miR-139 binding sites of ICAM-1 and CXCR4 to generate mutant-type ICAM-1 and CXCR4 plasmids for miR-141 and miR-139 binding, respectively. In the next step, MSC were cotransfected with wild-type/mutant-type ICAM-1 and CXCR4 plasmids and miR-141 or miR-139 using Lipofectamine 3000. Universally, transfection was

performed following the general protocol: the concentration of plasmid-based constructs was 0.2 μ g, and the concentration of miRNA mimics was 30 nM. The constructs and mimics were separately dissolved in PBS and added to the medium in a dish before shaking to mix. The luciferase activity of the cells was assayed 48 h posttransfection by using a Dual-Luciferase Reporter assay kit.

2.8. Western Blotting. Western blotting was done to assay the expression of ICAM-1 and CXCR4 proteins in samples using a conventional procedure. Anti-ICAM-1 and anti-CXCR4 primary antibodies were purchased from Abcam (Cambridge, MA).

2.9. MTT Assay. MSC proliferation was measured using an MTT assay kit (Beyotime Medical, Wuhan, China). Optical density was evaluated at 570 nm wavelength on a microplate reader (Bio-Rad 550, Bio-Rad Laboratories, Hercules, CA) in strict accordance with the manual provided by the machine manufacturer.

2.10. Transwell Assay. Transwells (8 μ m, Millipore, Billerica, MA) were used to examine the migration ability of MSC in a 48 h experiment.

2.11. Immunohistochemistry. Immunohistochemistry was carried out to determine the protein expression of ICAM-1 and CXCR4 in paraffin-embedded samples. After rehydration, the 4 μ m sliced tissue sample sections were blocked using 5% goat serum before they were incubated with anti-ICAM-1 (dilution: 1:1,000; Abcam, Cambridge, MA) and anti-CXCR4 primary antibodies (dilution: 1:1,000; Abcam, Cambridge, MA) at 4°C overnight. Then, the sections were incubated for twenty minutes at 37°C with biotinylated secondary antibodies (dilution: 1:2,000; Abcam), stained with 3,3'-diaminobenzidine (DAB, Thermo Fisher Scientific, Waltham, MA), counterstained with hematoxylin, and observed under an Olympus light microscope (Olympus Corporation).

2.12. Histological Analysis. HE stained transverse sections from colon samples were sliced into 4 μ m sections, fixed at 4°C overnight in 4% (v/v) formaldehyde, and embedded in paraffin. The extent of colonic inflammatory damage was assessed blindly according to previous publications [30].

2.13. Serum Analysis. The levels of peripheral blood biomarkers, such as C-reactive protein (CRP), were evaluated with a biochemistry analyzer (TBA-120FR; Toshiba Medical System Co., Tochigi, Japan) according to the manufacturer's instructions.

3. Statistical Analysis

One-way ANOVA (post hoc test: Tukey's test) and Student's *t*-tests were performed using SPSS 21.0 when appropriate to compare the results for different groups. A *P* value of 0.05 was taken to judge statistical significance.

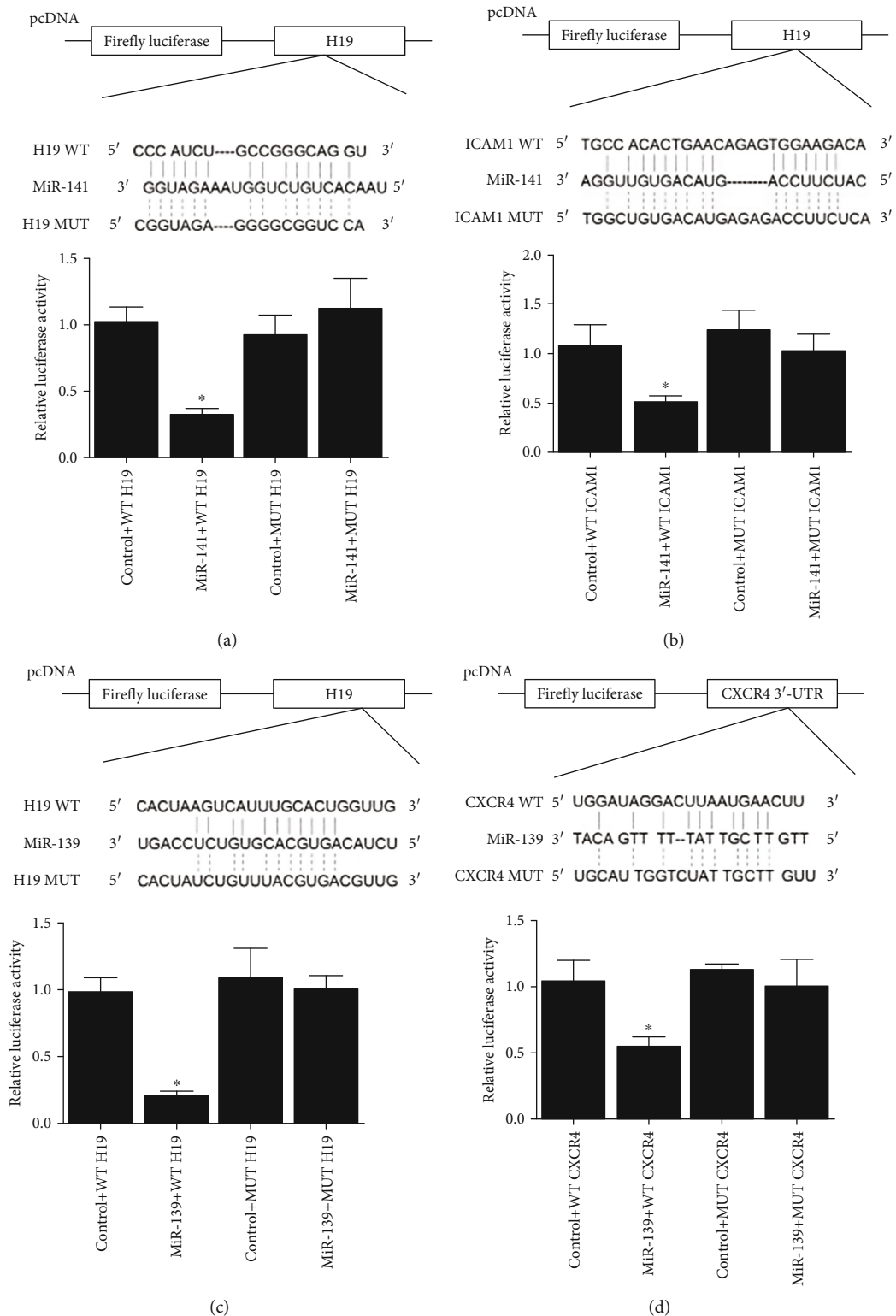


FIGURE 1: Luciferase assay of the H19-miR-141-ICAM-1 and H19-miR-139-CXCR4 axis. (a) Binding region between H19 and miR-141 was predicted, and the luciferase activity was the lowest in cells cotransfected with miR-141 and wild-type H19 (**P* value <0.05 vs. control + WT H19). (b) Binding region between miR-141 and ICAM-1 was predicted, and the luciferase activity was the lowest in cells cotransfected with miR-141 and wild-type ICAM-1 (**P* value <0.05 vs. control + WT ICAM1). (c) Binding region between H19 and miR-139 was predicted, and the luciferase activity was the lowest in cells cotransfected with miR-139 and wild-type H19 (**P* value <0.05 vs. control + WT ICAM1). (d) Binding region between miR-139 and CXCR4 was predicted, and the luciferase activity was the lowest in cells cotransfected with miR-139 and wild-type CXCR4 (**P* value <0.05 vs. control + WT CXCR4).

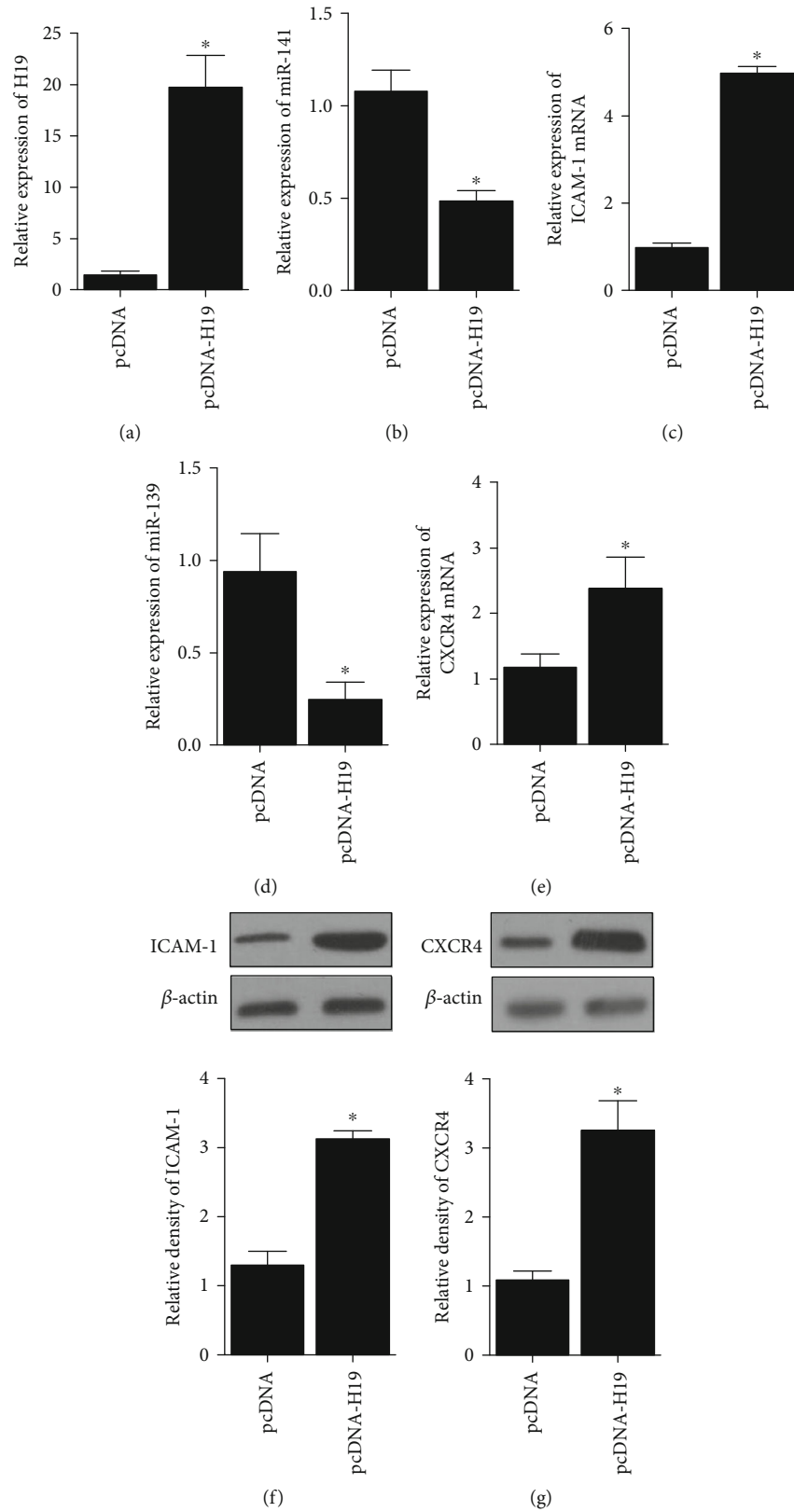


FIGURE 2: RNA and protein levels of miR-141, miR-139, ICAM-1, and CXCR4 in MSC was regulated by the transfection of H19 (**P* value <0.05 vs. pcDNA). (a) RNA level of H19 was boosted in MSC transfected with H19. (b) RNA level of miR-141 was decreased in MSC transfected with H19. (c) mRNA level of ICAM-1 was increased in MSC transfected with H19. (d) RNA level of miR-139 was decreased in MSC transfected with H19. (e) mRNA level of CXCR4 was increased in MSC transfected with H19. (f) protein level of ICAM-1 was higher in MSC transfected with H19. (g) Protein level of CXCR4 was higher in MSC transfected with H19.

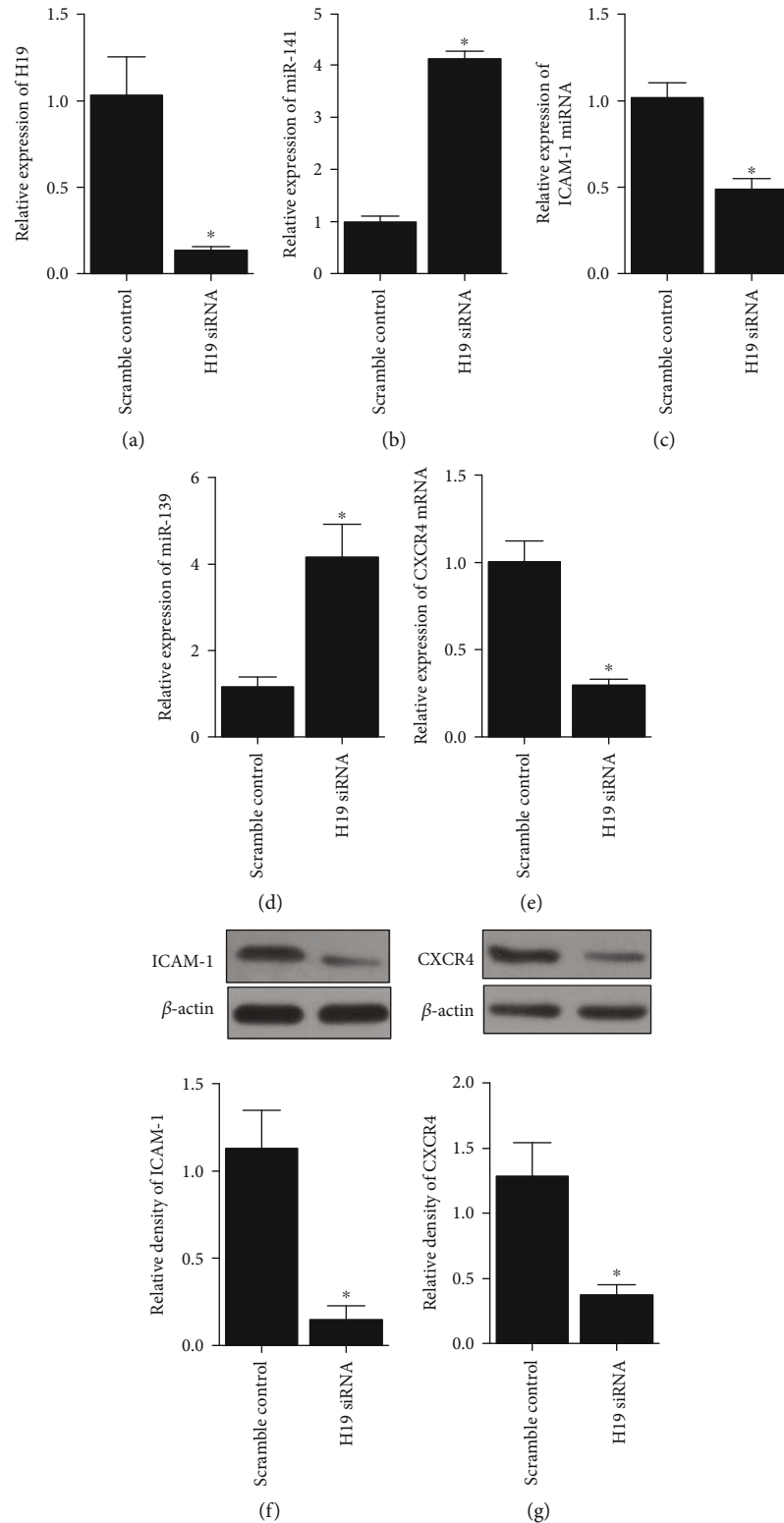


FIGURE 3: RNA and protein levels of miR-141, miR-139, ICAM-1, and CXCR4 in MSC transfected with scramble control or H19 siRNA (**P* value < 0.05 vs. control). (a) RNA level of H19 was reduced by the transfection of H19 siRNA in MSC. (b) RNA level of miR-141 was promoted by the transfection of H19 siRNA in MSC. (c) mRNA level of ICAM-1 was inhibited by the transfection of H19 siRNA in MSC. (d) RNA level of miR-139 was promoted by the transfection of H19 siRNA in MSC. (e) mRNA level of CXCR4 was inhibited by the transfection of H19 siRNA in MSC. (f) Protein level of ICAM-1 was reduced with the presence of H19 siRNA in MSC. (g) Protein level of CXCR4 was reduced with the presence of H19 siRNA in MSC.

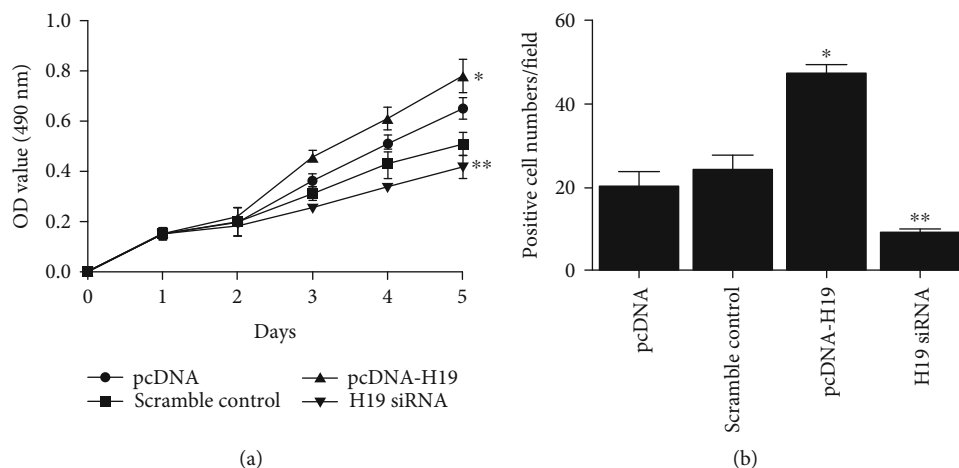


FIGURE 4: Proliferation and migration of MSC transfected with pcDNA, scramble control, pcDNA-H19, or H19 siRNA (* P value <0.05 vs. pcDNA; ** P value <0.05 vs. control). (a) MTT assay indicated that proliferation of MSC transfected with pcDNA-H19 was the highest among all cell groups. (b) Transwell assay indicated that migration of MSC transfected with pcDNA-H19 was the highest among all cell groups.

4. Results

4.1. Validation of the H19-miR-141-ICAM-1 and H19-miR-139-CXCR4 Axes. By searching public databases (<http://mirtarbase.mbc.nctu.edu.tw> and <http://www.mirdb.org>), H19 was predicted to bind to miR-141 (Figure 1(a)) and miR-139 (Figure 1(c)). We subsequently confirmed the binding of H19 to miR-141 and miR-139 by detecting the luciferase activity in cells cotransfected with control + WT/MUT H19 and in cells cotransfected with miR-141/miR-139 + WT/MUT H19. Accordingly, the results revealed that the luciferase activity was sharply decreased in cells cotransfected with WT H19 and miR-141 (Figure 1(a)) or WT H19 and miR-139 (Figure 1(c)). The downstream targets of miR-141 and miR-139 were further analyzed. ICAM-1 was predicted to be a downstream target of miR-141 (Figure 1(b)), and CXCR4 was predicted to be a downstream target of miR-139 (Figure 1(d)). Then, the luciferase activity was tested in cells cotransfected with control + WT/MUT ICAM-1 compared with cells cotransfected with miR-141 + WT/MUT ICAM-1 (Figure 1(b)) and in cells cotransfected with control + WT/MUT CXCR4 compared with cells cotransfected miR-139 + WT/MUT CXCR4 (Figure 1(d)). Accordingly, luciferase activity was significantly decreased in cells cotransfected with miR-141 and wild-type ICAM-1 (Figure 1(b)) and in cells cotransfected with CXCR4 and miR-139 (Figure 1(d)).

4.2. Regulatory Relationship among H19, miR-141/miR-139, and ICAM-1/CXCR4. Mesenchymal stem cells (MSC) were transfected with pcDNA or pcDNA-H19, followed by detection of the expression of miR-141, ICAM-1 mRNA/protein, miR-139, and CXCR4 mRNA/protein. The evidently upregulated H19 expression validated the successful transfection of pcDNA-H19 (Figure 2(a)), and the miR-141 (Figure 2(b)) and miR-139 (Figure 2(d)) expression was decreased in pcDNA-H19 cells, while the ICAM-1 (Figures 2(c) and 2(f))

and CXCR4 (Figures 2(e) and 2(g)) expression was increased in pcDNA-H19 cells. In addition, cells transfected with H19 siRNA (Figure 3(a)) had higher levels of miR-141 (Figure 3(b)) and miR-139 (Figure 3(d)) but lower levels of ICAM-1 (Figures 3(c) and 3(f)) and CXCR4 (Figures 3(e) and 3(g)).

4.3. The Impacts of H19 on Cell Proliferation and Migration. MSC were transfected with pcDNA, scramble control, pcDNA-H19, or H19 siRNA, and MTT and transwell assays were performed to detect cell proliferation and migration. MTT results showed that the proliferation rate of cells transfected with pcDNA-H19 was significantly higher than that of cells in other groups, while the proliferation rate of cells transfected with H19 siRNA was the lowest among all the cell groups (Figure 4(a)). Transwell assays revealed that higher expression of H19 had positive effects on cell migration, while downregulation of H19 inhibited cell migration (Figure 4(b)).

4.4. Impact of MSC and H19 on Ulcerative Colitis Mice. Mice were randomly divided into 4 groups: SHAM, DSS, DSS + MSC, and DSS + MSC-H19, and body weight was measured every three days. Accordingly, at day 90, mice treated with DSS showed significant weight loss (Figure 5(a)) and shortened colon length (Figure 5(b)), and the effects of DSS were attenuated by MSC treatment and further alleviated by MSC-H19 treatment (Figures 5(a) and 5(b)). Additionally, the level of the peripheral blood biomarker CRP was the lowest in the SHAM group and highest in the DSS group (Figure 5(c)). As shown in Figure 5(d), HE staining indicated that the level of inflammation was evidently increased by DSS, and MSC treatment and MSC-H19 treatment partially restored the increased histological inflammatory score in DSS mice.

Then, the levels of inflammatory cytokines (TNF- α , IL-1, IL-6, IL-8) were tested in the four groups. As expected, DSS

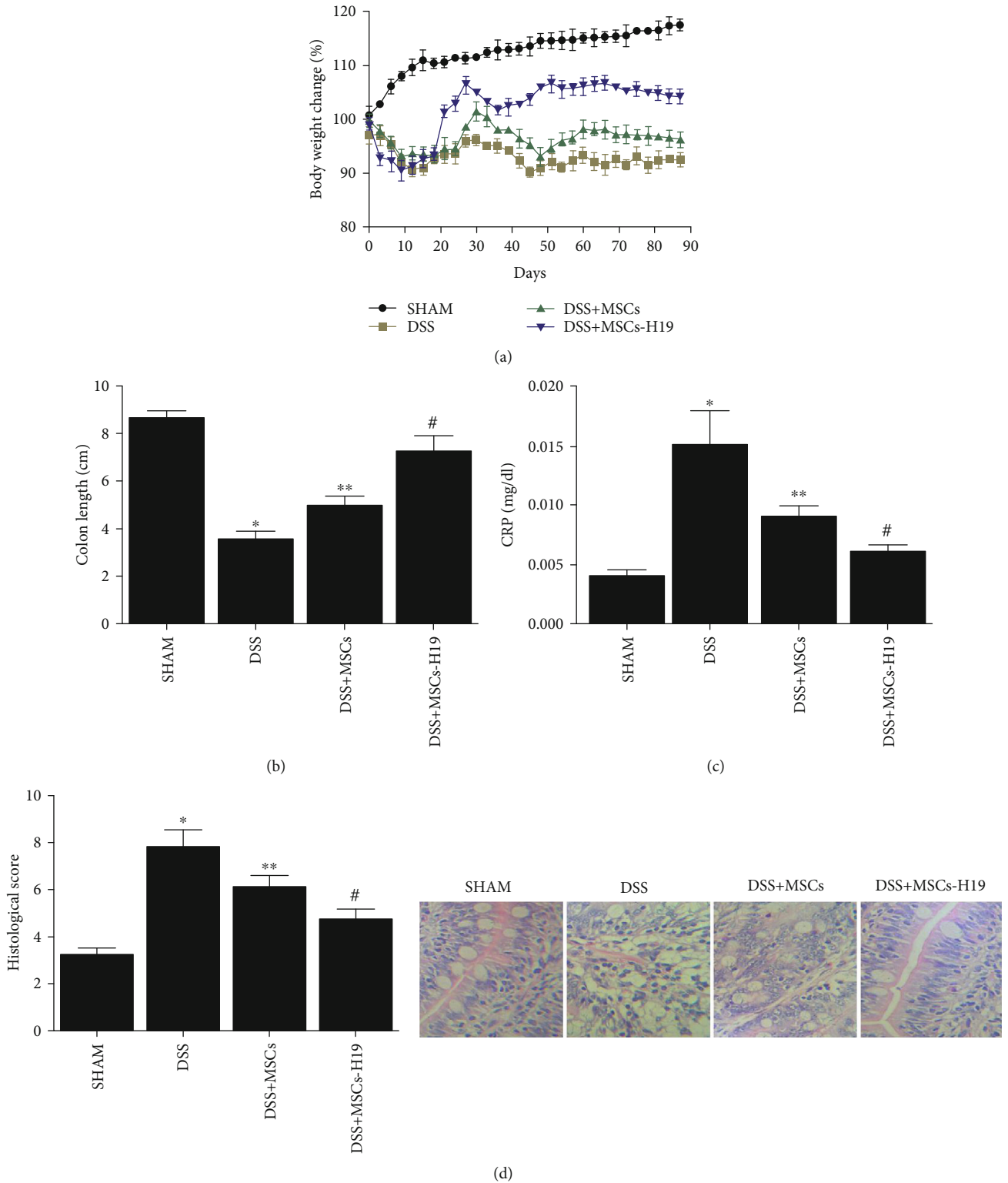


FIGURE 5: Effects of DSS, MSC, and MSC-H19 on mice weight and colon length. (a) Body weight loss of mice was highest in the DSS group, while MSC treated and MSC-H19 treated both obstructed this negative effect (body weight loss (%) = (weight at day X/weight at day 0) × 100). (b) Colon length of mice was shortest in the DSS group and longest in the SHAM group (**P* value <0.05 vs. control; ***P* value <0.05 vs. DSS; #*P* value <0.05 vs. DDS + MSC). (c) Histological inflammatory score of HE staining of mice was the highest in the DSS group and lowest in the SHAM group (**P* value <0.05 vs. control; ***P* value <0.05 vs. DSS; #*P* value <0.05 vs. DDS + MSC). (d) CRP level of mice was the highest in the DSS group and lowest in the SHAM group (**P* value <0.05 vs. control; ***P* value <0.05 vs. DSS; #*P* value <0.05 vs. DDS + MSC).

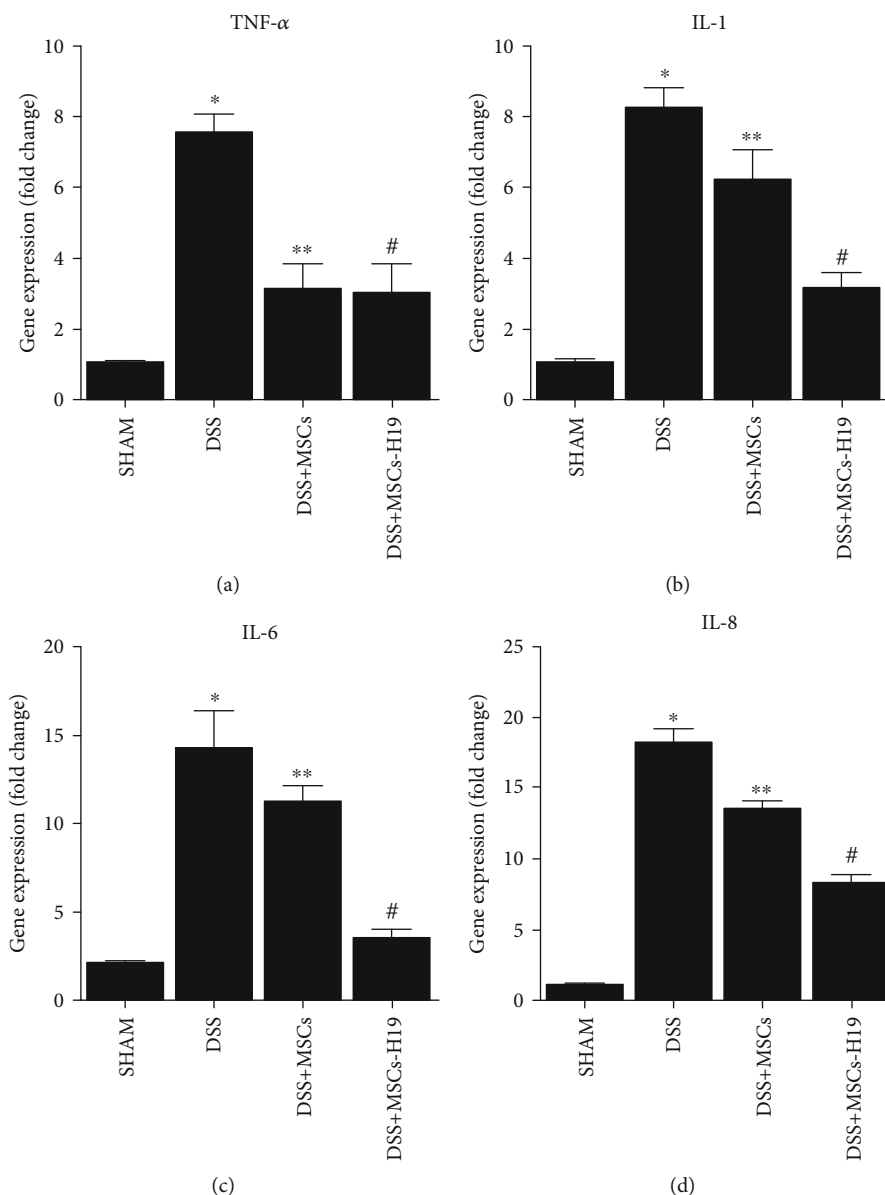


FIGURE 6: Effects of DSS, MSC, and MSC-H19 on the inflammatory response were measured by the detection of mRNA levels of TNF- α , IL-1, IL-6, and IL-8 (**P* value <0.05 vs. control; ***P* value <0.05 vs. DSS; #*P* value <0.05 vs. DSS + MSC). (a) Level of TNF- α mRNA in mice was the highest and lowest, respectively, in the DSS and SHAM groups. (b) Level of IL-1 mRNA in mice was the highest and lowest, respectively, in the DSS and SHAM groups. (c) Level of IL-6 mRNA in mice was the highest and lowest, respectively, in the DSS and SHAM groups. (d) Level of IL-8 mRNA in mice was the highest and lowest, respectively, in the DSS and SHAM groups.

treatment induced an inflammatory response, manifested by increased expression of TNF- α (Figure 6(a)), IL-1 (Figure 6(b)), IL-6 (Figure 6(c)), and IL-8 (Figure 6(d)). MSC injection reduced the effects of DSS, and MSC-H19 infusion further reduced the level of inflammatory responses.

4.5. Functions of MSC and H19 in Ulcerative Colitis Mice. We further tested the targets of H19 (i.e., miR-141 and miR-139) and their downstream genes (i.e., ICAM-1 and CXCR4) in the four mouse groups. As shown in Figure 7, administration of DSS evidently increased miR-141 (Figure 7(a)) and miR-139 (Figure 7(c)) expression while decreasing ICAM-1 mRNA (Figure 7(b)) and CXCR4

mRNA (Figure 7(d)) expression, which was also confirmed by RT-qPCR. MSC injection weakened the effects of DSS, and MSC-H19 further abated the effects of DSS. ICAM-1 and CXCR4 protein expression was measured via Western blotting. As shown in Figures 7(e) and 7(f), the protein expression of ICAM-1 and CXCR4 was significantly decreased by DSS, while MSC infusion elevated the protein expression of CXCR4 and ICAM-1, and MSC-H19 had a more prominent effect in raising the ICAM-1 and CXCR4 expression (Figures 7(e) and 7(f)). The protein expression of CXCR4 (Figure 8(b)) and ICAM-1 (Figure 8(a)) was further examined via IHC, and the results were consistent with the WB results.

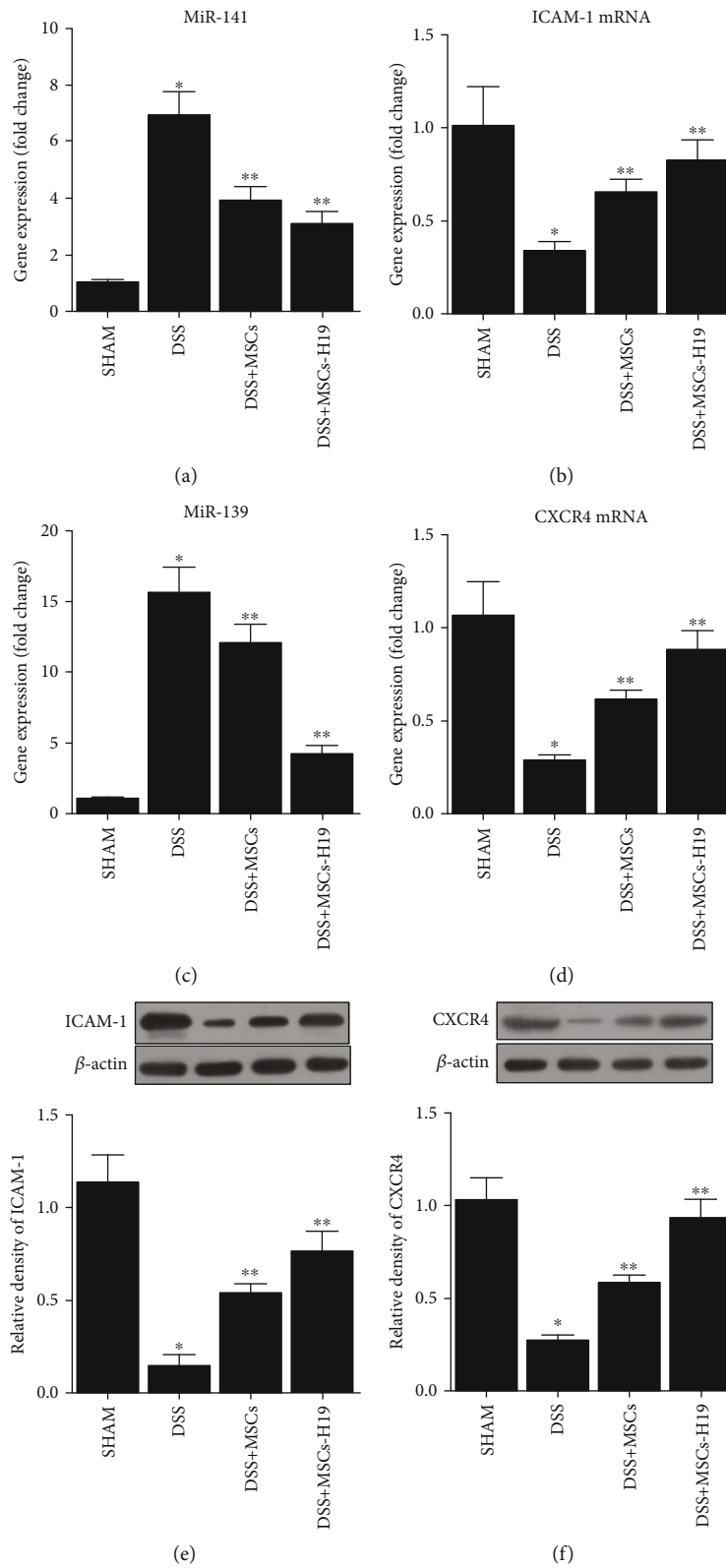


FIGURE 7: Effects of DSS, MSC, and MSC-H19 on miR-141, ICAM-1 mRNA, miR-139, and CXCR4 levels (**P* value <0.05 vs. control; ***P* value <0.05 vs. DSS). (a) RNA level of miR-141 in mice was the highest in the DSS group and the lowest in the SHAM group. (b) RNA level of ICAM-1 in mice was the highest and lowest, respectively, in the SHAM and DSS groups. (c) RNA level of miR-139 in mice was the highest in the DSS group and the lowest in the SHAM group. (d) RNA level of CXCR4 in mice was the highest and lowest, respectively, in the SHAM and DSS groups. (e) Protein level of ICAM-1 in mice was the highest and lowest, respectively, in the SHAM and DSS groups. (f) Protein level of CXCR4 in mice was the highest and lowest, respectively, in the SHAM and DSS groups.

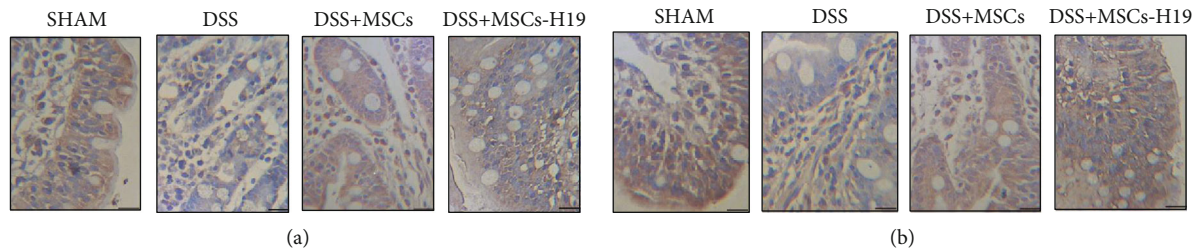


FIGURE 8: Protein levels of ICAM-1 and CXCR4 in transverse colon tissues of mice in SHAM, DSS, DSS + MSC, and DSS + MSC-H19 groups were detected by IHC (the brown color denotes the expression of ICAM-1 in (a) and CXCR4 in (b); scale bar: 50 μ m). (a) IHC assay indicated that the protein level of ICAM-1 was the lowest in the DSS group and highest in the SHAM group. (b) IHC assay indicated that the protein level of CXCR4 was the lowest in the DSS group and highest in the SHAM group.

5. Discussion

IBD, such as Crohn's disease and ulcerative colitis, is persistent and relapsing conditions with chronic inflammation of the intestinal tract and injuries to the mucus [31]. Mucosal recovery is linked to improved and lasting medical efficacy. Thus, mucosal recovery has been a major target for IBD treatment [32]. The absence of mucosal recuperation generally leads to difficulties in patient recovery and complications, such as blood loss, fistulas, and perforation, which demand a hospital stay and surgery. Less than 50% of IBD patients can be managed with standard treatments, such as immunomodulators, corticosteroids, and biologic drugs [33]. Standard treatments used to treat IBD rely on suppression of the immune system; for that reason, new techniques are required to enhance mucosal regrowth [34]. While intravenous transplants of stem cells are frequently used in common treatments, the distribution of MSC to wounded tissues is still extremely complicated [35]. Initiatives are being made to promote the delivery of MSC, such as by using nanoparticles [36]. In addition, chemokine CXC receptor (CXCR), vascular cell adhesion molecule 1 (VCAM1), and E-selectin ligands have been assessed to cover MSC surfaces to aid their targeted delivery to wounded sites, improving the therapeutic results of IBD therapy [35, 37]. In the present study, mice were randomly divided into 4 groups: SHAM, DSS, DSS + MSC, and DSS + MSC-H19. Mice treated with DSS showed significant weight loss and shortened colon length. The effects of DSS were obstructed by MSC treatment and were further alleviated by MSC-H19 treatment. In addition, the level of inflammatory cytokines was tested in the four groups. DSS treatment induced an inflammatory response, while MSC injection reduced the effects of DSS, and MSC-H19 infusion further reduced the inflammatory response. Furthermore, the levels of targets of H19 (miR-141 and miR-139) and their downstream genes (ICAM-1 and CXCR4) were tested in the four mouse groups. It was found that the expression of miR-141 and miR-139 was evidently increased while the expression of ICAM-1 and CXCR4 was decreased in DSS animals. MSC injection weakened the effects of DSS, and MSC-H19 injection further abated the effects of DSS.

Recently, the level of H19 was discovered to become substantially enhanced in osteoarthritis tissues, indicating a prospective role of H19 in the progression of inflammatory

conditions [38]. A previous report on the role of H19 in protection of the intestinal barrier in sepsis seems to conflict with our results [39]. Such a discrepancy could be attributed to the different disease backgrounds. The basic disease investigated in this study is ulcerative colitis, and the basic disease examined in the reference is sepsis. Recently, scientists utilized bioinformatic and luciferase assay to verify the binding between miR-141 and H19. As assumed, it was found that miR-141 could bind complementarily to H19, inhibiting translation of an RLuc-H19 gene. It was likewise revealed that miR-141 acts as a repressor of ICAM-1 expression, and the miR-141 overexpression decreases the ICAM-1 expression induced by ischemia to alleviate reperfusion injury. Therefore, miR-141 might act as a beneficial factor in the treatment of heart disease [40]. Here, ICAM-1 is predicted to be a downstream gene of miR-141, and CXCR4 is a downstream target of miR-139. The activity of miR-141/miR-139 was decreased in cells cotransfected with miR-141/miR-139 and ICAM-1/CXCR4. In addition, mesenchymal stem cells (MSC) were transfected with pcDNA, pcDNA-H19, or H19 siRNA. The expression levels of miR-141 and miR-139 were decreased in pcDNA-H19 cells and increased in H19 siRNA cells, while the levels of ICAM-1 and CXCR4 were increased in pcDNA-H19 cells but decreased in H19 siRNA cells. Furthermore, MSC were transfected with pcDNA, scramble control, pcDNA-H19, or H19 siRNA. MTT and transwell assays revealed that the higher H19 expression had positive effects on cell proliferation and migration, while downregulation of H19 inhibited cell proliferation and migration.

ICAM-1 has been shown to participate in the vital processes of immune reactions [9]. ICAM-1 can promote homing of numerous immune cells in secondary lymphoid organs. From a physiological standpoint, the ICAM-1 expression in MSC is very low, but ICAM-1 is dramatically enhanced in MSC located in an inflammatory environment [41, 42]. In addition, ICAM-1 up-regulation enhances the immunosuppressive role of MSC [41–43].

The expression of ICAM-1 in IBD indicates a possible function of ICAM-1 in IBD pathophysiology. ICAM-1 was shown to be elevated in colon lysates collected from patients with ulcerative colitis [44, 45].

The level of CXCR4 is an essential factor in promoting the proliferation and migration of stem cells. CXCR4 is mostly expressed in cell cytoplasm [46]. The level of CXCR4

is minimized with extended cell culture [47]. Various cytokines can promote the expression of CXCR4 on the cell membrane [48, 49]. Transforming growth factor- β 1 (TGF- β 1) might upregulate the CXCR4 expression in basal cell carcinoma (BCC) cells [50]. TGF- β 1 can also increase CXCR4 levels in MSC in acute I/R injury. Additionally, CXCR4 aids MSC migration to SDF-1.

The results of this study provided further understanding of the molecular mechanism underlying the therapeutic effect of stem cell in the treatment of IBD and identified the reinforcer, H19, to improve the therapeutic effect of stem cells. These findings may provide a basis for the future clinical use of stem cell as a modality to treat IBD.

6. Conclusion

In conclusion, collectively, the results of our study demonstrated that the overexpression of H19 in MSC downregulated the expression of miR-139 and miR-141, thus upregulating the expression of their target genes ICAM-1 and CXCR4, respectively. Since it has been verified that the overexpression of ICAM-1 and CXCR4 can promote the homing of MSC in the treatment of ulcerative colitis, the overexpression of H19 exhibited therapeutic effects in ulcerative colitis.

Data Availability

The data of this study are available from the corresponding author upon reasonable request.

Conflicts of Interest

The authors declare that they have no conflicts of interest.

Acknowledgments

This work was supported by grants from the Guangdong Provincial Key Laboratory of Precision Medicine for Gastrointestinal Cancer (2020B121201004).

References

- [1] D. Sheehan and F. Shanahan, "The Gut Microbiota in Inflammatory Bowel Disease," *Gastroenterology Clinics of North America*, vol. 46, no. 1, pp. 143–154, 2017.
- [2] K. M. de Lange and J. C. Barrett, "Understanding inflammatory bowel disease via immunogenetics," *Journal of Autoimmunity*, vol. 64, pp. 91–100, 2015.
- [3] A. I. Caplan, "New MSC: MSCs as pericytes are sentinels and gatekeepers," *Journal of Orthopaedic Research*, vol. 35, no. 6, pp. 1151–1159, 2017.
- [4] Y. Z. Zhu, H. B. Ma, T. Liu, L. B. Wang, and Y. K. Li, "Effects of IFN- γ on immunomodulation of mesenchymal stem cells isolated from fetal side of human placenta tissues," *Xi Bao Yu Fen Zi Mian Yi Xue Za Zhi*, vol. 28, no. 10, pp. 1058–1061, 2012.
- [5] K. Miteva, K. Pappritz, M. El-Shafeey et al., "Mesenchymal stromal cells modulate monocytes trafficking in coxsackievirus B3-induced myocarditis," *Stem Cells Translational Medicine*, vol. 6, no. 4, pp. 1249–1261, 2017.
- [6] A. T. Wang, Y. Feng, H. H. Jia, M. Zhao, and H. Yu, "Application of mesenchymal stem cell therapy for the treatment of osteoarthritis of the knee: a concise review," *World Journal of Stem Cells*, vol. 11, no. 4, pp. 222–235, 2019.
- [7] H. Yang, Y. Zheng, Y. Zhang, Z. Cao, and Y. Jiang, "Mesenchymal stem cells derived from multiple myeloma patients protect against chemotherapy through autophagy-dependent activation of NF- κ B signaling," *Leukemia Research*, vol. 60, pp. 82–88, 2017.
- [8] I. A. Ho, H. C. Toh, W. H. Ng et al., "Human bone marrow-derived mesenchymal stem cells suppress human glioma growth through inhibition of angiogenesis," *Stem Cells*, vol. 31, no. 1, pp. 146–155, 2013.
- [9] B. G. Cui, A. Campagne, G. W. Bell et al., "MSC-regulated microRNAs converge on the transcription factor FOXP2 and promote breast cancer metastasis," *Cell Stem Cell*, vol. 15, no. 6, pp. 762–774, 2014.
- [10] P. F. Li, S. C. Chen, T. Xia et al., "Non-coding RNAs and gastric cancer," *World Journal of Gastroenterology*, vol. 20, no. 18, pp. 5411–5419, 2014.
- [11] H. Bierhoff, A. Postepska-Igielska, and I. Grummt, "Noisy silence: non-coding RNA and heterochromatin formation at repetitive elements," *Epigenetics*, vol. 9, no. 1, pp. 53–61, 2014.
- [12] U. A. Orom and R. Shiekhattar, "Long noncoding RNAs usher in a new era in the biology of enhancers," *Cell*, vol. 154, no. 6, pp. 1190–1193, 2013.
- [13] A. Gabory, M. A. Ripoché, T. Yoshimizu, and L. Dandolo, "The H19 gene: regulation and function of a non-coding RNA," *Cytogenetic and Genome Research*, vol. 113, no. 1–4, pp. 188–193, 2006.
- [14] I. J. Matouk, N. DeGroot, S. Mezan et al., "The H19 non-coding RNA is essential for human tumor growth," *PLoS One*, vol. 2, no. 9, article e845, 2007.
- [15] H. M. Byun, H. L. Wong, E. A. Birnstein, E. M. Wolff, G. Liang, and A. S. Yang, "Examination of IGF2 and H19 loss of imprinting in bladder cancer," *Cancer Research*, vol. 67, no. 22, pp. 10753–10758, 2007.
- [16] F. Tian, Z. Tang, G. Song et al., "Loss of imprinting of IGF2 correlates with hypomethylation of the H19 differentially methylated region in the tumor tissue of colorectal cancer patients," *Molecular Medicine Reports*, vol. 5, no. 6, pp. 1536–1540, 2012.
- [17] S. Lottin, E. Adriaenssens, T. Dupressoir et al., "Overexpression of an ectopic H19 gene enhances the tumorigenic properties of breast cancer cells," *Carcinogenesis*, vol. 23, no. 11, pp. 1885–1895, 2002.
- [18] W. Wu, Q. Hu, E. Nie et al., "Hypoxia induces H19 expression through direct and indirect Hif-1 α activity, promoting oncogenic effects in glioblastoma," *Scientific Reports*, vol. 7, no. 1, 2017.
- [19] Y. Qu, J. Wu, D. Chen et al., "MiR-139-5p inhibits HGTD-P and regulates neuronal apoptosis induced by hypoxia-ischemia in neonatal rats," *Neurobiology of Disease*, vol. 63, pp. 184–193, 2014.
- [20] X. Zhou, F. Ye, C. Yin, Y. Zhuang, G. Yue, and G. Zhang, "The interaction between MiR-141 and lncRNA-H19 in regulating cell proliferation and migration in gastric cancer," *Cellular Physiology and Biochemistry*, vol. 36, no. 4, pp. 1440–1452, 2015.
- [21] L. C. Gong, H. M. Xu, G. L. Guo, T. Zhang, J. W. Shi, and C. Chang, "Long non-coding RNA H19 protects H9c2 cells

- against hypoxia-induced injury by targeting microRNA-139," *Cellular Physiology and Biochemistry*, vol. 44, no. 3, pp. 857–869, 2017.
- [22] L. Qin, H. Y. Deng, S. J. Chen, and W. Wei, "miR-139 acts as a tumor suppressor in T-cell acute lymphoblastic leukemia by targeting CX chemokine receptor 4," *American Journal of Translational Research*, vol. 9, no. 9, pp. 4059–4070, 2017.
- [23] J. Zheng, H. Li, L. He et al., "Preconditioning of umbilical cord-derived mesenchymal stem cells by rapamycin increases cell migration and ameliorates liver ischaemia/reperfusion injury in mice via the CXCR4/CXCL12 axis," *Cell Proliferation*, vol. 52, no. 2, article e12546, 2019.
- [24] L. Li, R. Z. L. Lim, L. S. U. Lee, and N. S. Y. Chew, "HIV glycoprotein gp120 enhances mesenchymal stem cell migration by upregulating CXCR4 expression," *Biochimica et Biophysica Acta - General Subjects*, vol. 1862, no. 8, pp. 1790–1800, 2018.
- [25] J. R. Philpott and P. B. Miner Jr., "Antisense inhibition of ICAM-1 expression as therapy provides insight into basic inflammatory pathways through early experiences in IBD," *Expert Opinion on Biological Therapy*, vol. 8, no. 10, pp. 1627–1632, 2008.
- [26] C. F. Bennett, D. Kornbrust, S. Henry et al., "An ICAM-1 antisense oligonucleotide prevents and reverses dextran sulfate sodium-induced colitis in mice," *The Journal of Pharmacology and Experimental Therapeutics*, vol. 280, no. 2, pp. 988–1000, 1997.
- [27] X. Li, Q. Wang, L. Ding et al., "Intercellular adhesion molecule-1 enhances the therapeutic effects of MSCs in a dextran sulfate sodium-induced colitis models by promoting MSCs homing to murine colons and spleens," *Stem Cell Research & Therapy*, vol. 10, no. 1, p. 267, 2019.
- [28] X. B. Zheng, X. W. He, L. J. Zhang et al., "Bone marrow-derived CXCR4-overexpressing MSCs display increased homing to intestine and ameliorate colitis-associated tumorigenesis in mice," *Gastroenterology Report*, vol. 7, no. 2, pp. 127–138, 2019.
- [29] B. R. Jin, K. S. Chung, S. Y. Cheon et al., "Rosmarinic acid suppresses colonic inflammation in dextran sulphate sodium (DSS)-induced mice via dual inhibition of NF- κ B and STAT3 activation," *Scientific Reports*, vol. 7, no. 1, p. ???, 2017.
- [30] A. Sarazin, A. Dendooven, M. Delbeke et al., "Treatment with P28GST, a schistosoma-derived enzyme, after acute colitis induction in mice: decrease of intestinal inflammation associated with a down regulation of Th1/Th17 responses," *PLoS One*, vol. 13, no. 12, article e0209681, 2018.
- [31] D. C. Baumgart and W. J. Sandborn, "Inflammatory bowel disease: clinical aspects and established and evolving therapies," *The Lancet*, vol. 369, no. 9573, pp. 1641–1657, 2007.
- [32] L. Peyrin-Biroulet, W. Sandborn, B. E. Sands et al., "Selecting therapeutic targets in inflammatory bowel disease (STRIDE): determining therapeutic goals for treat-to-target," *Official journal of the American College of Gastroenterology| ACG*, vol. 110, pp. 1324–1338, 2015.
- [33] M. F. Neurath and S. P. Travis, "Mucosal healing in inflammatory bowel diseases: a systematic review," *Gut*, vol. 61, no. 11, pp. 1619–1635, 2012.
- [34] M. F. Neurath, "New targets for mucosal healing and therapy in inflammatory bowel diseases," *Mucosal Immunology*, vol. 7, no. 1, pp. 6–19, 2014.
- [35] T. J. Kean, P. Lin, A. I. Caplan, and J. E. Dennis, "MSCs: Delivery Routes and Engraftment, Cell-Targeting Strategies, and Immune Modulation," *Stem Cells International*, vol. 2013, Article ID 732742, 13 pages, 2013.
- [36] Q. Chen, Y. Li, Z. Chen, H. Du, and J. Wan, "Anti-VCAM 1 antibody-coated mesenchymal stromal cells attenuate experimental colitis via immunomodulation," *Medical Science Monitor*, vol. 25, pp. 4457–4468, 2019.
- [37] S. Ansboro, U. Greiser, F. Barry, and M. Murphy, "Strategies for improved targeting of therapeutic cells: implications for tissue repair," *European Cells & Materials*, vol. 23, pp. 310–319, 2012.
- [38] X. Shi, M. Sun, H. Liu, Y. Yao, and Y. Song, "Long non-coding RNAs: a new frontier in the study of human diseases," *Cancer Letters*, vol. 339, no. 2, pp. 159–166, 2013.
- [39] T. X. Yu, H. K. Chung, L. Xiao et al., "Long Noncoding RNA H19 Impairs the Intestinal Barrier by Suppressing Autophagy and Lowering Paneth and Goblet Cell Function," *Cellular and Molecular Gastroenterology and Hepatology*, vol. 9, no. 4, pp. 611–625, 2020.
- [40] R. R. Liu, J. Li, J. Y. Gong et al., "MicroRNA-141 regulates the expression level of ICAM-1 on endothelium to decrease myocardial ischemia-reperfusion injury," *American Journal of Physiology. Heart and Circulatory Physiology*, vol. 309, no. 8, pp. H1303–H1313, 2015.
- [41] G. Ren, X. Zhao, L. Zhang et al., "Inflammatory cytokine-induced intercellular adhesion molecule-1 and vascular cell adhesion molecule-1 in mesenchymal stem cells are critical for immunosuppression," *Journal of Immunology*, vol. 184, no. 5, pp. 2321–2328, 2010.
- [42] Y. Rubtsov, K. Goryunov, A. Romanov, Y. Suzdaltseva, G. Sharonov, and V. Tkachuk, "Molecular Mechanisms of Immunomodulation Properties of Mesenchymal Stromal Cells: A New Insight into the Role of ICAM-1," *Stem Cells International*, vol. 2017, Article ID 6516854, 15 pages, 2017.
- [43] B. Tang, X. Li, Y. Liu et al., "The therapeutic effect of ICAM-1-overexpressing mesenchymal stem cells on acute graft-versus-host disease," *Cellular Physiology and Biochemistry*, vol. 46, no. 6, pp. 2624–2635, 2018.
- [44] B. Vainer and O. H. Nielsen, "Changed colonic profile of P-selectin, platelet-endothelial cell adhesion molecule-1 (PECAM-1), intercellular adhesion molecule-1 (ICAM-1), ICAM-2, and ICAM-3 in inflammatory bowel disease," *Clinical and Experimental Immunology*, vol. 121, no. 2, pp. 242–247, 2000.
- [45] R. J. Xavier and D. K. Podolsky, "Unravelling the pathogenesis of inflammatory bowel disease," *Nature*, vol. 448, no. 7152, pp. 427–434, 2007.
- [46] M. Abdel Aziz, H. Atta, N. Roshdy et al., "Amelioration of murine Schistosoma mansoni induced liver fibrosis by mesenchymal stem cells," *Journal of Stem Cells & Regenerative Medicine*, vol. 8, no. 1, pp. 28–34, 2012.
- [47] S. Guiducci, M. Manetti, E. Romano et al., "Bone marrow-derived mesenchymal stem cells from early diffuse systemic sclerosis exhibit a paracrine machinery and stimulate angiogenesis in vitro," *Annals of the Rheumatic Diseases*, vol. 70, no. 11, pp. 2011–2021, 2011.
- [48] H. K. Kim, M. de la Luz Sierra, C. K. Williams, A. V. Gulino, and G. Tosato, "G-CSF down-regulation of CXCR4 expression identified as a mechanism for mobilization of myeloid cells," *Blood*, vol. 108, no. 3, pp. 812–820, 2006.

- [49] Z. Wang and Q. Ma, “ β -Catenin is a promising key factor in the SDF-1/CXCR4 axis on metastasis of pancreatic cancer,” *Medical Hypotheses*, vol. 69, no. 4, pp. 816–820, 2007.
- [50] C. Y. Chu, Y. S. Sheen, S. T. Cha et al., “Induction of chemokine receptor CXCR4 expression by transforming growth factor- β 1 in human basal cell carcinoma cells,” *Journal of Dermatological Science*, vol. 72, no. 2, pp. 123–133, 2013.

Research Article

Effect of ORF7 of SARS-CoV-2 on the Chemotaxis of Monocytes and Neutrophils In Vitro

Gang Wang ¹, Jun Guan,¹ Guojun Li,² Fengtian Wu,¹ Qin Yang,¹ Chunhong Huang,¹ Junwei Shao,¹ Lichen Xu,¹ Zixuan Guo,¹ Qihui Zhou,¹ Haihong Zhu ¹, and Zhi Chen ¹

¹State Key Laboratory for Diagnosis and Treatment of Infectious Diseases, National Clinical Research Center for Infectious Diseases, Collaborative Innovation Center for Diagnosis and Treatment of Infectious Diseases, The First Affiliated Hospital, Zhejiang University School of Medicine, Hangzhou, China

²Department of Liver Diseases, National Clinical Research Center for Infectious Disease, Shenzhen Third People's Hospital, The Second Affiliated Hospital, School of Medicine, Southern University of Science and Technology, Shenzhen, 518000 Guangdong, China

Correspondence should be addressed to Haihong Zhu; zhuhh72@zju.edu.cn and Zhi Chen; zjuchenzhi@zju.edu.cn

Received 15 July 2021; Revised 29 August 2021; Accepted 13 September 2021; Published 28 September 2021

Academic Editor: Wen-Jun Tu

Copyright © 2021 Gang Wang et al. This is an open access article distributed under the Creative Commons Attribution License, which permits unrestricted use, distribution, and reproduction in any medium, provided the original work is properly cited.

Coronavirus disease 2019 (COVID-19) caused by the severe acute respiratory syndrome coronavirus 2 (SARS-CoV-2) is currently the most significant public health threat worldwide. Patients with severe COVID-19 usually have pneumonia concomitant with local inflammation and sometimes a cytokine storm. Specific components of the SARS-CoV-2 virus trigger lung inflammation, and recruitment of immune cells to the lungs exacerbates this process, although much remains unknown about the pathogenesis of COVID-19. Our study of lung type II pneumocyte cells (A549) demonstrated that ORF7, an open reading frame (ORF) in the genome of SARS-CoV-2, induced the production of CCL2, a chemokine that promotes the chemotaxis of monocytes, and decreased the expression of IL-8, a chemokine that recruits neutrophils. A549 cells also had an increased level of IL-6. The results of our chemotaxis Transwell assay suggested that ORF7 augmented monocyte infiltration and reduced the number of neutrophils. We conclude that the ORF7 of SARS-CoV-2 may have specific effects on the immunological changes in tissues after infection. These results suggest that the functions of other ORFs of SARS-CoV-2 should also be comprehensively examined.

1. Introduction

Coronavirus disease 2019 (COVID-19) is an infectious disease caused by the severe acute respiratory syndrome coronavirus 2 (SARS-CoV-2) that has become a worldwide pandemic [1–3]. The number of confirmed patients infected by SARS-CoV-2 continues to increase daily. As of Apr 2021, there were more than 0.14 billion SARS-CoV-2 infections and 3 million deaths from COVID-19 reported worldwide (<https://coronavirus.jhu.edu/map.html>). This global pandemic is still not under control, although there are encouraging trends in some regions. Other coronaviruses, such as MERS and SARS, had high transmissibility, but the epidemics were limited to certain regions and populations.

Thus, SARS virus led to more than 8000 infected cases and 700 deaths in 26 countries, and MERS led to about 2500 cases and 858 deaths in 27 countries [4–6]. In contrast, there has been an enormous disease burden associated with SARS-CoV-2 infection. Numerous vaccines are currently available in many regions, and clinical trials have shown they are effective and safe [7, 8].

SARS-CoV-2 infects lung epithelial cells, type II alveolar (ATII) cells, by binding to the membrane-associated angiotensin-converting enzyme 2 (ACE2) on the cell surface [9–12]. Once inside the host cell, SARS-CoV-2 begins to produce viral RNA polymerase, which then replicates the complementary genomic RNA, making double-stranded RNA [13]. Subsequently, cells translate the structural and

nonstructural proteins (NSPs) of SARS-CoV-2 in the cytosol [13, 14]. The structural proteins include nucleocapsid (N), spike (S), membrane (M), and envelope (E) proteins, and the NSPs include 16 NSPs from the ORF1ab [15]. There are at least 10 open reading frames (ORFs) in the genome of SARS-CoV-2: ORF1ab, ORF2 (S protein), ORF3, ORF4 (E protein), ORF5 (M protein), ORF6, ORF7, ORF8, ORF9 (N protein), and ORF10 [15, 16]. Viral polymerase and all 16 NSPs are translated from the ORF1ab subgenome [16]. The S, N, E, and M proteins are all structural proteins, and the 16 NSPs function in replication and transcription of the viral genome [15].

Emerging evidence indicates that almost all of these ORF proteins have important roles in the lifecycle of SARS-CoV-2. As an RNA virus, SARS-CoV-2 infection stimulates the innate immunity of cells for RNA sensor proteins in the cytosol, such as retinoic acid inducible gene-1 (RIG-I), melanoma differentiation-associated gene-5 (MDA-5), and toll-like receptors (TLR 3/7/8), which induce the expression of interferons (IFNs) [17]. ORF6, ORF8, and the N protein of SARS-CoV-2 inhibit these IFN-activated antiviral pathways, and this inhibits the IFN-stimulated response element (ISRE) [18]. Additionally, ORF3 upregulates markers of apoptosis in 293T, HepG2, and Vero E6 [19]. Although the functions of several ORFs are incompletely understood, all ORFs and NSPs have specific functions during the lifecycle of SARS-CoV-2.

The present *in vitro* study examined the function of ORF7 in SARS-CoV-2 by focusing on its regulation of numerous cytokines and chemokines (IL-6, TNF- α , IL-8, CXCL2, and CXCL7) that function in the chemotaxis of monocytes and neutrophils *in vitro*.

2. Materials and Methods

2.1. Cell Culture and Vector Construction of ORF7. A lung adenocarcinoma cell line (A549) was purchased from the Chinese Academy of Science (Shanghai, China), and cells were cultured in Dulbecco's modified Eagle medium (DMEM; Hyclone, Logan, UT, USA) with 10% fetal bovine serum (FBS; Corning, NY, USA) and 1% penicillin/streptomycin in a humidified incubator with 5% CO₂ at 37°C. For transfection, a lentiviral vector harboring FLAG-tagged ORF7 of SARS-CoV-2 was constructed using a specific SARS-CoV-2 strain (Wuhan-Hu-1 strain, NC_045512). Transfection was performed, and ORF7-expressing A549 cell was obtained. Control cells were transfected with control vector.

2.2. Quantitative Real-Time Polymerase Chain Reaction (qRT-PCR). RNA was extracted from cells using the TRIzol reagent (TaKaRa, Dalian) and was then reverse transcribed into cDNA using the PrimeScript RT Master Mix (TaKaRa, Dalian). The expression of mRNAs (*IL-1a*, *IL-1b*, *IFN- α* , *IFN- β* , *IL-6*, *IL-8*, *CCL2*, and *TNF- α*) was quantified using qRT-PCR with the TB Green Master Mix (TaKaRa, Japan). Expression was normalized to *GAPDH*, and relative expression was calculated using the $2^{-\Delta\Delta C_t}$ method (primers are listed in Table 1). qRT-PCR was performed with the Quant-

TABLE 1: Primers for real-time PCR.

Gene symbol	Sequences
Human-3552-IL-1a-F	TGGTAGTAGCAACCAACGGGA
Human-3552-IL-1a-R	ACTTTGATTGAGGGCGTCATTC
Human-3553-IL-1b-F	AGCTACGAATCTCCGACCAC
Human-3553-IL-1b-R	CGTTATCCCATGTGTGCGAAGAA
Human-3439-IFN-a-F	GCCTCGCCCTTTGCTTTACT
Human-3439-IFN-a-R	CTGTGGGTCTCAGGGAGATCA
Human-3456-IFN-b-F	GCTTGGATTCTACAAAAGAAGCA
Human-3456-IFN-b-R	ATAGATGGTCAATGCGGCGTC
Human-3569-IL-6-F	ACTCACCTCTTCAGAACGAATTG
Human-3569-IL-6-R	CCATCTTTGGAAGGTTCAAGTTG
Human-3576-IL-8-F	TTTTGCCAAGGAGTGCTAAAGA
Human-3576-IL-8-R	AACCCTCTGCACCCAGTTTTTC
Human-7124-TNF-F	CCTCTCTAATCAGCCCTCTG
Human-7124-TNF-R	GAGGACCTGGGAGTAGATGAG
Human-6347-CCL2-F	CAGCCAGATGCAATCAATGCC
Human-6347-CCL2-R	TGGAATCCTGAACCCACTTCT
Human-6354-CCL7-F	GACAAGAAAACCCAAACTCCAAAG
Human-6354-CCL7-R	TCAAAAACCCACCAAATCCA
Human-3586-IL-10-F	TCAAGGCGCATGTGAACTCC
Human-3586-IL-10-R	GATGTCAAACCTACTCATGGCT

Studio™ Dx system (ABI, Thermo, USA) using the following procedure: denaturation at 95°C for 5 min, 40 cycles of 95°C for 5 s and 60°C for 30 s, followed by a melting curve step of 95°C for 15 s and 60°C for 1 min, and a final increase to 95°C.

2.3. Immunofluorescence. ORF7-expressing A549 cells were cultured in 6-well plates with slides. After 24 h, when the cells were adhered to coverslips, cells were fixed with 4% paraformaldehyde for 15 min and permeabilized with 0.5% TritonX-100. After blocking for 30 min at room temperature using 3% BSA, the cells were incubated with a mouse anti-FLAG antibody (Sigma, USA) at 4°C overnight and were then stained with a fluorescein isothiocyanate- (FITC-) conjugated goat anti-mouse antibody (ProteinTech) at room temperature for 1 h. The nuclei were stained with DAPI (Abcam, ab104139), and the cellular distribution of ORF7 was observed using confocal microscopy.

2.4. Western Blot Analysis. Western blotting was conducted as previously described [20]. Briefly, cells were lysed with SDS sample buffer (1x), boiled for 10 min, separated using 4–20% SDS-PAGE (GenScript, USA), and then transferred onto a 0.22 μ m polyvinylidene difluoride (PVDF) membrane (Millipore, USA). After blocking for 1 h at room temperature with 3% BSA, the membranes were incubated with diluted primary antibodies at 4°C overnight. The secondary antibodies were added at room temperature for 2 h. Protein bands were detected using the Clarity Western ECL Substrate (Bio-Rad, USA).

2.5. Isolation of Human Neutrophils and Monocytes. Neutrophils were isolated from blood samples of healthy human

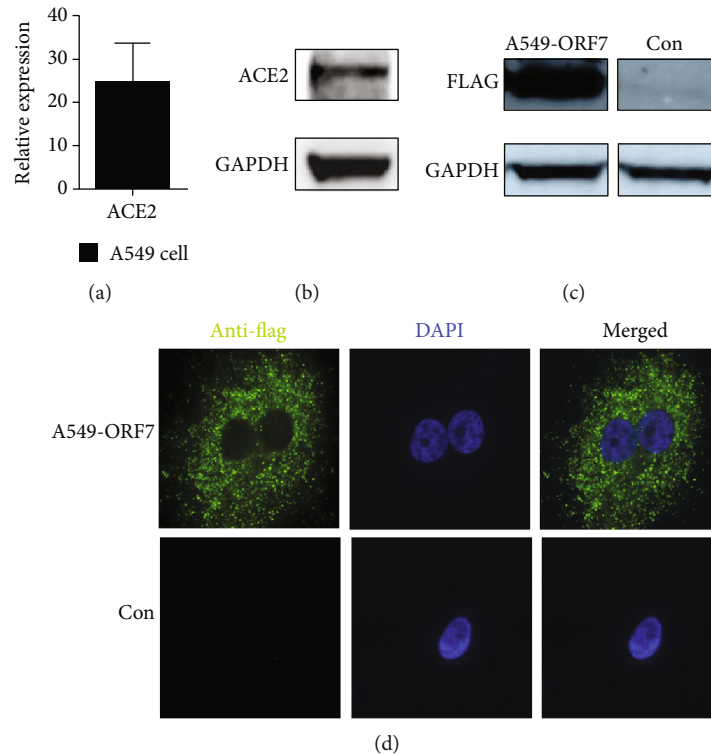


FIGURE 1: Expression of ACE2 and distribution of ORF7 in A549 cells. (a) Expression of ACE2 in A549 cells (qRT-PCR). (b) Expression of ACE2 in A549 cells (Western blotting). (c) FLAG-ORF7 expression in A549-ORF7 cells (Western blotting). (d) Cellular distribution of ORF7 in A549-ORF7 cells (immunofluorescence microscopy).

donors using PolymorphPrep (Alere Technologies AS, Oslo, Norway) as previously described [21, 22]. Briefly, 5 mL of blood was layered onto 5 mL of PolymorphPrep and centrifuged for 35 min (500 g) at room temperature. The neutrophil layer was transferred to a new tube, washed with PBS, diluted by 50% with ddH₂O, and then centrifuged for 10 min (400 g), followed by red blood cell lysis in a lysis buffer (Solarbio, China).

Peripheral blood mononuclear cells (PBMCs) were isolated from blood samples of healthy donors using a Ficoll density gradient [23]. Then, CD14 microbeads (Miltenyi Biotec, Germany) were used for the positive selection of human monocytes from these cells [24]. The purity of the CD14⁺ cells was evaluated using an APC-conjugated anti-human CD14 antibody (eBioscience, CatNo: 17-0149-42) with flow cytometry. The Institutional Ethics Committee of the First Affiliated Hospital of Zhejiang University approved this study.

2.6. Transwell Assay. Transwell assays were conducted using a 12 mm Transwell with a 3.0 μ m pore polycarbonate membrane insert (Corning, USA, CatNo: CLS3402) [25]. A549 cells that were transfected with lentiviruses were seeded in the lower chamber and cultured for 24 h in DMEM containing 10% FBS. Human-derived monocytes and neutrophils in serum-free DMEM were added to the upper chamber. After incubation for 1 h, cells in the reverse side of the upper chamber were fixed with 4% paraformaldehyde and then stained in crystal violet for observation with a microscope.

Cells in the lower chamber were collected and counted by flow cytometry, and counting beads were used for quantitation of different samples [26].

2.7. Enzyme-Linked Immunosorbent Assay (ELISA). ORF7-expressing A549 cells and control cells were plated into 6-well plates. The supernatant was collected and used for measurement of CCL2 (MultiSciences, CatNo: 70-EK187-96), CCL7 (Cloud-Clone Corp., CatNo: SEA089Hu), and IL-6 (MultiSciences, CatNo: 70-EK206/3-96) using ELISA kits according to each manufacturer's instructions.

2.8. Statistical Analysis. The significance of differences was determined using Student's *t*-test with GraphPad Prism version 7.0 (GraphPad Software, CA). A *P* value below 0.05 was considered significant.

3. Results

3.1. Construction of ORF7-Expressing A549 Cells. ACE2 occurs on the surface of pneumocytes and binds to SARS-CoV-2 during infections [27]. We therefore first examined the expression of ACE2 in A549 cells, a type II pneumocyte cell line [28]. The Western blotting and quantitative PCR results confirmed that these cells expressed ACE2 (Figures 1(a) and 1(b)). We then used the sequence of a SARS-CoV-2 isolate (Wuhan-Hu-1, NC_045512.2) to construct a lentiviral vector that expressed a FLAG-tagged ORF7 subgenomic sequence (Lenti-ORF7-FLAG) and

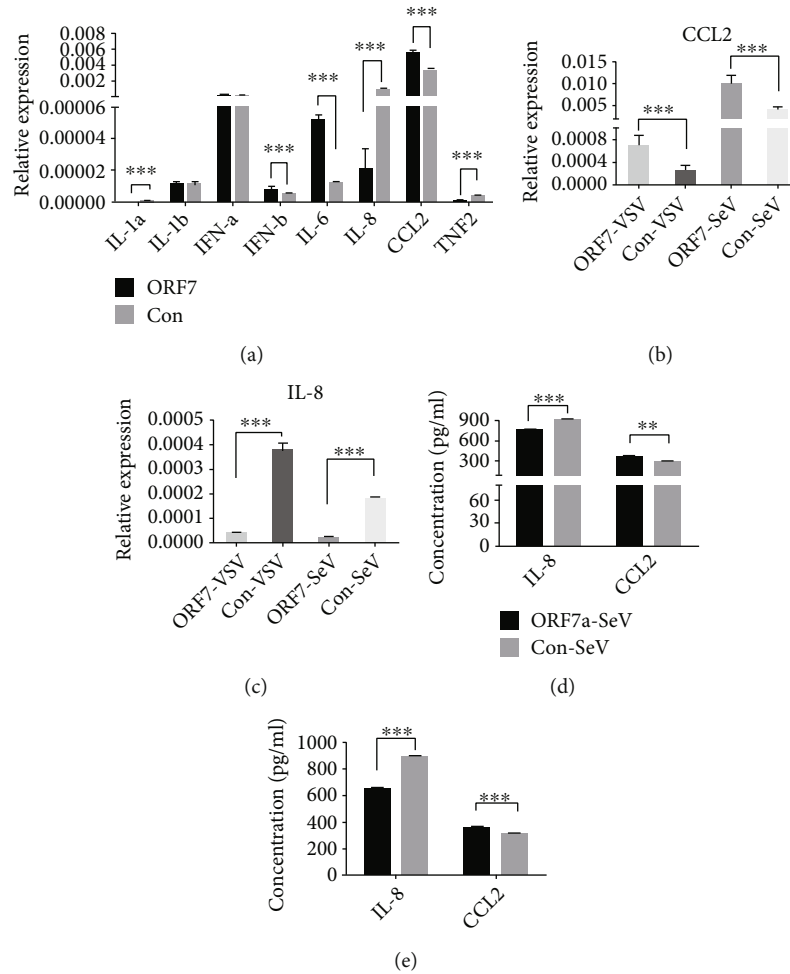


FIGURE 2: Effect of ORF7 on the expression of cytokines and chemokines in A549 cells. (a) Relative to control cells, A549-ORF7 cells had increased expression of *IL-6*, *CCL2*, and *IFN- β* (all $P < 0.01$), decreased expression of *IL-1 α* , *IL-8*, and *TNF- α* (all $P < 0.01$), but similar expression of *IL-1 β* and *IFN- α* (both $P > 0.05$). *CCL7* and *IL-10* were undetectable (qRT-PCR). (b) Activation of innate immunity by SeV/VSV infection increased the expression of *CCL2* and decreased the expression of *IL-8* in A549-ORF7 cells compared to control cells (both $P < 0.05$; qRT-PCR). (c) A549-ORF7 cells had increased levels of *CCL2* and decreased levels of *IL-8* relative to control cells (both $P < 0.01$; ELISA).

transfected A549 cells with Lenti-ORF7-FLAG to establish an ORF7-expressing cells. We confirmed the expression and the cellular distribution of ORF7 using Western blotting and immunofluorescence. The results indicated expression of ORF7 (Figure 1(c)) and that this protein was present in the cytosol (Figure 1(d)). These data thus demonstrated the successful establishment of ORF7-expressing A549 cells that could be used for further studies of the function of ORF7.

3.2. ORF7 Alters the Expression of Cytokines and Chemokines in A549 Cells. Innate immune cells, such as monocytes, macrophages, and neutrophils, are the first cells to respond when there is an infection in the lungs [29]. In particular, infection of pneumocytes leads to massive infiltration of monocytes into lung tissues [30], although there appears to be limited infiltration of neutrophils during SARS-CoV-2 infection [31–33]. During the early stage of viral infection, cytokines (*IL-1*, *IL-2*, *IL-8*, *IL-10*, *CCL2*, *CCL7*, *IFN- α* , *IFN- β* , and *TNF- α*) have essential functions in the recruit-

ment of immune cells, defense against the infection, and promotion of inflammation [34]. We therefore used qPCR to determine the expression of cytokines and chemokines in ORF7-expressing A549 cells compared to control cells (Figure 2(a)). The results demonstrated that *IL-6*, *CCL2*, and *IFN- β* had higher expression in A549-ORF7 cells (all $P < 0.01$); *IL-1 α* , *IL-8*, and *TNF- α* had lower expression in A549-ORF7 cells (all $P < 0.01$); the two groups had no differences in the levels of *IL-1 β* and *IFN- α* (both $P > 0.05$); and *CCL7* and *IL-10* were undetectable.

CCL-2 (MCP-1) and *IL-8* (CXCL8) function in the chemotaxis of monocytes and neutrophils, respectively [35, 36]. Sendai virus (SeV) and vesicular stomatitis virus (VSV) infections stimulate intracellular innate immunity and can be used to model RNA virus infections [37]. We therefore used qPCR to measure *CCL2* and *IL-8* expression in A549-ORF7 and control cells following infection by these viruses (Figure 2(b)). The results indicated that A549-ORF7 cells had greater expression of *CCL2* and decreased expression

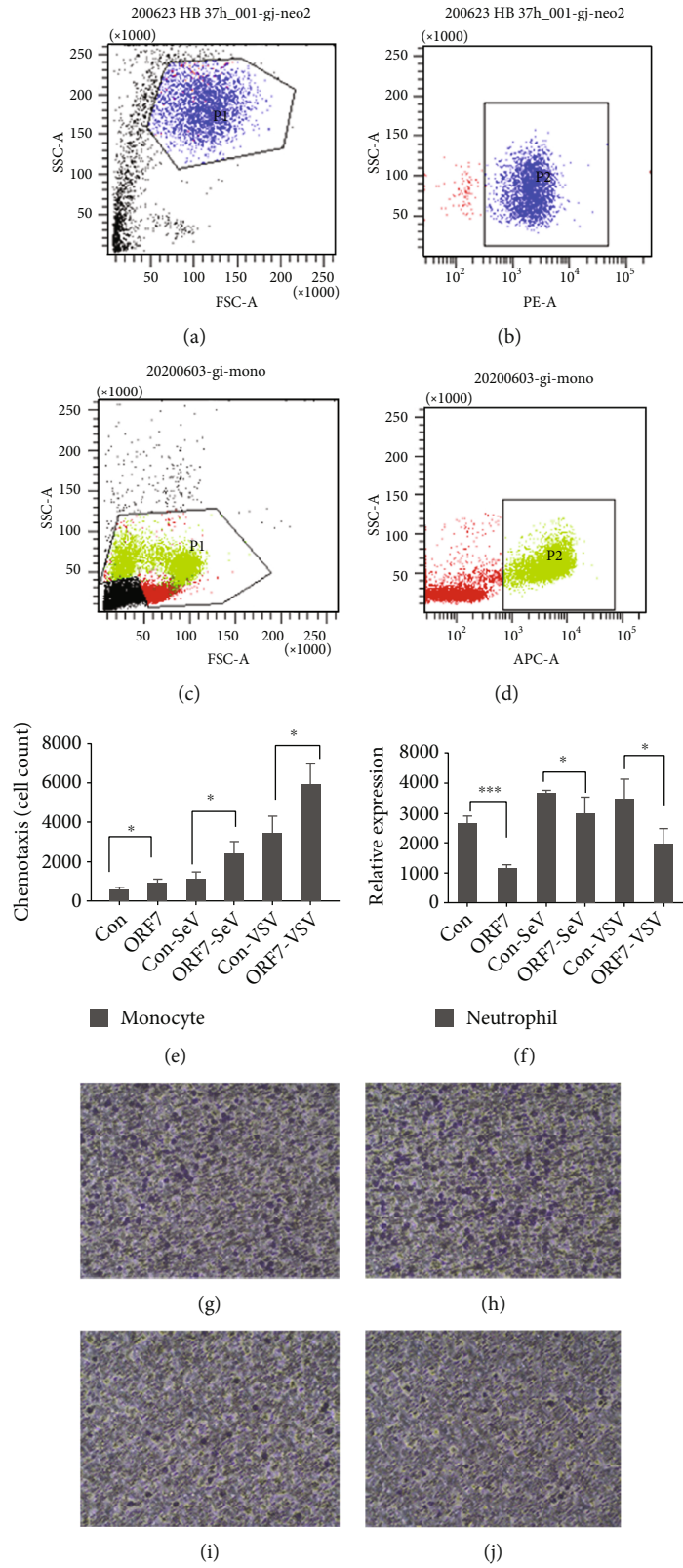


FIGURE 3: Continued.

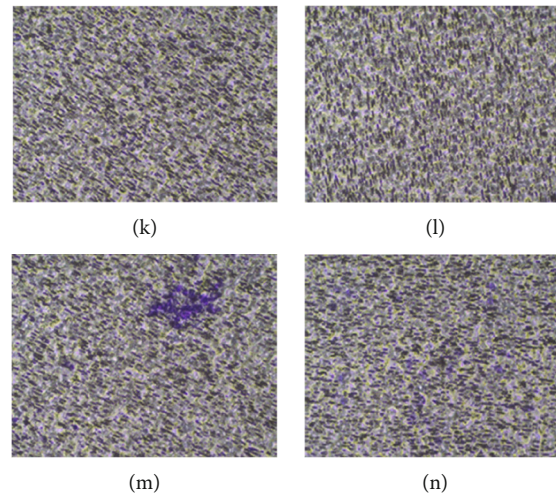


FIGURE 3: Effect of ORF7 on chemotaxis of neutrophils and monocytes. (a–d) Neutrophils were identified as CD11b+ cells and monocytes as CD14+ positive cells (flow cytometry). (g–n) Chemotaxis of monocytes and neutrophils (upper chamber) in response to A549-ORF cells (lower chamber) was examined by staining (Transwell assay). (e, f) Quantitation of chemotaxis results showing increased monocyte chemotaxis and decreased neutrophil chemotaxis (both $P < 0.01$).

of *IL-8* compared to control cells (both $P < 0.05$). We also used ELISA to measure the levels of *IL-8* and *CCL2* in the supernatant of A549-ORF7 and control cells (Figure 2(c)). These results confirmed that A549-ORF7 cells had increased expression of *CCL2* and decreased expression of *IL-8* with or without infection by SeV/VSV or the transduction of agonist, LMW and HMW RNAs (both $P < 0.01$).

3.3. ORF7 Affects the Chemotaxis of Monocytes and Neutrophils. We next examined the effects of ORF7 on the chemotaxis of monocytes and neutrophils. Flow cytometry provided identification of neutrophils as CD11b+ cells (Figures 3(a) and 3(b)) and monocytes as CD14+ positive cells (Figures 3(c) and 3(d)). Next, we implanted the A549-ORF7 and control cells in the lower chambers of 12-well plates, added monocytes and neutrophils in the upper chamber, and recorded chemotaxis after 6 h (monocytes) and 3 h (neutrophils) [25, 38]. The results indicated that monocytes had increased chemotaxis, and neutrophils had reduced chemotaxis (Figures 3(g)–3(n)).

During these experiments, we found numerous transmembrane cells, monocytes, and neutrophils on the lower wells with the A549-ORF7 cells. Thus, we used flow cytometry for the cell counting. The results indicated that more monocytes and fewer neutrophils migrated into the lower chamber with A549-ORF7 cells than with control A549 cells (all $P < 0.01$; Figures 3(e) and 3(f)). These results indicated that ORF7 attracted monocytes and repelled neutrophils in vitro.

4. Discussion

Previous postmortem examinations indicated that the lungs of COVID-19 patients, particularly the immune microenvironment, had significant alterations. These changes included alterations in T cells, B cells, macrophages, and neutrophils [39, 40]. Lymphocytes, T cells, and B cells were less abun-

dant and scattered in the lungs of these patients [30, 32, 39, 41], but there was increased infiltration by monocytes, macrophages, and neutrophils [42]. After infection of the lungs, macrophages and neutrophils function as the first defense of the innate immune system, and these cells phagocytize pathogens and produce cytokines and chemokines that attract other immune cells [29]. The early recruitment of immune cells determines the local immune response and can even cause more widespread inflammation, such as a cytokine storm. Our present work examined the influence of ORF7 of SARS-CoV-2 on innate immunity. Our major result is that expression of ORF7 in type II pneumocytes (A549 cells) increased the level of *CCL2*, decreased the level of *IL-8*, and increased the migration of primary monocytes but decreased the migration of neutrophils in vitro.

The ORF7 gene is located in a region of the genomes of the SARS-CoV-2, SARS-CoV-1, and MERS viruses that have a high frequency of mutations [1]. Our results indicated that ORF7 has a specific function in the immune response to coronavirus infection. Monocytes produce *IL-1*, *IL-6*, *IL-18*, *IL-33*, *TNF- α* , *CCLs*, and *VEGF*, and these molecules have critical roles in cytokine release and recruitment of other immune cells [43]. *IL-6* and *IL-1* are proinflammatory cytokines and the predominant inducers of the cytokine storm [43, 44]. Additionally, *IL-6* can activate macrophages, which produce more cytokines and chemokines [43]. Neutrophils are also produced early in response to infection, and neutrophil chemotaxis in humans is usually mediated by factors such as *IL-8*, *IL-1*, *TNF- α* , and complement *C5a* [45]. Neutrophils, like macrophages, produce a range of cytokines (*TNF- α* , *ILs*, *GCSF*, *MCSF*, and *GMCSF*) and chemokines (*IL-8*, *CXCL10*, *CXCL9*, *CCL2*, *CCL3*, and *CCL4*) [43, 46]. Thus, neutrophils have direct antipathogen effects (phagocytosis) and indirect antipathogen effects (stimulation by cytokines). Macrophages and neutrophils thus play critical roles during the acute phase of pneumonia following viral infection.

Patients with COVID-19 have greater levels of peripheral monocytes than healthy controls [47, 48]. Recent evidence showed massive macrophage infiltration of the lungs of deceased COVID-19 patients, including intra-alveolar CD68+ macrophages [30, 31, 49]. The monocytes in these tissues (macrophages) may be at a stage of active proliferation in the lung alveolar spaces of these patients [50].

Previous research reported that the blood neutrophil count of SARS patients was associated with the severity of their pneumonia [51]. In contrast, other studies reported that the blood neutrophil count of COVID-19 patients was inversely associated with disease severity [47, 52, 53]. Although virus infections, such as influenza, induce neutrophil infiltration in the respiratory tract, the status of neutrophils in the lungs of COVID-19 patients appears paradoxical [30–33, 54, 55]. Several autopsy reports found no neutrophil infiltration in the lungs of COVID-19 patients, but there was neutrophil infiltration of the liver [31]. Some reports that found minor infiltrations of neutrophils in the lungs attributed this to secondary infections [33]. A report of 4 patients with COVID-19 found that only 1 patient had neutrophil infiltration of the lungs [55]. Another report of two cases found neutrophil infiltration in 1 patient's pulmonary interstitium [30]. Other studies reported the presence of megakaryocytes, dendritic cells, and natural killer cells in the lungs of deceased COVID-19 patients [33, 40].

The present *in vitro* study found that overexpression of the SARS-CoV-2 ORF7 in cultured type II alveolar cells (A549) upregulated the expression of CCL2, a chemokine that functions in monocyte chemotaxis. This suggests that ORF7 may accelerate the progression of local inflammation after viral infection. Our *in vitro* studies also found that ORF7 downregulated the expression of IL-8. This suggests that ORF7 may block the migration of neutrophils. Greater neutrophil infiltration of the lungs could exacerbate the cytokine storm and worsen the patient's condition due to lymphopenia [56].

There is evidence that a specific variant of SARS-CoV-2 which has mutation N501Y in the S protein and was first reported in London [57] is now widespread. Because this mutation is in the receptor-binding domain of the S protein, this variant likely has altered binding capacity to its ACE2 receptor. Even though this mutation was in the S protein, recent research reported the efficacy of neutralizing antibodies in mice [58]. It is important to consider that the mutation frequency of RNA viruses, such as coronaviruses and influenza viruses, is higher than that of DNA viruses.

Our study indicated that ORF7 of SARS-CoV-2 had specific effects on the immunological changes. ORF7 may therefore contribute to the unique immunological profile of the lung tissues of patients with COVID-19, although the functions of other ORFs should also be examined. ORF7 can be the target for the development of anti-COVID-19 drugs in the future. The inflammation environment in the lung is one of the major risks for severe COVID-19 patients. In addition, ORF7 and other genes, including the structure and nonstructure proteins, combinatorially involve in the inflammatory environment in the lung after the infection.

However, there are limitations to our work. Many other physical and pathological factors impact the inflammation status of the lungs of patients with SARS-CoV-2 infections. For example, the genomic RNA sensor system triggers the innate immune reaction, stimulates the translation of other proteins from the genome or subgenome of the virus, and may thereby increase lung injury. Consequently, appropriated animal models can be employed for the determination of ORF7 *in vivo* in the future. Additionally, the effect of ORF7 on the microenvironment of the lung should not be considered alone. Instead, there should be a systematic examination of the impact of all factors and their interactions on lung inflammation.

Data Availability

There are no publicly archived datasets analysed in this study.

Ethical Approval

Our study was approved by the Institutional Ethics Committee of the First Affiliated Hospital of Zhejiang University.

Consent

Written informed consent of the legal guardian was obtained.

Conflicts of Interest

The authors declare no conflict of interest.

Authors' Contributions

Z.C. and H.Z. are responsible for the conceptualization; G.W., J.G., F.W., C.H., J.S., L.X., Z.G., and Q.Z. for the methodology; G.W. and J.G. for the formal analysis; G.W. and J.G. for the data curation; G.W. and J.G. for writing original draft preparation; Z.C., H.Z., and G.L. for writing—review and editing; Z.C. and H.Z. for the supervision; Z.C. for the project administration; and Z.C. for the funding acquisition, and Gang Wang and Jun Guan contributed equally to this work.

Acknowledgments

This research was funded by the National Science and Technology Major Project of China (2018ZX10302206-003, 2017ZX10202203-007, and 2017ZX10202203-008), Zhejiang Health and Family Planning Research Projects (2016KYA162 and 2015KYA046), and Major Science and Technology Projects for Liver Disease Research Fund of Ningbo.

References



- [1] P. Zhou, X.-L. Yang, X.-G. Wang et al., "Addendum: A pneumonia outbreak associated with a new coronavirus of probable bat origin," *Nature*, vol. 588, no. 7836, p. E6, 2020.

- [2] J. Bedford, D. Enria, J. Giesecke et al., "COVID-19: towards controlling of a pandemic," *Lancet*, vol. 395, no. 10229, pp. 1015–1018, 2020.
- [3] J. Cao, W. J. Tu, W. Cheng et al., "Clinical features and short-term outcomes of 102 patients with coronavirus disease 2019 in Wuhan, China," *Clinical Infectious Diseases*, vol. 71, no. 15, pp. 748–755, 2020.
- [4] Z. Zhu, X. Lian, X. Su, W. Wu, G. A. Marraro, and Y. Zeng, "From SARS and MERS to COVID-19: a brief summary and comparison of severe acute respiratory infections caused by three highly pathogenic human coronaviruses," *Respir Res*, vol. 21, no. 1, p. 224, 2020.
- [5] M. D. Christian, S. M. Poutanen, M. R. Loutfy, M. P. Muller, and D. E. Low, "Severe acute respiratory syndrome," *Clinical Infectious Diseases*, vol. 38, no. 10, pp. 1420–1427, 2004.
- [6] A. Al-Omari, A. A. Rabaan, S. Salih, J. A. Al-Tawfiq, and Z. A. Memish, "MERS coronavirus outbreak: implications for emerging viral infections," *Diagnostic Microbiology and Infectious Disease*, vol. 93, no. 3, pp. 265–285, 2019.
- [7] F. Krammer, "SARS-CoV-2 vaccines in development," *Nature*, vol. 586, no. 7830, pp. 516–527, 2020.
- [8] Y. Dong, T. Dai, Y. Wei, L. Zhang, M. Zheng, and F. Zhou, "A systematic review of SARS-CoV-2 vaccine candidates," *Signal Transduct Target Ther*, vol. 5, no. 1, p. 237, 2020.
- [9] R. Yan, Y. Zhang, Y. Li, L. Xia, Y. Guo, and Q. Zhou, "Structural basis for the recognition of SARS-CoV-2 by full-length human ACE2," *Science*, vol. 367, no. 6485, pp. 1444–1448, 2020.
- [10] Y. Wu, F. Wang, C. Shen et al., "A noncompeting pair of human neutralizing antibodies block COVID-19 virus binding to its receptor ACE2," *American Association for the Advancement of Science*, vol. 368, no. 6496, pp. 1274–1278, 2020.
- [11] J. Lan, J. Ge, J. Yu et al., "Structure of the SARS-CoV-2 spike receptor-binding domain bound to the ACE2 receptor," *Nature*, vol. 581, no. 7807, pp. 215–220, 2020.
- [12] X. Y. Ge, J. L. Li, X. L. Yang et al., "Isolation and characterization of a bat SARS-like coronavirus that uses the ACE2 receptor," *Nature*, vol. 503, no. 7477, pp. 535–538, 2013.
- [13] S. M. Khade, S. M. Yabaji, and J. Srivastava, "An update on COVID-19: SARS-CoV-2 life cycle, immunopathology, and BCG vaccination," *Preparative Biochemistry & Biotechnology*, vol. 51, no. 7, pp. 650–658, 2021.
- [14] P. S. Masters, "The molecular biology of coronaviruses," *Advances in Virus Research*, vol. 66, pp. 193–292, 2006.
- [15] P. V'Kovski, A. Kratzel, S. Steiner, H. Stalder, and V. Thiel, "Coronavirus biology and replication: implications for SARS-CoV-2," *Nature Reviews. Microbiology*, vol. 19, no. 3, pp. 155–170, 2021.
- [16] R. A. Khailany, M. Safdar, and M. Ozaan, "Genomic characterization of a novel SARS-CoV-2," *Gene Rep*, vol. 19, p. 100682, 2020.
- [17] N. Vabret and J. M. Blander, "Sensing microbial RNA in the cytosol," *Frontiers in Immunology*, vol. 4, p. 468, 2013.
- [18] J. Y. Li, C. H. Liao, Q. Wang et al., "The ORF6, ORF8 and nucleocapsid proteins of SARS-CoV-2 inhibit type I interferon signaling pathway," *Virus Research*, vol. 286, p. 198074, 2020.
- [19] Y. Ren, T. Shu, D. Wu et al., "The ORF3a protein of SARS-CoV-2 induces apoptosis in cells," *Cellular & Molecular Immunology*, vol. 17, no. 8, pp. 881–883, 2020.
- [20] X. Liu, W. Song, X. Zhang et al., "Downregulating LncRNA XIST attenuated contrast-induced nephropathy injury via regulating miR-133a-3p/NLRP3 axis," *Journal of Thrombosis and Thrombolysis*, 2021.
- [21] R. Corriden, A. Moshensky, C. M. Bojanowski et al., "E-cigarette use increases susceptibility to bacterial infection by impairment of human neutrophil chemotaxis, phagocytosis, and NET formation," *American Journal of Physiology. Cell Physiology*, vol. 318, no. 1, pp. C205–c214, 2020.
- [22] B. Xu, A. Janicova, J. T. Vollrath et al., "Club cell protein 16 in sera from trauma patients modulates neutrophil migration and functionality via CXCR1 and CXCR2," *Mol Med*, vol. 25, no. 1, p. 45, 2019.
- [23] B. Bonilauri, M. D. M. Santos, A. C. Camillo-Andrade et al., "The impact of blood-processing time on the proteome of human peripheral blood mononuclear cells," *Biochim Biophys Acta Proteins Proteom*, vol. 1869, no. 3, article 140581, 2020.
- [24] S. Vitale, A. Schmid-Alliana, V. Breuil et al., "Soluble fractalkine prevents monocyte chemoattractant protein-1-induced monocyte migration via inhibition of stress-activated protein kinase 2/p38 and matrix metalloproteinase activities," *Journal of Immunology*, vol. 172, no. 1, pp. 585–592, 2004.
- [25] I. Bournazou, J. D. Pound, R. Duffin et al., "Apoptotic human cells inhibit migration of granulocytes via release of lactoferrin," *The Journal of Clinical Investigation*, vol. 119, no. 1, pp. 20–32, 2009.
- [26] L. Saraiva, L. Wang, M. Kammel et al., "Comparison of volumetric and bead-based counting of CD34 cells by single-platform flow cytometry," *Cytometry. Part B, Clinical Cytometry*, vol. 96, no. 6, pp. 508–513, 2019.
- [27] M. Hoffmann, H. Kleine-Weber, S. Schroeder et al., "SARS-CoV-2 cell entry depends on ACE2 and TMPRSS2 and is blocked by a clinically proven protease inhibitor," *Cell*, vol. 181, no. 2, pp. 271–280.e8, 2020.
- [28] J. R. Cooper, M. B. Abdullatif, E. C. Burnett et al., "Long term culture of the A549 cancer cell line promotes multilamellar body formation and differentiation towards an alveolar type II pneumocyte phenotype," *PLoS One*, vol. 11, no. 10, article e0164438, 2016.
- [29] M. Galeas-Pena, N. McLaughlin, and D. Pociask, "The role of the innate immune system on pulmonary infections," *Biological Chemistry*, vol. 400, no. 4, pp. 443–456, 2019.
- [30] S. Li, L. Jiang, X. Li et al., "Clinical and pathological investigation of patients with severe COVID-19," *JCI Insight*, vol. 5, no. 12, 2020.
- [31] X.-W. Bian, "Autopsy of COVID-19 patients in China," *National Science Review*, vol. 7, no. 9, pp. 1414–1418, 2020.
- [32] L. M. Barton, E. J. Duval, E. Stroberg, S. Ghosh, and S. Mukhopadhyay, "Covid-19 autopsies, Oklahoma, USA," *American Journal of Clinical Pathology*, vol. 153, no. 6, pp. 725–733, 2020.
- [33] S. E. Fox, A. Akmatbekov, J. L. Harbert, G. Li, J. Quincy Brown, and R. S. Vander Heide, "Pulmonary and cardiac pathology in African American patients with COVID-19: an autopsy series from New Orleans," *The Lancet Respiratory Medicine*, vol. 8, no. 7, pp. 681–686, 2020.
- [34] G. Arango Duque and A. Descoteaux, "Macrophage cytokines: involvement in immunity and infectious diseases," *Frontiers in Immunology*, vol. 5, p. 491, 2014.
- [35] M. E. Hammond, G. R. Lapointe, P. H. Feucht et al., "IL-8 induces neutrophil chemotaxis predominantly via type I IL-8 receptors," *Journal of Immunology*, vol. 155, no. 3, pp. 1428–1433, 1995.

- [36] M. Gschwandtner, R. Derler, and K. S. Midwood, "More than just attractive: how CCL2 influences myeloid cell behavior beyond chemotaxis," *Frontiers in Immunology*, vol. 10, p. 2759, 2019.
- [37] Z. Liu, C. Wu, Y. Pan et al., "NDR2 promotes the antiviral immune response via facilitating TRIM25-mediated RIG-I activation in macrophages," *Sci Adv*, vol. 5, no. 2, article eaav0163, 2019.
- [38] R. Singh, T. Hui, A. Matsui et al., "Modulation of infection-mediated migration of neutrophils and CXCR2 trafficking by osteopontin," *Immunology*, vol. 150, no. 1, pp. 74–86, 2017.
- [39] D. Wichmann, J. P. Sperhake, M. Lutgehetmann et al., "Autopsy findings and venous thromboembolism in patients with COVID-19," *Annals of Internal Medicine*, vol. 173, no. 4, pp. 268–277, 2020.
- [40] Y. Zhang, Y. Gao, L. Qiao, W. Wang, and D. Chen, "Inflammatory response cells during acute respiratory distress syndrome in patients with coronavirus disease 2019 (COVID-19)," *Annals of Internal Medicine*, vol. 173, no. 5, pp. 402–404, 2020.
- [41] A. V. Rapkiewicz, X. Mai, S. E. Carsons et al., "Megakaryocytes and platelet-fibrin thrombi characterize multi-organ thrombosis at autopsy in COVID-19: a case series," *EClinicalMedicine*, vol. 24, p. 100434, 2020.
- [42] A. A. Stegelmeier, J. P. van Vloten, R. C. Mould et al., "Myeloid cells during viral infections and inflammation," *Viruses*, vol. 11, no. 2, p. 168, 2019.
- [43] D. C. Fajgenbaum and C. H. June, "Cytokine storm," *The New England Journal of Medicine*, vol. 383, no. 23, pp. 2255–2273, 2020.
- [44] W. J. Tu, J. Cao, L. Yu, X. Hu, and Q. Liu, "Clinicolaboratory study of 25 fatal cases of COVID-19 in Wuhan," *Intensive Care Medicine*, vol. 46, no. 6, pp. 1117–1120, 2020.
- [45] C. J. Thomas and K. Schroder, "Pattern recognition receptor function in neutrophils," *Trends in Immunology*, vol. 34, no. 7, pp. 317–328, 2013.
- [46] M. A. Cassatella, "Neutrophil-derived proteins: selling cytokines by the pound," *Advances in Immunology*, vol. 73, pp. 369–509, 1999.
- [47] R. Wang, M. Pan, X. Zhang et al., "Epidemiological and clinical features of 125 hospitalized patients with COVID-19 in Fuyang, Anhui, China," *International Journal of Infectious Diseases*, vol. 95, pp. 421–428, 2020.
- [48] L. Wang, Y. Duan, W. Zhang et al., "Epidemiologic and clinical characteristics of 26 cases of COVID-19 arising from patient-to-patient transmission in Liaocheng, China," *Clinical Epidemiology*, vol. Volume 12, pp. 387–391, 2020.
- [49] T. Adachi, J. M. Chong, N. Nakajima et al., "Clinicopathologic and immunohistochemical findings from autopsy of patient with COVID-19, Japan," *Emerg Infect Dis*, vol. 26, no. 9, pp. 2157–2161, 2020.
- [50] S. F. Lax, K. Skok, P. Zechner et al., "Pulmonary arterial thrombosis in COVID-19 with fatal outcome: results from a prospective, single-center, clinicopathologic case series," *Annals of Internal Medicine*, vol. 173, no. 5, pp. 350–361, 2020.
- [51] R. S. Wong, A. Wu, K. F. To et al., "Haematological manifestations in patients with severe acute respiratory syndrome: retrospective analysis," *BMJ*, vol. 326, no. 7403, pp. 1358–1362, 2003.
- [52] G. Zhang, C. Hu, L. Luo et al., "Clinical features and short-term outcomes of 221 patients with COVID-19 in Wuhan, China," *Journal of Clinical Virology*, vol. 127, p. 104364, 2020.
- [53] W. Yang, Q. Cao, L. Qin et al., "Clinical characteristics and imaging manifestations of the 2019 novel coronavirus disease (COVID-19): A multi-center study in Wenzhou city, Zhejiang, China," *The Journal of Infection*, vol. 80, no. 4, pp. 388–393, 2020.
- [54] T. Watanabe, J. Tisoncik-Go, N. Tchitchek et al., "1918 influenza virus hemagglutinin (HA) and the viral RNA polymerase complex enhance viral pathogenicity, but only HA induces aberrant host responses in mice," *Journal of Virology*, vol. 87, no. 9, pp. 5239–5254, 2013.
- [55] S. Tian, Y. Xiong, H. Liu et al., "Pathological study of the 2019 novel coronavirus disease (COVID-19) through postmortem core biopsies," *Modern Pathology*, vol. 33, no. 6, pp. 1007–1014, 2020.
- [56] A. Tufan, A. Avanoğlu Guler, and M. Matucci-Cerinic, "COVID-19, immune system response, hyperinflammation and repurposing antirheumatic drugs," *Turk J Med Sci*, vol. 50, no. SI-1, pp. 620–632, 2020.
- [57] J. Wise, "Covid-19: new coronavirus variant is identified in UK," *BMJ*, vol. 371, p. m4857, 2020.
- [58] H. Gu, Q. Chen, G. Yang et al., "Adaptation of SARS-CoV-2 in BALB/c mice for testing vaccine efficacy," *Science*, vol. 369, no. 6511, pp. 1603–1607, 2020.

Research Article

Association between Plasma Homocysteine Concentrations and the First Ischemic Stroke in Hypertensive Patients with Obstructive Sleep Apnea: A 7-Year Retrospective Cohort Study from China

Nanfang Li ¹, Xintian Cai ², Qing Zhu,² Xiaoguang Yao,¹ Mengyue Lin,² Lin Gan,² Le Sun,¹ Na Yue,¹ Yingli Ren,¹ Jing Hong,¹ Yue Ma,¹ Run Wang,¹ Jina Yili,¹ and Qin Luo¹

¹Hypertension Center of People's Hospital of Xinjiang Uygur Autonomous Region, Xinjiang Hypertension Institute, National Health Committee Key Laboratory of Hypertension Clinical Research, Xinjiang Clinical Medical Research Center for Hypertension Diseases, Urumqi, Xinjiang, China

²Xinjiang Medical University, Urumqi, Xinjiang, China

Correspondence should be addressed to Nanfang Li; lnanfang2016@sina.com and Xintian Cai; 278996834@qq.com

Received 24 August 2021; Revised 16 September 2021; Accepted 21 September 2021; Published 28 September 2021

Academic Editor: Wen-Jun Tu

Copyright © 2021 Nanfang Li et al. This is an open access article distributed under the Creative Commons Attribution License, which permits unrestricted use, distribution, and reproduction in any medium, provided the original work is properly cited.

Purpose. This study was aimed at investigating the association between baseline plasma homocysteine (Hcy) concentrations and the risk of the first ischemic stroke (IS) and at investigating any possible influential modifying factors in hypertensive patients with obstructive sleep apnea (OSA). **Methods.** Cox proportional hazards regression was employed to investigate the relationship between plasma Hcy concentration and the first IS. A generalized additive model was applied to determine the nonlinear relationship. In addition, we conducted subgroup analysis. **Results.** A total of 2350 hypertensive patients with OSA without a history of IS were enrolled in this study. At a median follow-up of 7.15 years, we identified 93 cases of the first IS. After adjusting for potential confounding, the findings revealed that plasma Hcy concentration was strongly and positively associated with the occurrence of the first IS (per SD increment; HR = 1.37, 95% CI: 1.30-1.44). A nonlinear relationship was found between plasma Hcy concentration and the risk of developing the first IS with inflection points for plasma Hcy of 5 $\mu\text{mol/L}$. In stratified analysis, a greater positive correlation was found between baseline plasma Hcy concentrations and new-onset IS in patients with DBP ≥ 90 mmHg (per SD increment; HR = 1.48, 95% CI: 1.33-1.65 vs. <90 mmHg: HR = 1.20, 95% CI: 1.02-1.42; P -interaction = 0.04) and BMI ≥ 24 and <28 kg/m² (per SD increment; HR = 1.46, 95% CI: 1.26-1.70 vs. <24 kg/m²: HR = 1.13, 95% CI: 0.95-1.33 vs. ≥ 28 kg/m²: HR = 1.46, 95% CI: 1.25-1.70; P -interaction = 0.03). **Conclusion.** Elevated plasma Hcy concentrations are independently associated with the risk of the first IS in hypertensive patients with OSA. Plasma Hcy concentrations ≥ 5 $\mu\text{mol/L}$ surely increased the risk of the first IS in hypertensive patients with OSA.

1. Introduction

Stroke is the leading cause of disability worldwide and the second leading cause of death after ischemic heart disease [1–3]. More importantly, according to China's National Disease Surveillance Point System, there were an estimated 2.4 million new-onset strokes and 1.1 million stroke-related deaths per year [4]. Researches have demonstrated that ischemic stroke (IS) is the most prevalent stroke subtype in

China, accounting for about 70-86% of all strokes [2, 5]. Therefore, early identification and management of associated risk factors are critical measures to prevent and treat the first IS [6, 7].

Obstructive sleep apnea (OSA) is a widespread sleep disturbance [8, 9]. The high prevalence of OSA in hypertensive patients is well demonstrated, and OSA is especially prevalent in patients with intractable hypertension [10–12]. Hypertension and OSA often cooccur, which may contribute

to a significantly enhanced risk of cardiovascular disease in hypertensive patients with OSA [13]. OSA is associated independently with carotid intima-media thickness in hypertensive patients [14]. OSA was additionally associated with an increased risk of new-onset ventricular fibrillation, and a significant dose-response correlation was identified between the severity of OSA and the degree of risk of developing ventricular fibrillation [15]. A meta-analysis of retrospective researches revealed that hypertensive patients with comorbid moderate to severe OSA had significantly increased mortality from cardiovascular disease compared with those without comorbid OSA [16, 17]. A few reports have indicated that people with hypertension combined with OSA have a two-fold elevated risk of developing IS compared to people without OSA [16–18].

Although previous investigations have reported a significant association between hyperhomocysteinemia (HHcy) caused by disorders of homocysteine (Hcy) metabolism and the first IS, the relationship between the degree of Hcy metabolism disorder and the first IS remains controversial [19]. In general, the normal reference range for plasma Hcy concentrations is 5 to 10 $\mu\text{mol/L}$. Thus, the definition of HHcy is disputable and is commonly defined as plasma Hcy concentrations $\geq 10 \mu\text{mol/L}$, but also as Hcy $\geq 15 \mu\text{mol/L}$ [20–23]. Current guidelines suggest plasma Hcy concentration control goals only in people with pure hypertension to prevent IS events [24]. However, available data from cohort investigations on the correlation between baseline plasma Hcy concentrations and incident first IS are limited and inconclusive, especially in hypertensive patients with OSA. It is worth noting that previous investigations have rarely thoroughly examined the potential moderators of the relationship between baseline plasma Hcy concentrations and incident first IS risk.

Therefore, we intended to evaluate the association between baseline plasma Hcy concentrations and the first IS and to investigate the appropriate plasma Hcy concentration target to reduce the incidence of the first IS in hypertensive patients with OSA.

2. Materials and Methods

2.1. Study Design. This retrospective cohort study included consecutive hypertensive patients with suspected OSA hospitalized at the Hypertension Center of People's Hospital of Xinjiang Uygur Autonomous Region from January 2011 to December 2013. The study protocol was authorized by the Medical Ethics Committee of the People's Hospital of Xinjiang Uygur Autonomous Region (no. 2019030662) and was conducted in adherence to the approved guidelines. Because of the retrospective nature of the study, patient consent and/or informed consent was not required.

A total of 2585 patients aged ≥ 18 years with hypertension combined with OSA determined by polysomnography (PSG) were enrolled in this study. Exclusion criteria for this study were age younger than 18 years ($n = 11$), severe systemic disease ($n = 25$) (i.e., severe pulmonary disease, malignancy, severe liver disease, or severe chronic kidney disease or other major diseases that affect long-term survival), cen-

tral sleep apnea ($n = 12$), pregnancy ($n = 6$), lacking a fasting blood sample and physical examination at baseline ($n = 61$), a history of stroke at baseline ($n = 24$), and loss to follow-up ($n = 96$). Ultimately, 2350 study participants were eligible for inclusion in the statistical analysis.

2.2. Baseline Examination. All participants finished the baseline examination between January 2011 and December 2013. Data on demographic features, lifestyle, personal disease records, history of regular CPAP treatment, and medication history were collected from all candidates through interviews.

Weight, height, neck circumference (NC), and waist circumference (WC) were measured three times, and the mean of the three times measurements was used for analysis. Systolic blood pressure (SBP) and diastolic blood pressure (DBP) were monitored using an electronic sphygmomanometer (HEM-1000, Omron, Kyoto, Japan). All participants underwent PSG examination throughout the night. All participants were instructed to refrain from coffee, alcohol, and sedative-hypnotics before the sleep study. Interpretation of PSG results was done by a professional polysomnography technician, and all steps were consistent with previous studies [25, 26]. Venous blood samples were retrieved from the antecubital vein in the early morning after 12 hours of fasting. Fasting plasma glucose (FPG), high-density lipoprotein (HDL-c), total cholesterol (TC), low-density lipoprotein (LDL-c), triglycerides (TG), creatinine (Cr), and high-sensitivity C-reactive protein (hs-CRP) levels were measured. Plasma Hcy concentrations were measured by a fluorescence polarization immunoassay on an automated immunoassay analyzer. The estimated glomerular filtration rate (eGFR) was calculated by using a formula derived from the CKD-EPI [27].

2.3. Definitions. The apnea hypopnea index (AHI) was defined as the sum of apnea and hypopnea events per hour of sleep on average. A diagnosis of OSA was determined as a minimum of 5 events per hour of AHI, with 5 to 14.9 events per hour recognized as mild OSA, 15 to 29.9 events per hour as moderate OSA, and 30 or more events per hour as severe OSA. Hypertension was defined as SBP ≥ 140 mmHg and/or DBP ≥ 90 mmHg and/or previously diagnosed hypertension and/or use of antihypertensive therapy within the past two weeks. Patients with diabetes were defined as those previously diagnosed with diabetes or newly diagnosed with diabetes (fasting glucose ≥ 7.0 mmol/L on 3 occasions during hospitalization, HbA1c $> 6.5\%$ at baseline), according to current guidelines. According to the frequency of drinking and smoking, we categorized them as never, former, and current.

2.4. Clinical Outcomes and Follow-Up. Endpoints were acquired through personal interview, records from medical insurance, and hospital discharge summaries. According to former investigations, the principal endpoint was to be determined as the first IS, including cerebral infarction and transient ischemic attack [28, 29]. The diagnosis of IS was on the basis of a contrast vascular computed tomography

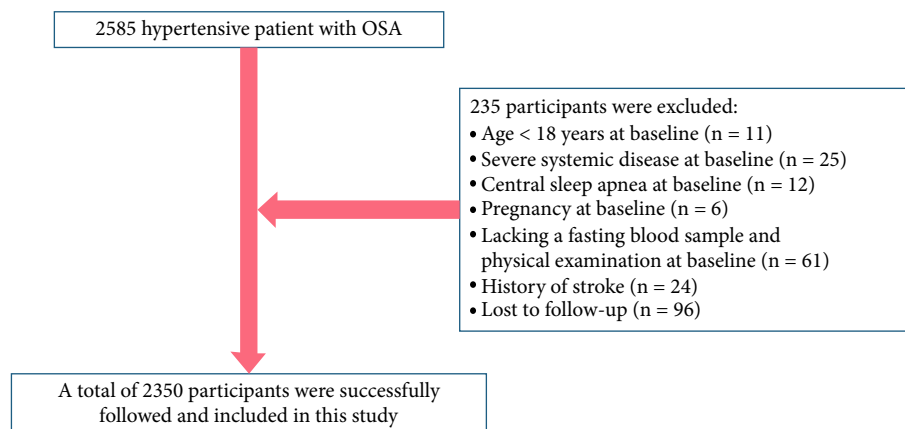


FIGURE 1: Flowchart.

(CT) scan or cranial CT scan, cerebrovascular angiography, or magnetic resonance imaging of the brain. The period of follow-up started at the first visit and ended on December 31, 2020.

2.5. Statistical Analysis. Differences between baseline characteristics of the different plasma Hcy groups were analyzed by one-way ANOVA, Kruskal-Wallis H , and χ^2 tests. Multivariate Cox proportional hazard regression was performed to evaluate the association between baseline plasma Hcy concentration and the risk of the first IS by estimating hazard ratios (HR) and 95% confidence intervals (CI). Adjustment for variables in this study showed varying degrees of adjustment results according to the statement of STROBE [30]. Adjust model I was adjusted for age and gender at baseline; adjusted model II was further adjusted for smoking status, drinking status, NC, BMI, and WC at baseline; adjusted model III was further adjusted for history of arrhythmia, diabetes, coronary heart disease, SBP, DBP, AHI, AI, HI, sleep duration, mean SaO₂ and lowest SaO₂, antidiabetic drugs, lipid-lowering drugs, antiplatelet drugs, regular CPAP treatment, antihypertensive drugs, and TC, TG, HDL-c, LDL-c, FPG, eGFR, Cr, and hs-CRP levels at baseline. Moreover, we calculated the cumulative IS incidence function of events over time using the Kaplan-Meier method. Further, we simulated the dose-response correlation between plasma Hcy concentration and IS risk using a generalized additive model, fitted the model with a recursive algorithm using maximum likelihood, and calculated the inflection points for the nonlinear correlation [31]. Considering that association between plasma Hcy concentrations and IS may differ in some populations, we performed exploratory stratified analysis by using a Cox proportional hazards model for some subgroups and used likelihood ratio tests to check for hierarchical differences to determine if there was an interaction. Finally, to estimate the reasonableness of the deviations caused by unmeasured and residual confounding factors, we also calculated the E -value of our main research results. The E -value estimates the strength of the unmeasured confounding variable needed to invalidate the observed association between our exposure and the result, taking into account all the measured covariables.

All statistical analyses were conducted using R version 4.0.1 software.

3. Results

3.1. Demographic Characteristics. In this cohort study, a total of 2350 participants, including 1611 males and 739 females, were evaluated. Participant screening details are shown in Figure 1. Table 1 shows the baseline characteristics of the participants grouped by plasma Hcy concentration tertile. Overall, the mean age of the 2350 participants was 49.45 ± 10.65 years, and 68.55% were male.

3.2. Follow-Up Results. During follow-up, 93 (3.96%) of the hypertensive patients with OSA in the study were diagnosed with IS. Of these, the incidence of IS corresponding to the plasma Hcy concentrations tertile grouping was 1.92% for T1, 4.99% for T2, and 4.71% for T3. Figure 2 illustrates the significant difference in IS risk between plasma Hcy concentration tertile groups (log-rank test, $P = 0.0022$). The cumulative risk of IS gradually increased with increasing plasma Hcy concentrations.

3.3. Association between Plasma Hcy Concentrations and the First IS in Hypertensive Patients with OSA. The association between plasma Hcy concentrations and the first IS is summarized in Table 2. We found that high plasma Hcy concentrations, expressed as a continuous variable and a categorical variable, were significantly and positively associated with the first IS. When plasma Hcy concentrations were expressed as a continuous variable, plasma Hcy concentrations were significantly associated with first IS in the crude model (per SD increment; HR = 1.37, 95% CI: 1.30-1.44, $P < 0.01$; E -value = 2.08). In adjust model I, plasma Hcy concentrations were still an independent risk factor for the first IS (per SD increment; HR = 1.35, 95% CI: 1.27-1.42, $P < 0.01$; E -value = 2.03). In adjust model II, plasma Hcy concentrations were still an independent risk factor for the first IS (per SD increment; HR = 1.34, 95% CI: 1.26-1.43, $P < 0.01$; E -value = 2.01), as well as the fully adjusted model (adjust model III), where plasma Hcy concentrations (per SD increment; HR = 1.32, 95% CI: 1.24-1.38, $P < 0.01$; E -value = 1.97) were

TABLE 1: Participants sorted by tertiles of Hcy.

Variable	Hcy tertiles (mmol/L)			P value
	Tertile 1 (<11.6)	Tertile 2 (11.6–18.2)	Tertile 3 (>18.2)	
No. of participants	783	782	785	
Age (years)	48.87 ± 9.94	50.36 ± 10.59	49.15 ± 11.29	0.01
BMI (kg/m ²)	28.46 ± 3.78	28.43 ± 3.89	28.46 ± 3.79	0.98
NC (cm)	40.04 ± 3.89	40.38 ± 3.93	40.76 ± 3.60	<0.01
WC (cm)	100.66 ± 10.06	101.24 ± 10.74	101.11 ± 10.30	0.51
SBP (mmHg)	138.52 ± 18.66	139.65 ± 18.89	142.19 ± 21.28	<0.01
DBP (mmHg)	91.10 ± 13.93	91.04 ± 13.08	93.63 ± 15.30	<0.01
Gender (<i>n</i> (%))				<0.01
Female	293 (37.42%)	264 (33.76%)	179 (22.80%)	
Male	490 (62.58%)	518 (66.24%)	606 (77.20%)	
Smoking status (<i>n</i> (%))				<0.01
Never	484 (61.81%)	463 (59.21%)	393 (50.06%)	
Former	72 (9.20%)	80 (10.23%)	97 (12.36%)	
Current	227 (28.99%)	239 (30.56%)	295 (37.58%)	
Drinking status (<i>n</i> (%))				0.10
Never	528 (67.43%)	527 (67.90%)	502 (63.95%)	
Former	39 (4.98%)	54 (6.91%)	63 (8.03%)	
Current	216 (27.59%)	197 (25.19%)	220 (28.03%)	
History of disease				
Arrhythmia (<i>n</i> (%))	109 (13.92%)	178 (22.76%)	153 (19.49%)	<0.01
Diabetes (<i>n</i> (%))	151 (19.28%)	150 (18.77%)	115 (14.65%)	0.06
Laboratory examinations				
TC (mmol/L)	4.61 ± 1.31	4.47 ± 0.95	4.59 ± 1.34	0.06
TG (mmol/L)	1.77 (1.28-2.47)	1.73 (1.22-2.48)	1.76 (1.25-2.54)	0.25
HDL-c (mmol/L)	1.11 ± 0.29	1.11 ± 0.31	1.09 ± 0.28	0.32
LDL-c (mmol/L)	2.61 ± 0.81	2.72 ± 0.80	2.63 ± 0.81	0.02
hs-CRP (mg/L)	2.21 (0.90-4.07)	2.01 (0.96-4.19)	2.12 (0.99-3.83)	0.85
FPG (mmol/L)	5.30 ± 1.35	5.33 ± 1.59	5.21 ± 1.48	0.26
Hcy (μmol/L)	7.70 ± 3.32	14.70 ± 1.87	29.22 ± 10.15	<0.01
eGFR (mL/min/1.73 m ²)	99.26 ± 21.08	95.75 ± 20.50	93.39 ± 22.11	<0.01
Cr (μmol/L)	73.60 ± 24.55	76.21 ± 20.98	81.62 ± 25.22	<0.01
Polysomnography examinations				
AHI (events/hour)	17.40 (10.00-33.80)	19.40 (10.40-34.95)	18.50 (10.50-32.80)	0.52
AI (events/hour)	2.50 (0.40-9.80)	3.20 (0.50-12.28)	3.10 (0.60-11.30)	0.79
HI (events/hour)	12.40 (7.20-21.40)	12.85 (7.30-21.17)	12.10 (7.20-19.20)	0.10
Sleep duration (minutes)	368.17 ± 73.55	366.11 ± 73.24	367.05 ± 72.27	0.86
Mean SaO ₂ (%)	90.83 ± 9.62	91.35 ± 6.86	91.16 ± 8.01	0.46
Lowest SaO ₂ (%)	76.54 ± 12.32	77.12 ± 10.00	77.51 ± 11.04	0.23
Medication use				
Antidiabetic drugs (<i>n</i> (%))	133 (16.99%)	79 (10.10%)	102 (12.99%)	<0.01
Lipid-lowering drugs (<i>n</i> (%))	417 (53.26%)	536 (68.54%)	605 (77.07%)	<0.01
Antihypertensive drugs (<i>n</i> (%))	713 (91.06%)	737 (94.25%)	766 (97.58%)	<0.01
Antiplatelet drugs (<i>n</i> (%))	541 (69.09%)	620 (79.28%)	508 (64.71%)	<0.01
Regular CPAP treatment (<i>n</i> (%))	22 (3.07%)	41 (6.27%)	34 (2.04%)	<0.01
Follow-up duration (days)	2627.00 (2313.00-2995.00)	2655.00 (2287.50-2984.75)	2563.00 (2265.00-2973.00)	0.26
Incident ischemic stroke (<i>n</i> (%))				<0.01

TABLE 1: Continued.

Variable	Hcy tertiles (mmol/L)			P value
	Tertile 1 (<11.6)	Tertile 2 (11.6–18.2)	Tertile 3 (>18.2)	
No	768 (98.08%)	743 (95.01%)	748 (95.29%)	
Yes	15 (1.92%)	39 (4.99%)	37 (4.71%)	

Data are n (%), mean \pm SD, or median (interquartile range). BMI: body mass index; NC: neck circumference; WC: waist circumference; SBP: systolic blood pressure; DBP: diastolic blood pressure; TC: total cholesterol; TG: triglyceride; HDL-c: high-density lipoprotein cholesterol; LDL-c: low-density lipoprotein cholesterol; hs-CRP: high-sensitivity C-reactive protein; FPG: fasting plasma glucose; Hcy: homocysteine; eGFR: estimated glomerular filtration rate; Cr: creatinine; AHI: apnea hypopnea index; AI: apnea index; HI: hypopnea index; mean SaO₂: mean oxygen saturation; lowest SaO₂: lowest oxygen saturation; CPAP: continuous positive airway pressure.

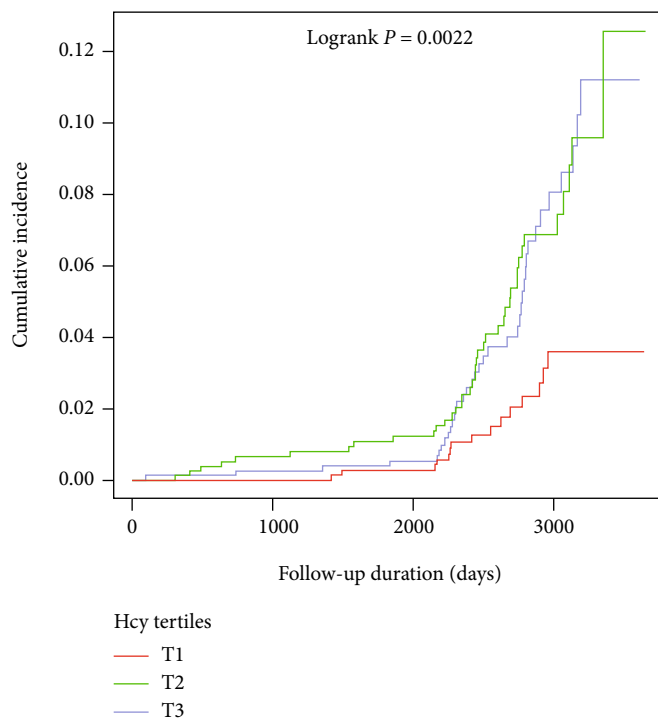


FIGURE 2: Kaplan-Meier curves of incidence of ischemic stroke according to tertiles of baseline plasma Hcy concentrations.

positively associated with the first occurrence of IS (Table 2). In the sensitivity analysis, all E -values were more than one, indicating that the current association tends to be stable and that our main findings are unlikely to be offset by unmeasured confounding variables. Moreover, when plasma Hcy concentrations were divided into different categories, there were obvious changes in effect sizes. The risk of the first IS increased over time by baseline plasma Hcy concentration tertiles and was still significant despite adjustment for potential confounders, and the fully adjusted HRs (adjusted model III) were 2.13 (95% CI: 1.74-2.59) and 1.76 (95% CI: 1.43-2.17) for tertiles 2 and 3, respectively, versus tertile 1 of the baseline plasma Hcy concentrations.

3.4. Threshold Effect Analysis of Plasma Hcy Concentrations on Incident First IS. After adjusting for potential confounders, a nonlinear relationship was observed between plasma Hcy concentration and the first IS (Figure 3). The inflection point, determined by the two-piecewise recursive algorithm and linear regression, was 5 μ mol/L. The P value

of the log-likelihood ratio test was less than 0.01, indicating that the two-piecewise linear regression was more appropriate for fitting the relationship between plasma Hcy concentrations and the risk of the first IS. On the right of the inflection point (plasma Hcy concentrations ≥ 5 μ mol/L), we observed a positive association between plasma Hcy concentrations and the occurrence of the first IS (HR = 1.35, 95% CI: 1.08-1.69, $P < 0.01$). On the left side of the inflection point (plasma Hcy concentrations < 5 μ mol/L), however, their relationship saturated (HR = 1.02, 95% CI: 0.97-1.07, $P = 0.28$) (Table 3).

3.5. Stratified Analyses. To better identify plasma Hcy concentrations and other possible influences on the risk of the first IS, we performed stratified analyses and interaction tests in prespecified subgroups. In stratified analyses, a greater positive correlation between baseline plasma Hcy concentrations and new-onset IS was observed for participants with DBP ≥ 90 mmHg (per SD increment; HR = 1.48, 95% CI: 1.33-1.65 vs. < 90 mmHg: HR = 1.20, 95% CI: 1.02-1.42, P -

TABLE 2: Association between Hcy and incident of the first IS in different models.

Exposure	Crude model (HR to 95% CI to P)	Adjust model I (HR to 95% CI to P)	Adjust model II (HR to 95% CI to P)	Adjust model III (HR to 95% CI to P)
Continuous				
Hcy (per SD increment)	1.37 (1.30 to 1.44) <0.01	1.35 (1.27 to 1.42) <0.01	1.34 (1.26 to 1.43) <0.01	1.32 (1.24 to 1.38) <0.01
Categorical				
Hcy tertiles ($\mu\text{mol/L}$)				
Tertile 1 (<11.6)	Reference	Reference	Reference	Reference
Tertile 2 (11.6–18.2)	2.91 (2.42 to 3.49) <0.01	2.67 (2.22 to 3.20) <0.01	2.33 (1.94 to 2.72) <0.01	2.13 (1.74 to 2.59) <0.01
Tertile 3 (>18.2)	2.75 (2.29 to 3.31) <0.01	2.23 (1.85 to 2.70) <0.01	1.96 (1.73 to 2.19) <0.01	1.76 (1.43 to 2.17) <0.01

Crude model: adjusted for none. Adjust model I: adjusted for age and gender at baseline. Adjust model II: adjusted for variables in adjusted model I plus smoking status, drinking status, NC, WC, and BMI at baseline. Adjust model III: fully adjusted model. Adjusted for variables in adjusted model II plus SBP, DBP, history of arrhythmia and diabetes, AHI, AI, HI, sleep duration, mean SaO_2 and lowest SaO_2 , antidiabetic drugs, antiplatelet drugs, lipid-lowering drugs, regular CPAP treatment, antihypertensive drugs, and TC, TG, HDL-c, LDL-c, FPG, eGFR, Cr, and hs-CRP levels at baseline. Abbreviations are the same as in Table 1.

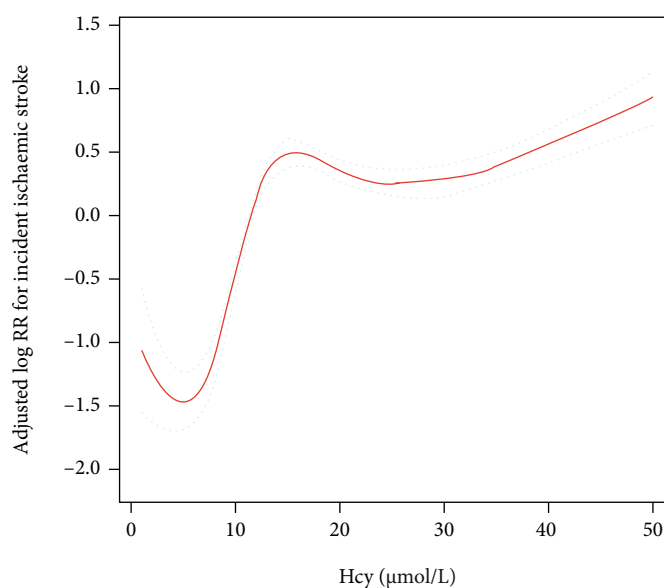


FIGURE 3: A piecewise linear regression model was used to detect the association of plasma Hcy concentrations and the first IS according to the plasma Hcy concentration cut points. All were adjusted for age, gender, smoking status, drinking status, NC, WC, BMI, SBP, DBP, history of arrhythmia, diabetes, AHI, AI, HI, sleep duration, mean SaO_2 and lowest SaO_2 , antidiabetic drugs, antiplatelet drugs, lipid-lowering drugs, regular CPAP treatment, antihypertensive drugs, and TC, TG, HDL-c, LDL-c, FPG, eGFR, Cr, and hs-CRP levels at baseline.

interaction = 0.04) and $\text{BMI} \geq 24$ and $<28 \text{ kg/m}^2$ (per SD increment; HR = 1.46, 95% CI: 1.26-1.70 vs. $<24 \text{ kg/m}^2$: HR = 1.13, 95% CI: 0.95-1.33 vs. $\geq 28 \text{ kg/m}^2$: HR = 1.46, 95% CI: 1.25-1.70, P -interaction = 0.03) (Table 4). However, other variables, including gender (female vs. male), diabetes (no vs. yes), smoking status (never vs. ever vs. current), arrhythmia (no vs. yes), drinking status (never vs. ever vs. current), age (<60 vs. ≥ 60 years), FPG (<6.1 vs. ≥ 6.1 mmol/L), SBP (<140 vs. ≥ 140 mmHg), AHI (≥ 5 and <15 vs. ≥ 15 and <30 vs. ≥ 30 events/hour), and eGFR (<90 vs. $\geq 90 \text{ mL/min/1.73 m}^2$) at baseline, did not dramatically

modify the relationship between plasma Hcy concentrations and the first IS (all P -interactions > 0.05) (Table 4).

4. Discussion

In China, IS is the most prevalent type of cerebrovascular event. Therefore, the prevention of IS is an important and urgent public health issue [6, 7, 32]. Since the discovery of the association of Hcy with the pathogenesis of atherosclerosis, Hcy-lowering therapies have attracted considerable attention among the various prevention strategies for IS

[33, 34]. In addition, a compelling and developing body of epidemiological evidence demonstrates a significant correlation between increased Hcy concentrations and enhanced risk of IS [35, 36]. However, the relationship between Hcy and IS is inconclusive. Iso et al. conducted a prospective, nested case-control study of 11846 Japanese subjects aged 40 to 85 years. Their findings showed odds ratios (95% CI) of 3.89 (1.60 to 9.46) for the highest ($\geq 11.0 \mu\text{mol/L}$) versus the lowest quartile ($< 7.0 \mu\text{mol/L}$) of Hcy for IS after adjusting for cardiovascular risk factors. The respective odds ratio associated with a $5 \mu\text{mol/L}$ increase in Hcy was 1.52 (1.07 to 2.14) [37]. Sacco et al. followed a population-based cohort for vascular events. Their findings suggest that Hcy elevations above $15 \mu\text{mol/L}$ are an independent risk factor for IS, whereas mild tHcy elevations of 10 to $15 \mu\text{mol/L}$ are not predictive. Hcy has the greatest vascular impact in Whites and Hispanics and less in Blacks [38]. However, the Caerphilly study conducted by Fallon et al. yielded the opposite results to the above study. A total of 2254 male participants aged 50 to 64 years were included in the Caerphilly study, and after a mean follow-up of 10.2 years, a total of 107 participants experienced IS. However, after adjusting for confounding, no significant association was found between Hcy and IS [39].

In the current study, we found a meaningful relationship between plasma Hcy concentrations and the incidence of the first IS in hypertensive patients with OSA. Similar results have been reported in several previous studies in patients with simple hypertension or healthy populations, but these studies did not identify a nonlinear association [38, 40, 41]. We found a threshold saturation effect association between plasma Hcy concentrations and the first IS even after removing adjusted covariates from the model. This is the first study to explore the nonlinear association between plasma Hcy concentration and the first IS, calculated for plasma Hcy concentrations at the inflection points of 5 and $15 \mu\text{mol/L}$. Notably, this association between plasma Hcy concentrations and the first IS has opposite effects in the middle of the two inflection points versus the left and right sides. Plasma Hcy concentrations were positively associated with the risk of the first IS when plasma Hcy concentrations were between 5 and $15 \mu\text{mol/L}$. This suggests that the risk of the first IS in hypertensive patients with OSA increases rapidly when plasma Hcy concentrations are between 5 and $15 \mu\text{mol/L}$. In contrast, there was no significant association between plasma Hcy concentrations and the risk of the first IS when plasma Hcy concentrations were $< 5 \mu\text{mol/L}$ or $> 15 \mu\text{mol/L}$. However, the mechanism behind the threshold saturation effect association between plasma Hcy concentrations and the first IS and the inflection point is not clear. To better understand the association between plasma Hcy concentrations and the risk of the first IS, we included significant variables in univariate analysis and noncollinear variables in the multivariate analysis. After adjustment for covariates, participants in the highest tertile of plasma Hcy concentrations had a 1.76-fold greater risk of the first IS compared with those in the lowest tertile.

Subgroup analysis and exploration of interactions are essential for clinical research to better understand plasma

TABLE 3: A piecewise linear regression model was applied to detect the association of Hcy and IS according to the Hcy cut points.

Outcome: incident of ischemic stroke	HR (95% CI)	P value
Linear regression	1.13 (1.02 to 1.24)	<0.01
Two-piecewise linear regression model		
Hcy < $5 \mu\text{mol/L}$	1.02 (0.97 to 1.07)	0.28
Hcy $\geq 5 \mu\text{mol/L}$	1.35 (1.08 to 1.69)	<0.01
P for the log-likelihood ratio test	<0.01	

Notes: adjusted for age, gender, smoking status, drinking status, NC, WC, BMI, SBP, DBP, history of arrhythmia, diabetes, AHI, AI, HI, sleep duration, mean SaO₂ and lowest SaO₂, antidiabetic drugs, antiplatelet drugs, lipid-lowering drugs, regular CPAP treatment, antihypertensive drugs, and TC, TG, HDL-c, LDL-c, FPG, eGFR, Cr, and hs-CRP levels at baseline. Abbreviations are the same as in Table 1.

Hcy concentrations and the risk of the first IS in different populations. In this study, these factors, including gender, diabetes, coronary heart disease, arrhythmia, smoking status, drinking status, age, BMI, FPG, SBP, DBP, AHI, and eGFR, and stronger correlations were identified in participants with BMI $\geq 24 \text{ kg/m}^2$ and DBP $\geq 90 \text{ mmHg}$. In China, the prevalence of obesity in hypertensive patients with OSA is high [42]. A meta-analysis identified a 40% increase in IS mortality for every 5 kg/m^2 increase in BMI among those with a BMI between 25 and 50 kg/m^2 . However, there was no association between BMI and IS mortality in those with a BMI of $15\text{-}24 \text{ kg/m}^2$ [43]. The exact biological mechanism of the interaction between high BMI and high Hcy is unclear. In available studies, a reasonable biological interpretation of this interaction may be due to the fact that elevated Hcy and obesity may share several cellular and molecular mechanisms (e.g., impaired mitochondrial function and the onset of oxidative stress) that are responsible for the development of stroke [44, 45]. In addition, we found that baseline DBP ($\geq 90 \text{ mmHg}$ vs. $< 90 \text{ mmHg}$) significantly altered the effect of Hcy on the risk of the first IS. Zheng et al. [46] found that in Chinese patients with uncontrolled hypertension, the prevalence of IS increased with increasing DBP, suggesting that DBP has an important contribution to the incidence of IS in hypertensive patients. This suggests that DBP serves an essential role in the incidence of IS in hypertensive patients. DBP is traditionally thought to reflect structural changes in small arteries or thinning of microvessels. Thus, elevated DBP may reflect dysfunction of peripheral microvessels, whereas elevated Hcy reflects damage to large- and medium-sized arteries; thus, elevated levels of Hcy and DBP may reflect damage to peripheral vessels and large- and medium-sized arteries, which helps explain the apparent concerted impact of DBP and Hcy on the risk of the first IS [47, 48]. The optimal blood pressure level for controlling Hcy on the risk of the first IS should be explored in future studies.

TABLE 4: Association between Hcy and the first IS in various subgroups.

Stratification variable	No. of participants.	HR (95% CI)	95% CI low	95% CI high	<i>P</i> value	<i>P</i> for interaction
Gender						0.63
Female	744	1.20	0.65	2.22	0.56	
Male	1606	1.40	1.13	1.74	<0.01	
Diabetes						0.51
No	1937	1.39	1.12	1.73	<0.01	
Yes	413	1.16	0.70	1.92	0.57	
Arrhythmia						0.18
No	2306	1.24	1.05	1.46	0.01	
Yes	440	1.41	1.27	1.57	<0.01	
Smoking status						0.63
Never	1342	1.33	0.94	1.88	0.10	
Former	258	1.78	1.04	3.05	0.04	
Current	750	1.34	0.99	1.80	0.05	
Drinking status						0.65
Never	1557	1.43	1.12	1.82	<0.01	
Former	166	1.24	0.63	2.46	0.54	
Current	627	1.13	0.72	1.79	0.59	
Age (years)						0.87
<60	1911	1.36	1.07	1.73	0.01	
≥60	439	1.42	0.96	2.08	0.08	
BMI (kg/m ²)						0.03
<24	221	1.13	0.95	1.33	0.16	
≥24, <28	934	1.46	1.26	1.70	<0.01	
≥28	1195	1.46	1.25	1.70	<0.01	
SBP (mmHg)						0.41
<140	1084	1.25	0.86	1.82	0.23	
≥140	1266	1.51	1.18	1.92	<0.01	
DBP (mmHg)						0.04
<90	887	1.20	1.02	1.42	0.03	
≥90	1463	1.48	1.33	1.65	<0.01	
AHI (events/hour)						0.37
≥5, <15	934	1.46	1.04	2.07	0.03	
≥15, <30	722	1.47	1.04	2.09	0.03	
≥30	694	1.07	0.73	1.56	0.74	
FPG (mmol/L)						0.72
<6.1	1991	1.38	1.23	1.54	<0.01	
≥6.1	359	1.32	1.04	1.66	0.02	
eGFR (mL/min/1.73 m ²)						0.59
<90	941	1.42	1.08	1.85	0.01	
≥90	1409	1.27	0.93	1.72	0.13	

Note 1: adjusted for age, gender, smoking status, drinking status, NC, WC, BMI, SBP, DBP, history of arrhythmia, diabetes, AHI, AI, HI, sleep duration, mean SaO₂ and lowest SaO₂, antidiabetic drugs, antiplatelet drugs, lipid-lowering drugs, regular CPAP treatment, antihypertensive drugs, and TC, TG, HDL-c, LDL-c, FPG, eGFR, Cr, and hs-CRP levels at baseline. Note 2: in each case, the model was not adjusted for hierarchical covariates. Abbreviations are the same as in Table 1.

Our findings may have important implications for public health concerns [19, 49]. In hypertensive patients with OSA, increased Hcy levels are probably a changeable risk factor for IS. Lowering Hcy levels may reduce the risk of stroke in hypertensive patients with OSA, and the prog-

nostic effect of Hcy levels has important clinical implications. However, the relationship between slightly increased Hcy levels and the risk of IS is disputable [38]. Our study revealed a nonlinear dose-response relationship between Hcy levels and the first IS in hypertensive patients

with OSA, and slightly increased Hcy levels may increase the risk of the first IS in hypertensive patients with OSA. However, a few investigations have shown that slightly increased Hcy levels do not enhance the risk of IS [38, 50]. Further, in IS patients with marginal or slightly increased Hcy levels, reducing Hcy with high-dose vitamin therapy did not reduce the risk of IS recurrence [51]. Therefore, additional investigations are necessary to verify whether the risk of IS in hypertensive patients with OSA can be reduced by intensive control or maintenance of lower Hcy levels through folic acid and vitamin B12 supplementation.

The present study has some unique strengths. First, it is the first report of a nonlinear relationship between Hcy and the first IS in hypertensive patients with OSA. Second, the present study is a retrospective cohort research and thus vulnerable to potential influences. However, we applied rigorous statistical adjustments to reduce remnant confounders as much as possible. Finally, we conducted subgroup analyses and interaction tests to further demonstrate reliability for the results and to identify potential interactions with other variables.

Limitations of the study are mainly in the areas of the following. First, levels of Hcy were tested only once at baseline, so we were unable to investigate the effect of changes in levels of Hcy on IS. Second, levels of Hcy could be affected by genetic background, dietary habits, and/or medication usage. It is possible that a single plasma Hcy concentration test may not provide us with sufficient information to determine a causal relationship between Hcy and IS. Third, participants were limited to hypertensive patients with OSA in northwest China. Therefore, the findings of the present investigation should be approached with caution for extrapolation to the general population or other ethnic communities. Fourth, data on adiponectin, IL-6, and TNF- α levels are lacking in this cohort study, so it is not possible to compare the accuracy of Hcy levels and other biomarkers for predicting the risk of IS [2, 5]. Finally, recall bias may have existed during data collection. However, recall bias was minimized during data collection through rigorous training in survey methodology and the application of standard operating procedures.

5. Conclusion

In conclusion, elevated plasma Hcy concentrations were independently associated with the risk of the first IS in hypertensive patients with OSA. Plasma Hcy concentrations $\geq 5 \mu\text{mol/L}$ obviously increase the risk of the first IS in hypertensive patients with OSA. Undoubtedly, lowering plasma Hcy concentrations to $<5 \mu\text{mol/L}$ is an efficient and modest approach to minimize the risk of the first IS in hypertensive patients with OSA.

Data Availability

All relative data are in the paper.

Ethical Approval

This study was approved by the Ethics Committee of the People's Hospital of Xinjiang Uygur Autonomous Region (no. 2019030662).

Conflicts of Interest

The authors declare that they have no conflicts of interest.

Authors' Contributions

Nanfang Li and Xintian Cai contributed equally to this paper.

Acknowledgments

This work was financially supported by the Special Research Project for Young Medical Science and Technology Talents (No. WJWY-202031) and the Research Project of Xinjiang People's Hospital (No. 20190419).

References

- [1] J. D. Pandian, S. L. Gall, M. P. Kate et al., "Prevention of stroke: a global perspective," *Lancet*, vol. 392, no. 10154, pp. 1269–1278, 2018.
- [2] W. J. Tu, H. C. Qiu, Y. K. Liu, Q. Liu, X. Zeng, and J. Zhao, "Elevated levels of adiponectin associated with major adverse cardiovascular and cerebrovascular events and mortality risk in ischemic stroke," *Cardiovascular Diabetology*, vol. 19, no. 1, p. 125, 2020.
- [3] W. J. Tu, B. H. Chao, L. Ma et al., "Case-fatality, disability and recurrence rates after first-ever stroke: A study from bigdata observatory platform for stroke of China," *Brain Research Bulletin*, vol. 175, pp. 130–135, 2021.
- [4] S. Wu, B. Wu, M. Liu et al., "Stroke in China: advances and challenges in epidemiology, prevention, and management," *The Lancet Neurology*, vol. 18, no. 4, pp. 394–405, 2019.
- [5] L. S. Cheng, W. J. Tu, Y. Shen, L. J. Zhang, and K. Ji, "Combination of high-sensitivity C-reactive protein and homocysteine predicts the post-stroke depression in patients with ischemic stroke," *Molecular Neurobiology*, vol. 55, no. 4, pp. 2952–2958, 2018.
- [6] T. Li, J. Zhu, Q. Fang et al., "Association of H-type hypertension with stroke severity and prognosis," *BioMed Research International*, vol. 2018, Article ID 8725908, 7 pages, 2018.
- [7] C. Wang, Z. du, N. Ye et al., "Using the atherogenic index of plasma to estimate the prevalence of ischemic stroke within a general population in a rural area of China," *BioMed Research International*, vol. 2020, Article ID 7197054, 7 pages, 2020.
- [8] A. S. Jordan, D. G. McSharry, and A. Malhotra, "Adult obstructive sleep apnoea," *Lancet*, vol. 383, no. 9918, pp. 736–747, 2014.
- [9] P. Lévy, M. Kohler, W. T. McNicholas et al., "Obstructive sleep apnoea syndrome," *Nature Reviews. Disease Primers*, vol. 1, no. 1, article 15015, 2015.
- [10] H. Hou, Y. Zhao, W. Yu et al., "Association of obstructive sleep apnea with hypertension: a systematic review and meta-analysis," *Journal of Global Health*, vol. 8, no. 1, article 010405, 2018.

- [11] M. A. Martínez-García, C. Navarro-Soriano, G. Torres et al., “Beyond resistant hypertension,” *Hypertension*, vol. 72, no. 3, pp. 618–624, 2018.
- [12] R. P. Pedrosa, L. F. Drager, C. C. Gonzaga et al., “Obstructive sleep apnea: the most common secondary cause of hypertension associated with resistant hypertension,” *Hypertension*, vol. 58, no. 5, pp. 811–817, 2011.
- [13] L. A. Salman, R. Shulman, and J. B. Cohen, “Obstructive sleep apnea, hypertension, and cardiovascular risk: epidemiology, pathophysiology, and management,” *Current Cardiology Reports*, vol. 22, no. 2, p. 6, 2020.
- [14] I. Cano-Pumarega, J. Durán-Cantolla, F. Aizpuru et al., “Obstructive sleep apnea and systemic hypertension: longitudinal study in the general population: the Vitoria Sleep Cohort,” *American Journal of Respiratory and Critical Care Medicine*, vol. 184, no. 11, pp. 1299–1304, 2011.
- [15] E. Zhao, S. Chen, Y. Du, and Y. Zhang, “Association between sleep apnea hypopnea syndrome and the risk of atrial fibrillation: a meta-analysis of cohort study,” *BioMed Research International*, vol. 2018, Article ID 5215868, 2018.
- [16] J. Y. Dong, Y. H. Zhang, and L. Q. Qin, “Obstructive sleep apnea and cardiovascular risk: meta-analysis of prospective cohort studies,” *Atherosclerosis*, vol. 229, no. 2, pp. 489–495, 2013.
- [17] Y. K. Loke, J. W. Brown, C. S. Kwok, A. Niruban, and P. K. Myint, “Association of obstructive sleep apnea with risk of serious cardiovascular events: a systematic review and meta-analysis,” *Circulation. Cardiovascular Quality and Outcomes*, vol. 5, no. 5, pp. 720–728, 2012.
- [18] C. Xie, R. Zhu, Y. Tian, and K. Wang, “Association of obstructive sleep apnoea with the risk of vascular outcomes and all-cause mortality: a meta-analysis,” *BMJ open*, vol. 7, no. 12, article e013983, 2017.
- [19] X. Wu, Q. Zhou, Q. Chen et al., “Association of homocysteine level with risk of stroke: A dose-response meta-analysis of prospective cohort studies,” *Nutrition, Metabolism, and Cardiovascular Diseases*, vol. 30, no. 11, pp. 1861–1869, 2020.
- [20] S. S. Kang and R. S. Rosenson, “Analytic approaches for the treatment of hyperhomocysteinemia and its impact on vascular disease,” *Cardiovascular Drugs and Therapy*, vol. 32, no. 2, pp. 233–240, 2018.
- [21] B. Yang, S. Fan, X. Zhi et al., “Prevalence of hyperhomocysteinemia in China: a systematic review and meta-analysis,” *Nutrients*, vol. 7, no. 1, pp. 74–90, 2015.
- [22] J. Skeete and D. J. DiPette, “Relationship between homocysteine and hypertension: new data add to the debate,” *The Journal of Clinical Hypertension*, vol. 19, no. 11, pp. 1171–1172, 2017.
- [23] R. L. Sacco, R. Adams, G. Albers et al., “Guidelines for prevention of stroke in patients with ischemic stroke or transient ischemic attack: a statement for healthcare professionals from the American Heart Association/American Stroke Association Council on Stroke: co-sponsored by the Council on Cardiovascular Radiology and Intervention: the American Academy of Neurology affirms the value of this guideline,” *Circulation*, vol. 113, no. 10, pp. e409–e449, 2006.
- [24] W. J. Powers, A. A. Rabinstein, T. Ackerson et al., “Guidelines for the early management of patients with acute ischemic stroke: 2019 update to the 2018 guidelines for the early management of acute ischemic stroke: a guideline for healthcare professionals from the American Heart Association/American Stroke Association,” *Stroke*, vol. 50, no. 12, pp. e344–e418, 2019.
- [25] W. Yang, L. Shao, M. Heizhati et al., “Oropharyngeal microbiome in obstructive sleep apnea: decreased diversity and abundance,” *Journal of Clinical Sleep Medicine*, vol. 15, no. 12, pp. 1777–1788, 2019.
- [26] L. Wang, N. Li, X. Yao et al., “Detection of secondary causes and coexisting diseases in hypertensive patients: OSA and PA are the common causes associated with hypertension,” *BioMed Research International*, vol. 2017, Article ID 8295010, 8 pages, 2017.
- [27] A. S. Levey, L. A. Inker, and J. Coresh, “GFR estimation: from physiology to public health,” *American Journal of Kidney Diseases*, vol. 63, no. 5, pp. 820–834, 2014.
- [28] Y. Yu, L. Liu, J. Huang et al., “Association between systolic blood pressure and first ischemic stroke in the Chinese older hypertensive population,” *The Journal of International Medical Research*, vol. 48, no. 4, p. 030006052092009, 2020.
- [29] Y. Q. Huang, K. Lo, X. C. Liu, S. T. Tang, C. Huang, and Y. Q. Feng, “The relationship between fasting blood glucose levels and first ischemic stroke in elderly hypertensive patients,” *Risk Management and Healthcare Policy*, vol. Volume 13, pp. 777–784, 2020.
- [30] E. von Elm, D. G. Altman, M. Egger, S. J. Pocock, P. C. Gøtzsche, and J. P. Vandenbroucke, “The strengthening of reporting of observational studies in epidemiology (STROBE) statement: guidelines for reporting observational studies,” *Lancet*, vol. 370, no. 9596, pp. 1453–1457, 2007.
- [31] J. Wang, D. Zhou, and X. Li, “The association between neutrophil-to-lymphocyte ratio and diabetic depression in U.S. adults with diabetes: findings from the 2009-2016 National Health and Nutrition Examination Survey (NHANES),” *BioMed Research International*, vol. 2020, Article ID 8297628, 7 pages, 2020.
- [32] T. Li, X. Liu, S. Diao et al., “H-type hypertension is a risk factor for cerebral small-vessel disease,” *BioMed Research International*, vol. 2020, Article ID 6498903, 6 pages, 2020.
- [33] D. S. Wald, M. Law, and J. K. Morris, “Homocysteine and cardiovascular disease: evidence on causality from a meta-analysis,” *BMJ*, vol. 325, no. 7374, pp. 1202–1206, 2002.
- [34] G. N. Welch and J. Loscalzo, “Homocysteine and atherothrombosis,” *The New England Journal of Medicine*, vol. 338, no. 15, pp. 1042–1050, 1998.
- [35] Y. Huo, J. Li, X. Qin et al., “Efficacy of folic acid therapy in primary prevention of stroke among adults with hypertension in China: the CSPPT randomized clinical trial,” *JAMA*, vol. 313, no. 13, pp. 1325–1335, 2015.
- [36] T. Zhang, T. Lin, Y. Wang et al., “Estimated stroke-free survival of folic acid therapy for hypertensive adults: projection based on the CSPPT,” *Hypertension*, vol. 75, no. 2, pp. 339–346, 2020.
- [37] H. Iso, Y. Moriyama, S. Sato et al., “Serum total homocysteine concentrations and risk of stroke and its subtypes in Japanese,” *Circulation*, vol. 109, no. 22, pp. 2766–2772, 2004.
- [38] R. L. Sacco, K. Anand, H. S. Lee et al., “Homocysteine and the risk of ischemic stroke in a triethnic cohort: the Northern Manhattan Study,” *Stroke*, vol. 35, no. 10, pp. 2263–2269, 2004.
- [39] U. B. Fallon, P. Elwood, Y. Ben-Shlomo, J. B. Ubbink, R. Greenwood, and G. D. Smith, “Homocysteine and ischaemic stroke in men: the Caerphilly study,” *Journal of Epidemiology and Community Health*, vol. 55, no. 2, pp. 91–96, 2001.

- [40] R. Kawamoto, T. Kajiwar, Y. Oka, and Y. Takagi, "An association between plasma homocysteine concentrations and ischemic stroke in elderly Japanese," *Journal of Atherosclerosis and Thrombosis*, vol. 9, no. 2, pp. 121–125, 2002.
- [41] L. Han, Q. Wu, C. Wang et al., "Homocysteine, ischemic stroke, and coronary heart disease in hypertensive patients: a population-based, prospective cohort study," *Stroke*, vol. 46, no. 7, pp. 1777–1786, 2015.
- [42] X. Qin, Y. Zhang, Y. Cai et al., "Prevalence of obesity, abdominal obesity and associated factors in hypertensive adults aged 45-75 years," *Clinical Nutrition*, vol. 32, no. 3, pp. 361–367, 2013.
- [43] Prospective Studies Collaboration, G. Whitlock, S. Lewington et al., "Body-mass index and cause-specific mortality in 900 000 adults: collaborative analyses of 57 prospective studies," *Lancet*, vol. 373, no. 9669, pp. 1083–1096, 2009.
- [44] A. Laha, A. Majumder, M. Singh, and S. C. Tyagi, "Connecting homocysteine and obesity through pyroptosis, gut microbiome, epigenetics, peroxisome proliferator-activated receptor γ , and zinc finger protein 407," *Canadian Journal of Physiology and Pharmacology*, vol. 96, no. 10, pp. 971–976, 2018.
- [45] N. Komorniak, M. Szczuko, B. Kowalewski, and E. Stachowska, "Nutritional deficiencies, bariatric surgery, and serum homocysteine level: review of current literature," *Obesity Surgery*, vol. 29, no. 11, pp. 3735–3742, 2019.
- [46] L. Zheng, Z. Sun, J. Li et al., "Pulse pressure and mean arterial pressure in relation to ischemic stroke among patients with uncontrolled hypertension in rural areas of China," *Stroke*, vol. 39, no. 7, pp. 1932–1937, 2008.
- [47] M. J. Cipolla, D. S. Liebeskind, and S. L. Chan, "The importance of comorbidities in ischemic stroke: impact of hypertension on the cerebral circulation," *Journal of Cerebral Blood Flow and Metabolism*, vol. 38, no. 12, pp. 2129–2149, 2018.
- [48] P. Sun, L. Liu, C. Liu et al., "Carotid intima-media thickness and the risk of first stroke in patients with hypertension," *Stroke*, vol. 51, no. 2, pp. 379–386, 2020.
- [49] F. Pan, M. Heizhati, L. Wang et al., "Distribution characteristics of circulating homocysteine and folate and related factors in agriculture, stock-raising and urban populations: a cross-sectional survey," *Public Health Nutrition*, vol. 24, no. 5, pp. 1001–1008, 2021.
- [50] A. G. Bostom, I. H. Rosenberg, H. Silbershatz et al., "Nonfasting plasma total homocysteine levels and stroke incidence in elderly persons: the Framingham Study," *Annals of Internal Medicine*, vol. 131, no. 5, pp. 352–355, 1999.
- [51] J. F. Toole, M. R. Malinow, L. E. Chambless et al., "Lowering homocysteine in patients with ischemic stroke to prevent recurrent stroke, myocardial infarction, and death: the vitamin intervention for stroke prevention (VISP) randomized controlled trial," *JAMA*, vol. 291, no. 5, pp. 565–575, 2004.

Review Article

Immune Checkpoints: Therapeutic Targets for Pituitary Tumors

Ding Nie,¹ Yimeng Xue,² Qiuyue Fang,³ Jianhua Cheng,³ Bin Li,³ Dawei Wang,³ Chuzhong Li,³ Songbai Gui,¹ Yazhuo Zhang,³ and Peng Zhao¹ 

¹Department of Neurosurgery, Beijing Tiantan Hospital, Capital Medical University, Beijing, China

²Savaid Medical School, University of Chinese Academy of Sciences, Beijing, China

³Beijing Neurosurgical Institute, Beijing, China

Correspondence should be addressed to Peng Zhao; zhaopeng@ccmu.edu.cn

Received 14 June 2021; Accepted 6 August 2021; Published 17 August 2021

Academic Editor: Xianwei Zeng

Copyright © 2021 Ding Nie et al. This is an open access article distributed under the Creative Commons Attribution License, which permits unrestricted use, distribution, and reproduction in any medium, provided the original work is properly cited.

Pituitary tumors are the third most common intracranial tumors in adults. Treatment of refractory pituitary tumors is known to be difficult due to limited treatment options. As a promising therapeutic method, tumor immunotherapy has been applied in the treatment of many tumors, including pituitary tumors. Immune checkpoint blocking is one of the effective strategies to activate antitumor immunity. Immune checkpoints prevent tissue damage by regulating the immune response of peripheral tissues and participate in the maintenance of a normal immune environment. In the presence of a tumor, inhibition of T cell activity by tumor cells binding to immune checkpoints and their ligands is an important mechanism for tumor cells to escape immune injury. In this review, we summarize the latest findings of immune checkpoints and their potential as immunotherapeutic targets for pituitary tumors.

1. Introduction

A pituitary tumor is a nonmetastatic tumor that occurs in the pituitary gland and accounts for 15% of all tumors of the central nervous system [1, 2]. A small proportion of pituitary tumors are clinically invasive and are likely to remain or recrudescence after surgery and radiotherapy [3]. Temozolomide (TMZ) is effective in some invasive pituitary tumors, but up to 50% of patients do not respond to TMZ, and the median time of progression is short [4]. Targeted therapies, including growth factors and their receptors, intracellular signaling pathways, and proteins that regulate cell cycles, are also of limited effectiveness [5]. At the same time, some pathologists have suggested that invasive pituitary tumors have malignant potential, and early identification and aggressive treatment of these invasive tumors are needed to reduce tumor recurrence and prolong survival [6]. Thus, it is urgent to propose a new treatment regimen. In recent years, based on the deep understanding of tumor immune microenvironment, immune checkpoint suppressive therapy has made great progress in cancer treatment which applied to the treatment of various malignant tumors including melanoma,

lymphoma, lung cancer, bladder cancer, liver cancer, and gastroesophageal cancer [7–9]. Different immune checkpoints work together to regulate the immune system, which is a double-edged sword, and in physiological situations, these checkpoints are usually responsible for maintaining the immune response within the required physiological range and protecting the host from autoimmunity. In the presence of a tumor, immune checkpoints may be used to inhibit the activation of T cells, thereby preventing T cells from damaging tumor cells and eventually leading to tumor proliferation or migration [10–12] (Figure 1). Thus, targeted immune checkpoint therapy is a new hot spot in tumor immunotherapy. Immune checkpoint inhibitors (ICIs) mediated immunotherapy has become a turning point in oncology therapy by targeting immune checkpoints, relieving T cell suppression, and promoting antitumor immunity [13, 14]. So far, the cytotoxic T-lymphocyte antigen, 4 (CTLA-4) and programmed cell death protein 1 (PD-1)/programmed cell death ligand 1 (PD-L1) are the main representative immune checkpoints. Meanwhile, Lymphocyte activation-gene-3 (LAG-3), T cell immunoglobulin domain and mucin domain-3 (TIM-3), and T cell immunoreceptor with Ig and Itim

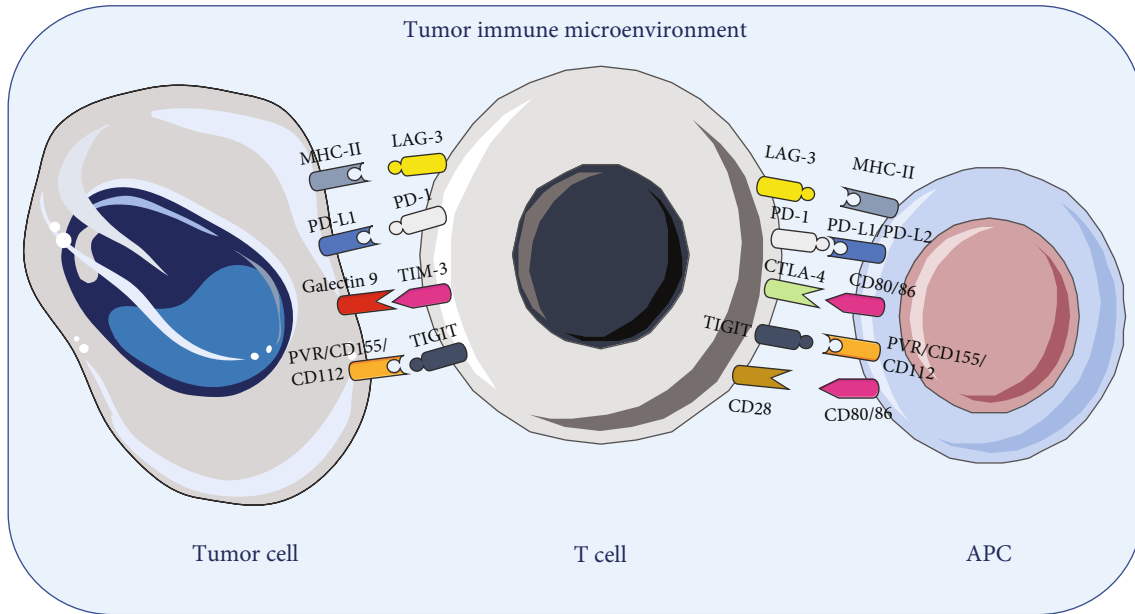


FIGURE 1: Binding patterns of immune checkpoints. Immune checkpoint binding with ligand in the immune microenvironment.

domains (TIGIT) have been identified (Table 1) [13, 15, 16]. In the case of pituitary tumors, with the further study of its immune microenvironment, the use of immune checkpoint inhibitors may be the next effective choice for the treatment of refractory pituitary tumors or even pituitary cancer. [10]. Therefore, this review article introduces the current research progress of different immune checkpoints and discusses their application prospects in pituitary tumors.

2. PD-1/PD-L1

PD-1 is often expressed on the surface of B cells, T cells, NK cells, and other cells, and the combination with PD-L1 and PD-L2 will block the cytokine secretion and proliferation of these cells [17, 18]. Although PD-L2 can also inhibit T cell function, PD-1/PD-L1 blockers have received more attention because PD-L1 expression is higher in tumor cells than PD-L2, that is, in many human tumors, the high expression of PD-L1 leads to poor prognosis [19–22]. PD-1/PD-L1 axis inhibitors exert their antitumor effects by alleviating PD-L1-mediated inhibition of tumor-infiltrating T lymphocytes and enhancing the proliferation of tumor-infiltrating T-regulatory cells (Treg) [23, 24]. For example, inhibitors block the interaction of PD-1 receptors on CD8⁺ and CD4⁺ T cells with PD-L1 on target tumor cells [25, 26]. The expression of PD-L1 is a predictive biomarker of anti-PD-1/PD-L1 treatment response. It has been reported that in different tumor types, PD-L1-positive patients with tumors have a much higher response rate to PD-1/PD-L1 axis inhibitors than the negative ones [27]. Several studies have described the expression of PD-L1 in pituitary neuroendocrine tumors (PitNETs). In general, the present studies indicated that PD-L1 is highly expressed in invasive pituitary tumors as well as in some functional pituitary tumors, particularly in somatotrophs and lactotrophs [28–33]. Furthermore, in a recent

study of 264 pituitary adenoma specimens, researchers found a high incidence of significant overexpression of PD-L1 in Pit-1-positive tumors [34]. Compared to tumor tissues, a study involving 10 pituitary samples showed no increase in PD-L1 expression in normal endocrine tissues [35]. Although some types of pituitary tumors show high levels of PD-L1 expression, it does not mean that these tumors will necessarily respond to immune checkpoint suppression. Still, these facts suggest that immune checkpoint suppression may represent a reasonable treatment for some pituitary tumors and even pituitary carcinomas [34]. Likewise, pituitary tumors themselves exhibit T cell infiltrates, a prerequisite for checkpoint blockade efficacy [28]. In preclinical studies, after subcutaneous tumor implantation, anti-PD-L1 treatment significantly inhibited tumor growth and serum ACTH secretion, and some mice achieved complete tumor regression, compared with tumor-bearing mice without anti-PD-L1 treatment, which also have been observed in models of intracranial tumors [32]. There has been strong evidence of the effectiveness of immunotherapy in the treatment of pituitary tumors. In 2018, Lin et al. reported about a patient with ACTH-secreting pituitary carcinomas who was successfully treated with combined immunotherapy with ipilimumab (anti-CTLA-4) and nivolumab (anti-PD-1) [36]. Recently, Sol et al. reported about a patient with ACTH-secreting pituitary carcinomas who was stabilized with the same combination immunotherapy [37]. Caccese et al. also reported about a patient with a MMRd pituitary adrenocorticotropic hormone- (ACTH-) secreting adenoma treated with the checkpoint inhibitor pembrolizumab [38]. Similarly, Lamb et al. treated a case of prolactin pituitary cancer using ipilimumab and nivolumab in combination with vascular endothelial growth factor inhibition therapy [39]. In conclusion, the exploration of immunotherapy in pituitary tumors or pituitary carcinomas with high PD-L1 expression is a promising work.

TABLE 1: Possible immune checkpoints in pituitary tumors.

Immune checkpoint	Application in pituitary tumors	Research type	Recommendation	Ref.	Year
PD-1/PD-L1	Cushing's disease			[32]	2020
	ACTH pituitary carcinomas	Preclinical	Used in pituitary tumors with high expression of PD-L1, combined with other target inhibitors when necessary	[37]	2021
	Prolactin pituitary carcinomas	Clinical		[38]	2020
	Clinical	[39]		2020	
CTLA-4	ACTH pituitary carcinomas	Clinical	Combination therapy of CTLA-4 inhibitors with PD-1/PD-L1 inhibitors	[37]	2021
	Prolactin pituitary carcinomas	Clinical		[39]	2020
TIM-3	—	—	Tim-3 blocking combined with PD-L1 blocking	—	—
LAG-3	—	—	Combined with other targets, dual blocking	—	—
TIGIT	—	—	Combined with other targets, dual blocking (functional pituitary tumors)	—	—

PD-1/PD-L1: programmed cell death protein 1/programmed cell death ligand 1; CTLA-4: cytotoxic T-lymphocyte antigen, 4; TIM-3: T cell immunoglobulin domain and mucin domain-3; LAG-3: lymphocyte activation-gene-3; TIGIT: T cell immunoreceptor with Ig and Itim domains.

3. CTLA-4

CTLA-4 is a kind of representative immune checkpoint pathway like PD-1/PD-L1 and is also involved in the negative regulation of immune function at different stages of T cell activation [13]. CTLA-4, expressed on activated T and Treg cells, is homologous to CD28 and has a higher affinity for CD80 and CD86 [40]. Unlike the first antigen-dependent receptor (CD28), CTLA-4 is antigen independent [41]. It is the second receptor of the T cell costimulatory ligand CD80/86, and its function is critical for the downregulation of the immune response. Typically, CD28 binds to the B7 ligand and signals through phosphoinositol 3-kinase (PI3K) to enhance downstream activation pathways [42]. The binding of CTLA-4 to CD80/CD86 prevents T cell proliferation stimulation provided by the binding of CD28 to CD80/CD86 during initiation [40]. In addition, the involvement of CTLA-4 in T cell activation prevents cell cycle progression [43]. In animal experiments, Brunner et al. demonstrated that CTLA-4 prevented cell cycle progression by inhibiting the production of cyclin D3 and CDK4 and CDK6, as well as altering the degradation of cell cycle inhibitor p27. Moreover, they also observed CTLA-4-mediated effects on cyclins when cells were stimulated only by CD3, suggesting that CTLA-4 inhibited the CD28-independent pathway in T cell activation [44]. CTLA-4 blocks the binding of antibodies to CTLA-4 expressed on T lymphocytes, leading to the beneficial expansion of effector T cells that recognize tumor antigens and eliminate tumors, thereby inhibiting tumor growth [45]. Currently, CTLA-4 has been rarely reported in pituitary tumors. In one study, the transcriptome of 115 pituitary tumors was analyzed and no differences in CTLA-4 expression among tumor subtypes were observed which showed that the expression of CTLA-4 was not specific in each subtype of pituitary tumor [31]. In another study, CTLA-4 expression was confirmed in 37 surgical pituitary adenomas and 11 normal pituitary glands [45]. These shreds of evidence explain that the application of CTLA-4 antibodies binds to the pituitary CTLA-4 and triggers a series of cyto-

pathic immune responses leading to side effects such as pituitary inflammation [46]. At the same time, it is also a kind of evidence of the therapeutic effect of CTLA-4 antibody on pituitary tumors. Considering that the combination of CTLA-4 antibody with the “ectopic” expression of CTLA-4 antigen on normal pituitary endocrine cells can cause damage to normal pituitary tissue, the use of the CTLA-4 antibody as an adjuvant to other checkpoint inhibitors, such as anti-PD-1 and anti-PD-L1, for the treatment of pituitary tumors, may be a promising approach. CTLA-4 inhibitors are used in combination with PD-1/PD-L1 inhibitors in the treatment of pituitary tumors reported so far [36].

4. TIM-3, LAG-3, and TIGIT

The success of CTLA-4 inhibitors and PD-1/PD-L1 inhibitors in the treatment of many types of tumors has inspired researchers to investigate targets beyond these [47]. Although to the best of our knowledge, no studies have targeted these targets in pituitary tumors, they remain a viable and promising option.

TIM-3, a member of the TIM gene family, is expressed in tumor cells and immune cells [48–50]. The interaction of TIM-3 with its ligand induces T cell inhibition, while blocking TIM-3 expression leads to T cell proliferation and cytokine production, thus triggering immune activation [51]. Notably, Tim-3 and PD-1 are often coexpressed in T cells, which are dysfunctional or failing. In one study, anti-TIM-3 treatment alone had little or no effect on mice carrying solid tumor CT26 colon cancer, and anti-PD-L1 treatment alone showed a tendency to delay tumor growth [48]. However, the combination of anti-TIM-3 and anti-PD-L1 led to a significant reduction in tumor growth, with 50% of the mice showing complete tumor regression [48]. This suggests that combined targeting of the TIM-3 and PD-1 pathways is more effective in controlling tumor growth than targeting the TIM-3 and PD-1 pathways alone. Song et al. reported that Tim-3⁺ Foxp3⁺ Treg cell levels in PBMC of patients with nonfunctional pituitary adenoma were significantly higher than those

of healthy controls, and the level of Foxp3⁺ Treg cells expressing Tim-3 was significantly reduced in patients after surgery [52]. Therefore, it is worth further exploration whether combined blocking of TIM-3 and PD-L1 can effectively treat pituitary tumors.

LAG-3 is expressed in activated CD4⁺ and CD8⁺ T cells, NK cells, B cells, and dendritic cells (DC) and induces immune failure by binding to major histocompatibility complex class II (MHC-II) and other ligands [53–56]. Coexpression of LAG-3 with other targets (such as PD-1, TIGIT, and TIM-3) leads to T cell failure, exemplified by lack of proliferation and cytokine secretion [57]. In some preclinical studies on different tumor types, LAG-3 monotherapy has largely failed, often in combination with other targets, i.e., the use of dual coblocking will enhance tumor inhibition [58–60]. For example, in mice with MC38 tumor, dual LAG-3/PD-1 coblocking synergism restricted the growth of MC38 and resulted in 80% tumor clearance in mice [57]. It seems that coblocking of LAG-3 with PD-1 or other targets can enhance the effect of immunotherapy, and whether it can also be applied in pituitary tumors is a direction of future research.

TIGIT expression in NK cells and T cells, binding with CD155, CD112, or PVRL3, can inhibit interferon- γ production of NK cells and promote the generation of mature immunoregulatory DCS and inhibitory differentiation and function of T cells [47, 61–63]. Similar to TIM-3 and LAG-3, TIGIT is often coexpressed with other targets, and double blockade restates T cell and NK cell function in the preclinical environment [62, 64, 65]. Studies have shown that activation of the hypothalamic-pituitary-adrenal (HPA) axis causes the adrenal cortex to release glucocorticoid (GC) hormones into the circulatory system, and these GCs may promote the expression of TIGIT by key effector cells in an environmental, tissue-specific, and system-specific manner, thereby suppressing the immune response [66]. Whether the secretion of hormones in functional pituitary tumors can also affect the expression of TIGIT and the coinhibition of TIGIT and other targets can affect the immunotherapy of pituitary tumors are two problems facing us at present.

5. The Dilemma of Immune Checkpoint Inhibitors

The use of immune checkpoint inhibitors has revolutionized the management of some tumors, but with different responses in different patients, and these drugs can cause unique adverse reactions that can be life threatening [67–69]. How to enhance the efficacy of immunosuppressive agents and reduce adverse reactions are two major challenges facing us.

The combination of immunosuppressive agents, such as CTLA-4 inhibitors combined with PD-1 inhibitors, or TIM-3 and PD-L1 inhibitors combined with blocking, is currently the best choice to enhance the therapeutic effect [17, 36, 48]. Some researchers are exploring other ways, too. For example, Deng et al. proposed that the combination of radiotherapy and anti-PD-L1 therapy can enhance the activity of CD8⁺ T cells, optimize the tumor immune microenvironment, and lead to tumor regression [70]. Liu et al. believed that abnormal mechanical properties and immunosuppres-

sion were the two key factors limiting the antitumor efficacy of T cell immune checkpoint blocking inhibitors against solid tumors in clinical practice, and they found that hyperbaric oxygen could promote PD-1 antibody delivery and destroy hypoxic-mediated immunosuppression through the consumption of extracellular matrix [71]. Melero et al. suggested that intratumoral drug delivery and targeted drug delivery of tumor tissue should be used instead of traditional intravenous infusion [72]. Such explorations provide broad ideas for finding ways to improve the efficacy of immunosuppressants.

In clinical treatment, immune-related adverse events (irAE) caused by ICIs are more toxic than conventional chemotherapy and often involve different organ systems [73, 74]. For example, the cardiovascular system presents with pericarditis, pericardial effusion, and various types of arrhythmias, including the development of the complete atrioventricular block, myocardial infarction, heart failure, and myocarditis [75]. In the skin lesions, the manifestations are psoriasis, erythema pleomorphic, leukocyte cataclastic vasculitis, and eczema [76]. In the gastrointestinal system, diseases such as colitis, hepatitis, cholangitis, and gastritis are common [77]. In the blood system, it is often manifested as autoimmune hemolytic anemia, immune thrombocytopenia, and aplastic anemia [78]. In the nervous system, it is manifested as myasthenia gravis, encephalitis, and demyelination of the central nervous system [79]. In the urinary system, acute kidney injury and acute tubulointerstitial nephritis often occur [73]. When considering the introduction of ICIs in the treatment of pituitary tumors, it is of concern that ICIs can damage the endocrine system and cause endocrine diseases involving the thyroid, pituitary, adrenal, and pancreas [80]. How to reduce the damage to normal pituitary tissue while making ICI damage to pituitary tumor cells is the key to make immune checkpoint suppression therapy suitable for a pituitary tumor.

6. Future Perspectives and Conclusions

While ICIs have been extensively used to target immune checkpoints in many tumors, their use in pituitary tumors has just commenced. With the increasing research on the microenvironment of pituitary tumors, the recognized infiltration of lymphocytes and the expression of immune checkpoints seem to give us a strong implication that immunotherapy targeting immune checkpoints is the next effective treatment approach for pituitary tumors. Before that, to clarify the specific mechanism of the interaction between pituitary tumors and the human immune system, improve the efficacy of ICIs, and reduce irAE are the first three problems to solve. There are reasons to believe that immune checkpoints will be the next therapeutic target for pituitary tumors.

Conflicts of Interest

The authors have no conflict of interest relevant to this study.

References

- [1] S. Banskota and D. C. Adamson, "Pituitary adenomas: from diagnosis to therapeutics," *Biomedicine*, vol. 9, no. 5, 2021.
- [2] K. A. McNeill, "Epidemiology of brain tumors," *Neurologic Clinics*, vol. 34, no. 4, pp. 981–998, 2016.
- [3] M. P. Yavropoulou, M. Tsoli, K. Barkas, G. Kaltsas, and A. Grossman, "The natural history and treatment of non-functioning pituitary adenomas (non-functioning PitNETs)," *Endocrine-Related Cancer*, vol. 27, no. 10, pp. R375–r390, 2020.
- [4] A. L. Lin, M. T. A. Donoghue, S. L. Wardlaw et al., "Approach to the treatment of a patient with an aggressive pituitary tumor," *The Journal of Clinical Endocrinology & Metabolism*, vol. 105, no. 12, pp. 3807–3820, 2020.
- [5] L. S. Lamb, H. W. Sim, and A. I. McCormack, "Exploring the role of novel medical therapies for aggressive pituitary tumors: a review of the literature—"Are we there yet?," *Cancers*, vol. 12, no. 2, p. 308, 2020.
- [6] J. Trouillas, M. L. Jaffrain-Rea, A. Vasiljevic et al., "Are aggressive pituitary tumors and carcinomas two sides of the same coin? Pathologists reply to clinician's questions," *Reviews in Endocrine and Metabolic Disorders*, vol. 21, no. 2, pp. 243–251, 2020.
- [7] J. J. Havel, D. Chowell, and T. A. Chan, "The evolving landscape of biomarkers for checkpoint inhibitor immunotherapy," *Nature Reviews Cancer*, vol. 19, no. 3, pp. 133–150, 2019.
- [8] H. O. Alsaab, S. Sau, R. Alzhrani et al., "PD-1 and PD-L1 checkpoint signaling inhibition for cancer immunotherapy: mechanism, combinations, and clinical outcome," *Frontiers in Pharmacology*, vol. 8, p. 561, 2017.
- [9] S. Lyford-Pike, S. Peng, G. D. Young et al., "Evidence for a role of the PD-1:PD-L1 pathway in immune resistance of HPV-associated head and neck squamous cell carcinoma," *Cancer Research*, vol. 73, no. 6, pp. 1733–1741, 2013.
- [10] D. Nie, Q. Fang, B. Li et al., "Research advances on the immune research and prospect of immunotherapy in pituitary adenomas," *World Journal of Surgical Oncology*, vol. 19, no. 1, p. 162, 2021.
- [11] C. Dai, S. Liang, B. Sun, and J. Kang, "The progress of immunotherapy in refractory pituitary adenomas and pituitary carcinomas," *Frontiers in Endocrinology*, vol. 11, article 608422, 2020.
- [12] E. Munari, F. R. Mariotti, L. Quatrini et al., "PD-1/PD-L1 in cancer: pathophysiological, diagnostic and therapeutic aspects," *International Journal of Molecular Sciences*, vol. 22, no. 10, p. 5123, 2021.
- [13] H. Zhang, Z. Dai, W. Wu et al., "Regulatory mechanisms of immune checkpoints PD-L1 and CTLA-4 in cancer," *Journal of Experimental & Clinical Cancer Research*, vol. 40, no. 1, p. 184, 2021.
- [14] N. McGranahan, A. J. S. Furness, R. Rosenthal et al., "Clonal neoantigens elicit T cell immunoreactivity and sensitivity to immune checkpoint blockade," *Science*, vol. 351, no. 6280, pp. 1463–1469, 2016.
- [15] S. Qin, L. Xu, M. Yi, S. Yu, K. Wu, and S. Luo, "Novel immune checkpoint targets: moving beyond PD-1 and CTLA-4," *Molecular Cancer*, vol. 18, no. 1, p. 155, 2019.
- [16] L. Zhai, E. Ladomersky, A. Lenzen et al., "IDO1 in cancer: a Gemini of immune checkpoints," *Cellular & Molecular Immunology*, vol. 15, no. 5, pp. 447–457, 2018.
- [17] S. Mehdizadeh, H. Bayatipoor, S. Pashangzadeh, R. Jafarpour, Z. Shojaei, and M. Motallebnezhad, "Immune checkpoints and cancer development: therapeutic implications and future directions," *Pathology - Research and Practice*, vol. 223, article 153485, 2021.
- [18] A. Swaika, W. A. Hammond, and R. W. Joseph, "Current state of anti-PD-L1 and anti-PD-1 agents in cancer therapy," *Molecular Immunology*, vol. 67, no. 2, pp. 4–17, 2015.
- [19] S. L. Topalian, J. M. Taube, R. A. Anders, and D. M. Pardoll, "Mechanism-driven biomarkers to guide immune checkpoint blockade in cancer therapy," *Nature Reviews Cancer*, vol. 16, no. 5, pp. 275–287, 2016.
- [20] C. Steidl, S. P. Shah, B. W. Woolcock et al., "MHC class II transactivator *CIITA* is a recurrent gene fusion partner in lymphoid cancers," *Nature*, vol. 471, no. 7338, pp. 377–381, 2011.
- [21] H. Dong, S. E. Strome, D. R. Salomao et al., "Tumor-associated B7-H1 promotes T-cell apoptosis: a potential mechanism of immune evasion," *Nature Medicine*, vol. 8, no. 8, pp. 793–800, 2002.
- [22] Y. Zhang, S. Huang, D. Gong, Y. Qin, and Q. Shen, "Programmed death-1 upregulation is correlated with dysfunction of tumor-infiltrating CD8⁺ T lymphocytes in human non-small cell lung cancer," *Cellular & Molecular Immunology*, vol. 7, no. 5, pp. 389–395, 2010.
- [23] I. A. Vathiotis, G. Gomatou, D. J. Stravopodis, and N. Syrigos, "Programmed death-ligand 1 as a regulator of tumor progression and metastasis," *International Journal of Molecular Sciences*, vol. 22, no. 10, p. 5383, 2021.
- [24] L. M. Francisco, V. H. Salinas, K. E. Brown et al., "PD-L1 regulates the development, maintenance, and function of induced regulatory T cells," *Journal of Experimental Medicine*, vol. 206, no. 13, pp. 3015–3029, 2009.
- [25] A. Marchetti, A. Di Lorito, and F. Buttitta, "Why anti-PD1/PDL1 therapy is so effective? Another piece in the puzzle," *Journal of Thoracic Disease*, vol. 9, no. 12, pp. 4863–4866, 2017.
- [26] S. R. Gordon, R. L. Maute, B. W. Dulken et al., "PD-1 expression by tumour-associated macrophages inhibits phagocytosis and tumour immunity," *Nature*, vol. 545, no. 7655, pp. 495–499, 2017.
- [27] S. P. Patel and R. Kurzrock, "PD-L1 expression as a predictive biomarker in cancer immunotherapy," *Molecular Cancer Therapeutics*, vol. 14, no. 4, pp. 847–856, 2015.
- [28] Y. Mei, W. L. Bi, N. F. Greenwald et al., "Increased expression of programmed death ligand 1 (PD-L1) in human pituitary tumors," *Oncotarget*, vol. 7, no. 47, pp. 76565–76576, 2016.
- [29] P. F. Wang, T. J. Wang, Y. K. Yang et al., "The expression profile of PD-L1 and CD8⁺ lymphocyte in pituitary adenomas indicating for immunotherapy," *Journal of Neuro-Oncology*, vol. 139, no. 1, pp. 89–95, 2018.
- [30] M. Sato, R. Tamura, H. Tamura et al., "Analysis of tumor angiogenesis and immune microenvironment in non-functional pituitary endocrine tumors," *Journal of Clinical Medicine*, vol. 8, no. 5, p. 695, 2019.
- [31] W. Zhou, C. Zhang, D. Zhang et al., "Comprehensive analysis of the immunological landscape of pituitary adenomas: implications of immunotherapy for pituitary adenomas," *Journal of Neuro-Oncology*, vol. 149, no. 3, pp. 473–487, 2020.
- [32] H. R. Kemeny, A. A. Elsamadicy, S. H. Farber et al., "Targeting PD-L1 initiates effective antitumor immunity in a murine model of Cushing disease," *Clinical Cancer Research*, vol. 26, no. 5, pp. 1141–1151, 2020.

- [33] G. Zhao, W. Chen, J. He et al., "Analysis of cyclooxygenase 2, programmed cell death ligand 1, and arginase 1 expression in human pituitary adenoma," *World Neurosurgery*, vol. 144, pp. e660–e673, 2020.
- [34] J. Turchini, L. Sioson, A. Clarkson, A. Sheen, and A. J. Gill, "PD-L1 is preferentially expressed in PIT-1 positive pituitary neuroendocrine tumours," *Endocrine Pathology*, 2021.
- [35] R. Pollack, M. Kagan, R. Dresner-Pollak, and T. Neuman, "PD-L1 expression in normal endocrine tissues is not increased despite high incidence of PD-1 inhibitor-associated endocrinopathies," *Endocrine Practice*, vol. 27, no. 1, pp. 34–37, 2021.
- [36] A. L. Lin, P. Jonsson, V. Tabar et al., "Marked response of a hypermutated ACTH-secreting pituitary carcinoma to ipilimumab and nivolumab," *The Journal of Clinical Endocrinology & Metabolism*, vol. 103, no. 10, pp. 3925–3930, 2018.
- [37] B. Sol, J. M. K. de Filette, G. Awada et al., "Immune checkpoint inhibitor therapy for ACTH-secreting pituitary carcinoma: a new emerging treatment?," *European Journal of Endocrinology*, vol. 184, no. 1, pp. K1–K5, 2021.
- [38] M. Caccese, M. Barbot, F. Ceccato et al., "Rapid disease progression in patient with mismatch-repair deficiency pituitary ACTH-secreting adenoma treated with checkpoint inhibitor pembrolizumab," *Anti-Cancer Drugs*, vol. 31, no. 2, pp. 199–204, 2020.
- [39] L. S. Lamb, H. W. Sim, and A. I. McCormack, "Case report: a case of pituitary carcinoma treated with sequential dual immunotherapy and vascular endothelial growth factor inhibition therapy," *Frontiers in Endocrinology*, vol. 11, article 576027, 2020.
- [40] J. G. Egen, M. S. Kuhns, and J. P. Allison, "CTLA-4: new insights into its biological function and use in tumor immunotherapy," *Nature Immunology*, vol. 3, no. 7, pp. 611–618, 2002.
- [41] J. Foell, B. Hewes, and R. S. Mittler, "T cell costimulatory and inhibitory receptors as therapeutic targets for inducing anti-tumor immunity," *Current Cancer Drug Targets*, vol. 7, no. 1, pp. 55–70, 2007.
- [42] F. A. Harding, J. G. McArthur, J. A. Gross, D. H. Raulet, and J. P. Allison, "CD28-mediated signalling co-stimulates murine T cells and prevents induction of anergy in T-cell clones," *Nature*, vol. 356, no. 6370, pp. 607–609, 1992.
- [43] P. J. Blair, J. L. Riley, B. L. Levine et al., "CTLA-4 ligation delivers a unique signal to resting human CD4 T cells that inhibits interleukin-2 secretion but allows Bcl-X(L) induction," *The Journal of Immunology*, vol. 160, no. 1, pp. 12–15, 1998.
- [44] M. C. Brunner, C. A. Chambers, F. K. Chan, J. Hanke, A. Winoto, and J. P. Allison, "CTLA-4-mediated inhibition of early events of T cell proliferation," *The Journal of Immunology*, vol. 162, no. 10, pp. 5813–5820, 1999.
- [45] P. Caturegli, G. di Dalmazi, M. Lombardi et al., "Hypophysitis secondary to cytotoxic T-lymphocyte-associated protein 4 blockade: insights into pathogenesis from an autopsy series," *The American Journal of Pathology*, vol. 186, no. 12, pp. 3225–3235, 2016.
- [46] J. Jaafar, M. Mavromati, and J. Philippe, "Endocrinopathies induced by immune checkpoint inhibitors," *Revue Médicale Suisse*, vol. 14, no. 588–589, pp. 34–38, 2018.
- [47] J. B. Lee, S.-J. Ha, and H. R. Kim, "Clinical insights into novel immune checkpoint inhibitors," *Frontiers in Pharmacology*, vol. 12, article 681320, 681320 pages, 2021.
- [48] K. Sakuishi, L. Apetoh, J. M. Sullivan, B. R. Blazar, V. K. Kuchroo, and A. C. Anderson, "Targeting Tim-3 and PD-1 pathways to reverse T cell exhaustion and restore anti-tumor immunity," *Journal of Experimental Medicine*, vol. 207, no. 10, pp. 2187–2194, 2010.
- [49] X. Gao, Y. Zhu, G. Li et al., "TIM-3 expression characterizes regulatory T cells in tumor tissues and is associated with lung cancer progression," *PLoS One*, vol. 7, no. 2, article e30676, 2012.
- [50] L. Monney, C. A. Sabatos, J. L. Gaglia et al., "Th1-specific cell surface protein Tim-3 regulates macrophage activation and severity of an autoimmune disease," *Nature*, vol. 415, no. 6871, pp. 536–541, 2002.
- [51] L. Golden-Mason, B. E. Palmer, N. Kassam et al., "Negative immune regulator Tim-3 is overexpressed on T cells in hepatitis C virus infection and its blockade rescues dysfunctional CD4⁺ and CD8⁺ T cells," *Journal of Virology*, vol. 83, no. 18, pp. 9122–9130, 2009.
- [52] S. Han, E. Ma, W. Jiang, Y. Lu, X. Sun, and S. Feng, "Overrepresentation of highly functional T regulatory cells in patients with nonfunctioning pituitary adenoma," *Human Immunology*, vol. 81, no. 6, pp. 314–319, 2020.
- [53] S. Andrae, F. Piras, N. Burdin, and F. Triebel, "Maturation and activation of dendritic cells induced by lymphocyte activation gene-3 (CD223)," *The Journal of Immunology*, vol. 168, no. 8, pp. 3874–3880, 2002.
- [54] L. P. Andrews, A. E. Marciscano, C. G. Drake, and D. A. A. Vignali, "LAG 3 (CD 223) as a cancer immunotherapy target," *Immunological Reviews*, vol. 276, no. 1, pp. 80–96, 2017.
- [55] B. Huard, P. Prigent, M. Tournier, D. Bruniquel, and F. Triebel, "CD4/major histocompatibility complex class II interaction analyzed with CD4- and lymphocyte activation gene-3 (LAG-3)-Ig fusion proteins," *European Journal of Immunology*, vol. 25, no. 9, pp. 2718–2721, 1995.
- [56] B. Huard, M. Tournier, T. Hercend, F. Triebel, and F. Faure, "Lymphocyte-activation gene 3/major histocompatibility complex class II interaction modulates the antigenic response of CD4⁺ T lymphocytes," *European Journal of Immunology*, vol. 24, no. 12, pp. 3216–3221, 1994.
- [57] S.-R. Woo, M. E. Turnis, M. V. Goldberg et al., "Immune inhibitory molecules LAG-3 and PD-1 synergistically regulate T-cell function to promote tumoral immune escape," *Cancer Research*, vol. 72, no. 4, pp. 917–927, 2012.
- [58] F.-J. Li, Y. Zhang, G. X. Jin, L. Yao, and D. Q. Wu, "Expression of LAG-3 is coincident with the impaired effector function of HBV-specific CD8⁺ T cell in HCC patients," *Immunology Letters*, vol. 150, no. 1–2, pp. 116–122, 2013.
- [59] N. Lakhani, A. Spreafico, A. W. Tolcher et al., "1019O phase I studies of Sym021, an anti-PD-1 antibody, alone and in combination with Sym022 (anti-LAG-3) or Sym023 (anti-TIM-3)," *Annals of Oncology*, vol. 31, p. S704, 2020.
- [60] L. P. Andrews, A. E. Marciscano, C. G. Drake, and D. A. A. Vignali, "LAG3 (CD223) as a cancer immunotherapy target," *Immunological Reviews*, vol. 276, no. 1, pp. 80–96, 2017.
- [61] X. Yu, K. Harden, L. C. Gonzalez et al., "The surface protein TIGIT suppresses T cell activation by promoting the generation of mature immunoregulatory dendritic cells," *Nature Immunology*, vol. 10, no. 1, pp. 48–57, 2009.
- [62] N. Joller, E. Lozano, P. R. Burkett et al., "Treg cells expressing the coinhibitory molecule TIGIT selectively inhibit

- proinflammatory Th1 and Th17 cell responses,” *Immunity*, vol. 40, no. 4, pp. 569–581, 2014.
- [63] E. Lozano, M. Dominguez-Villar, V. Kuchroo, and D. A. Hafler, “The TIGIT/CD226 axis regulates human T cell function,” *Journal of Immunology*, vol. 188, no. 8, pp. 3869–3875, 2012.
- [64] J. M. Chauvin, O. Pagliano, J. Fourcade et al., “TIGIT and PD-1 impair tumor antigen-specific CD8⁺ T cells in melanoma patients,” *The Journal of Clinical Investigation*, vol. 125, no. 5, pp. 2046–2058, 2015.
- [65] Q. Zhang, J. Bi, X. Zheng et al., “Blockade of the checkpoint receptor TIGIT prevents NK cell exhaustion and elicits potent anti-tumor immunity,” *Nature Immunology*, vol. 19, no. 7, pp. 723–732, 2018.
- [66] P. T. Rudak, R. Gangireddy, J. Choi et al., “Stress-elicited glucocorticoid receptor signaling upregulates TIGIT in innate-like invariant T lymphocytes,” *Brain, Behavior, and Immunity*, vol. 80, pp. 793–804, 2019.
- [67] S. L. Topalian, F. S. Hodi, J. R. Brahmer et al., “Safety, activity, and immune correlates of anti-PD-1 antibody in cancer,” *The New England Journal of Medicine*, vol. 366, no. 26, pp. 2443–2454, 2012.
- [68] C. Gutierrez, C. McEvoy, D. Reynolds, and J. L. Nates, “Toxicity of immunotherapeutic agents,” *Critical Care Clinics*, vol. 37, no. 3, pp. 605–624, 2021.
- [69] A. J. Lee, K. W. Kim, Y. C. Cho et al., “Incidence of immune-mediated pseudoprogression of lymphoma treated with immune checkpoint inhibitors: systematic review and meta-analysis,” *Journal of Clinical Medicine*, vol. 10, no. 11, p. 2257, 2021.
- [70] L. Deng, H. Liang, B. Burnette et al., “Irradiation and anti-PD-L1 treatment synergistically promote antitumor immunity in mice,” *The Journal of Clinical Investigation*, vol. 124, no. 2, pp. 687–695, 2014.
- [71] X. Liu, N. Ye, S. Liu et al., “Hyperbaric oxygen boosts PD-1 antibody delivery and T cell infiltration for augmented immune responses against solid tumors,” *Advanced Science*, vol. 8, no. 15, article 2100233, 2021.
- [72] I. Melero, E. Castanon, M. Alvarez, S. Champiat, and A. Marabelle, “Intratumoural administration and tumour tissue targeting of cancer immunotherapies,” *Nature Reviews Clinical Oncology*, 2021.
- [73] K. Manaka, J. Sato, M. Takeuchi et al., “Immune checkpoint inhibitor combination therapies very frequently induce secondary adrenal insufficiency,” *Scientific Reports*, vol. 11, no. 1, pp. 11617–11617, 2021.
- [74] C. J. Smith, Y. Almodallal, and A. Jatoi, “Rare adverse events with programmed death-1 and programmed Death-Ligand 1 inhibitors: justification and rationale for a systematic review,” *Current Oncology Reports*, vol. 23, no. 8, p. 86, 2021.
- [75] R. Esposito, T. Fedele, S. Orefice et al., “An encephalitis related to cancer treatment with immune checkpoint inhibitors: systematic rnhibitors,” *Biomolecules*, vol. 11, no. 6, p. 785, 2021.
- [76] C. Criscitiello, C. Corti, G. Pravettoni, and G. Curigliano, “Managing side effects of immune checkpoint inhibitors in breast cancer,” *Critical Reviews in Oncology/Hematology*, vol. 162, article 103354, 2021.
- [77] T. Ouyang, Y. Cao, X. Kan et al., “Treatment-related serious adverse events of immune checkpoint inhibitors in clinical trials: a systematic review,” *Frontiers in Oncology*, vol. 11, article 621639, 621639 pages, 2021.
- [78] H. Zhou, N. Li, H. Tang et al., “Delayed thrombocytopenia as a rare but serious adverse event secondary to immune checkpoint inhibitor: a case report,” *Annals of Palliative Medicine*, vol. 10, no. 5, pp. 5881–5886, 2021.
- [79] V. Nersesjan, O. McWilliam, L. H. Krarup, and D. Kondziella, “Autoimmune encephalitis related to cancer treatment with immune checkpoint Inhibitors,” *Neurology*, vol. 97, no. 2, pp. e191–e202, 2021.
- [80] J. J. Wright, A. C. Powers, and D. B. Johnson, “Endocrine toxicities of immune checkpoint inhibitors,” *Nature Reviews Endocrinology*, vol. 17, no. 7, pp. 389–399, 2021.

Research Article

Plaque Length Predicts the Incidence of Microembolic Signals in Acute Anterior Circulation Stroke

Liming Zhao,^{1,2} Hongqin Zhao,³ Yicheng Xu,⁴ Aijuan Zhang,⁵ Jiatang Zhang ¹,
and Chenglin Tian ¹

¹Department of Neurology, Medical School of Chinese People's Liberation Army, Chinese People's Liberation Army General Hospital, Beijing 100039, China

²Department of Neurology, Affiliated Hospital of Weifang Medical College, Weifang 261055, China

³Department of Neurology, Affiliated Hospital of Qingdao University, Qingdao 266000, China

⁴Department of Neurology, Aerospace Center Hospital, Beijing 100049, China

⁵Department of Neurology, Weifang People's Hospital, Weifang 261021, China

Correspondence should be addressed to Jiatang Zhang; zhangjt1128@sina.com and Chenglin Tian; tianchenglin2020@163.com

Received 5 June 2021; Revised 5 July 2021; Accepted 11 July 2021; Published 29 July 2021

Academic Editor: Xianwei Zeng

Copyright © 2021 Liming Zhao et al. This is an open access article distributed under the Creative Commons Attribution License, which permits unrestricted use, distribution, and reproduction in any medium, provided the original work is properly cited.

Microembolic signals (MES) of the carotid artery are associated with plaque destabilization and recurrence of stroke. Previous studies have focused primarily on the degree of carotid artery stenosis and plaque components, and the relationship between plaque length and microembolic sign has received little attention. We aimed to find the association between carotid plaque length (CPL) and the presence of MES. We conducted a retrospective observational cross-sectional study. A total of 84 acute anterior-circulation ischemic stroke/transient ischemic attack (TIA) patients with carotid artery atherosclerosis were classified into an MES-positive (MES+) group and MES-negative (MES-) group. We measured multiple parameters of carotid plaque size (length, thickness) in each patient and evaluated the relationship between different plaque parameters and occurrence of MES. We found that male, carotid artery stenosis (CAS), CPL, carotid plaque thickness (CPT), and intima-media thickness (IMT) of the carotid artery were each significantly different between two groups (all $P < 0.05$). The multivariate analysis showed CPL (odds ratio (OR), 1.109; 95% CI, 1.044–1.177; $P = 0.001$) to be independently associated with the presence of MES. The areas under the ROC curves (AUCs) for CPL for predicting MES were 0.777 (95% CI, 0.640–0.914; $P < 0.001$). The cutoff value of CPL for predicting MES was 16.7 mm, with a sensitivity of 88.2% and a specificity of 77.6%. We found that CPL was a meaningful independent predictor of MES. Therefore, CPL may be useful for risk stratification of long and nonstenotic plaques in anterior circulation stroke.

1. Introduction

Microembolic signals (MES) of the cerebral artery are associated with plaque destabilization and predict the occurrence of stroke [1–5]. Furthermore, MES can cause recessionary cognition [6]. Detection of MES may provide a diagnostic stratification in patients with asymptomatic carotid stenosis and aid in optimizing therapies for such patients [1], as well as serve as a tool for elucidating the mechanisms of stroke and evaluating efficacies of antiplatelet therapies [2, 5, 7].

Hence, MES should be widely used in observational and interventional studies [7, 8].

A previous study [9] found that carotid plaque thickness (CPT) > 3 mm may be a source of thromboembolic stroke. Another study shows CPT > 3 mm failed to be significantly different with ipsilateral embolic stroke of undetermined source [10]. Growth of plaque length of carotid artery is faster than their corresponding thicknesses [11]. Thus, plaque length may be an underestimated indicator of carotid artery atherosclerosis. Only a few studies focus on the search of

CPL [12, 13]. Therefore, the relationship between lengths of plaques of the carotid artery and MES requires further investigation. Importantly, assessment of the lengths of carotid plaques may be useful for discerning high-risk plaques. The purpose of our study was to discover the relationship between CPL and MES.

2. Materials and Methods

2.1. Patients and Study Design. This was a retrospective observational cross-sectional study. We investigated the relationship between CPL and MES lasting 60 min during Transcranial Doppler (TCD) monitoring within 72 h after the onset of acute stroke. Consecutive patients with acute anterior-circulation ischemic stroke or transient ischemic attack (TIA), admitted to the Department of Neurology at Weifang Brain Hospital, were enrolled in the present study from January 2015 through October 2019. Stroke was diagnosed based on imaging characteristics obtained via magnetic resonance imaging (MRI) and neurological deficits lasting for more than 24 h. TIA was defined based on the criteria of the American Heart Association/American Stroke Association (AHA/ASA) [14]. CAS was diagnosed based on ultrasound examination. Our study was approved by Changyi People's Hospital Ethics Committee. The approval no. of the Ethics Committee was CYRM20171014. Our study was a retrospective observational study. Patient informed consent for inclusion in this study was waived. The patients' general data, relevant medical history, treatments, and laboratory examinations were evaluated and recorded by a neurologist.

Exclusion criteria for candidate patients were as follows: (1) <40 years old, (2) carotid artery occlusion or middle cerebral artery occlusion, (3) the absence of a temporal acoustic window for TCD monitoring, (4) bilateral anterior infarctions and/or anterior- and posterior-circulation infarctions, (5) cardioembolic stroke or strokes with other etiologies, (6) severe nephritis or liver disease or definitive or suspected cancer, (7) no enduring MES for 60 min during TCD monitoring, and (8) a history of carotid endarterectomy or a carotid artery stent.

2.2. Assessment of CAS via Ultrasonography. Ultrasound examination was conducted by two skilled doctors. The carotid artery stenosis (CAS) was defined by criteria of ECST (arrange 50% to 99%) (16). Other ultrasonic parameters [15] that we assessed were as follows: (1) CPL was defined as the maximum length of all ipsilateral carotid artery plaques [13]; (2) CPT was defined as the maximal thickness of all plaques within ipsilateral carotid arteries; (3) resistance index (RI) was defined by the Mannheim Carotid IMT Consensus, and IMT was assessed at the thickness of segments without plaques and was measured in the far wall of the common carotid artery at approximately 10 mm proximal to the carotid artery bifurcation, as previously described [16]; (4) plaques of ipsilateral carotid arteries were categorized as either predominantly echolucent, predominantly echogenic, or as mixed echolucent/echogenic; and (5) ulcerative plaques were defined by common criteria in ultrasonography [17], including plaque surface craters measuring 2×2 mm or those

with concavity with an echogenic line at the plaque base. Timing of ultrasound examination was not limited, and most of the patients were detected within 3 days after stroke.

2.3. Assessment of MES via TCD Monitoring. MES were detected via TCD monitoring (Delica EMS-9A); for this purpose, skilled technicians fixed a 2 MHz probe to the patients head frame and monitored occurrence of MES in the initial and distal segments of the symptomatic middle cerebral artery for 1 hour. All patients were detected within 3 days after stroke/TIA. Distances ≥ 6 mm between two points were applicable for MES monitoring. Typically, the middle cerebral artery was monitored at depths between 50 and 65 mm. The sample volume based on a nearly 8 mm vessel length, combined with a relative low gain, was used to distinguish emboli signals from background noise. The skilled technicians identified the presence of MES as unidirectional, short duration signals (less than 0.3 s) with intensity threshold above 3 dB, accompanied by "chirping" sound and occurring randomly throughout the cardiac cycle, as previously described [18].

2.4. Statistical Analysis. The SPSS 22.0 software package (Chicago, IL, USA) was utilized for data analysis. Quantitative data are expressed as the mean \pm standard deviation, while qualitative data are expressed as frequencies and percentages. After testing for normality, quantitative data were compared between two groups by *t*-tests, and qualitative or categorical data were compared by χ^2 tests or Fisher's exact tests.

Statistically significant factors ($P < 0.05$) in univariate analyses were entered into stepwise forward logistic regression analysis to identify the independent factors for MES. Odds ratios (ORs) and their 95% CIs were used to evaluate the independent contributions of significant factors. The Hosmer-Lemeshow test was used to estimate the appropriateness of the model.

We measured the correlations between CPT and CPL by calculating Pearson correlation coefficients.

Receiver operating characteristic (ROC) curves were obtained to determine the optimal cutoff values for the independent risk factors, as well as their sensitivities, specificities, and areas under the ROC curves (AUCs). $P < 0.05$ was reckoned statistically significant.

3. Results

3.1. Baseline Demographics. During the study period, 596 consecutive patients with acute stroke/TIA were potentially eligible for our study. After removing patients that fit the exclusion criteria, a total of 84 anterior-circulation ischemic stroke/TIA patients were enrolled in our present study (Figure 1). These patients' demographic and clinical features are presented in Table 1. The mean age was 62.05 ± 9.29 years. There were 55 (65.5%) males. MES occurred in 17 out of 84 cases. There were no significant differences between MES+ and MES- patients in terms of age or the presence of hypertension, diabetes mellitus, ischemic heart disease, smoking, or drinking. However, the percentage of males in the MES+ group was significantly higher than that in the

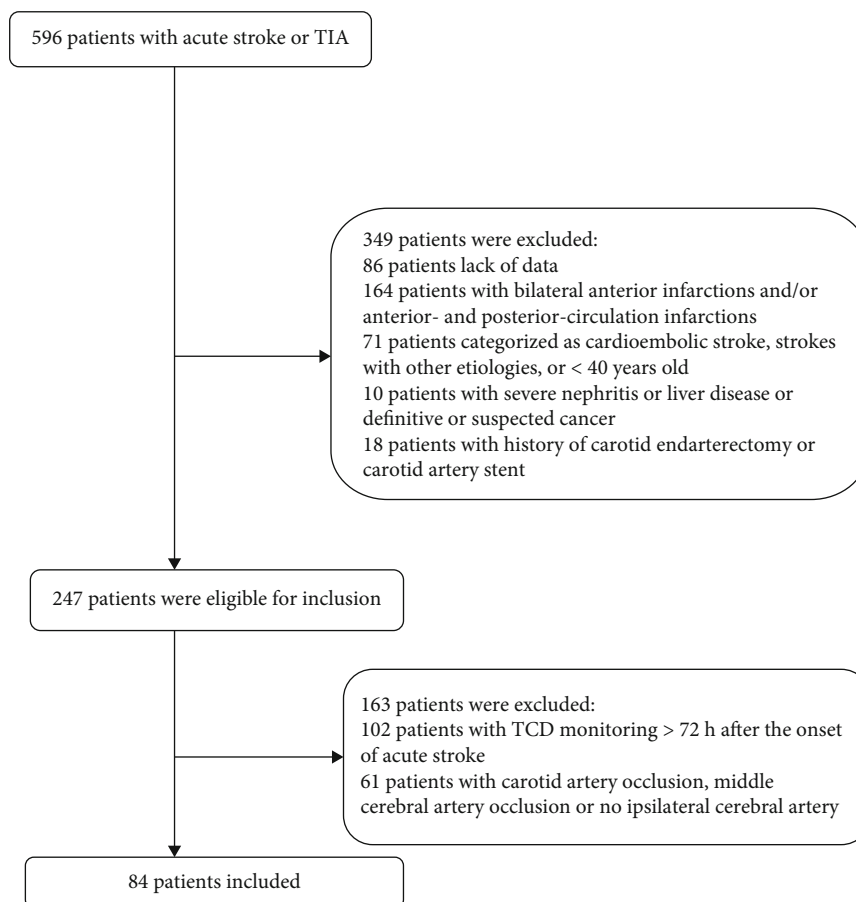


FIGURE 1: Flowchart of the patients included in the present study.

TABLE 1: Baseline demographics.

	MES+ (n = 17)	MES- (n = 67)	T/ χ^2	P
Age (years)	62.53 ± 4.75	61.93 ± 10.15	0.357	0.722
Gender (male/female)	15 (86.7%)	40 (59.7%)	4.884	0.027
Hypertension	13 (76.5%)	56 (83.6%)	0.108	0.742
Diabetes mellitus	6 (35.3%)	11 (16.4%)	1.938	0.164
CAD	4 (23.5%)	13 (19.4%)	1.317	0.251
History of stroke or TIA	4 (23.5%)	11 (16.4%)	0.108	0.742
Smoking	8 (47.1%)	19 (22.4%)	2.056	0.152
Drinking	6 (35.3%)	19 (28.4%)	0.312	0.576
TC (mmol/L)	4.25 ± 0.71	4.57 ± 1.08	-1.178	0.242
TG (mmol/L)	1.69 ± 1.00	1.82 ± 0.86	-0.684	0.496
LDL (mmol/L)	2.15 ± 0.61	2.42 ± 0.95	-1.128	0.263
HDL (mmol/L)	1.29 ± 0.512	1.24 ± 0.647	0.122	0.903
Cr (μ mol/L)	62.59 ± 13.72	63.49 ± 13.56	0.258	0.797
BUN (mmol/L)	5.34 ± 1.42	5.10 ± 1.66	0.568	0.572
Clopidogrel plus aspirin	3 (17.6%)	24 (35.8%)	2.056	0.152

BUN: blood urea nitrogen; CAD: coronary artery disease; Cr: creatinine; HDL: high-density lipoprotein; LDL: low-density lipoprotein; MES: microembolic signals; TC: total cholesterol; TG: triglycerides; TIA: transient ischemic attack.

TABLE 2: Plaque ultrasound characteristics within the ipsilateral carotid artery.

	MES+ ($n = 17$)	MES- ($n = 67$)	T/χ^2	P
IMT	0.960 ± 0.112	0.848 ± 0.152	2.073	0.041
RI	0.768 ± 0.055	0.762 ± 0.054	0.377	0.707
Plaque ulceration	2/17	1/67	3.046	0.110
CAS	9/17	14/67	5.302	0.021
CPL (mm)	23.10 ± 9.18	12.99 ± 8.87	4.167	<0.001
CPT (mm)	2.750 ± 1.135	1.953 ± 750	2.320	0.031
<i>Plaque echo</i>				
Echolucent	27/57	51/125	1.426	0.490
Mixed echolucent/echogenic	28/57	65/125		
Echogenic	2/57	9/125		

CAS: carotid artery stenosis; CPL: carotid plaque length; CPT: carotid plaque thickness; IMT: intima-media thickness; MES: microembolic signals; RI: resistance index.

MES- group. Finally, laboratory parameters—including total cholesterol (TC), triglycerides (TG), low-density lipoprotein (LDL), high-density lipoprotein (HDL), creatinine (Cr), and blood urea nitrogen (BUN) levels—were not significantly different between the MES+ group and MES- group ($P > 0.05$).

3.2. Characterization of Carotid Plaques. The patients' ultrasound characteristics are listed in Table 2. CAS, CPL, CPT, and IMT of the carotid artery were each significantly different between the MES+ group and the MES- group (all $P < 0.05$). In contrast, there was no significant difference in the RI between the MES+ group and the MES- group ($P = 0.707$).

We found that the percentage of plaque echolucency was not significantly different between the MES+ group and the MES- group (47.4% vs. 40.8%, respectively).

3.3. Multiple Collinear Analysis of Independent Variables and Multivariable Analysis. Variance inflation factors (VIF) of CAS, CPL, CPT, and IMT were less than 5. Multicollinearity was considered nonexistent.

Gender was adjusted because there was a statistically significant difference between male and female. CAS, CPL, CPT, and IMT were entered into logistic regression analysis. Multivariable analysis showed that CPL (OR: 1.109; 95% CI: 1.044–1.177; $P = 0.001$; B : 0.103; S.E.: 0.031) was an independent risk factor for MES. Factors including gender, CAS, CPT, and IMT were not in the equation. The P value of the Hosmer-Lemeshow test was 0.213.

3.4. Correlational Analysis between CPL and CPT. The correlation between CPL and CPT was $R^2 = 0.539$ and $P < 0.01$, and this correlation was moderate level.

3.5. AUC for CPL for Predicting MES. The AUC for CPL for predicting MES was 0.777 (95% CI, 0.640–0.914; $P < 0.001$) (Figure 2). The optimal cutoff value of CPL for predicting MES was 16.7 mm, with a sensitivity of 88.2%, specificity of 77.6%, positive predictive value of 88.2%, and negative predictive value of 77.6%.

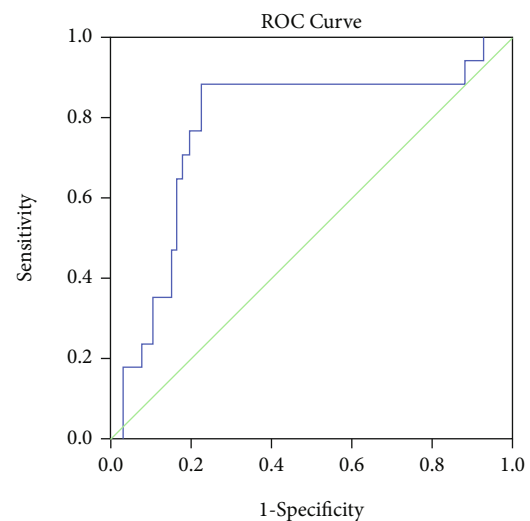


FIGURE 2: Points along the diagonal dotted line represent an AUC of 0.5. The AUCs for CPL of carotid arteries for predicting MES were 0.777 (95% CI, 0.640–0.914; $P < 0.001$). AUCs: areas under the ROC curves; CPL: carotid plaque length; MES: microembolic signals.

4. Discussion

The present study evaluated the predictive value of CPL for MES in patients with acute anterior-circulation ischemic stroke/TIA. Vulnerable plaque characteristics such as intra-plaque hemorrhages, plaque ulcerations, and thinned or disrupted fibrous caps can be clearly identified by high-resolution magnetic resonance imaging (MRI) or PET-CT [19]. However, due to their relatively low occurrences, costliness, and difficulty to quantify, these specific plaque characteristics have not been widely adopted clinically and may be far from ideal markers of MES [19]. Alternatively, CPL is noninvasive, cost-effective, and easily quantified and may thus be sufficient for predicting MES [13].

In the current study, conventional stroke-related risks such as hypertension, diabetes mellitus, coronary artery disease (CAD), smoking history, and drinking history were

not significantly different between the MES+ group and the MES- group. These findings are consistent with those of a previous study [4, 20, 21]. We found that the percentage of males in the MES+ group was significantly higher than that in the MES- group. Related to this finding, a previous study has noted that males have a higher smoking rate, drinking rate, and other increased risk factors compared to those of females in China [18]. Our study and previous studies all found that there were no significant differences about plasma lipid level (TC, TG, LDL, or HDL), Cr, and BUN between the two groups [20]. Previous studies also deem that dual antiplatelet therapy can reduce MES more effectively than single antiplatelet therapy [2, 4]. In our study, dual antiplatelet therapy in the MES- group was nearly two times more frequent than in the MES+ group (35.8% vs. 17.6%, respectively) despite the lack of any statistically significant difference, which may be due to the limited sample size.

In the present study, CAS, CPL, CPT, and IMT were significantly different between the MES+ group and the MES- group. Most of the studies suggested that MES was associated with symptomatic carotid stenosis [5, 22]. However, some studies showed MES had no relationship with symptomatic CAS [23]. IMT is traditionally considered an important arteriosclerosis factor for stroke and its recurrence [21]. Our present study found that IMT was also associated with MES. Only three cases with ulcerative plaques were found in our data, due to rigorous criteria of ulcerative plaques requiring a concavity greater than 2×2 mm. In a Chinese study, the proportion of ulcerative plaque was only 8% in 287 patients with moderate internal CAS [24]. Another carotid plaque morphology research also deems the prevalence of ulcerative was fairly low [23], just like our research. These findings suggest that ulcerative plaques (greater than 2×2 mm) may not represent a sensitive parameter for predicting MES. Echolucent plaques have been commonly suggested responsible for the presence of MES. Our research showed that the percentage of echolucent plaques was not different between the two groups. Part of the reason may be that plaque morphology will change after stroke or releasing MES.

Logistic regression analysis supported that CPL was independently associated with the occurrence of MES, while CAS, CPT, and IMT were not independent factors for MES in acute anterior stroke. Part of the reason may be due to the limited sample size. The cutoff value of CPL for predicting MES was 16.7 mm. Carotid artery plaques increase in length much faster than in thickness and have a large dynamic scope [11]. In conclusion, CPL may be a meaningful independent sensitive predictor for MES. The relationship between CPL and MES has rarely been reported previously. A recent article reported that plasma osteoprotegerin levels (an inflammatory biomarker) was predictive of MES [20] and that the corresponding AUC (0.734) was also effective; however, laboratory testing for osteoprotegerin levels is not exactly practical compared with CPL in most Chinese hospitals. CPL belongs to plaque morphology parameter and osteoprotegerin level reflects unstable plaque inflammation. Another recent study [13] reported that CPL is an independent indicator of the severity of CAD, and our study showed that

CPL would be a useful tool to evaluate high-risk recurrence of stroke instead of CPT and IMT. There were only a few literatures on carotid plaque length. To our knowledge, our study is the first to discover the relationship between CPL and MES. Our research showed that CPL has a correlation with CPT. This relationship needs future exploration.

CPL which is convenient to measure by ultrasound could make up for the limitation of MES. TCD monitoring requires special equipment as well as skilled technicians, and its clinical applications have been limited. Some older people have unilateral or bilateral poor temporal windows and are unable to endure a 1-hour MES monitoring session [20].

CPL may be beneficial for rethinking etiological classifications of stroke via large and nonstenotic plaques. It has been increasingly recognized that there are limitations in Trial of Org10172 in Acute Stroke Treatment (TOAST) classifications, especially in Asian countries with higher rates of LAA (Large Artery Atherosclerosis) [25–28]. For example, the percentage of “undermined stroke” via TOAST classifications is much higher than that of other etiologic stroke classifications [26, 29]. For instance, large and nonstenotic plaques are classified as “undermined stroke” or small-vessel-disease subgroups via TOAST classifications. The total plaque area (TPA ≥ 1.19 mm²) is a criterion for indicating nonstenotic LAA stroke with a heavy plaque burden in SPARKLE [30]. Nevertheless, measurement of total plaque area (TPA) is also time-consuming and consequently difficult to be used widely in clinical practice compared with CPL. Our study showed that CPL was a valuable independent marker for the presence of MES, and this result means measuring of CPL would identify the nonstenotic carotid with high risk.

The present study had some limitations. First, the sample sizes were relatively small. Because of our limited sample sizes, a few traditional risk factors failed to meet the criteria for independent risk factors of binary regressions. Therefore, future studies with larger sample sizes and other measurement instruments are needed to confirm or refute our present findings. Second, the MES monitoring that we employed had limitations. Since we only conducted MES monitoring for 1 h, this monitoring time may not have been long enough and may have led to false-negative errors. Finally, since this was a retrospective cross-sectional study, our findings need to be validated by prospective cohort studies in the future.

5. Conclusions

Our present findings suggest that ultrasound CPL was a dependent parameter and meaningful predictor for MES, thus suggesting that high CPL may discern the high-risk plaque undermined stroke and small-vessel-disease with high recurrence. CPL may be widely implemented in clinical practice and research.

Data Availability

The data that support this study are available from the responding author upon reasonable request.

Conflicts of Interest

The authors declare that there is no conflict of interest regarding the publication of this paper.

Authors' Contributions

LZ conceived the study, participated in the design, collected the data, performed statistical analyses, and drafted the first manuscript. AZ participated in the design and collected the data. HZ participated in the design and drafted the first manuscript. YX performed statistical analyses and helped to draft the manuscript. JZ and CT performed statistical analyses and helped to revise.

Acknowledgments

We thank LetPub (<http://www.letpub.com>) for its linguistic assistance and scientific consultation during the preparation of this manuscript. Thanks are due to Mingyi Hu, Xiaohua Mu, Yingying Shan, and Honghai Wang for their work on TCD microemboli monitoring. Thanks are due to Jinhua Xia and Song Qiu for their work on carotid ultrasound monitoring. Thanks are due to Dr. Xiaochen Liu for his guidance and advice on data processing.

References

- [1] H. S. Markus, A. King, M. Shipley et al., "Asymptomatic embolisation for prediction of stroke in the Asymptomatic Carotid Emboli Study (ACES): a prospective observational study," *The Lancet Neurology*, vol. 9, no. 7, pp. 663–671, 2010.
- [2] K. S. L. Wong, C. Chen, J. Fu et al., "Clopidogrel plus aspirin versus aspirin alone for reducing embolisation in patients with acute symptomatic cerebral or carotid artery stenosis (CLAIR study): a randomised, open-label, blinded-endpoint trial," *The Lancet Neurology*, vol. 9, no. 5, pp. 489–497, 2010.
- [3] R. Topakian, A. King, S. U. Kwon et al., "Ultrasonic plaque echolucency and emboli signals predict stroke in asymptomatic carotid stenosis," *Neurology*, vol. 77, no. 8, pp. 751–758, 2011.
- [4] J. Jiang, Y. Jiang, S. Feng et al., "Microembolic signal monitoring of TOAST-classified cerebral infarction patients," *Molecular Medicine Reports*, vol. 8, no. 4, pp. 1135–1142, 2013.
- [5] A. King and H. S. Markus, "Doppler embolic signals in cerebrovascular disease and prediction of stroke risk," *Stroke*, vol. 40, no. 12, pp. 3711–3717, 2009.
- [6] I. Goldberg, E. Auriel, D. Russell, and A. D. Korczyn, "Microembolism, silent brain infarcts and dementia," *Journal of the Neurological Sciences*, vol. 322, no. 1–2, pp. 250–253, 2012.
- [7] H. S. Markus, D. W. Droste, M. Kaps et al., "Dual antiplatelet therapy with clopidogrel and aspirin in symptomatic carotid stenosis evaluated using doppler embolic signal detection: the Clopidogrel and Aspirin for Reduction of Emboli in Symptomatic Carotid Stenosis (CARESS) trial," *Circulation*, vol. 111, no. 17, pp. 2233–2240, 2005.
- [8] J. D. Spence, "Transcranial Doppler emboli identifies asymptomatic carotid patients at high stroke risk: why this technique should be used more widely," *Angiology*, vol. 68, no. 8, pp. 657–660, 2017.
- [9] J. M. Coutinho, S. Derkatch, A. R. J. Potvin et al., "Nonstenotic carotid plaque on CT angiography in patients with cryptogenic stroke," *Neurology*, vol. 87, no. 7, pp. 665–672, 2016.
- [10] J. M. Ospel, N. Singh, M. Marko et al., "Prevalence of ipsilateral nonstenotic carotid plaques on computed tomography angiography in embolic stroke of undetermined source," *Stroke*, vol. 51, no. 6, pp. 1743–1749, 2020.
- [11] J. D. Spence and R. A. Hegele, "Non-invasive assessment of atherosclerosis risk," *Current Drug Target -Cardiovascular & Hematological Disorders*, vol. 4, no. 2, pp. 125–128, 2004.
- [12] A. M. Elhfnawy, P. U. Heuschmann, M. Pham, J. Volkman, and F. Fluri, "Stenosis length and degree interact with the risk of cerebrovascular events related to internal carotid artery stenosis," *Frontiers in Neurology*, vol. 10, p. 317, 2019.
- [13] W. Tang, X. Shen, H. Li et al., "The independent and incremental value of ultrasound carotid plaque length to predict the presence and severity of coronary artery disease: analysis from the carotid plaque length prospective registry," *European Heart Journal-Cardiovascular Imaging*, vol. 21, no. 4, pp. 389–396, 2020.
- [14] W. N. Kernan, B. Ovbiagele, H. R. Black et al., "Guidelines for the prevention of stroke in patients with stroke and transient ischemic attack: a guideline for healthcare professionals from the American Heart Association/American Stroke Association," *Stroke*, vol. 45, no. 7, pp. 2160–2236, 2014.
- [15] W. Brinjikji, A. A. Rabinstein, G. Lanzino et al., "Ultrasound characteristics of symptomatic carotid plaques: a systematic review and meta-analysis," *Cerebrovascular Diseases*, vol. 40, no. 3–4, pp. 165–174, 2015.
- [16] P. J. Touboul, M. G. Hennerici, S. Meairs et al., "Mannheim carotid intima-media thickness consensus (2004–2006). An update on behalf of the Advisory Board of the 3rd and 4th Watching the Risk Symposium, 13th and 15th European Stroke Conferences, Mannheim, Germany, 2004, and Brussels, Belgium, 2006," *Cerebrovascular Diseases*, vol. 23, no. 1, pp. 75–80, 2007.
- [17] M. Muraki, T. Mikami, T. Yoshimoto et al., "New criteria for the sonographic diagnosis of a plaque ulcer in the extracranial carotid artery," *American Journal of Roentgenology*, vol. 198, no. 5, pp. 1161–1166, 2012.
- [18] X. Wu, H. Zhang, H. Liu, Y. Xing, and K. Liu, "Microembolic signals detected with transcranial Doppler sonography differ between symptomatic and asymptomatic middle cerebral artery stenoses in Northeast China," *PLoS One*, vol. 9, no. 2, article e88986, 2014.
- [19] H. F. G. Müller, A. Viaccoz, L. Fisch et al., "18FDG-PET-CT: an imaging biomarker of high-risk carotid plaques. Correlation to symptoms and microembolic signals," *Stroke*, vol. 45, no. 12, pp. 3561–3566, 2014.
- [20] Y. Cao, C. Cui, H. Zhao et al., "Plasma osteoprotegerin correlates with stroke severity and the occurrence of microembolic signals in patients with acute ischemic stroke," *Disease Markers*, vol. 2019, Article ID 3090364, 7 pages, 2019.
- [21] E. Higuchi, S. Toi, Y. Shirai et al., "Prevalence of microembolic signals in embolic stroke of undetermined source and other subtypes of ischemic stroke," *Stroke*, vol. 51, no. 2, pp. 655–658, 2020.
- [22] E. V. Zuilen, J. Van Gijn, and R. G. A. Ackerstaff, "The clinical relevance of cerebral microemboli detection by transcranial Doppler ultrasound," *Journal of Neuroimaging*, vol. 8, no. 1, pp. 32–37, 1998.

- [23] I. Mayor, M. Comelli, E. Vassileva, P. Burkhard, and R. Sztajzel, "Microembolic signals and carotid plaque morphology: a study of 71 patients with moderate or high grade carotid stenosis," *Acta Neurologica Scandinavica*, vol. 108, no. 2, pp. 114–117, 2003.
- [24] Y. Liu, Y. Hua, R. Liu et al., "Ultrasonographical features associated with progression of atherosclerosis in patients with moderate internal carotid artery stenosis," *Translational Stroke Research*, vol. 9, no. 4, pp. 375–381, 2018.
- [25] B. J. Kim and J. S. Kim, "Ischemic stroke subtype classification: an Asian viewpoint," *Journal of Stroke*, vol. 16, no. 1, pp. 8–17, 2014.
- [26] H. Zhang, Z. Li, Y. Dai, E. Guo, C. Zhang, and Y. Wang, "Ischaemic stroke etiological classification system: the agreement analysis of CISS, SPARKLE and TOAST," *Stroke and Vascular Neurology*, vol. 4, no. 3, pp. 123–128, 2019.
- [27] S. Gao, Y. J. Wang, A. D. Xu, Y. S. Li, and D. Z. Wang, "Chinese ischemic stroke subclassification," *Frontiers in Neurology*, vol. 2, p. 6, 2011.
- [28] B. H. Chao, F. Yan, Y. Hua et al., "Stroke prevention and control system in China: CSPPC-Stroke Program," *International Journal of Stroke*, vol. 16, no. 3, pp. 265–272, 2021.
- [29] E. M. Arsava, J. Helenius, R. Avery et al., "Assessment of the predictive validity of etiologic stroke classification," *JAMA Neurology*, vol. 74, no. 4, pp. 419–426, 2017.
- [30] C. Bogiatzi, T. Wannarong, A. I. McLeod, M. Heisel, D. Hackam, and J. D. Spence, "SPARKLE (Subtypes of Ischaemic Stroke Classification System), incorporating measurement of carotid plaque burden: a new validated tool for the classification of ischemic stroke subtypes," *Neuroepidemiology*, vol. 42, no. 4, pp. 243–251, 2014.

Research Article

The Prognostic Determinant of Interleukin-10 in Patients with Acute Ischemic Stroke: An Analysis from the Perspective of Disease Management

Wen Sun ¹, Shuhui Wang ², and Shanji Nan ³

¹School of Public Health, Weifang Medical University, Weifang, China

²Department of Clinical Laboratory, Qingdao Central Hospital, Qingdao, China

³Department of Neurology, Second Hospital of Jilin University, Changchun, China

Correspondence should be addressed to Shanji Nan; nansj@jlu.edu.cn

Received 22 June 2021; Revised 2 July 2021; Accepted 10 July 2021; Published 19 July 2021

Academic Editor: Wen-Jun Tu

Copyright © 2021 Wen Sun et al. This is an open access article distributed under the Creative Commons Attribution License, which permits unrestricted use, distribution, and reproduction in any medium, provided the original work is properly cited.

Background. In patients with ischemic stroke, the role of anti-inflammatory cytokine Interleukin-10 (IL-10) in predicting risk and outcomes is not very clear. This study is aimed at prospectively assessing the prognostic determinant value of IL-10 in patients with acute ischemic stroke in a cohort of Chinese people. **Methods.** In a prospective cohort study, consecutive first-ever patients with acute ischemic stroke admitted to our hospital were included from October 2019 to October 2020. The serum level of IL-10 was measured at baseline. A structured follow-up telephone interview was performed on day 90 after admission. Logistic regression analyses were used to assess the prognostic value of IL-10 to predict the poor functional outcome (defined as a modified Rankin Scale score of 3 to 6) and mortality. **Results.** The median age of the 236 enrolled patients was 65 years (interquartile range (IQR), 56-76), and 57.6% were male. There was a negative correlation between the National Institutes of Health Stroke Scale (NIHSS) score and IL-10 serum levels (r (Spearman) = -0.221, P = 0.001). Patients with elevated IL-10 levels (> the highest quartile = 5.24 pg/mL; n = 79) were at significantly lower risk of poor functional outcomes (odds ratio (OR), 0.35; 95% confidence interval (CI), 0.19 to 0.63; P < 0.001) and mortality (OR = 0.24; 95% CI = 0.11–0.52; P < 0.001) compared with patients with IL-10 levels in the lowest three quartiles. **Conclusions.** Reduced serum levels of IL-10 were independently associated with both the clinical severity at admission and a poor functional prognosis in ischemic stroke patients, suggesting that the anti-inflammatory cytokine IL-10 was an important prognostic determinant.

1. Introduction

Acute ischemic stroke is one of the main causes of death and the leading cause of disability in adults worldwide [1, 2]. In China, ischemic stroke is a common disorder with almost 2 million new or recurrent events per year [3], and one study indicated annual estimates of 11 million prevalent cases of stroke in 2013 [4]. Stroke leads to the highest disability-adjusted life-year loss of any disease in China [3]. In the past ten years, China has made outstanding achievements in stroke prevention and control [5]. However, with the increase of population aging and the poor management of

chronic risk factors, future stroke prevention and treatment work still face challenges [3].

Inflammation and oxidative stress pathways are the pathophysiological mechanisms involved during ischemic stroke [6]. Global brain inflammation after a stroke might continuously affect the patients' long-term functional outcomes [7]. Inflammation is a double-edged sword at particular stages after a stroke, which could be both detrimental and beneficial [8]. Various proinflammatory and anti-inflammatory responses after ischemic stroke are potential therapeutic strategies [9]. The mechanisms between systemic inflammation and poor stroke outcome had been proposed [10].

Elevated blood levels of inflammatory cytokines such as C-reactive protein (CRP) [11], Interleukin-6 (IL-6) [12, 13], IL-18 [14], IL-12 [15], tumor necrosis factor- α [16], and C-C chemokine ligand 2 (CCL-2) [17] were associated with poor outcome and increased mortality after stroke. Anti-inflammatory cytokines could inhibit the proinflammatory cytokine production and might be used for stroke treatment. Vila et al. [18] showed that a reduced level of IL-10 (an anti-inflammatory cytokine) was associated with neurological worsening in acute ischemic stroke. Similarly, another study also reported that reduced IL-10 concentrations were associated with a degree of neurological deficit and poor stroke outcome [19]. Interestingly, not all the literature conclusions are very consistent. One study showed that higher IL-10 levels were associated with poor outcomes in female patients with ischemic stroke [20], while another study reported that more elevated serum IL-10 was an independent prognosticator of ischemic stroke outcome [21]. In addition, the prognostic value of IL-10 in ischemic stroke patients in another study was not confirmed [22].

The prognostic value of IL-10 in patients after acute ischemic stroke is not well documented. Further research is recommended to explain and unify these differences. Thus, this study is aimed at prospectively assessing the prognostic determinant value of anti-inflammatory cytokine IL-10 in patients with acute ischemic stroke in a cohort of Chinese people.

2. Subjects and Methods

2.1. Patients and Study Design. A single-center prospective cohort study was performed from October 1, 2019, to October 30, 2020. All patients with acute ischemic stroke diagnosed as the first onset were consecutively enrolled in our hospital during this period. The enrolled patients also needed to meet the following criteria: the diagnosis met the criteria of the World Health Organization [23] and was confirmed by Magnetic Resonance Imaging (MRI), with symptom onset within 3 days. Patients with (1) cerebral hemorrhage, (2) malignant tumor, (3) renal insufficiency, (4) surgery or trauma < 3 months, and (5) autoimmune diseases would be excluded. In addition, those patients without informed consent or fasting blood samples also would be excluded.

2.2. Clinical Variables. Within 24 hours of hospitalization, we collect primary patient data, including sex, age, residence (urban and rural), ethnicity, education, and marital status, medical insurance information, vascular risk factors (smoking status (nonsmokers, past smokers, and current smokers), consumption of alcohol, family history of stroke, history of transient ischemic attack (TIA), hypertension, diabetes, hyperlipidemia, and atrial fibrillation), therapies before admission (antihypertensive, hypoglycemic, anticoagulant, and statins), and acute treatment (IV thrombolysis and/or mechanical thrombectomy). We also record the following measurement information: height and weight (body mass index (BMI) was calculated based on height and weight, and $\text{BMI} \geq 28 \text{ kg/m}^2$ was defined as obesity), arterial pressure (systolic and diastolic), body temperature, stroke severity at

admission (assessed by the National Institutes of Health Stroke Scale (NIHSS) score (0-42, the higher the score, the more serious the disease)) [24], and lesion size (brain MRI was performed within 48 hours after admission to verify the stroke diagnosis; the infarct volume was calculated by using the formula $0.5 \times a \times b \times c$ according to the diffusion-weighted imaging (DWI) sequences) [25]. Trial of ORG 10172 in Acute Stroke Treatment (TOAST) classification was used to classified ischemic strokes, which distinguishes large-vessel occlusive, small-vessel occlusive, cardioembolic, other, and unknown subtypes [26].

2.2.1. Blood Sampling and Follow-Up. Fasting serum samples were routinely collected within the first 24 h after admission. Those samples were stored at -80°C before being tested for biomarkers. At discharge, length, cost, and treatment information during hospitalization were recorded. A structured follow-up telephone interview with the patient or the closest relative was performed on day 90 after admission. The patient's survival information was recorded. The functional outcome of surviving patients was assessed by the modified Rankin Scale (mRS) score [27], blinded to clinical data and laboratory tests. Patients were classified according to the mRS scores: poor functional outcome (defined as an mRS score of 3 to 6 points) and good outcome (defined as an mRS score of 0 to 2 points) [28].

2.3. Laboratory Testing. The measurement of the serum level of IL-10 was performed by the enzyme-linked immunosorbent assay (ELISA) sandwich method. The Human IL-10 ELISA Kit (No. ab100549) was used (Abcam plc., Shanghai, 201203, China). In this study, the testing sensitivity was 1.00 pg/mL, and the testing range was from 1.00 pg/mL to 100.00 pg/mL. The precision of intra-assay and interassay was 8.0% and 9.5%, respectively. The serum level of IL-6 was also tested by the Human IL-6 ELISA Kit (No. ab178013). In addition, serum levels of CRP, glucose, triglycerides, total cholesterol, high-density lipoprotein (HDL), and LDL (low-density lipoprotein) were also tested in our laboratory department.

2.4. Statistical Analysis. The study results were shown as the number (percentage) for categorical variables and the median (interquartile range (IQR)) for continuous variables. Correlation analysis between IL-10 and different variables was assessed by Spearman's rank correlation. The Mann-Whitney *U* test for continuous variables and chi-squared test for categorical variables were used to compare differences between groups. Stroke clinical severity at admission was dichotomized as minor (NIHSS, 0-5), moderate (NIHSS, 6-11), and severe (NIHSS ≥ 12) [29].

The prognostic determinant value of IL-10 for stroke functional outcome and mortality was assessed, and the odds ratios (OR) and 95% confidence intervals (CI) of the highest quartile IL-10 level (vs. lowest three quartiles) as compared with other risk factors were calculated by univariate and multivariate logistic regression analyses. In multivariate analysis, we included age, sex, obesity, vascular risk factors, therapies before admission, acute stroke treatment, stroke subtype,

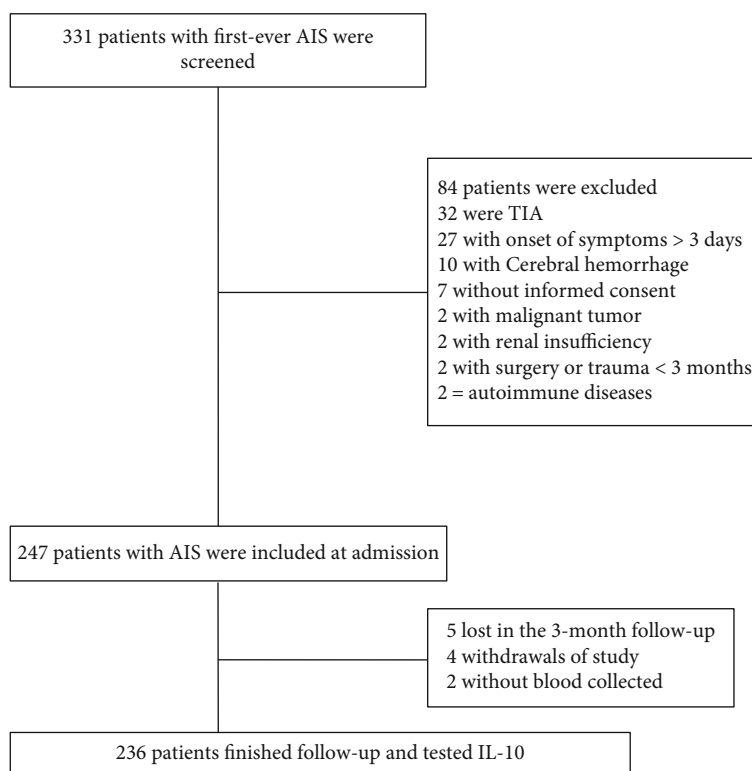


FIGURE 1: Research flow chart.

NIHSS at admission, infarct size, and serum levels of IL-6, Hs-CRP, and glucose.

Receiver operating characteristic (ROC) curve analysis was used to assess the cut-off value of IL-10 serum level as an indicator for screening of poor outcome and mortality, and results were reported as the area under the curve (AUC) and 95% CI. Diagnostic sensitivity and specificity also would be presented. Statistical software SPSS 24.0 (SPSS Inc., Chicago, IL, USA) was used for data statistics, and P values less than 0.05 (two-tailed) were considered to indicate significance.

2.5. Ethics Approval. The Ethics Committee of the First Affiliated Hospital of Jilin University reviewed and approved the research protocol (2019-08-007). Before entering the group, patients understood the research protocol, rights, and obligations and signed written informed consent. For patients who could not provide signatures, family members' signatures were also acceptable.

3. Results

3.1. Patients. In the beginning, 331 patients with suspected first-ever ischemic stroke entered the scope of our study; 247 patients with acute ischemic stroke were included at admission. Finally, 236 patients with collected blood samples finished follow-up and tested IL-10 (Figure 1). The basic information of the enrolled patients was comparable to that of all screened patients (age ($P = 0.08$), sex ($P = 0.55$), and BMI ($P = 0.21$)).

3.2. Descriptive Characteristics of Included Patients. The median age of the enrolled patients was 65 years (IQR, 56-76), and 57.6% ($n = 136$) of the patients were male. Most of the enrolled patients were Han (95.3%) and enjoyed medical insurance (96.6%). The most common vascular risk factors were hypertension (74.2%), diabetes (28.8%), and hyperlipidemia (26.7%). In addition, a history of atrial fibrillation (10.2%), TIA (11.9%), and obesity (11.4%) were also uncommon. At admission, the NIHSS score and the median infarct size were 7 (IQR, 3-11) points and 15.8 (7.2-28.7) mL, respectively. More than one in ten patients (13.3%) received acute mechanical thrombectomy and/or IV thrombolysis therapy during hospitalization. At discharge, the median mRS score was 2 (IQR, 0-3), and the median length of hospitalization and hospitalization costs were 12 (9-17) days and 9988 (8315-14153) CNY, respectively. More information is presented in Table 1.

3.3. Main Results. Serum IL-10 levels decreased with the increasing severity of stroke (evaluation by NIHSS score). As shown in Figure 2, there was a negative correlation between NIHSS score and IL-10 serum levels (r (Spearman) = -0.221 , $P = 0.001$). Furthermore, serum IL-10 levels in minor stroke patients with an NIHSS score of 0 to 5 points ($N = 92$) were 4.00 (IQR, 2.72-6.59) pg/mL, in moderate patients with an NIHSS score of 6 to 11 ($n = 98$) were 3.49 (IQR, 2.65-5.14) pg/mL, and in severe patients with an NIHSS score greater than 11 ($n = 46$) were 2.95 (IQR, 2.23-4.59) pg/mL (Figure 3). As shown in Table 2, negative correlations between IL-10 serum levels and IL-6 ($P = 0.012$) and infarct size ($P = 0.033$) were also reported, unlike all others assessed.

TABLE 1: Characteristics of the included patients.

Characteristics [†]	Patients with AIS
Participants	<i>N</i> = 236
Age (years)	
Median (IQR)	65 (56-76)
Mean age (SD)	65 (12.5)
Age groups	
<40	5 (2.1)
40-59	75 (31.8)
60-79	121 (51.3)
≥80	35 (14.8)
Sex	
Men	136 (57.6)
Women	100 (42.4)
Residence: urban	164 (69.5)
BMI (kg/m ²)	
Mean (SD)	24.4 ± 3.9
Median (IQR)	24.2 (22.5-25.7)
Ethnicity	
Minority	11 (4.7)
Han	225 (95.3)
Education: college and above	35 (14.8)
Medical insurance	228 (96.6)
Marital status: married	224 (94.9)
Vascular risk factors	
Smoking status	
Nonsmokers	202 (85.6)
Past smokers	4 (1.7)
Current smokers	30 (12.7)
Consumption of alcohol	33 (14.0)
Family history of stroke	35 (14.8)
History of TIA	28 (11.9)
Hypertension	175 (74.2)
Diabetes	68 (28.8)
Hyperlipidemia	63 (26.7)
Atrial fibrillation	24 (10.2)
Obesity ^{††}	27 (11.4)
Stroke severity, median NIHSS score (IQR)	7 (3-11)
DWI lesion size, median (mL) (IQR)	15.8 (7.2-28.7)
Median arterial pressure (mm Hg) (IQR)	
Systolic	159 (145-167)
Diastolic	92 (80-106)
Median body temperature (°C) (IQR)	37.0 (36.5-37.5)
Stroke causative factors, <i>n</i> (%)	
Large-vessel occlusive	69 (29.2)
Small-vessel occlusive	55 (23.3)
Cardioembolic	42 (17.8)
Other	18 (7.6)
Unknown	52 (22.0)

TABLE 1: Continued.

Characteristics [†]	Patients with AIS
Therapies before admission, <i>n</i> (%)	
Antihypertensive	142 (60.2)
Hypoglycemic	53 (22.5)
Anticoagulant	25 (10.6)
Statins	55 (23.3)
Acute treatment, <i>n</i> (%)	
IV thrombolysis	28 (11.9)
Mechanical thrombectomy	5 (2.1)
Mechanical thrombectomy and/or IV thrombolysis	31 (13.3)
Laboratory findings, median (IQR)	
Serum IL-10 level (pg/mL)	3.51 (2.61-5.24)
Serum IL-6 level (ng/mL)	16.1 (12.1-20.8)
Serum Hs-CRP (mg/dL)	0.82 (0.24-1.48)
Serum glucose level (mmol/L)	5.96 (5.15-6.77)
Triglycerides (mmol/L)	1.44 (1.14-1.89)
Total cholesterol (mmol/L)	4.13 (3.36-5.02)
HDL (mmol/L)	1.31 (1.08-1.62)
LDL (mmol/L)	2.10 (1.38-2.78)
Hospital stays, median days (IQR)	12 (9-17)
Hospital costs, median CNY (IQR)	9988 (8315-14153)
mRS at discharge, median (IQR)	2 (0-3)

[†]The results were presented as *n* (percentages) for categorical variables and as mean (standard deviation (SD)) for continuous variables. ^{††}Obesity was defined as BMI ≥ 28.0 kg/m². BMI: body mass index; CNY: Chinese Yuan Renminbi; TIA: transient ischemic attack; IQR: interquartile range; SD: standard deviation; NIHSS: National Institutes of Health Stroke Scale; DWI: diffusion-weighted imaging; mRS: modified Rankin Scale; IL-6: Interleukin-6; IL-10: Interleukin-10; Hs-CRP: hypersensitive-c-reactive-protein; LDL: high-density lipoprotein; LDL: low-density lipoprotein.

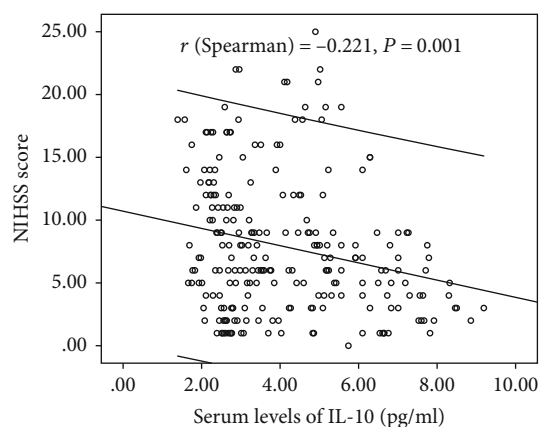


FIGURE 2: The correlation between NIHSS score and IL-10 serum levels. NIHSS: National Institutes of Health Stroke Scale; IL-10: Interleukin-10.

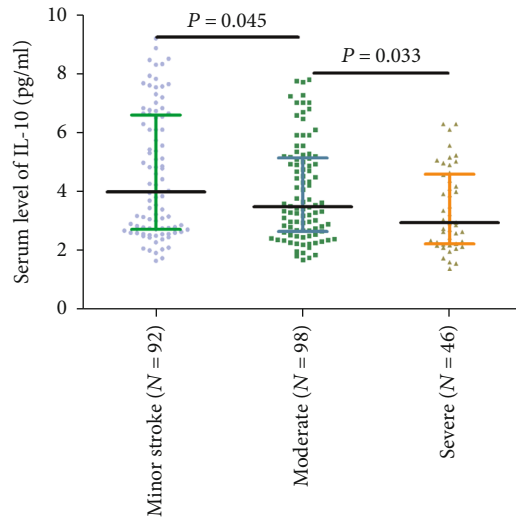


FIGURE 3: Serum IL-10 levels in groups stratified by stroke severity. All data are medians (IQR). *P* values refer to Mann–Whitney *U* tests. IL-10: Interleukin-10; IQR: interquartile ranges.

TABLE 2: Correlation analysis between IL-10 and different variables.

Variables	<i>r</i> (Spearman)	<i>P</i>
Age	0.052	0.425
Sex	-0.081	0.215
NIHSS	-0.221	0.001
Infarct size	-0.142	0.033
IL-6	-0.166	0.012
Hs-CRP	-0.108	0.103
Serum glucose	0.067	0.315
Stroke causative factors	0.134	0.044

NIHSS: National Institutes of Health Stroke Scale; IL-6: Interleukin-6; IL-10: Interleukin-10; Hs-CRP: hypersensitive-c-reactive-protein.

3.4. IL-10 and Functional Outcome after 3 Months. At follow-up, 70 patients (29.7%) had a poor functional outcome (mRS > 2). In these patients, the median IL-10 serum level was lower than in those patients with a good outcome (3.31 (IQR, 2.46-4.70) vs. 3.72 (IQR, 2.6-5.79); *P* = 0.033) (Figure 4). The ORs of the highest quartile IL-10 level (vs. lowest three quartiles) as compared with other risk factors were calculated by univariate and multivariate logistic regression analyses. With an unadjusted OR of 0.20 (95% CI, 0.09–0.42), IL-10 had a strong association with functional outcomes. In multivariable models adjusted for age, sex, obesity, vascular risk factors, therapies before admission, acute stroke treatment, stroke subtype, NIHSS at admission, infarct size, and serum levels of IL-6, Hs-CRP, and glucose, IL-10 levels in the highest quartile (>5.24 pg/mL) were associated with a reduced risk of a poor functional outcome (OR = 0.35; 95% CI = 0.19–0.63; *P* < 0.001). Conversely, the IL-6 serum level was positively associated with poor outcome (OR = 1.13; 95%CI = 1.04–1.21; *P* = 0.003) (Table 3).

In ROC curve analysis, we calculated the cut-off value of IL-10 serum level as an indicator for screening of poor outcome, as presented in Figure 5. The critical value was

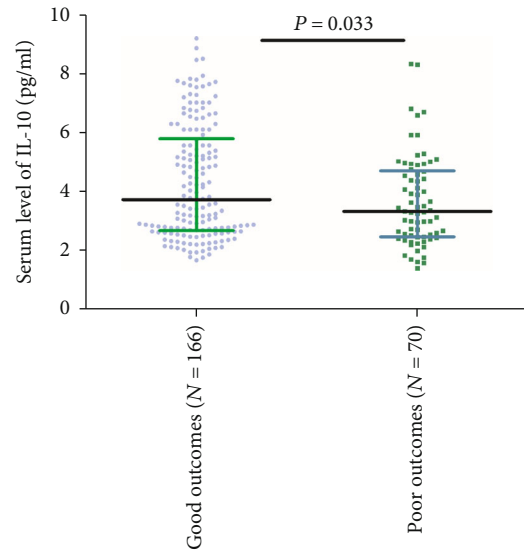


FIGURE 4: Serum IL-10 levels in groups stratified by the functional outcome. Poor functional outcome was defined as an mRS score of 3 to 6 points, and good outcome was defined as an mRS score of 0 to 2 points. All data are medians (IQR). *P* values refer to Mann–Whitney *U* tests. IL-10: Interleukin-10; IQR: interquartile ranges; mRS: modified Rankin Scale.

5.11 pg/mL with an AUC of 0.59 (95% CI, 0.51–0.66), showing a sensitivity of 87.14% and a specificity of 34.34%. With an AUC of 0.59, IL-10 was superior to CRP (AUC, 0.55; 95% CI, 0.50–0.59; *P* = 0.001) and white blood cell count (AUC, 0.53; 95% CI, 0.48–0.59; *P* < 0.001) and was within the range of the IL-6 (AUC, 0.61; 95% CI, 0.54–0.69; *P* = 0.103).

3.5. IL-10 and Death after 3 Months. Twenty-four patients died during the follow-up. In these patients, the median IL-10 serum level was lower than in those surviving patients (2.91 (IQR, 1.90-4.05) vs. 3.55 (IQR, 2.67-5.37); *P* = 0.006) (Figure 6). The ORs of the highest quartile IL-10 level (vs. lowest three quartiles) as compared with other risk factors were also calculated by univariate and multivariate logistic regression analyses. With an unadjusted OR of 0.14 (95% CI, 0.06–0.30), IL-10 had a strong association with mortality. In multivariable models adjusted for age, sex, obesity, vascular risk factors, therapies before admission, acute stroke treatment, stroke subtype, NIHSS at admission, infarct size, and serum levels of IL-6, Hs-CRP, and glucose, IL-10 levels in the highest quartile (>5.24 pg/mL) were associated with a reduced risk of mortality (OR = 0.24; 95%CI = 0.11–0.52; *P* < 0.001). Conversely, the IL-6 serum level was positively associated with poor outcome (OR = 1.16; 95%CI = 1.02–1.25; *P* = 0.002) (Table 3).

In ROC curve analysis, we calculated the cut-off value of the IL-10 serum level as an indicator for screening of death events as presented in Figure 7. The critical value was 2.54 pg/mL with an AUC of 0.67 (95% CI, 0.55–0.79), showing a sensitivity of 50.00% and a specificity of 81.13%. With an AUC of 0.67, IL-10 was superior to CRP (AUC, 0.61; 95% CI, 0.54–0.69; *P* < 0.001) and white blood cell count

TABLE 3: Multivariate analysis of predictors of poor functional outcome (Rankin 3–6) and mortality[†].

Variables	Poor functional outcome			Mortality		
	OR	95% CI	<i>P</i>	OR	95% CI	<i>P</i>
Age (increase per unit)	1.07	1.02-1.14	0.002	1.08	1.02-1.15	<0.001
Stroke severity, NIHSS > 6	15.14	3.03-30.11	<0.001	10.15	2.25-22.32	0.009
Acute stroke treatment	0.50	0.20-0.85	0.005	0.26	0.12-0.61	<0.001
IL-10 > 5.24 pg/mL [‡]	0.35	0.19-0.63	<0.001	0.24	0.11-0.52	<0.001
IL-6 (increase per unit)	1.13	1.04-1.21	0.003	1.16	1.02-1.25	0.002
Obesity (BMI ≥ 28 kg/m ²)	1.85	1.05-2.82	0.032	2.05	1.07-4.05	0.183

[†]Multivariable model included the following variables: age, sex, obesity, vascular risk factors, therapies before admission, acute stroke treatment, stroke subtype, NIHSS at admission, infarct size, and serum levels of IL-6, Hs-CRP, and glucose. [‡]IL-10 ≤ 5.24 pg/mL corresponding to the combination of the lowest three quartiles used as the reference. OR: odds ratio; CI: confidence interval; NIHSS: National Institutes of Health Stroke Scale; IL-6: Interleukin-6; IL-10: Interleukin-10; Hs-CRP: hypersensitive-c-reactive-protein.

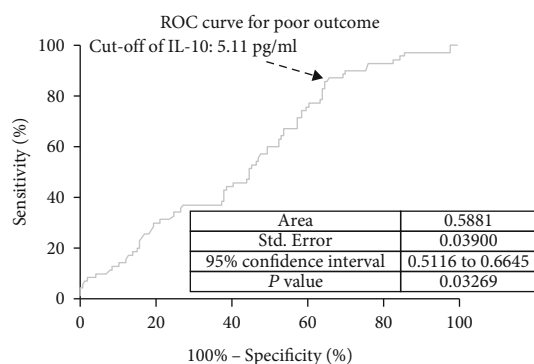


FIGURE 5: Receiver operating characteristic curve analysis was used to assess the value of IL-10 serum level as an indicator for screening of poor outcomes. Poor functional outcome was defined as an mRS score of 3 to 6 points. IL-10: Interleukin-10; mRS: modified Rankin Scale.

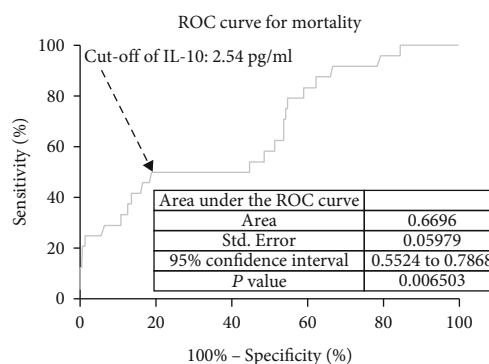


FIGURE 7: Receiver operating characteristic curve analysis was used to assess the value of IL-10 serum level as an indicator for screening of mortality. IL-10: Interleukin-10.

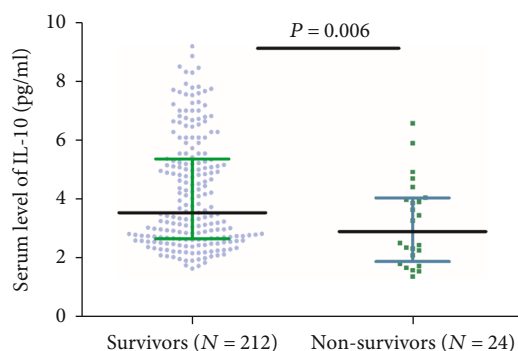


FIGURE 6: Serum IL-10 levels in groups stratified by survival state. All data are medians (IQR). *P* values refer to Mann-Whitney *U* tests. IL-10: Interleukin-10.

(AUC, 0.57; 95% CI, 0.50-0.68; *P* < 0.001) and was within the range of the IL-6 (AUC, 0.69; 95% CI, 0.60-0.81; *P* = 0.075).

4. Discussion

IL-10, a quintessential immunosuppressive anti-inflammatory cytokine, can resolve inflammation and promote wound repair at peripheral sites. In this prospective, cohort study, we found that low serum levels of IL-10 were

independently associated with both the clinical severity at admission and a poor functional prognosis in ischemic stroke patients, suggesting that the anti-inflammatory cytokine IL-10 was an important prognostic determinant.

In patients with ischemic stroke, the role of IL-10 in predicting risk and outcomes is not very clear [30]. In the limited number of clinical studies, higher IL-10 levels seen postictus are related to worse outcomes [20, 21]. However, in this study, we showed that elevated IL-10 was associated with a more favorable prognosis, which had been supported by two previous studies [18, 19]. Similarly, reduced IL-10 serum levels were associated with a more unfavorable prognosis in patients with acute coronary syndromes [31]. IL-10 was an early outcome predictor in traumatic brain injury patients [32]. The differences in these studies might be caused by differences in the number of patients, time of onset of the disease, population, testing methods, and reagents. Additional large sample and multicenter studies assessing the role of IL-10 in ischemic stroke are warranted.

Welsh et al. [33] found that baseline circulating levels of IL-10 were positively associated with the risk of cardiovascular events among the elderly without prior cardiovascular events. Another study showed that the elevated serum IL-10 levels were related to the presence of depressive mood in patients with cardiovascular risk factors [34]. Dziedzic et al. [35] demonstrated that increased serum levels of IL-10 were significantly correlated with the Glasgow Coma Scale score in

intracerebral hemorrhage patients. In addition, the temporospatial expression of IL-10 in the rat brain may contribute to worse outcomes [36]. The IL-10 level in serum did not show any significant correlation with the NIHSS score at the time of admission [37], which was not confirmed in our study.

The neuroprotective role of IL-10 in an experimental mouse stroke model had been verified [38]. Administration of hematopoietic cytokines could increase the expression of IL-10, which might provide a favorable microenvironment for neurogenesis after ischemic stroke [39]. A meta-analysis study showed that reduced serum levels of IL-10 might be a major player in the development and progression of cerebral infarction [40]; another cross-sectional study found that the lower serum IL-10 concentration and its selected genetic variations were significantly associated with an increased likelihood of ischemic stroke [41]. Serum levels of IL-10 in patients with unstable angina were significantly lower than those with chronic stable angina, suggesting that IL-10 has a protective role in atherosclerosis [42].

The elevated level of IL-10 in ischemic stroke patients might play a neuroprotective role through the following pathways: (1) the IL-10/STAT3 axis presents anti-inflammatory activities [43]. The use of anti-inflammatory medications might improve the prognosis following ischemic stroke. (2) IL-10 can play roles in limiting neuronal damage [43], increasing neuronal survival [44], and regulating adult neurogenesis [45]. IL-10 also can reduce the vulnerability of neurons to CNS ischemia and trauma [46]. (3) IL-10 could promote the activity of M2 macrophages in adipose tissue [47] or act directly on adipocytes to decrease their inflammatory response [48]. Cell-based therapies using M2-like macrophages could be protective therapeutic strategies against stroke [49]. Li et al. [50] showed that IL-10 could regulate microglial phagocytosis and macrophage infiltration after intracerebral hemorrhage by regulating CD36. Adipocyte fatty acid-binding protein plays a role in the stroke prognosis [51]. (4) IL-10 could provide neuroprotection by acting via IL-10 receptor and PI3K/AKT and STAT3 signal transduction pathways [52].

The following limitations need to be considered: (1) single-center and small sample ($N = 236$) researches need further verification. More samples with subtle designs are warranted in the future. (2) This cohort observational study cannot draw causal conclusions. (3) Blood samples were collected one time after admission. We could not obtain the change in serum IL-10 concentration after the onset of stroke patients. (4) We only tested serum levels of IL-10; other members of the IL-10 cytokine family, such as IL-19, IL-20, IL-22, and IL-24 [53], were not assessed. Thus, the relationship between IL-10, IL-10 cytokine family, and stroke prognosis could not be performed. (5) A meta-analysis indicated that IL-10-1082 A/G polymorphism was associated with ischemic stroke susceptibility in Asians [54]. However, in this study, the genetic polymorphism of IL-10 was not tested. Thus, the role of genetic polymorphism of IL-10 in stroke prognosis could not be confirmed. (6) IL-10 plays an important role in the cardiovascular system, and the blood, digestion, and especially diseases of the cardiovascular system

are closely related [55]. However, we did not obtain that information in our study. Thus, the influence of other factors on IL-10 and stroke prognosis could not be excluded.

5. Conclusions

Reduced serum levels of IL-10 were independently associated with both the clinical severity at admission and a poor functional prognosis in ischemic stroke patients, suggesting that the anti-inflammatory cytokine IL-10 was an important prognostic determinant. Further studies are warranted to confirm whether the protective association of IL-10 with prognosis represents a causal pathway involved in the pathogenesis or the predictive effect of poor prognosis on ischemic stroke patients. This study may open up new strategies for the treatment and secondary prevention of stroke in the future.

Data Availability

Please contact the corresponding author (Dr. Nan) for data requirements.

Consent

Consent was not needed.

Conflicts of Interest

The authors declare that they have no conflicts of interest.

Acknowledgments

We thank all patients who participated in the study.

References

- [1] M. S. Phipps and C. A. Cronin, "Management of acute ischemic stroke," *BMJ*, vol. 368, 2020.
- [2] W. J. Tu, H. C. Qiu, Y. Zhang et al., "Lower serum retinoic acid level for prediction of higher risk of mortality in ischemic stroke," *Neurology*, vol. 92, no. 15, pp. e1678–e1687, 2019.
- [3] S. Wu, B. Wu, M. Liu et al., "Stroke in China: advances and challenges in epidemiology, prevention, and management," *The Lancet Neurology*, vol. 18, no. 4, pp. 394–405, 2019.
- [4] W. Wang, B. Jiang, H. Sun et al., "Prevalence, incidence, and mortality of stroke in China: results from a nationwide population-based survey of 480 687 adults," *Circulation*, vol. 135, no. 8, pp. 759–771, 2017.
- [5] B. H. Chao, F. Yan, Y. Hua et al., "Stroke prevention and control system in China: CSPPC-Stroke Program," *International Journal of Stroke*, vol. 16, no. 3, pp. 265–272, 2021.
- [6] S. E. Lakhan, A. Kirchgessner, and M. Hofer, "Inflammatory mechanisms in ischemic stroke: therapeutic approaches," *Journal of Translational Medicine*, vol. 7, no. 1, pp. 1–11, 2009.
- [7] K. Shi, D. C. Tian, Z. G. Li, A. F. Ducruet, M. T. Lawton, and F. D. Shi, "Global brain inflammation in stroke," *The Lancet Neurology*, vol. 18, no. 11, pp. 1058–1066, 2019.
- [8] K. L. Lambertsen, B. Finsen, and B. H. Clausen, "Post-stroke inflammation—target or tool for therapy?," *Acta Neuropathologica*, vol. 137, no. 5, pp. 693–714, 2019.

- [9] R. Jin, L. Liu, S. Zhang, A. Nanda, and G. Li, "Role of inflammation and its mediators in acute ischemic stroke," *Journal of Cardiovascular Translational Research*, vol. 6, no. 5, pp. 834–851, 2013.
- [10] T. Dziedzic, "Systemic inflammation as a therapeutic target in acute ischemic stroke," *Expert Review of Neurotherapeutics*, vol. 15, no. 5, pp. 523–531, 2015.
- [11] L. S. Cheng, W. J. Tu, Y. Shen, L. J. Zhang, and K. Ji, "Combination of high-sensitivity C-reactive protein and homocysteine predicts the post-stroke depression in patients with ischemic stroke," *Molecular Neurobiology*, vol. 55, no. 4, pp. 2952–2958, 2018.
- [12] T. Nakase, T. Yamazaki, N. Ogura, A. Suzuki, and K. Nagata, "The impact of inflammation on the pathogenesis and prognosis of ischemic stroke," *Journal of the Neurological Sciences*, vol. 271, no. 1-2, pp. 104–109, 2008.
- [13] K. Kowalska, E. Klimiec, K. Weglarczyk et al., "Reduced ex vivo release of pro-inflammatory cytokines and elevated plasma interleukin-6 are inflammatory signatures of post-stroke delirium," *Journal of Neuroinflammation*, vol. 15, no. 1, pp. 111–116, 2018.
- [14] Y. Hao, J. Ding, R. Hong et al., "Increased interleukin-18 level contributes to the development and severity of ischemic stroke," *Aging (Albany NY)*, vol. 11, no. 18, pp. 7457–7472, 2019.
- [15] T. V. Arumugam, D. N. Granger, and M. P. Mattson, "Stroke and T-cells," *Neuromolecular Medicine*, vol. 7, no. 3, pp. 229–242, 2005.
- [16] C. Lin, X. Tang, Z. Shi et al., "Serum tumor necrosis factor α levels are associated with new ischemic brain lesions after carotid artery stenting," *Journal of Vascular Surgery*, vol. 68, no. 3, pp. 771–778, 2018.
- [17] J. Zaremba, J. Ilkowski, and J. Losy, "Serial measurements of levels of the chemokines CCL2, CCL3 and CCL5 in serum of patients with acute ischaemic stroke," *Folia Neuropathologica*, vol. 44, no. 4, pp. 282–289, 2006.
- [18] N. Vila, J. Castillo, A. Dávalos, A. Esteve, A. M. Planas, and A. Chamorro, "Levels of anti-inflammatory cytokines and neurological worsening in acute ischemic stroke," *Stroke*, vol. 34, no. 3, pp. 671–675, 2003.
- [19] V. Basic Kes, A. M. Simundic, N. Nikolac, E. Topic, and V. Demarin, "Pro-inflammatory and anti-inflammatory cytokines in acute ischemic stroke and their relation to early neurological deficit and stroke outcome," *Clinical Biochemistry*, vol. 41, no. 16-17, pp. 1330–1334, 2008.
- [20] S. E. Conway, M. Roy-O'Reilly, B. Friedler, I. Staff, G. Fortunato, and L. D. McCullough, "Sex differences and the role of IL-10 in ischemic stroke recovery," *Biology of Sex Differences*, vol. 6, no. 1, pp. 1–5, 2015.
- [21] L. T. Chang, C. M. Yuen, C. W. Liou et al., "Link between interleukin-10 level and outcome after ischemic stroke," *Neuroimmunomodulation*, vol. 17, no. 4, pp. 223–228, 2010.
- [22] X. Li, S. Lin, X. Chen et al., "The prognostic value of serum cytokines in patients with acute ischemic stroke," *Aging and Disease*, vol. 10, no. 3, pp. 544–556, 2019.
- [23] S. Hatano, "Experience from a multicentre stroke register: a preliminary report," *Bulletin of the World Health Organization*, vol. 54, no. 5, pp. 541–553, 1976.
- [24] T. Brott, H. P. Adams Jr., C. P. Olinger et al., "Measurements of acute cerebral infarction: a clinical examination scale," *Stroke*, vol. 20, no. 7, pp. 864–870, 1989.
- [25] J. R. Sims, L. R. Gharai, P. W. Schaefer et al., "ABC/2 for rapid clinical estimate of infarct, perfusion, and mismatch volumes," *Neurology*, vol. 72, no. 24, pp. 2104–2110, 2009.
- [26] H. P. Adams, B. H. Bendixen, L. J. Kappelle et al., "Classification of subtype of acute ischemic stroke. Definitions for use in a multicenter clinical trial. TOAST. Trial of Org 10172 in Acute Stroke Treatment," *Stroke*, vol. 24, no. 1, pp. 35–41, 1993.
- [27] R. B. R. Bonita and R. Beaglehole, "Recovery of motor function after stroke," *Stroke*, vol. 19, no. 12, pp. 1497–1500, 1988.
- [28] W. J. Tu, H. C. Qiu, J. L. Cao, Q. Liu, X. W. Zeng, and J. Z. Zhao, "Decreased concentration of irisin is associated with poor functional outcome in ischemic stroke," *Neurotherapeutics*, vol. 15, no. 4, pp. 1158–1167, 2018.
- [29] M. Katan, F. Fluri, N. G. Morgenthaler et al., "Copeptin: a novel, independent prognostic marker in patients with ischemic stroke," *Annals of Neurology*, vol. 66, no. 6, pp. 799–808, 2009.
- [30] J. M. Garcia, S. A. Stillings, J. L. Leclerc et al., "Role of interleukin-10 in acute brain injuries," *Frontiers in Neurology*, vol. 8, p. 244, 2017.
- [31] C. Heeschen, S. Dimmeler, C. W. Hamm et al., "Serum level of the anti-inflammatory cytokine interleukin-10 is an important prognostic determinant in patients with acute coronary syndromes," *Circulation*, vol. 107, no. 16, pp. 2109–2114, 2003.
- [32] L. Lagerstedt, L. Azurmendi, O. Tenovuo et al., "Interleukin 10 and heart fatty acid-binding protein as early outcome predictors in patients with traumatic brain injury," *Frontiers in Neurology*, vol. 11, p. 376, 2020.
- [33] P. Welsh, H. M. Murray, I. Ford et al., "Circulating interleukin-10 and risk of cardiovascular events," *Arteriosclerosis, Thrombosis, and Vascular Biology*, vol. 31, no. 10, pp. 2338–2344, 2011.
- [34] T. Meyer, B. Stanske, M. M. Kochen et al., "Serum levels of interleukin-6 and interleukin-10 in relation to depression scores in patients with cardiovascular risk factors," *Behavioral Medicine*, vol. 37, no. 3, pp. 105–112, 2011.
- [35] T. Dziedzic, S. Bartus, A. Klimkowicz, M. Motyl, A. Slowik, and A. Szczudlik, "Intracerebral hemorrhage triggers interleukin-6 and interleukin-10 release in blood," *Stroke*, vol. 33, no. 9, pp. 2334–2335, 2002.
- [36] A. Y. Fouda, A. Kozak, A. Alhusban, J. A. Switzer, and S. C. Fagan, "Anti-inflammatory IL-10 is upregulated in both hemispheres after experimental ischemic stroke: hypertension blunts the response," *Experimental & translational stroke medicine*, vol. 5, no. 1, p. 12, 2013.
- [37] H. V. Singh, A. Pandey, A. K. Shrivastava, A. Raizada, S. K. Singh, and N. Singh, "Prognostic value of neuron specific enolase and IL-10 in ischemic stroke and its correlation with degree of neurological deficit," *Clinica Chimica Acta*, vol. 419, pp. 136–138, 2013.
- [38] A. Liesz, A. Bauer, J. D. Hoheisel, and R. Veltkamp, "Intracerebral interleukin-10 injection modulates post-ischemic neuroinflammation: an experimental microarray study," *Neuroscience Letters*, vol. 579, pp. 18–23, 2014.
- [39] Y. Morita, S. Takizawa, H. Kamiguchi, T. Uesugi, H. Kawada, and S. Takagi, "Administration of hematopoietic cytokines increases the expression of anti-inflammatory cytokine (IL-10) mRNA in the subacute phase after stroke," *Neuroscience Research*, vol. 58, no. 4, pp. 356–360, 2007.
- [40] Y. Zhu, H. Yang, Z. Diao, Y. Li, and C. Yan, "Reduced serum level of interleukin-10 is associated with cerebral infarction: a

- case-control and meta-analysis study," *Molecular Neurobiology*, vol. 53, no. 4, pp. 2698–2704, 2016.
- [41] G. Xie, P. K. Myint, M. J. S. Zaman et al., "Relationship of serum interleukin-10 and its genetic variations with ischemic stroke in a Chinese general population," *PLoS One*, vol. 8, no. 9, article e74126, 2013.
- [42] D. A. Smith, S. D. Irving, J. Sheldon, D. Cole, and J. C. Kaski, "Serum levels of the anti-inflammatory cytokine interleukin-10 are decreased in patients with unstable angina," *Circulation*, vol. 104, no. 7, pp. 746–749, 2001.
- [43] M. Saraiva, P. Vieira, and A. O'Garra, "Biology and therapeutic potential of interleukin-10," *The Journal of experimental medicine*, vol. 217, no. 1, p. e20190418, 2020.
- [44] Z. Zhou, X. Peng, R. Insolera, D. J. Fink, and M. Mata, "Interleukin-10 provides direct trophic support to neurons," *Journal of Neurochemistry*, vol. 110, no. 5, pp. 1617–1627, 2009.
- [45] L. Pereira, M. Font-Nieves, C. van den Haute, V. Baekelandt, A. M. Planas, and E. Pozas, "IL-10 regulates adult neurogenesis by modulating ERK and STAT3 activity," *Frontiers in Cellular Neuroscience*, vol. 9, 2015.
- [46] M. Grilli, I. Barbieri, H. Basudev et al., "Interleukin-10 modulates neuronal threshold of vulnerability to ischaemic damage," *The European Journal of Neuroscience*, vol. 12, no. 7, pp. 2265–2272, 2000.
- [47] Y. Xue, D. Nie, L. J. Wang et al., "Microglial polarization: novel therapeutic strategy against ischemic stroke," *Aging and Disease*, vol. 12, no. 2, pp. 466–479, 2021.
- [48] F. S. Lira, J. C. Rosa, G. D. Pimentel et al., "Both adiponectin and interleukin-10 inhibit LPS-induced activation of the NF- κ B pathway in 3T3-L1 adipocytes," *Cytokine*, vol. 57, no. 1, pp. 98–106, 2012.
- [49] M. Kanazawa, I. Ninomiya, M. Hatakeyama, T. Takahashi, and T. Shimohata, "Microglia and monocytes/macrophages polarization reveal novel therapeutic mechanism against stroke," *International Journal of Molecular Sciences*, vol. 18, no. 10, p. 2135, 2017.
- [50] Q. Li, X. Lan, X. Han et al., "Microglia-derived interleukin-10 accelerates post-intracerebral hemorrhage hematoma clearance by regulating CD36," *Brain, Behavior, and Immunity*, vol. 94, pp. 437–457, 2021.
- [51] W. J. Tu, X. W. Zeng, A. Deng et al., "Circulating FABP4 (fatty acid-binding protein 4) is a novel prognostic biomarker in patients with acute ischemic stroke," *Stroke*, vol. 48, no. 6, pp. 1531–1538, 2017.
- [52] S. Sharma, B. Yang, X. Xi, J. C. Grotta, J. Aronowski, and S. I. Savitz, "IL-10 directly protects cortical neurons by activating PI-3 kinase and STAT-3 pathways," *Brain Research*, vol. 1373, pp. 189–194, 2011.
- [53] S. Xu, J. Zhang, J. Liu et al., "The role of interleukin-10 family members in cardiovascular diseases," *International Immunopharmacology*, vol. 94, p. 107475, 2021.
- [54] J. Jin, W. Li, L. Peng et al., "Relationship between interleukin-10-1082A/G polymorphism and risk of ischemic stroke: a meta-analysis," *PLoS One*, vol. 9, no. 4, article e94631, 2014.
- [55] M. I. Yilmaz, Y. Solak, M. Saglam et al., "The relationship between IL-10 levels and cardiovascular events in patients with CKD," *Clinical Journal of the American Society of Nephrology*, vol. 9, no. 7, pp. 1207–1216, 2014.